University of Strathclyde

Department of Mathematics and Statistics

THE HYDRODYNAMICS OF FERROELECTRIC SMECTIC C LIQUID CRYSTALS

Lawrence Joseph Seddon

A thesis presented in fulfilment of the requirements

for the degree of Doctor of Philosophy.

September 2010

This thesis is the result of the authors original research. It has been composed by the author and has not been previously submitted for examination which has led to the award of a degree.

The copyright of this thesis belongs to the author under the terms of the United Kingdom Copyright Acts as qualified by University of Strathclyde Regulation 3.50. Due acknowledgement must always be made of the use of any material contained in, or derived from, this thesis.

Signed :

Date :

Acknowledgements

First things first, I must extend a very considerable degree of thanks to Professor Iain Stewart, who has throughout my PhD, patiently guided me and given advice and assistance whenever I needed it. I could not have wished for a better supervisor, it's been a privilege working with you.

Additional thanks go to my colleagues in the Department of Mathematics and Statistics. In particular I'd like to thank Dr Andrew Davidson, Dr Alan Walker, Dr Julie Sullivan and Dr Kim McCosh for all the coffee club mornings and afternoons and general chats and advice, cheers ladies and gents! Big thanks also to my old office mate Dr Michael Strauss for a lot of gigantic laughs, coffee breaks, politics Thursdays and invaluable discussions on operator theory. Yet more thanks go to Darren Knox, Lindsey Ritchie, Jill Miscandlon and Stephen Corson for lots of friendly stress relieving conversation, very much appreciated chaps! An extra big thank you goes to my family and friends for all their support, especially my cousin Wendy Ellis and her husband Rob and my old UKC chums Paul Litjens and Uniti Bhalla, for all their help and hospitality. And thanks also to the EPSRC who provided financial support for both my MSc and PhD.

Which brings me, finally, to my parents, my dad Lawrence Percival Seddon, my mum Maria Carmen Seddon and my step dad Eric Ronald Seddon. Without their love, encouragement and support absolutely none of this would have been possible. I can't thank them enough for all they did for me.

Abstract

A continuum model incorporating flow is developed as an extension to the work of Stewart and Momoniat who considered a mechanical soliton travelling through a sample of smectic C* liquid crystal. Here we study a wave front propagating through an infinite sample of ferroelectric liquid crystal in a planar geometry, under the influence of an inclined electric field of constant magnitude. We use the dynamic theory for smectic C liquid crystals of Leslie, Stewart and Nakagawa, appropriately extended to include the spontaneous polarisation and elastic energy terms encountered in smectic C* materials. We incorporate flow terms into our model giving a total of five dynamic equations. The resulting dynamic equations have infinitesimal perturbations imposed upon them. The perturbation equations are linearised and, by exploiting an exact solution in the case where the field is co-planar with the sample, a set of linear perturbation equations are developed. Simplifying assumptions lead to a pair of equations which, when suitable time decaying, spatially dependent perturbations are applied yield an eigenvalue problem. By employing a suitable numerical scheme we examine the resulting stability problem and use the results to identify critical electric field strengths below which we conjecture, travelling waves are not initiated. We also present a novel method for determining wave front profiles for a mechanical soliton in a planar sample of ferroelectric smectic C liquid crystal. We end by looking at numerical method for determining wave speeds in ferroelectric smectic C liquid crystals which employs discretised nonlinear Volterra integral equations

of the second kind. The method is completely general in scope, and may in fact be used to tackle wave speed problems for any appropriate reaction-diffusion equation which admits travelling wave solutions.

For Lawrie, Maria and Eric.

Contents

Chapter 1

Introducing Liquid Crystals

1.1 Introduction

Since their discovery in 1888 by the Austrian botanist Reinitzer liquid crystals have assumed huge importance in our modern technological world. From the display screen on a desk in an office to the shampoo people use to wash their hair liquid crystals have been crucial in the development of many branches of science and engineering. An extraordinary list of objects which incorporate liquid crystals in some form has been compiled by Peter Palffy-Muhoray [1] and makes for entertaining reading

> Liquid crystals are all around us: in high-strength plastics, snail slime, laundry detergent, textile fibres such as silk and Kevlar, crude oil, insect wings, mineral slurries, lipstick, Bose-Einstein condensates, and the mantles of neutron stars. We eat them as aligned molecules in gluten and drink them as phospholipids in milk, where they stabilize fat globules. In our bodies they transport fats, make up cell membranes and affect the functioning of hair cells in the inner ear, and even DNA.

Needless to say the list is not exhaustive! Probably the most important use of liquid crystals has been in the application to LCD display technology. Liquid

crystal displays are found in mobile phones, calculators, watches, hand-held games devices, touch screens and televisions. Electronics manufacturers use them as steerable waveguides in antennas, switches in opto-electronic devices and doped with dye they can be pumped with an external light source and used as lasers. The range of applications of liquid crystals is quite simply vast.

Our interest so far as this thesis is concerned centres around a class of liquid crystals known as ferroelectrics. Ferroelectric liquid crystalline materials have been actively researched for many years. Of particular importance is the application of ferroelectric liquid crystals to fast switching display devices. Current display technologies employ approaches such as in-plane switching [2] or twisted nematic cells [3, p.101-109] to guide light. Both in-plane switched and twisted nematic devices are well understood and are relatively straightforward and cheap to manufacture. Each uses nematic liquid crystals as the fundamental building blocks on which they are constructed.

The big drawback with devices based on nematic technology is the slow switching speed of the order of 10 ms [4, p.317]. This is adequate for the most applications but can be a problem in LCD televisions for example when reproducing fast moving objects such as balls in say a game of football. The individual pixels which make up the display must be switched quickly, and with a switching time of 10 ms, most display devices struggle to reproduce fast moving picture facets without the addition of very expensive buffering circuitry.

Ferroelectric devices offer the promise of displays which can in theory switch many times faster than their nematic counterparts. Experimental work on electro-optic switching in ferroelectric smectic C liquid crystals, in particular the work by Clark and Lagerwall [5], indicates microsecond to submicrosecond switching times are achievable. In addition theoretical calculations have also predicted microsecond switching times, see for instance calculations performed

by Stewart [4, p.317]. Achieving switching speeds of even microsecond order would signal a huge leap forwards in display technology and would open up new areas of application in the opto-electronics industry.

A great deal of effort is being devoted to the study of smectic C* liquid crystals. However the continuum modelling of smectic C* liquid crystals is perhaps not as well developed as other areas of theoretical liquid crystals research such as nematics [6]. Our aim in this thesis is to investigate some less well explored areas relating to theoretical aspects of ferroelectric smectic C modelling. Broadly speaking the work is split into three main parts.

In this chapter we cover a little of the history of liquid crystals, attempt to offer a definition of what a liquid crystal is and how they are categorised and then go on to explore some of the principle ideas behind the continuum models we shall be considering in later chapters.

Chapter 2 introduces the hydrodynamic flow model that forms a large part of this study. In it we shall introduce the travelling wave equation for a wave front propagating in a thin film of smectic C* liquid crystal about which much of the work is centred, along with conditions which are necessary in order to extract an exact solution for the propagating wave front. Then we go on to consider the continuum model used to generate the wave equation but augment it by introducing infinitesimal flow in the form of perturbations. Ultimately this will yield a total of five nonlinear perturbation equations which form the focus of study in the two chapters which follow.

In Chapter 3 we linearise the perturbation equations and use the exact solution for the front propagation equation to derive linear perturbation equations expressed in terms of hyperbolic functions.

In the following chapter, Chapter 4, we introduce time decaying spatial perturbations and demonstrate how the linearised perturbation equations may be

reduced in form to give a constant coefficient non-self-adjoint eigenvalue problem and a non-constant coefficient non-self-adjoint eigenvalue problem. We go on to solve the eigenvalue problems using an extended Galerkin method, and then go on to investigate system stability using numerical methods to determine critical electric field strengths. We then present some power law results derived using the data collected.

In Chapter 5 we present a novel method for understanding the shape of propagating wave front by adapting a technique used by Stewart and Wigham [7] to investigate wave front propagation in circular domain walls in smectic C liquid crystals. Instead of considering circular wave fronts under the influence of a concentric magnetic field we consider planar waves under the influence of an linear electric field which may or may not lie in the plane of the sample.

In Chapter 6 we present work by Seddon and Stewart that is already in print [8]. This chapter details a novel method for determining wave speeds for front propagation in smectic C^* liquid crystals under the influence of an inclined electric field. We present a solution method using integral equations and discuss some results of the work. So we begin in the next section, as promised, with a short tour of the history of liquid crystal research.

1.2 A brief history of liquid crystals

Liquid crystals were first discovered in 1888 by the Austrian botanist Frederich Reinitzer as a result of work he had conducted at the Charles University of Prague. In his paper of 3rd May 1888 entitled *Beiträge zur Kenntniss des Cholesterins* [9] Reinitzer reported the existence of two melting points for the compound $C_{27}H_{45} \cdot C_7H_5O_2$ or *cholesteryl benzoate*. He noticed that on heating *cholesteryl benzoate* from a solid at room temperature the compound appeared to melt at 145.5°C to form a cloudy liquid and on further heating the liquid cleared

at 178.5°C. Although *cholesteryl benzoate* had been investigated by other researchers who observed similar behaviour at the same temperatures, Reinitzer alone recognized the significance of the two melting points. He had infact described the phase characteristics of the first naturally occurring cholesteric liquid crystalline material to be formally identified.

Reinitzer had in essence discovered a new form of matter. Prior to 1888 all forms of matter were thought to exist in one of three phases: solid, liquid and gas. At standard atmospheric pressure (1 atmosphere) a substance in solid form on heating would reach a prescribed melting point where it would undergo a phase change to a liquid. Further heating would take the liquid to its boiling point and continued heating would result in the liquid vapourising to a gaseous phase. In some cases compounds, like for example frozen *carbon dioxide*, were known to sublimate directly from the solid to the gas phase at 1 atmosphere without undergoing a phase change to liquid form.

The phase discovered by Reinitzer, what we now call a *cholesteric phase*, represented science's first encounter with a new class of materials known today as *liquid crystals*. Reinitzer sent samples of the material to his collaborator, Physicist Otto Lehmann. Lehmann, then a Professor in Aachen set about the task of characterising the material Reinitzer had sent him. In time Lehmann came to form the opinion that the substance was chemically uniform in nature [10]. Then in 1889 Gatterman and Ritschke observed the liquid crystalline phase of *p*-azoxyanisole also known as PAA, and further work by Lehmann led to PAA being described in 1890. In 1922 Friedel [11] coined the terminology commonly used today to describe liquid crystal phases these being *nematic*, *smectic* and *cholesteric*.

Serious attempts at describing liquid crystals theoretically began in the 1900's. In 1907, Vörlander discovered that a crucial requirement in order for

a material to posses two melting points was the existence of rod like molecules [4]. This in turn opened up the field of theoretical liquid crystal research. In particular it allowed molecules in liquid crystals to be modeled as rod like structures and would proves to be of critical importance in attempting to model liquid crystal phenomena. In the early years however and at about the time of Vörlander discovery theoretical descriptions centred on the work by Bose [12] using the recently introduced idea of statistical physics of Boltzmann. Bose developed a theoretical framework known as swarm theory and this idea came to dominate mathematical research into liquid crystal phenomena for many decades.

The first essentially correct *isothermal* (fixed temperature) mathematical description of liquid crystalline phases was due to Oseen who reported his work in a series of articles dating back to 1925 [13, 14], followed by Zocher in 1927 [15]. Ossen's work on the static theory of the nematic phase was further developed by Frank in 1958 [16] and incorporates the notion of a director $\mathbf{n}$ and its possible distortions, giving us what is now known as the Frank-Ossen elastic energy.

In 1961 Eriksen [17] generalised the static theory of nematics to propose balance laws which were needed to introduce dynamical behaviour. Leslie in two papers [18, 19] published between 1966 and 1968 formulated constitutive equations which allowed him to complete a dynamic theory for nematic liquid crystals. In so doing he placed the capstone on what has come to be known as the Eriksen-Leslie theory of nematic liquid crystals. General acceptance of this theory came when Fisher and Frederikson [20] compared experimental observations for an unusual scaling law for Poiseuille flow which confirmed theoretical predictions made by Atkin [21] in 1970. From this point the Eriksen-Leslie theory became established as the generally accepted dynamic theory for liquid crystals.

Over the next 20 years theoretical modeling of liquid crystal phases con-

tinued culminating in the dynamical continuum theory of non-chiral smectic C introduced by Leslie, Stewart and Nakagawa [22] in 1991. This theory together with extensions required to model ferroelectric materials forms the backbone around which the bulk of this thesis is based.

1.3 Liquid Crystals

In the work The Physics of Liquid Crystals de Gennes and Prost [23] remark that liquid crystals are phases of matter whose mechanical and symmetry properties lie somewhere between those of liquids and solids. Furthermore they provide a somewhat more specific definition when they state that a liquid crystal is a system "in which a liquid like order exists at least in one direction of space and in which some degree of anisotropy is present".

To push the point further de Gennes and Prost employ notions from condensed matter theory to realise a description of a liquid crystal phase. Condensed matter theory typically employs the notion of three-dimensional lattices on which the centres of gravity of the elements of a crystal (molecules or groups of molecules) are regularly stacked. The centres of gravity of the elements of a liquid are not ordered in this sense.

Furthermore de Gennes and Prost define liquid crystal in the following way. If a primitive pattern or basis is located at point $\mathbf{x}_0$ the probability of finding an equivalent pattern at the point $\mathbf{x} = \mathbf{x}_0 + n_1\mathbf{a}_1 + n_2\mathbf{a}_2 + n_3\mathbf{a}_3$ (n_i = integer and $i \in 1, 2, 3$) and basis vectors a_i stays finite when $|\mathbf{x} - \mathbf{x}_0| \to \infty$. In otherwords

$$\lim_{|\mathbf{x}-\mathbf{x}_0|\to\infty} \langle \rho(\mathbf{x})\rho(\mathbf{x}') \rangle = F(\mathbf{x} - \mathbf{x}'), \tag{1.1}$$

where $\langle \rho(\mathbf{x})\rho(\mathbf{x}') \rangle$ is the density-density correlation function and $F(\mathbf{x} - \mathbf{x}')$ is a periodic function of basis vectors $\mathbf{a_i}$ and $\rho(\mathbf{x})$ and $\rho(\mathbf{x}')$ are the particle densities at $\mathbf{x}$ and $\mathbf{x}'$ respectively.

Isotropic liquids are defined using density-density correlation functions in a similar way. If one can find a molecule or group of molecules at some point $\mathbf{x}_0$ there is no way to express the probability of finding a similar one at a point $\mathbf{x}$ far from $\mathbf{x}_0$, except through the average particle density $\bar{\rho}$. We may express this in the following way

$$\lim_{|\mathbf{x}-\mathbf{x}_0|\to\infty} \langle \rho(\mathbf{x})\rho(\mathbf{x}')\rangle \simeq \bar{\rho}^2, \tag{1.2}$$

So, we have from de Gennes and Prost a definition of a liquid crystal (also known as a *mesomorphic phase*) and two contrasting definitions of crystals and liquids. They follow this by observing that the density-density correlation function does not depend solely on the modulus $|\mathbf{x}-\mathbf{x}'|$, but also on the orientation of $\mathbf{x}-\mathbf{x}'$ with respect to macroscopically defined axes and this encapsulates the notion that liquid crystals possess some degree of anisotropy. These remarks allow de Gennes and Prost to make the case for mesophases being obtained in two different ways.

Firstly, a mesophase may be obtained by imposing no positional order, or imposing positional order in one or two rather than three dimensions leading to the following conclusions.

- The first case represents a liquid but if the correlation function is anisotropic it is not an isotropic liquid it is a *nematic*.

- The second case describes one-dimensional order in three-dimensions. Here the system is viewed as a set of two-dimensional liquid layers stacked one on top of the other with well defined spacing giving us a mesophase known as *smectic*.

- The third case corresponds to two-dimensionally ordered systems in three dimensions. They may be described as a two-dimensional array of tubes and are called *hexatic smectic phases*.

The second way of obtaining a mesophase involves introducing degrees of freedom that are distinct from the localisation of the centres of gravity.

Nematic, smectic and columnar mesophases are in fact the only known forms of liquid crystal. The type of liquid crystal that may be observed depends on the structure of the of the constituent molecules. Nematics and smectics are often constructed from elongated objects while some nematics and most columnar phases are often made up of disk-like molecules.

To generate a liquid crystal we must use anisotropic objects which are elongated or disk-like. There are a number of ways in which such liquid crystals may be constructed. The first is to use small elongated organic molecules such as *p*-azoxyanisole (PAA) which has a rigid rod length of ~ 20 Å and a width of ~ 5 Å. Another example is *N*-(*p*-methoxybenzylidene)-*p*-butylaniline (MBBA). Both PAA and MBBA are *nematogens* meaning that they give rise to the nematic type of mesophase. However PAA is a nematic state only at high temperatures between 116° C and 135° C at atmospheric pressure whereas MBBA is nematic from $\sim 20°$ C to 47° C but is chemically unstable. The simplest way to induce phase transitions in these types of materials (MBBA, PAA, cholesterol etc.) is to vary the temperature. For this reason these nematogens are commonly called *thermotropic*.

Small discoid organic molecules may also be employed, the simplest examples of which are materials composed of hexasubstituted phenylesters, which can give rise to columnar phases and thermotropic disk-like nematogens.

Another way of generating liquid crystals is to use long helical rods. For instance synthetic polypeptides in a suitable solvent have a rod-like structure with rod lengths of the order of 300 Å and widths of 20 Å. In concentrated solutions these systems give rise to mesophases. Similar phases are found with deoxyribonucleic acids (DNA) and certain viruses for example the tobacco mosaic virus

(TMV) with length 3000 Å and width $\sim$ 200 Å. Mesophases such as these are often called *lyotropic* because the mesophase manifests itself in response to a change in concentration of a solvent [4].

Rigid polymers in a suitable solvent can give rise to mesophases because they behave as rigid rods. These materials offer a greater degree of flexibility in terms of the type of mesogenic groups that can be synthesised. Typically the two main classes are of interest are main-chain polymers and side-group polymers. In both cases thermotropic mesomorphism is obtained, the resulting phases are stable and exhibit large mesomorphic ranges [23].

Associated structures represent another mechanism by which liquid crystal mesophases may be generated. Examples of these structures may be found in soap and water systems. Here we have what is known as an aliphatic anion $CH_3 - (CH_2)_{n-2} - CO_2^-$ (with n in the range $12 - 20$) plus a positive ion (Na^+, K^+, NH_4^+ or others). The polar head of the acid (the $-CO_2^-$ group) tends to be in close contact with water molecules while the apolar aliphatic chain avoids water. These two opposite requirements define an amphiphile. A single molecule in solution cannot satisfy both, but a cluster of molecules can. Other examples of amphiphilic chains organised in similar geometries are *block copolymers* [23]. Building blocks such as these may give rise to nematic, smectic and columnar phases and so are much more flexible than the simpler molecular structures discussed earlier. Amphiphilic compounds may be either lyotropic or thermotropic.

Our principal interest throughout this thesis is the smectic C^* mesophase. We shall discuss it in more detail later in this chapter but first we stop to survey some of the other mesophases discussed here starting with the nematic phase.

1.4 Nematic liquid crystal

Our description of the nematic phase is based on that given by Stewart in [4, p.3-4]. The word nematic comes from the Greek word $\nu\eta\mu\alpha$ meaning thread. In the nematic mesophase the long axis of the constituent molecules tend to align parallel to each other along some common preferred direction. The diagram presented in Figure 1.1 shows a basic representation of the molecular ordering expected in a nematic mesophase with molecules represented by elongated rods. The preferred direction along which the director is defined is commonly known as the *anisotropic axis*. There is no long range correlation between the centres of mass of the molecules. They can translate freely whilst being aligned on average parallel to one another. Rotational symmetry about the anisotropic axis means that the nematic phase is generally uniaxial. The axis of uniaxial symmetry is non-polar. The unit vector **n**, known as the *director*, describes the local direction

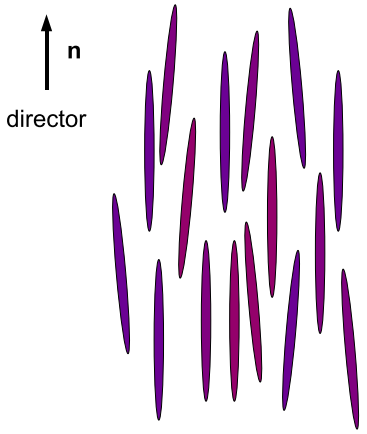

Figure 1.1: A basic representation of a nematogen mesophase. The molecules in this case represented by coloured rods have no overall positional order but they do possess orientational order. The average molecular orientation which we denote with a vector **n** called the *director* points in a direction parallel to the average orientation of the long axes of the molecules.

of the average molecular alignment of the liquid crystal. The notion of a director

is ubiquitous in liquid crystal continuum theory and occurs in all areas of study in nematics, smectics and columnar mesophase research. Since nematogens are non-polar the quantities $\mathbf{n}$ and $-\mathbf{n}$ are indistinguishable.

We note here that the first nematic liquid crystal phase was PAA discussed earlier. The material PAA was first synthesised by the chemists Gattermann and Ritschke [24] which they reported in 1890. It is important in the field of liquid crystals for another reason, it was the first liquid crystal not based on a naturally occurring substance. The first room temperature liquid crystal was MBBA synthesised by Kelker and Scheurle [25].

1.5 Smectic liquid crystals

From the Greek word $\sigma\mu\eta\gamma\mu\alpha$ meaning soap comes the word smectic. Smectic liquid crystals possess mechanical properties akin to those of soaps and occur in many substances. As we discussed earlier, smectics are layered structures. A smectic substance posses the general characteristic of positional order of the centres of mass of its constituent molecules. On average these molecular centres of mass arrange in layers with the projection of the centres of mass onto the smectic layers showing isotropic orientation as discussed in Dierking [26, p.9].

Characteristically, smectic mesophases being possessed of more structural order than nematics generally occur at lower temperatures than nematic mesophases. We shall give some basic qualitative information about smectic A, C and C* phases in the sections below. Further information regarding other smectic phases may be found in de Gennes and Prost [23] and Sackmann [27] provides a historical perspective on some of the key developments in the understanding of smectics.

1.6 Smectic A liquid crystals

When a smectic A phase occurs the molecules arrange in layers and the director **n** is on average aligned perpendicular to the layers and is parallel to the layer normal as shown in Figure 1.2. In thermotropic liquid crystals the smectic layer

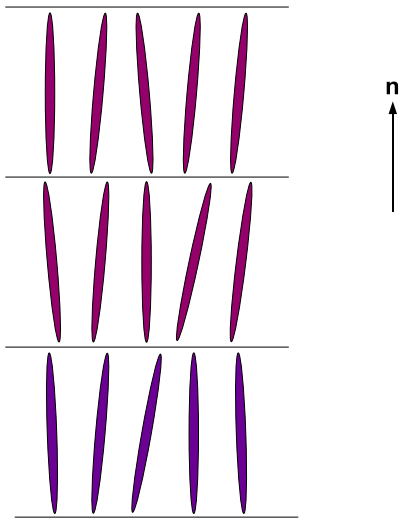

Figure 1.2: Basic schematic of the planar layer structure of a smectic A liquid crystalline material. The molecules indicated by coloured rods have an average local alignment indicated by the director **n**. The straight horizontal lines indicate the smectic planes.

thickness may be anything from the length of the molecules in extent up to twice their length so of the order $20 \sim 80$ Å. In lamella phases the interlayer separation may be several thousand angstrom (see Section 1.3). Once again the director **n** represents the average molecular orientation of the molecules and satisfies the symmetry condition that **n** and $-\mathbf{n}$ are physically indistinguishable. A full dynamic theory for smectic A liquid crystals recently became available due to Stewart [28].

1.7 Smectic C liquid crystals

Smectic C liquid crystals occur at generally lower temperatures than smectic A or nematic phases. The planar layer structure of the smectic C phase is shown in Figure 1.3. Typical of such phases is the presence of a temperature dependent *cone angle* denoted by θ. The cone angle represents the angle the director makes with the smectic layer normal here denoted by **a**. As the temperature within the smectic C phase increases the cone angle gets smaller until finally at the smectic C-smectic A transition temperature the cone angle vanishes as we enter the smectic A phase. Once again the director **n** indicates the average molecular

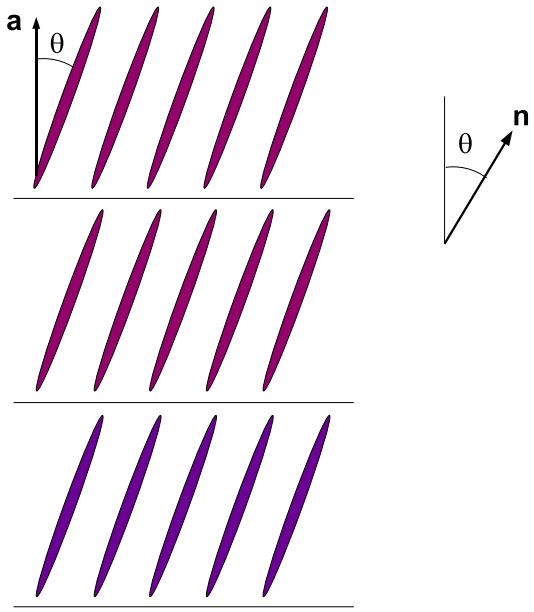

Figure 1.3: Basic schematic of the planar layer structure of a smectic C liquid crystalline material. The molecules indicated by coloured rods have an average local alignment indicated by the director **n**. The straight horizontal lines indicate the smectic planes. A layer normal **a** is oriented perpendicular to the smectic planes. The material possess a characteristic *cone angle* θ which is temperature dependent.

alignment and **n** and $-\mathbf{n}$ are once again indistinguishable. Smectic C liquid crystal are non-chiral in nature and in the absence of external influences the director is uniformly aligned.

It is common to model the director $\mathbf{n}$ in smectic C liquid crystals by considering two other unit vectors $\mathbf{a}$ which represents the normal to the smectic planes and $\mathbf{c}$ which represents the projection of the unit vector $\mathbf{n}$ onto the smectic planes. Then we have

$$\mathbf{n} = \mathbf{a}\cos\theta + \mathbf{c}\sin\theta. \tag{1.3}$$

It proves convenient when we go on to discuss smectic C* liquid crystals to introduce a unit vector $\mathbf{b}$ which is define as

$$\mathbf{b} = \mathbf{a} \times \mathbf{c}. \tag{1.4}$$

Clearly $\mathbf{b}$ is perpendicular to both $\mathbf{a}$ and $\mathbf{c}$ and in smectic C* lies in the direction of the spontaneous polarisation.

1.8 Smectic C* liquid crystals

Smectic C* liquid crystals were first discovered in 1975 by Meyer, Liébert, Strzelecki and Keller [29] who used symmetry arguments to conclude that chiral tilted smectic phases posses a spontaneous polarisation [26]. When the spontaneous polarisation can be reoriented between two stable states by application of an electric field we call the resulting arrangement *ferroelectric*. In fact this ferroelectric property lies behind the Surface Stabilized Ferroelectric Liquid Crystal (SSFLC) device which we shall discuss briefly later in this section.

In the bulk smectic C* phase, in a field free state, the spontaneous polarisation is supressed due to the presence of a helical superstructure. In this case the chiral smectic C phase is better refered to as *helielectric* [26]. The field free helical superstructure of the chiral smectic C* phase is illustrated in Figure 1.4.

These chiral smectic C materials have a planar layer structure much like their smectic C counterparts along with a characteristic temperature dependent cone angle θ. However unlike smectic C, smectic C* materials possess a chiral property

where the director **n** rotates about a twist axis oriented in the direction of the normal to the smectic planes. The figure shows the director rotating about the

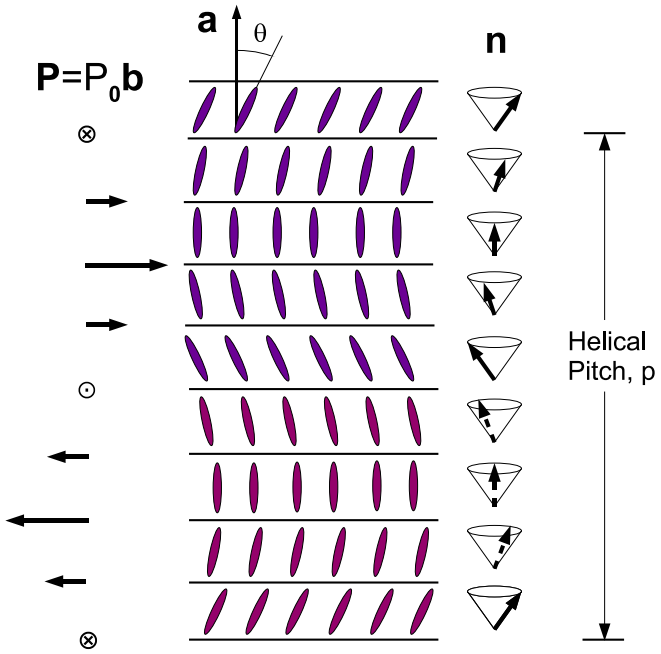

Figure 1.4: The helical superstructure of the chiral bulk smectic C* phase. The helicity of the liquid crystal manifests itself as we follow the planar layer normal **a**. The distance p represents the pitch of the material. Over a distance p the director **n** rotates around the smectic cone and undergoes one complete rotation of 2π radians. By assuming a liquid depth $d \ll p$ we can suppress the chirality of the material sufficiently for it to play no significant role in the systems we shall be investigating. The spontaneous polarisation **P** is positive in this instance, the polarisation vector rotates in a clockwise sense as we move parallel to the layer normal **a**.

smectic cone as we travel along the twist axis in the direction of the layer normal **a**. Smectic C* liquid crystals have what is known as a spontaneous polarisation which is a property of the material and is commonly denoted by the vector **P** where the polarisation may be expressed as either $\mathbf{P} = P_0\mathbf{b}$ or $\mathbf{P} = -P_0\mathbf{b}$ with $P_0 = |\mathbf{P}|$ depending on whether the spontaneous polarisation **P** is positive or negative respectively, for details we refer the reader to [4, p.307] and [23, 30].

The director in a ferroelectric exhibits a helical structure with a characteristic pitch length p as shown in the figure. A typical pitch length might be of the order of $1 \sim 10$ μm and might contain 10^3 smectic layers.

In the figure the director rotates in a clockwise sense. The symbol $\otimes$ indicates that the polarisation is directed into the page whilst the symbol $\odot$ indicates that the polarisation is directed out of the page. In the figure the polarisation is assumed to be positive. The sense of the helix is right handed but as Lagerwall [30] points out there is currently no known correspondence between the sense of $\mathbf{P}$ and the sense of the helix.

Typical values for the magnitude of the polarisation P_0 are of the order of $10 \sim 10^3$ μC m^{-2}. In fact some smectic C* materials are known to exhibit polarisation strengths of 2200 μC m^{-2} [30]. Worth noting is the fact that when an electric field is applied across a sample of smectic C* liquid crystal the polarisation $\mathbf{P}$ has a preference to align itself parallel to, and in the same direction as, the applied electric field.

Throughout this work we shall be exploring various aspects of chiral smectic C* materials. Probably the most important application is in the field of fast switching devices first proposed by Clark and Lagerwall in 1980 [5]. They consider a thin sample of bookshelf aligned smectic C* confined between two subtstrates separated by a gap smaller than the pitch of the helical superstructure in the bulk. The effect of this is to suppresses the helical structure of the material. Then with the application of appropriate boundary conditions at the substrate surfaces, the molecules in the bulk may be switched by exploiting the linear coupling of the polarisation with a d.c. electric field. If we force the director to lie in two stable positions on the surfaces of the substrates, with the polarisation vector pointing down into the bulk of the sample at the upper substrate surface, whilst at the lower substrate the polarisation points up

into the bulk [26], the resultant device may be switched in a bistable fashion by applying a suitable controlling voltage. This in effect is the SSFLC device mentioned above. SSFLC devices have the potential to switch very much faster than standard devices based on nematic technology [23, p.401].

However, before SSFLC devices see widespread use a number of technical challenges need to be overcome. In particular the switching processes involved in these devices is complicated. Physical phenomena such as *pumping* where a sample of bookshelf aligned ferroelectric material is placed between two glass plates and a field reversal takes place results in mechanical vibrations of the top plate. This has been recently investigated again by Stewart in [31].

Not all theoretical studies in the field of ferroelectrics are aimed at the development of fast devices. Among the more exotic applications of ferroelectrics is the work by Das and Schwarz [32] where they consider a smectic C* model in electrical solitary wave propagation along a biomolecular structure such as the cell membrane of a nerve axon.

Our focus will be on smectic C* liquid crystals in this thesis. We begin by exploring the connection between smectic C and smectic C* liquid crystals with a brief study of elastic energies in smectic C mesophases after we review some important material regarding the treatment of electric and magnetic fields which follows below.

1.9 Electric fields and electric energy

If we apply an electric field $\mathbf{E}$ across a sample of liquid crystal, a dipole moment per unit volume is induced. We call this dipole moment the polarisation and we denote it by $\mathbf{P_i}$. We note that the induced polarisation $\mathbf{P_i}$ is not the same as the spontaneous polarisation $\mathbf{P}$ we encounter in ferroelectric materials.

Anisotropy generally forces the electric field $\mathbf{E}$ and the induced polarisation

$\mathbf{P_i}$ to lie in different directions. We relate $\mathbf{P_i}$ to $\mathbf{E}$ via the electric susceptibility tensor $\boldsymbol{\chi}_e$ via the equation

$$\mathbf{P_i} = \epsilon_0 \boldsymbol{\chi}_e \mathbf{E}, \;\; \boldsymbol{\chi}_e = \begin{bmatrix} \chi_{e_\perp} & 0 & 0 \\ 0 & \chi_{e_\perp} & 0 \\ 0 & 0 & \chi_{e_\parallel} \end{bmatrix}. \tag{1.5}$$

Here ϵ_0 is the permittivity of free space. Note that $\chi_{e_\perp}$ and $\chi_{e_\parallel}$ denote the electric susceptibilities parallel and perpendicular to the director respectively. The electric displacement $\mathbf{D}$ induced by $\mathbf{E}$ and $\mathbf{P_i}$ is defined in SI units by

$$\mathbf{D} = \epsilon_0 \mathbf{E} + \mathbf{P_i}, \tag{1.6}$$

and so by considering equation (1.5)

$$\mathbf{D} = \epsilon_0 \boldsymbol{\epsilon} \mathbf{E}, \;\; \boldsymbol{\epsilon} = \mathbf{I} + \boldsymbol{\chi}_e, \tag{1.7}$$

where $\mathbf{I}$ is the identity tensor and $\boldsymbol{\epsilon}$ is called the dielectric tensor which we may write as

$$\boldsymbol{\epsilon} = \begin{bmatrix} \epsilon_\perp & 0 & 0 \\ 0 & \epsilon_\perp & 0 \\ 0 & 0 & \epsilon_\parallel \end{bmatrix}, \;\; \epsilon_\parallel = 1 + \chi_{e_\parallel}, \;\; \epsilon_\perp = 1 + \chi_{e_\perp}. \tag{1.8}$$

The coefficients $\epsilon_\parallel$ and $\epsilon_\perp$ denote the (relative) dielectric permittivities also called dielectric constants of the liquid crystal when the field and director are parallel and perpendicular respectively.

For a director $\mathbf{n}$ we have that in general the electric displacement is given by

$$\mathbf{D} = \epsilon_0 \epsilon_\perp \mathbf{E} + \epsilon_0 \epsilon_a (\mathbf{n} \cdot \mathbf{E}) \mathbf{n}, \tag{1.9}$$

where $\epsilon_a = \epsilon_\parallel - \epsilon_\perp$. We call ϵ_a the dielectric anisotropy of the liquid crystal. Note that the dielectric constants $\epsilon_\parallel$ and $\epsilon_\perp$ and ϵ_a are *unitless* since they are measured relative to ϵ_0. Note also that $\epsilon_a = \chi_{e_\parallel} - \chi_{e_\perp}$ sometimes written as $\Delta\chi_e$. Values of ϵ_a can be negative or positive depending on the type of liquid crystal under investigation.

Throughout this thesis we only consider models where the electric field is uniform and d.c. in nature. However it must be noted that in the presence of an a.c. field the dielectric anisotropy has a frequency dependence and this must be taken into account when considering, for example, the electro-optic performance of devices with a smectic C* component [33].

We note that when $\epsilon_a > 0$ the director is attracted to be parallel to the field and when $\epsilon_a < 0$ its preferred orientation is perpendicular to the field.

The total electric energy w_{elec} arising when a fixed voltage is maintained and applied on external conductors (see de Gennes and Prost [23, p.134]) is given by the expression

$$w_{elec} = -\int_{\mathbf{0}}^{\mathbf{E}} \mathbf{D} \cdot d\mathbf{E}, \tag{1.10}$$

and hence we find that

$$w_{elec} = -\frac{1}{2}\mathbf{D} \cdot \mathbf{E} = -\frac{1}{2}\epsilon_0\epsilon_\perp E^2 - \frac{1}{2}\epsilon_0\epsilon_a(\mathbf{n} \cdot \mathbf{E})^2, \tag{1.11}$$

where $E = |\mathbf{E}|$. The term $-\frac{1}{2}\epsilon_0\epsilon_\perp E^2$ is independent of the orientation of $\mathbf{n}$ and is therefore usually omitted. When $\epsilon_a > 0$ the last term in the above electric energy is minimised when $\mathbf{n}$ and $\mathbf{E}$ are parallel. For $\epsilon_a < 0$ the energy is minimized when $\mathbf{n}$ is perpendicular to $\mathbf{E}$. The most commonly adopted form of the electrical energy is therefore

$$w_{elec} = -\frac{1}{2}\epsilon_0\epsilon_a(\mathbf{n} \cdot \mathbf{E})^2. \tag{1.12}$$

1.10 Magnetic fields and magnetic energy

In this section we follow the discussion in [4]. When a magnetic field $\mathbf{H}$ is applied across a liquid crystal sample a magnetisation $\mathbf{M}$ is induced in the liquid crystal due to weak dipole moments imposed upon the molecular alignment by the magnetic field. We know that the magnetisation induced by $\mathbf{H}$ satisfies

$$\mathbf{M} = \chi_{m_\parallel}\mathbf{H}, \text{ if } \mathbf{H} \text{ is parallel to } \mathbf{n},$$

$$\mathbf{M} \;=\; \chi_{m_\perp}\mathbf{H}, \;\; \text{if } \mathbf{H} \text{ is perpendicular to } \mathbf{n},$$

where the coefficients $\chi_{m_\parallel}$ and $\chi_{m_\perp}$ denote the diamagnetic (negative) susceptibilities when the field and the director are parallel and perpendicular respectively.

Relative to the orientation of the director $\mathbf{n}$ we can write from simple geometric considerations $\mathbf{H} = \mathbf{H}_\parallel + \mathbf{H}_\perp$ with

$$\begin{aligned} \mathbf{H}_\parallel &= (\mathbf{n}.\mathbf{H})\mathbf{n}, \\ \mathbf{H}_\perp &= \mathbf{H} - \mathbf{H}_\parallel = \mathbf{H} - (\mathbf{n}\cdot\mathbf{H})\mathbf{n}. \end{aligned}$$

Assuming a linear dependence on the field and taking into account the invariance with respect to the sign of $\mathbf{n}$, when $\mathbf{H}$ makes an arbitrary angle with $\mathbf{n}$ the magnetisation defined by $\mathbf{M} = \chi_{m_\perp}\mathbf{H}_\perp + \chi_{m_\parallel}\mathbf{H}_\parallel$ becomes

$$\mathbf{M} = \chi_{m_\perp}\mathbf{H} + (\chi_{m_\parallel} - \chi_{m_\perp})(\mathbf{n}\cdot\mathbf{H})\mathbf{n}. \tag{1.13}$$

This is the generally accepted form for the magnetisation and discussions regarding it may be found in Ericksen [34].

Just as the electric displacement $\mathbf{D}$ is used in the construction of the electric energy density, the magnetic induction plays a similar part in the construction of the magnetic energy density, which in SI units is given by

$$\mathbf{B} = \mu_0(\mathbf{H} + \mathbf{M}), \tag{1.14}$$

where $\mu_0 = 4\pi \times 10^{-7}$ Hm^{-1} is the permeability of free space. Inserting the magnetisation into (1.14) means that we may write

$$\mathbf{B} = \mu_0\mu_\perp\mathbf{H} + \mu_0\Delta\chi(\mathbf{n}\cdot\mathbf{H})\mathbf{n}, \tag{1.15}$$

where

$$\mu_\perp = 1 + \chi_{m_\perp},\; \mu_\parallel = 1 + \chi_{m_\parallel},\; \Delta\chi = \mu_\parallel - \mu_\perp = \chi_{m_\parallel} - \chi_{m_\perp}. \tag{1.16}$$

We call the *unitless* quantity $\Delta\chi = \mu_{\parallel} - \mu_{\perp} = \chi_{m_{\parallel}} - \chi_{m_{\perp}}$ the *magnetic anisotropy*.

As with the electric field case, when $\Delta\chi > 0$ the director prefers to be parallel to the magnetic field and when $\Delta\chi < 0$ its preferred orientation lies perpendicular to the field.

In a completely analogous way to that used for obtaining the electric energy density w_{elec} we have that the magnetic energy density w_{mag} is given by

$$w_{mag} = -\int_{\mathbf{0}}^{\mathbf{H}} \mathbf{B} \cdot d\mathbf{H}. \tag{1.17}$$

From this we find that

$$w_{mag} = -\frac{1}{2}\mathbf{B} \cdot \mathbf{H} = -\frac{1}{2}\mu_0\mu_{\perp}H^2 - \frac{1}{2}\mu_0\Delta\chi(\mathbf{n} \cdot \mathbf{H})^2, \tag{1.18}$$

where $H = |\mathbf{H}|$. The contribution $-\frac{1}{2}\mu_0\mu_{\perp}H^2$ is independent of the orientation of $\mathbf{n}$ and $\mathbf{H}$ and is therefore often omitted.

When $\Delta\chi > 0$ the last term in the magnetic energy is minimised when $\mathbf{n}$ and $\mathbf{H}$ are parallel. Similarly, when $\Delta\chi < 0$ the last term is minimised when $\mathbf{n}$ and $\mathbf{H}$ are perpendicular. Typically then the most generally employed form of the magnetic density is

$$w_{mag} = -\frac{1}{2}\mu_0\Delta\chi(\mathbf{n} \cdot \mathbf{H})^2. \tag{1.19}$$

An alternative form of the magnetic energy density appropriate for non-ferromagnetic materials was given by de Jeu [35] and may be derived in terms of the magnetic induction $\mathbf{B}$ and is written as

$$w_{mag} = -\frac{1}{2}\mu_0^{-1}\mu_{\perp}B^2 - \frac{1}{2}\mu_0^{-1}\Delta\chi(\mathbf{n} \cdot \mathbf{B})^2, \tag{1.20}$$

where $B = |\mathbf{B}|$. As before when the term independent of the orientation of the director is neglected we arrive at the expression

$$w_{mag} = -\frac{1}{2}\mu_0^{-1}\Delta\chi(\mathbf{n} \cdot \mathbf{B})^2. \tag{1.21}$$

Once again the results quoted here for w_{mag} are valid provided the magnetic susceptibilities $\chi_{m_\parallel}$ and $\chi_{m_\perp}$ are smaller.

1.11 Energies for Smectic C liquid crystals

We shall follow the treatment given by Stewart [4] as we discuss smectic C and C* energies. We begin by pointing out that the difference in energies between non-chiral and chiral smectic C liquid crystals arises is essentially given by the difference between the associated elastic energies and electric and ferroelecric energies. We shall outline briefly below the energies for smectic C below the constituent energies for smectic C both elastic and electric. In addition we shall introduce extensions which are needed to model fully the ferroelectric smectic C phase.

1.11.1 Smectic C elastic energy

We begin by assuming a free energy density associated with the distortions of the director $\mathbf{n}$. This in turn may be related to distortions of the $\mathbf{a}$ and $\mathbf{c}$ vectors in smectic C. We shall state some results for the energy and give a brief physical interpretation of the elastic terms. We take the energy density to be of the form

$$w = w(\mathbf{a}, \mathbf{c}, \nabla\mathbf{a}, \nabla\mathbf{c}). \tag{1.22}$$

Then the total free energy is given by

$$W = \int_V w(\mathbf{a}, \mathbf{c}, \nabla\mathbf{a}, \nabla\mathbf{c})\, dV, \tag{1.23}$$

where V is the sample volume. We assume that the energy density w is quadratic in the gradients of $\mathbf{a}$ and $\mathbf{c}$. In addition the energy density must be invariant to arbitrary superposed rigid body rotations. Then we require that

$$w(\mathbf{a}, \mathbf{c}, \nabla\mathbf{a}, \nabla\mathbf{c}) = w(Q\mathbf{a}, Q\mathbf{c}, Q\nabla\mathbf{a}Q^T, Q\nabla\mathbf{c}Q^T), \tag{1.24}$$

where Q is any proper orthogonal matrix $\det Q = 1$ and Q^T is its transpose. These requirements must be met by smectic C* materials also. In addition for smectic C the requirement must also hold for any orthogonal matrix Q ($\det Q = \pm 1$) we expect the energy to be invariant to simultaneous changes in sign

$$\mathbf{a} \to -\mathbf{a}, \quad \mathbf{c} \to -\mathbf{c}. \tag{1.25}$$

This invariance arises from a consideration of the symmetry invariance required when

$$\mathbf{n} \to -\mathbf{n}. \tag{1.26}$$

The resulting elastic energy density w for non-chiral smectic C then takes the form stated by Leslie, Stewart, Carlsson and Nakagawa [36]

$$\begin{aligned} w &= \frac{1}{2}K_1(\nabla \cdot \mathbf{a})^2 + \frac{1}{2}K_2(\nabla \cdot \mathbf{c})^2 + \frac{1}{2}K_3(\mathbf{a} \cdot \nabla \times \mathbf{c})^2 \\ &\quad + \frac{1}{2}K_4(\mathbf{c} \cdot \nabla \times \mathbf{c})^2 + \frac{1}{2}K_5(\mathbf{b} \cdot \nabla \times \mathbf{c})^2 \\ &\quad + K_6(\nabla \cdot \mathbf{a})(\mathbf{b} \cdot \nabla \times \mathbf{c}) + K_7(\mathbf{a} \cdot \nabla \times \mathbf{c})(\mathbf{c} \cdot \nabla \times \mathbf{c}) \\ &\quad + K_8(\nabla \cdot \mathbf{c})(\mathbf{b} \cdot \nabla \times \mathbf{c}) + K_9(\nabla \cdot \mathbf{a})(\nabla \cdot \mathbf{c}), \end{aligned} \tag{1.27}$$

where we have omitted surface terms. The K_i, $i = 1, 2, \ldots, 9$ represent elastic constants. Also we recall that $\mathbf{b} = \mathbf{a} \times \mathbf{c}$. In addition we suppose that the elastic energy density is such that

$$w(\mathbf{a}, \mathbf{c}, \nabla\mathbf{a}, \nabla\mathbf{c}) \geq 0. \tag{1.28}$$

We may also write the elastic energy density in the equivalent Cartesian form when surface terms which can be written as a divergence are neglected. This form can be expressed as

$$\begin{aligned} w &= \frac{1}{2}K_1(a_{i,i})^2 + \frac{1}{2}(K_2 - K_4)(c_{i,i})^2 + \frac{1}{2}(K_3 - K_4)c_{i,j}c_jc_{i,k}c_k \\ &\quad + \frac{1}{2}K_4c_{i,j}c_{i,j} + \frac{1}{2}(K_5 - K_3)(c_ia_{i,j}c_j)^2 \\ &\quad + K_6a_{i,i}(c_ja_{j,k}c_k) - K_7c_{i,j}c_jc_{i,k}a_k \\ &\quad + K_9a_{i,i}c_{j,j} + (K_8 - K_7)c_{i,i}(c_ja_{j,k}c_k). \end{aligned} \tag{1.29}$$

We note that the constraint $\nabla \times \mathbf{a} = \mathbf{0}$ is equivalent to the condition $a_{i,j} = a_{j,i}$ in Cartesian component form. Other equivalent forms of the energy in terms of any two of the vectors **a**, **b** and **c** are available in [36] and may be compared to results developed by other workers in particular the Orsay group [37], Rapini [38] and Nakagawa [39].

Notice that three surface terms have been identified for the smectic C phase namely [36]

$$S_1 \equiv \nabla \cdot [\mathbf{c}(\nabla \cdot \mathbf{c}) - (\mathbf{c} \cdot \nabla)\mathbf{c}] = (c_i c_{j,j} - c_j c_{i,j})_{,i} \tag{1.30}$$

$$S_2 \equiv \nabla \cdot [\mathbf{a}(\nabla \cdot \mathbf{c}) - (\mathbf{a} \cdot \nabla)\mathbf{c}] = (a_i c_{j,j} - a_j c_{i,j})_{,i} \tag{1.31}$$

$$\begin{aligned} S_3 &\equiv \nabla \cdot [(\nabla \cdot \mathbf{a})\mathbf{a}] = (a_{i,i})^2 - a_{i,j}a_{i,j} \\ &= -2(\mathbf{b} \cdot \nabla \times \mathbf{c})(\mathbf{c} \cdot \nabla \times \mathbf{b}) - 2[\tfrac{1}{2}(\mathbf{c} \cdot \nabla \times \mathbf{c} - \mathbf{b} \cdot \nabla \times \mathbf{b})]^2. \end{aligned} \tag{1.32}$$

The equality that arises in (1.32) shall be of use when we come to discuss the elastic properties of smectic C* materials. To derive (1.32) requires detailed manipulations of the identities contained in references [40, 36] and we shall not pursue this further here.

Instead we once again follow the discussion given by Stewart [4] regarding the study of small perturbative effects on the smectic C elastic energy. For small perturbations to planar aligned layers of smectic C liquid crystal the nonlinear energy coincides with the approximate energy introduced by the Orsay Group [37]. This treatment allows us to gain a physical insight into the interpretation of the elastic constants. We review these interpretations briefly here.

The Orsay Group consider small deformations to planar aligned smectic layers which initially have the Cartesian z-axis parallel to the layer normal **a** with the c-director parallel to the x-axis. We define the elastic deformations to be

$$\mathbf{a} = \hat{\mathbf{a}} + \boldsymbol{\Omega} \times \hat{\mathbf{a}}, \quad \mathbf{b} = \hat{\mathbf{b}} + \boldsymbol{\Omega} \times \hat{\mathbf{b}}, \quad \mathbf{c} = \hat{\mathbf{c}} + \boldsymbol{\Omega} \times \hat{\mathbf{c}}, \tag{1.33}$$

where

$$\hat{\mathbf{a}} = (0,0,1), \quad \hat{\mathbf{b}} = (0,1,0), \quad \mathbf{c} = (0,0,1) \text{ and } \boldsymbol{\Omega} = (\Omega_x, \Omega_y, \Omega_z), \tag{1.34}$$

with $\boldsymbol{\Omega}$ being an arbitrary small rotation of the smectic layers. Note that

$$\mathbf{a} = (\Omega_y, -\Omega_x, 1), \quad \mathbf{b} = (-\Omega_z, 1, \Omega_x), \quad \mathbf{c} = (1, \Omega_z, -\Omega_y). \tag{1.35}$$

The constraint $\nabla \times \mathbf{a} = \mathbf{0}$ forces the requirements

$$\Omega_{x,z} = \Omega_{y,z} = 0, \quad \Omega_{x,x} + \Omega_{y,y} = 0. \tag{1.36}$$

Inserting (1.35) and (1.36) into the energy given by (1.27) and using the constraints

$$\mathbf{a} \cdot \mathbf{a} = 1, \quad \mathbf{c} \cdot \mathbf{c} = 1, \quad \mathbf{a} \cdot \mathbf{c} = 0, \quad \nabla \cdot \mathbf{a} = \mathbf{0}, \tag{1.37}$$

and ignoring quantities that enter through the surface terms S_1, S_2 and S_3 gives the Orsay version of the energy

$$\begin{aligned} w \;=\; & \frac{1}{2}A_{12}(\Omega_{y,x})^2 + \frac{1}{2}A_{21}(\Omega_{x,y})^2 - A_{11}(\Omega_{x,x})^2 + \frac{1}{2}B_1(\Omega_{z,x})^2 \\ & + \frac{1}{2}B_2(\Omega_{z,y})^2 + \frac{1}{2}B_3(\Omega_{z,z})^2 + B_{13}\Omega_{z,x}\Omega_{z,z} \\ & - C_1\Omega_{x,x}\Omega_{z,x} + C_2\Omega_{x,y}\Omega_{z,y}, \end{aligned} \tag{1.38}$$

provided we set

$$\begin{array}{lll} K_1 = A_{21}, & K_2 = B_2, & K_3 = B_1, \\ K_4 = B_3, & K_5 = 2A_{11} + A_{12} + A_{21} + B_3, & K_6 = -(A_{11} + A_{21} + \frac{1}{2}B_3), \\ K_7 = -B_{13}, & K_8 = C_1 + C_2 - B_{13}, & K_9 = -C_2. \end{array} \tag{1.39}$$

The above elastic constants are those used by the Orsay Group, except that for notational convenience we have set $A_{11} = -\frac{1}{2}A_{11}^{Orsay}$ and $C_1 = -C_1^{Orsay}$. The constants A_{12}, A_{21} and A_{11} are related to bending of the smectic layers. The constants B_1, B_2, B_3 and B_{13} from Saupe [41] are related to the re-orientation of the c-director within or across layers. The constants C_1 and C_2 are related

to various couplings of these deformations. It has been identified by Carlsson, Stewart and Leslie in [42] and Leslie, Stewart, Carlsson and Nakagawa [36] that the smectic C elastic energy expressed in (1.27) may be written in terms of the vectors **b** and **c**, then

$$\begin{aligned} w &= \frac{1}{2}A_{12}(\mathbf{b}\cdot\nabla\times\mathbf{c})^2+\frac{1}{2}A_{21}(\mathbf{c}\cdot\nabla\times\mathbf{b})^2+A_{11}(\mathbf{b}\cdot\nabla\times\mathbf{c})(\mathbf{c}\cdot\nabla\times\mathbf{b}) \\ &\quad +\frac{1}{2}B_1(\nabla\cdot\mathbf{b})^2+\frac{1}{2}B_2(\nabla\cdot\mathbf{c})^2+\frac{1}{2}B_3[\frac{1}{2}(\mathbf{b}\cdot\nabla\times\mathbf{b}+\mathbf{c}\cdot\nabla\times\mathbf{c})]^2 \\ &\quad +B_{13}(\nabla\cdot\mathbf{b})[\frac{1}{2}(\mathbf{b}\cdot\nabla\times\mathbf{b}+\mathbf{c}\cdot\nabla\times\mathbf{c})] \\ &\quad +C_1(\nabla\cdot\mathbf{c})(\mathbf{b}\cdot\nabla\times\mathbf{c})+C_2(\nabla\cdot\mathbf{c})(\mathbf{c}\cdot\nabla\times\mathbf{b}). \end{aligned} \tag{1.40}$$

The elastic energy density given in (1.40) may be related to the energy density given by the Orsay group formulation (1.38). Then using the **b** and **c** formulation it is possible to visualise the basic deformations A_{12}, A_{21}, B_1, B_2 and B_3 and we illustrate these in Figure 1.5. The model we shall be studying in later chapters incorporates only two elastic constants B_2 and B_1 using the Orsay Group notation (K_2 and K_3 respectively using the Leslie, Stewart, Carlsson and Nakagawa formulation). Full details on the physical interpretation of all nine smectic C elastic deformations may be found in [4, 42]. For brevity we highlight only the two most relevant to the current investigation, the B_1 and B_2 distortions, and briefly explain the significance of each.

The physical interpretation of B_1 and B_2 assumes that the smectic layers may remain planar while the c-director undergoes a rotation. Specifically, in Figure 1.5(d) the c-director rotates as we move parallel to the original local alignment of the c-director. This in turn means that the y-component of the c-director must change with respect to x and since $\mathbf{c}=(1,\Omega_z,-\Omega_y)$ we conclude that the Ω_z component of the rotation $\mathbf{\Omega}$ changes with respect to x as the material undergoes this particular type of distortion. In other words this distortion occurs when $\Omega_{z,x}\neq 0$ or comparing the coefficients of (1.40) to those of (1.38)

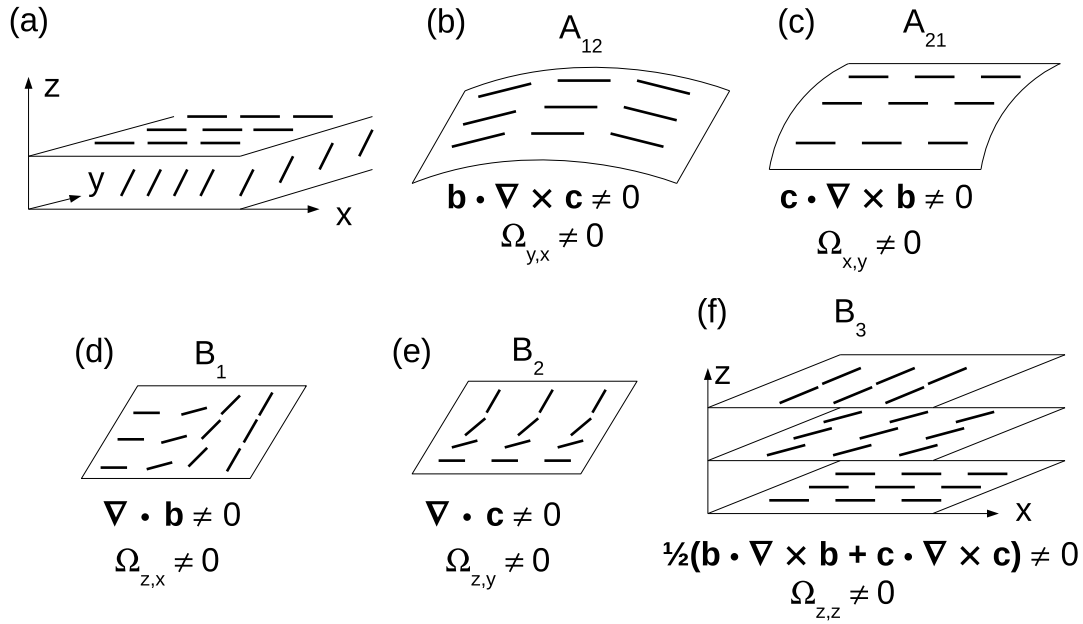

Figure 1.5: The five principal elastic deformations for smectic C liquid crystals reproduced from Stewart [4, p.253]. The bold lines parallel to the smectic planes indicate the c-director. Each one of figures (b)-(e) relates an elastic constant to the $\mathbf{b}$ and $\mathbf{c}$ vector functions and the Orsay deformations. Figure (a) represents the undistorted state. Four coupling terms may be constructed from combinations of these five basic deformations.

this is equivalent to the condition $\nabla \cdot \mathbf{b} \neq 0$.

In Figure 1.5(e) the c-director rotates as we move in a direction perpendicular to the original local alignment of the c-director. Here the y component of the c-director changes with respect to y and since $\mathbf{c} = (1, \Omega_z, -\Omega_y)$ we conclude that the Ω_z component of the rotation $\mathbf{\Omega}$ changes with respect to y as the material undergoes this particular type of distortion. That means that this type of distortion corresponds to $\Omega_{z,y} \neq 0$, and once again comparing coefficients in (1.40) and (1.38) we find that this deformation corresponds to $\nabla \cdot \mathbf{c} \neq 0$.

1.11.2 Smectic C magnetic and electric energy

It is common to assume that the magnetic and electric energy densities for smectic C liquid crystals are generally of the same form as the expressions developed in Sections 1.9 and 1.10. Here the discussion on the influence of electric and

magnetic fields remains valid except that smectic C materials may have different magnitudes of dielectric or magnetic anisotropy.

Recalling from Section 1.10 that the expression for the magnetic energy density is given by $w_{mag} = -\frac{1}{2}\mu_0\Delta\chi(\mathbf{n}\cdot\mathbf{H})^2$, we simply replace the nematic director $\mathbf{n}$ with the equivalent form used in smectic theory namely $\mathbf{n} = \mathbf{a}\cos\theta + \mathbf{c}\sin\theta$. Inserting this into the expression for the magnetic energy we find the expression for the magnetic energy density in SI units is given by

$$w_{mag} = -\frac{1}{2}\mu_0\Delta\chi(\mathbf{a}\cdot\mathbf{H}\cos\theta + \mathbf{c}\cdot\mathbf{H}\sin\theta)^2, \tag{1.41}$$

where $\mathbf{H}$ is the magnetic field μ_0 is the permeability of free space and $\Delta\chi$ once again represents the unitless magnetic anisotropy.

It is also possible to specify a magnetic energy in terms of the magnetic induction where we define w_{mag} as

$$w_{mag} = -\frac{1}{2}\mu_0^{-1}\Delta\chi(\mathbf{a}\cdot\mathbf{B}\cos\theta + \mathbf{c}\cdot\mathbf{B}\sin\theta)^2. \tag{1.42}$$

where $\mathbf{B}$ is the magnetic induction. Generally, throughout this thesis we shall be concerned with the interaction of liquid crystal samples under the influence of electric fields, so the two forms of the magnetic energy density given here are stated purely for reference.

For the smectic C electric energy density, if the contribution independent of the orientation of $\mathbf{a}$ and $\mathbf{c}$ is neglected, then the electric energy density may be constructed using the expression $w_{elec} = -\frac{1}{2}\epsilon_0\epsilon_a(\mathbf{n}\cdot\mathbf{E})^2$ and the smectic C director expression to give

$$w_{elec} = -\frac{1}{2}\epsilon_0\epsilon_a(\mathbf{a}\cdot\mathbf{E}\cos\theta + \mathbf{c}\cdot\mathbf{E}\sin\theta)^2, \tag{1.43}$$

where E is the electric field ϵ_0 the permittivity of free space and ϵ_a is the unitless dielectric anisotropy which may be positive or negative. Generally (1.43) is regarded as a suitable approximation for the electric energy density of the

smectic C phase when its dielectric biaxiality is considered small as discussed by Lagerwall [30, p.212-213].

1.12 Tilt angle dependence of the elastic constants

As the smectic cone angle θ tends toward zero the elastic energy should converge to that for the smectic A phase, given by [23, p.258] as

$$w_{Aelast} = \frac{1}{2}K_1(\nabla \cdot \mathbf{a})^2, \tag{1.44}$$

where $K_1 \geq 0$ is the splay elastic constant from nematic theory. Carlsson *et al* [42] employed the symmetry of the smectic C phase and utilised work conducted by Dahl and Lagerwall [43] in order to construct the tilt angle dependence of the smectic C elastic constants for small θ. Their results showed that

$$\begin{array}{lll} A_{12} = K_1 + \bar{A}_{12}\theta^2, & A_{21} = K_1 + \bar{A}_{21}\theta^2, & A_{11} = -K_1 + \bar{A}_{11}\theta^2, \\ B_1 = \bar{B}_1\theta^2, & B_2 = \bar{B}\theta^2, & B_3 = \bar{B}_3\theta^2, \\ B_{13} = \bar{B}_{13}\theta^3, & C_1 = \bar{C}_1\theta, & C_2 = \bar{C}_2\theta, \end{array} \tag{1.45}$$

where the elastic constants K_1, $\bar{A}_i$, $\bar{B}_i$ and $\bar{C}_i$ are assumed to be only weakly dependent on temperature. We shall make use of the tilt angle dependent form for the elastic constants in later chapters.

1.13 Energies for smectic C* liquid crystals

Smectic C* liquid crystals vary from their non-ferroelectric counterparts primarily in terms of the formulation of the elastic and electric energy density terms. For a full description of the elastic and electric energies for smectic C* materials a number of extra terms must be added to the elastic and electric energy densities of smectic C in order to model smectic C* accurately. We shall see that the new electric energy density for ferroelectrics incorporates a spontaneous polarisation term which we must incorporate in order to adequately reflect the linear

coupling of the field with the polarisation. On the other hand the additional terms required in the elastic energy are less important certainly so far as the models considered in this thesis are concerned. We shall discuss both the elastic and energy contributions in the sections below and we shall give reasons why the elastic ferroelectric terms may be neglected.

1.13.1 Smectic C* elastic energy

Once again following Stewart [4] we shall explore the additional energy contributions required to model ferroelectric materials and consider whether or not to incorporate these additional terms in the models we shall be constructing. In the smectic C* phase we extend the elastic energy density given by any of the energy density expressions (1.40), (1.29) or (1.27) of the smectic C phase with two additional energy terms

$$\begin{aligned} w_1^* &= A_{11}\delta(\mathbf{c}\cdot\nabla\times\mathbf{c}-\mathbf{b}\cdot\nabla\times\mathbf{b}) \\ &= 2A_{11}\delta b_i c_{j,i}a_j \\ &= 2A_{11}\delta\epsilon_{ipk}a_p c_k c_{j,i}a_j, \qquad (1.46) \\ w_2^* &= \frac{1}{2}B_3 q(\mathbf{c}\cdot\nabla\times\mathbf{c}+\mathbf{b}\cdot\nabla\times\mathbf{b}) \\ &= -B_3 q b_i c_{i,j}a_j \\ &= -B_3 q\epsilon_{ipk}a_p c_k c_{i,j}a_j. \qquad (1.47) \end{aligned}$$

Here the wave vector q satisfies

$$q = 2\pi/p, \qquad (1.48)$$

where p represents the helical pitch. In de Gennes and Prost [23, p.110] equivalent energy terms are given as D_2 and $-D_3$ respectively. The authors also discuss additional terms. The first of these $D_1(\mathbf{c}\cdot\nabla\mathbf{c}\cdot\mathbf{b}) = -D_1(\nabla\cdot\mathbf{b})$ (see also Carlsson *et al* [40] and Alexander [44]) is a divergence term which may

be converted to a surface term via the divergence theorem. Since we are only considering the *bulk energy* we may discard this contribution. The next term is $D_4(\mathbf{b}\cdot\nabla\gamma)$, where γ is related to the dilation in the smectic layers. Since we are assuming an incompressible liquid with constant interlayer distance we may discard the D_4 contribution.

As for the two principle energy terms given above the term $-w_2^*$ corresponds to the c-director rotating in a positive sense as an observer moves along the direction of the layer normal $\mathbf{a}$ and is responsible for the helical ordering of the c-director that appears in the smectic C* phase.

The elastic energy we adopt for the ferroelectric phase typically includes contributions from w_1^* and w_2^* and we may choose to use any of the equivalent elastic energy definitions for the smectic C phase given by w which we outlined earlier. Then we may write the smectic C* elastic energy contribution as

$$w_f = w + w_1^* + w_2^*. \tag{1.49}$$

For instance if we choose to ignore surface terms entering via divergence terms we may express the bulk elastic energy w_f in terms of $\mathbf{b}$ and $\mathbf{c}$. Using the expressions (1.32), (1.40), (1.46) and (1.47) we find that the ferroelectric elastic energy w_f may be written [4, 40] as

$$\begin{aligned} w_f \;=\; & \frac{1}{2}A_{12}(\mathbf{b}\cdot\nabla\times\mathbf{c})^2 + \frac{1}{2}A_{21}(\mathbf{c}\cdot\nabla\times\mathbf{b})^2 \\ & - A_{11}\left[\frac{1}{2}(\mathbf{c}\cdot\nabla\times c - \mathbf{b}\cdot\nabla\times\mathbf{b}) - \delta\right]^2 \\ & + \frac{1}{2}B_1(\nabla\cdot\mathbf{b})^2 + \frac{1}{2}B_2(\nabla\cdot\mathbf{c})^2 + \frac{1}{2}B_3\left[\frac{1}{2}(\mathbf{b}\cdot\nabla\times\mathbf{b} + \mathbf{c}\cdot\nabla\times\mathbf{c}) + q\right]^2 \\ & + B_{13}(\nabla\cdot\mathbf{b})\left[\frac{1}{2}(\mathbf{b}\cdot\nabla\times\mathbf{b} + \mathbf{c}\cdot\nabla\times\mathbf{c})\right] \\ & + C_1(\nabla\cdot\mathbf{c})(\mathbf{b}\cdot\nabla\times\mathbf{c}) + C_2(\nabla\cdot\mathbf{c})(\mathbf{c}\cdot\nabla\times\mathbf{b}), \end{aligned} \tag{1.50}$$

In practice throughout the work which follows we shall disregard the helical pitch brought about by considering the term w_2^*. We shall be studying planar samples

of ferroelectric material and specifically studying the hydrodynamic stability of solitonic waves travelling in the plane of the sample. For this reason since the helical structure lies along the normal to the smectic planes along the vector **a** we may suppress this component of the ferroelectric energy by assuming the layer is sufficiently thin that the helicity may be safely ignored.

The term w_1^* models the non-uniformity of the smectic layer normal in space [44, p.28]. Since we assume that the layers maintain a constant layer separation and the fluid is incompressible we may also disregard this term and set $\delta = 0$ to a first approximation. It is worth noting that Gill and Leslie [45] found that the contribution introduced into the simple models of shear flow which they investigated played no significant rôle. Because of these assumptions and omissions we may base the elastic energy of the ferroelectric systems under investigation on the elastic energy density for smectic C materials.

1.13.2 Smectic C* electric energy

The chief difference between the electric energy density found in non-chiral smectic C and chiral smectic C* lies in the addition of an electric energy density term $-\mathbf{P} \cdot \mathbf{E}$ to the dielectric energy density w_{elec} which takes account of the linear interaction of the spontaneous polarisation $\mathbf{P}$ with the electric field $\mathbf{E}$ via

$$w_{pol} = -\mathbf{P} \cdot \mathbf{E}. \tag{1.51}$$

We remark here that the polarisation $\mathbf{P}$ referred to in (1.51) refers to the spontaneous polarisation which is a *persistent* feature of ferroelectrics as opposed to the concept of induced polarisation introduced earlier in this chapter during the discussion on electric fields and denoted by $\mathbf{P_i}$. The energy given here is clearly minimised when $\mathbf{P}$ and $\mathbf{E}$ are co-parallel to each other. In other words this means that $\mathbf{P}$ has a preference to align in the same direction parallel to the electric field. The total electric energy density for smectic C* materials in the

presence of an applied electric field is

$$w_{elec} + w_{pol} = -\frac{1}{2}\epsilon_0\epsilon_a(\mathbf{a}\cdot\mathbf{E}\cos\theta + \mathbf{c}\cdot\mathbf{E}\sin\theta)^2 - \mathbf{P}\cdot\mathbf{E}. \tag{1.52}$$

Typically the unitless dielectric anisotropy ϵ_a is of similar order to that of smectic C materials and may be positive or negative depending on the smectic C* liquid crystal under consideration.

Notice that the dielectric biaxiality $\partial\epsilon$ of liquid crystals is very small, typically of the order of 10^{-3} as noted by Dierking in [26]. Consequently the dielectric biaxiality of the smectic C* liquid crystals studied here may be neglected. In fact throughout this thesis we consider only the uniaxial case. However, in some cases it does play an important and dominant rôle in models of cell switching and examples of these models may be found in Maltese, Piccolo and Ferrara [46] and Brown, Dunn and Jones [47].

1.14 The total energy for smectic C* liquid crystals

The total energy density for the smectic C* liquid crystal phase in the presence of an applied electric field $\mathbf{E}$ is given by

$$w^* = w_f + w_{elec} + w_{pol}, \tag{1.53}$$

where w_f is given by the appropriate elastic energy density for ferroelectrics, for instance the expression given in (1.50) with the electric and polarisation energy densities given by (1.52). Additional energy contributions, for instance a layer compression energy w_{comp}, may be incorporated via the expression

$$w_{comp} = \frac{1}{2}\bar{B}\left(\frac{\partial u}{\partial z}\right)^2, \tag{1.54}$$

an early form of which was proposed by de Gennes 1969 [48] and reported also in de Gennes and Prost [23, p.345-346]. The form given above is reproduced

from Stewart [4], where $u = u(x, y, z)$ is the vertical displacement of the layers relative to their original state and $\bar{B}$ is the associated layer compression constant. However in the models we shall tackle the total energy density for the energy in the bulk in the smectic C* phase shall be represented by

$$w^* = w + w_{elec} + w_{pol}, \tag{1.55}$$

where w may be any one of the smectic C elastic energy representations given previously at (1.40), (1.27), (1.29) or indeed any other suitable representation. The energy expression (1.55) is of the form we shall employ throughout the chapters which follow.

1.15 The dynamic equations for smectic C

We defer a full discussion on the dynamic equations for smectic C until Chapter 2 when we summarise the dynamic equations required including a description of the viscous stress tensor and it components, the balance of linear momentum equations and the balance of angular momentum equations. We make note for reference that the dynamic theory for incompressible smectic C liquid crystals was introduced by Leslie, Stewart and Nakagawa [22]. Instead at this point we take a brief detour to investigate the smectic viscosity coefficients which appear in smectic C theory. We note here that the smectic C* viscosities are *identical* to those present in smectic C theory.

1.16 The Smectic C viscosities

We present here some detail on smectic viscosities. A fuller exposition is given in Stewart [4]. Here we focus on listing and characterising the viscosities and draw attention to the tilt angle dependence of the viscous coefficients.

In total the dynamic theory of smectic C liquid crystals introduced twenty

viscous coefficients. The viscous coefficients can be classified into one of four groups and we list these here.

isotropic:	μ_0
smectic A-like:	μ_1, μ_2, λ_1, λ_4
nematic-like:	μ_3, μ_4, λ_2, λ_5
ac-coupling:	μ_5, λ_3, λ_6, κ_1, κ_2, κ_3, τ_1, τ_2, τ_3, τ_4, τ_5

The first viscous term μ_0 is associated with a term in the viscous stress which is independent of the vectors **a** and **c** and corresponds to the usual isotropic contribution to the viscous stress.

The second group of viscosity coefficients consists of viscosities which are connected to terms which are independent of the vector **c** and only depend on **a**. These viscous terms include μ_1, μ_2, λ_1 and λ_4. We suppose they should be present in the smectic A phase when $\theta = 0$. We expect the five viscosities μ_0, μ_1, μ_2, λ_1 and λ_4 are therefore anticipated to be connected to the dynamical properties of smectic A liquid crystals.

The group μ_3, μ_4, λ_2 and λ_5 have been designated nematic like and depend only on the vector **c**. The term nematic-like arises as a result of the fact that the contributions to the viscous stress associated with these four viscous coefficients resemble those for nematics. However, the similarity with nematics must be treated with care as noted in [49]. Whereas the viscous stress in nematics is described in terms of **n** the viscous stress in smectic C is described in terms of **c** so a like for like comparison would be inappropriate.

The remaining viscous terms μ_5, λ_3, λ_6, κ_1, κ_2, κ_3, τ_1, τ_2, τ_3, τ_4 and τ_5 are regarded as coupling terms since they depend on **a** and **c** and have no counterpart in nematic theory.

The smectic viscosity tilt angle dependence was investigated by Carlsson *et al* in [49] using ideas introduced by Dahl and Lagerwall [43]. For temperatures close to the smectic A-smectic C phase transition temperature T_{AC} the smectic

tilt angle may be assumed to be relatively small. If the smectic layer normal **a** is unchanged while the changes θ to $-\theta$ and **c** to $-\mathbf{c}$ are carried out simultaneously the smectic C description of the material should remain intact and the viscous stress must be invariant to such changes.

Then terms in the viscous stress tensor which are odd in **c** must have corresponding viscosity coefficients which are odd in θ. Similarly, terms even in **c** must have corresponding coefficients which are even in **c**. In particular the smectic A-like viscosities μ_1, μ_2, λ_1, λ_4 remain in the smectic A phase when $\theta \equiv 0$. We list these viscosities and their tilt angle dependence below

$$\begin{aligned}
&\mu_3 = \bar{\mu}_3\theta^4, \quad \mu_4 = \bar{\mu}_4\theta^2, \quad \mu_5 = \bar{\mu}_5\theta^2, \\
&\lambda_2 = \bar{\lambda}_2\theta^2, \quad \lambda_3 = \bar{\lambda}_3\theta^2, \quad \lambda_5 = \bar{\lambda}_5\theta^2, \quad \lambda_6 = \bar{\lambda}_6\theta^2, \\
&\kappa_1 = \bar{\kappa}_1\theta, \quad \kappa_2 = \bar{\kappa}_2\theta, \quad \kappa_3 = \bar{\kappa}_3\theta^3, \\
&\tau_1 = \bar{\tau}_1\theta, \quad \tau_2 = \bar{\tau}_2\theta, \quad \tau_3 = \bar{\tau}_3\theta, \quad \tau_4 = \bar{\tau}_4\theta^3, \quad \tau_5 = \bar{\tau}_5\theta.
\end{aligned}$$

Note that all of the coefficients $\bar{\mu}_i$, $\bar{\lambda}_i$, $\bar{\kappa}_i$ and $\bar{\tau}_i$ are only weakly temperature dependent. Osipov, Sluckin and Terentjev [50] note that four of the viscous coefficients which appear exclusively in the skew-symmetric contribution of the viscous stress, may be considered as rotational viscosities these being λ_4, λ_5, λ_6 and τ_5. Here λ_4 is related to the rotation of the local smectic layer normal **a**. The most prominent rotational viscosity in smectic C is λ_5, whilst λ_6 and τ_5 are **ac**-coupling viscosities.

This completes the survey of prerequisites regarding smectic C and smectic C* continuum theory. The continuum equations we shall be using will be discussed in full in Chapter 2 when we begin to construct a model we shall use to investigate hydrodynamic flow in ferroelectric smectic C materials.

Chapter 2

Modelling Hydrodynamic Flow in an Infinite Sample of Smectic C*

2.1 Introduction

In this chapter we focus our attention on developing a continuum model which accounts for the effects of hydrodynamic flow within a sample of ferroelectric SmC liquid crystal under the influence of an applied electric field. In particular we focus our attention on a wave front travelling under the influence of an electric field in the ferroelectric material and study the hydrodynamic phenomena that result when the wave front propagates in the ferroelectric. Front propagation is a heavily researched field in ferroelectric liquid crystal theory and numerous authors have published in the area. For instance van Saarloos *et al* [51] investigated front propagation into unstable and metastable states in smectic C* liquid crystals using linear and nonlinear marginal stability analysis. In [52] Maclennan *et al* study wave fronts in infinite samples of liquid crystal of the kind we shall be investigating here but do not study flow effects. Das and Schwarz used models of ferroelectrics which result in dynamic equations giving rise to wave fronts while studying solitons in cell membranes [32]. Experimental work, for instance the work of Stannarius and Langer [53] has investigated front

propagation in freely suspended smectic C* films.

The starting point for our investigation is the work of Stewart and Momoniat [54]. In this paper the orientation $\phi(x,t)$ of the unit orthogonal projection $\mathbf{c}$ of the molecular director $\mathbf{n}$ in an infinite sample of ferroelectric smectic C is modelled in the presence of an inclined electric field $\mathbf{E}$. The electric field $\mathbf{E}$ rests at an angle α with respect to the smectic layers. If $\alpha = 0$, the problem yields an exactly solvable nonlinear partial differential equation, with a soliton like solution. If $\alpha \neq 0$ the resulting differential equation cannot be solved exactly and numerical techniques must be employed. Crucially, throughout the analysis presented in [54] hydrodynamic flow is assumed to be negligible.

Following a brief review of the main points discussed in [54], we shall extended the model to incorporate an infinitesimal flow. By taking advantage of the fact that the original problem may be solved exactly for $\alpha = 0$, we go on to construct a set of dynamical equations which govern the motion of the director, and in addition describe the flow profile. Consequently we find that five coupled nonlinear partial differential equations provide a complete description of the system, accounting for both the director re-orientation and flow.

Once the flow equations have been derived we shall show how the dynamical equation found in [54] may be recovered by setting all of the flow velocities to zero.

2.2 Director re-orientation when flow is negligible

Following [54], imagine a sample of ferroelectric SmC confined by the geometry shown in Figure (2.1(a)). The normal to the smectic planes $\mathbf{a}$ is oriented along the z-axis. The director $\mathbf{n}$ is oriented at an angle θ to the layer normal $\mathbf{a}$. The unit orthogonal projection of the director $\mathbf{n}$ onto the smectic planes is given by

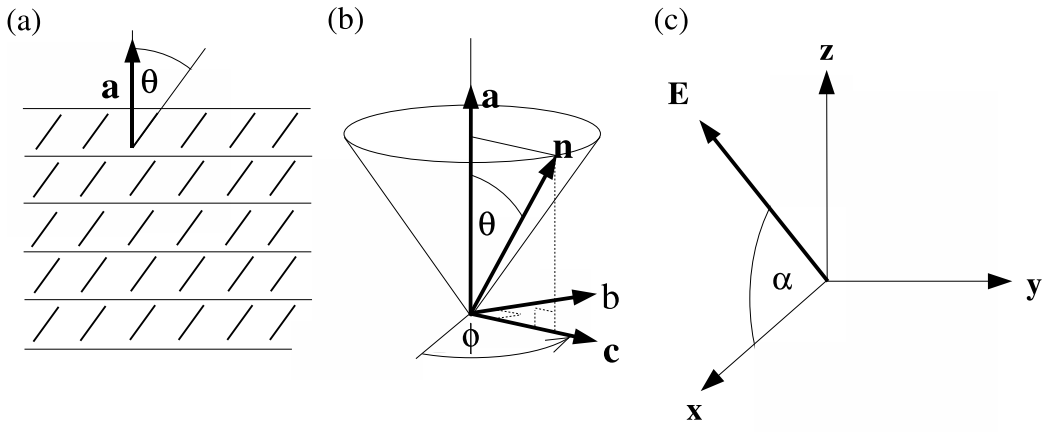

Figure 2.1: (a) The planar layer arrangement of the liquid crystal sample being considered. The molecules are tilted at a fixed angle θ to the layer normal $\mathbf{a}$ which is aligned with the z-axis. (b) The average molecular alignment is denoted by the unit vector $\mathbf{n}$, called the director. The vector $\mathbf{c}$ is the unit orthogonal projection of $\mathbf{n}$ onto the smectic planes. The orientation angle of the c-director is ϕ. Note also that smectic C* has a spontaneous polarisation which lies along the vector $\mathbf{b}$ and is denoted by $\mathbf{P} = P_0\mathbf{b}$ where $\mathbf{b} = \mathbf{a} \times \mathbf{c}$. (c) The electric field $\mathbf{E}$ at an angle of incline $\alpha \geq 0$ with respect to the smectic layers in the xy-plane.

$\mathbf{c}$ so that

$$\mathbf{n} = \mathbf{a}\cos\theta + \mathbf{c}\sin\theta. \tag{2.1}$$

Both $\mathbf{a}$ and $\mathbf{c}$ are mutually perpendicular to the polarisation vector $\mathbf{P} = P_0\mathbf{b}$ where the vector $\mathbf{b}$ is defined by

$$\mathbf{b} = \mathbf{a} \times \mathbf{c}. \tag{2.2}$$

Therefore the polarisation vector $\mathbf{P}$ is constrained always to lie in the same plane as the smectic layers. The model is described vectorially as follows

$$\mathbf{a} = (0, 0, 1), \tag{2.3}$$

$$\mathbf{c} = (\cos(\phi(x,t)), \sin(\phi(x,t)), 0), \tag{2.4}$$

$$\mathbf{b} = (-\sin(\phi(x,t)), \cos(\phi(x,t)), 0), \tag{2.5}$$

$$\mathbf{P} = P_0\mathbf{b}, \tag{2.6}$$

$$\mathbf{E} = E(\cos\alpha, 0, \sin\alpha). \tag{2.7}$$

Solving the continuum equations for the system above yields one dynamical equation for $\phi(x,t)$, which in the special case where $\alpha = 0$ leads to an exactly solvable PDE. The governing dynamical equation from [54] for the system is

$$\begin{aligned} 2\lambda_5 \frac{\partial \phi}{\partial t} &= B\frac{\partial^2 \phi}{\partial x^2} - P_0 E \cos\alpha \cos\phi \\ &\quad -\epsilon_0 \epsilon_a E^2 \left(\tfrac{1}{4}\sin 2\alpha \sin 2\theta \sin\phi + \tfrac{1}{2}\cos^2\alpha \sin^2\theta \sin 2\phi\right). \end{aligned} \tag{2.8}$$

When $\alpha = 0$ (2.8) reduces to

$$2\lambda_5 \frac{\partial \phi}{\partial t} = B\frac{\partial^2 \phi}{\partial x^2} - P_0 E \cos\phi - \epsilon_0 \epsilon_a E^2 \sin^2\theta \sin\phi \cos\phi, \tag{2.9}$$

and noting that $\epsilon_a = -|\epsilon_a|$ when $\epsilon_a < 0$, it may be shown that (2.9) possess the exact solution

$$\phi(x,t) = \frac{\pi}{2} - 2\arctan\left[\exp\left\{\sqrt{\frac{\beta}{B}}\,(x \pm ct)\right\}\right], \tag{2.10}$$

where

$$\beta = \epsilon_0 |\epsilon_a| E^2 \sin^2\theta, \tag{2.11}$$

and the wavespeed c is given by

$$c = \frac{|P_0 E|}{2\lambda_5}\sqrt{\frac{B}{\beta}}. \tag{2.12}$$

The solution (2.10) represents a soliton. We note here that the term $x + ct$ in (2.10) corresponds to $P_0 E > 0$, whilst the term $x - ct$ in (2.10) corresponds to $P_0 E < 0$. Moreover, for $P_0 E > 0$, $\phi \to +\pi/2$ as $t \to -\infty$ and $\phi \to -\pi/2$ as $t \to +\infty$. In other words when $P_0 E > 0$ the favoured state is $-\pi/2$. Conversely, if $P_0 E < 0$ we find that $\phi \to -\pi/2$ as $t \to -\infty$ and $\phi \to +\pi/2$ as $t \to +\infty$. So when $P_0 E < 0$ the favoured state is $+\pi/2$.

If we apply the transformation $\phi(x,t) = \frac{\pi}{2} - u(x,t)$ and substitute this into (2.9) we recover the equation given in [4, p.317]

$$2\lambda_5 \frac{\partial u}{\partial t} = B\frac{\partial^2 u}{\partial x^2} + a\sin u - b\sin u \cos u, \tag{2.13}$$

where

$$a = P_0 E \quad \text{and} \quad b = \epsilon_0 \left|\epsilon_a\right| E^2 \sin^2\theta, \tag{2.14}$$

having the solution

$$u(x,t) = 2\arctan\left[\exp\left\{\sqrt{\frac{b}{B}}\,(x \pm ct)\right\}\right], \tag{2.15}$$

provided

$$\left|\frac{a}{b}\right| < 1. \tag{2.16}$$

2.3 Director re-orientation in the presence of flow

We shall now consider the problem of modelling hydrodynamic flow in a sample of smectic C* liquid crystal. Our aim here is to extend the model described in [54] so as to include flow effects. Retaining the geometry of the original problem, we augment the model by assuming the presence of an infinitesimal flow velocity $\mathbf{v}(x,t)$. Stewart and Momoniat assumed negligible flow resulting in only one dynamical equation, a consequence of considering angular momentum conservation. By introducing flow we encounter four additional equations, one to take account of mass conservation, the remaining three are to take care of the need for the system to conserve linear momentum. We shall show how, when $\mathbf{v} = \mathbf{0}$, we recover the dynamical equation for the non-flow problem. We will describe a model in which we assume that flow occurs in three spatial directions where we regard the components of the velocity u, v and w to be infinitesimally small so that $|u(x,t)| \ll 1$, $|v(x,t)| \ll 1$ and $|w(x,t)| \ll 1$.

We shall appeal to a number of results from [4] as we develop our model. The dynamical equations for smectic C* are identical to the equations for smectic C with w^* replacing w. We summarise the main results below following [4, p.295].

The vectors a and c satisfy the constraints

$$\mathbf{a}\cdot\mathbf{a}=1,\quad \mathbf{c}\cdot\mathbf{c}=1,\quad \mathbf{a}\cdot\mathbf{c}=0,\quad \nabla\times\mathbf{a}=\mathbf{0}, \tag{2.17}$$

whilst the velocity vector must satisfy

$$v_{i,i}=0. \tag{2.18}$$

The expression (2.18) is a consequence of the fact that we choose to model the liquid crystal sample as an incompressible fluid with constant mass density throughout the sample. A compressible hydrodynamic theory for smectic C* is presented in [55, 56]. Conservation of linear momentum results in the following balance equation

$$\rho\dot{v}_i=\rho F_i-\tilde{p}_{,i}+G^a_k a_{k,i}+G^c_k c_{k,i}+\tilde{g}^a_k a_{k,i}+\tilde{g}^c_k c_{k,i}+\tilde{t}_{ij,j}, \tag{2.19}$$

with

$$\tilde{p}=p+w. \tag{2.20}$$

The balance of angular momentum yields two coupled sets of equations

$$\left(\frac{\partial w^*}{\partial a_{i,j}}\right)_{,j}-\frac{\partial w^*}{\partial a_i}+G^a_i+\tilde{g}^a_i+\gamma a_i+\mu c_i+\epsilon_{ijk}\beta_{k,j} = 0, \tag{2.21}$$

$$\left(\frac{\partial w^*}{\partial c_{i,j}}\right)_{,j}-\frac{\partial w^*}{\partial c_i}+G^c_i+\tilde{g}^c_i+\tau c_i+\mu a_i = 0, \tag{2.22}$$

where γ, μ, τ and the vector function $\boldsymbol{\beta}$ are Lagrange multipliers. In equation (2.19) the vector $\mathbf{F}$ represents the external body force per unit mass, whilst $\mathbf{G^a}$ and $\mathbf{G^c}$ are generalised body forces per unit volume related to $\mathbf{a}$ and $\mathbf{c}$, p is the pressure, w^* is the energy density defined by (2.45). Following [4, p.294], the quantities $\tilde{g}^a_i$ and $\tilde{g}^c_i$ are defined by

$$\begin{aligned}\tilde{g}^a_i &= -2(\lambda_1 D^a_i+\lambda_3 c_i c_j D^a_j+\lambda_4 A_i+\lambda_6 c_i c_j A_j\\ &\qquad +\tau_2 D^c_i+\tau_3 c_i a_j D^a_j+\tau_4 c_i c_j D^c_j+\tau_5 C_i),\end{aligned} \tag{2.23}$$

$$\tilde{g}^c_i = -2\left(\lambda_2 D^c_i+\lambda_5 C_i+\tau_1 D^a_i+\tau_5 A_i\right). \tag{2.24}$$

Here the quantities D_i^a and D_i^c are given by the expressions

$$D_i^a = D_{ij}a_j, \tag{2.25}$$

$$D_i^c = D_{ij}c_j. \tag{2.26}$$

The vectors A_i and C_i are defined by

$$A_i = \dot{a}_i - W_{ij}a_j, \tag{2.27}$$

$$C_i = \dot{c}_i - W_{ij}c_j, \tag{2.28}$$

and we note that the superposed dot represents the *material time derivative*, which from [57, p.4] is

$$\frac{D}{Dt} = \frac{\partial}{\partial t} + \mathbf{v}\cdot\nabla. \tag{2.29}$$

For instance, the material time derivative of the vector $\mathbf{c}$ is, in co-ordinate free form

$$\dot{\mathbf{c}} = \left(\frac{\partial}{\partial t} + \mathbf{v}\cdot\nabla\right)\mathbf{c}, \tag{2.30}$$

and here the vector $\mathbf{v}$ represents the flow velocity. We define the rate of strain tensor D_{ij} and the vorticity tensor W_{ij} to be

$$D_{ij} = \tfrac{1}{2}(v_{i,j} + v_{j,i}), \tag{2.31}$$

$$W_{ij} = \tfrac{1}{2}(v_{i,j} - v_{j,i}). \tag{2.32}$$

The vectors $\mathbf{A}$ and $\mathbf{C}$ represent the *co-rotational time fluxes* of the vectors $\mathbf{a}$ and $\mathbf{c}$ respectively. It is worth mentioning at this point that the vectors $\mathbf{A}$ and $\mathbf{C}$ have an analogue in the theory of nematics as described in [4, p.134-5], where the vector $\mathbf{N}$ defined by

$$\mathbf{N} = \boldsymbol{\omega}\times\mathbf{n}, \tag{2.33}$$

measures the rotation of the nematic director $\mathbf{n}$ relative to the surrounding fluid. Here the vector $\boldsymbol{\omega}$ is known as the *relative angular velocity*. It measures

the difference between the *local angular velocity* $\mathbf{w}$ of the nematic director and the *regional angular velocity* $\hat{\mathbf{w}}$ given by

$$\hat{\mathbf{w}} = \tfrac{1}{2}\boldsymbol{\nabla} \times \mathbf{v}, \tag{2.34}$$

where $\mathbf{v}$ is the velocity of the fluid, so that

$$\boldsymbol{\omega} = \mathbf{w} - \hat{\mathbf{w}} = \mathbf{w} - \tfrac{1}{2}\boldsymbol{\nabla} \times \mathbf{v}. \tag{2.35}$$

The $\mathbf{A}$ and $\mathbf{C}$ vectors are defined in an identical manner to the vector $\mathbf{N}$. That is we define $\mathbf{A}$ and $\mathbf{C}$ to be

$$\mathbf{A} = \boldsymbol{\omega} \times \mathbf{a}, \quad \mathbf{C} = \boldsymbol{\omega} \times \mathbf{c}. \tag{2.36}$$

Taking the first of these expressions (the argument is identical for both $\mathbf{A}$ and $\mathbf{C}$), it is straightforward to show that the vector $\mathbf{A}$ in (2.36) is equivalent to (2.27). We have that

$$\begin{aligned} A_i &= \epsilon_{ijk}\omega_j a_k \\ &= \epsilon_{ijk}\left(w_j - \tfrac{1}{2}\epsilon_{jpq}v_{q,p}\right)a_k \\ &= \epsilon_{ijk}w_j a_k - \tfrac{1}{2}\epsilon_{ijk}\epsilon_{jpq}v_{q,p}a_k \\ &= \epsilon_{ijk}w_j a_k + \tfrac{1}{2}\epsilon_{jik}\epsilon_{jpq}v_{q,p}a_k \\ &= \epsilon_{ijk}w_j a_k + \tfrac{1}{2}\left(\delta_{ip}\delta_{kq} - \delta_{iq}\delta_{kp}\right)v_{q,p}a_k \\ &= \epsilon_{ijk}w_j a_k + \tfrac{1}{2}\left(v_{k,i} - v_{i,k}\right)a_k, \end{aligned} \tag{2.37}$$

whereupon relabelling the k's in the second term on the right hand side with j's we have that

$$A_i = \epsilon_{ijk}w_j a_k - \tfrac{1}{2}(v_{i,j} - v_{j,i})a_j, \tag{2.38}$$

and, since $\mathbf{w}$ represents the angular velocity of $\mathbf{a}$, and $\mathbf{a}$ is a unit vector such that

$$\mathbf{a} \cdot \mathbf{a} = 1, \tag{2.39}$$

we may write the *material time derivative* of $\mathbf{a}$ as

$$\dot{\mathbf{a}} = \mathbf{w} \times \mathbf{a}. \tag{2.40}$$

Then we find that

$$\mathbf{A} = \dot{\mathbf{a}} - \mathsf{W}\mathbf{a}, \tag{2.41}$$

where W represents the vorticity tensor, which corresponds to (2.27). As an aside, the justification for (2.40) may be found in Chisolm [58]. The proof is given in (A.1) for convenience.

Finally from equation (2.19) we define the viscous stress $\tilde{t}_{ij}$ to be the sum of the symmetric and skew-symmetric tensors $\tilde{t}^s_{ij}$ and $\tilde{t}^{ss}_{ij}$ thus

$$\tilde{t}_{ij} = \tilde{t}^s_{ij} + \tilde{t}^{ss}_{ij}. \tag{2.42}$$

We define the symmetric part $\tilde{t}^s_{ij}$ to be given by

$$\begin{aligned}
\tilde{t}^s_{ij} \;=\; & \mu_0 D_{ij} + \mu_1 a_p D^a_p a_i a_j + \mu_2 (D^a_i a_j + D^a_j a_i) + \mu_3 c_p D^c_p c_i c_j \\
& + \mu_4 (D^c_i c_j + D^c_j c_i) + \mu_5 c_p D^a_p (a_i c_j + a_j c_i) \\
& + \lambda_1 (A_i a_j + A_j a_i) + \lambda_2 (C_i c_j + C_j c_i) + \lambda_3 c_p A_p (a_i c_j + a_j c_i) \\
& + \kappa_1 (D^a_i c_j + D^a_j c_i + D^c_i a_j + D^c_j a_i) \\
& + \kappa_2 (a_p D^a_p (a_i c_j + a_j c_i) + 2 a_p D^c_p a_i a_j) \\
& + \kappa_3 (c_p D^c_p (a_i c_j + a_j c_i) + 2 a_p D^c_p c_i c_j) \\
& + \tau_1 (C_i a_j + C_j a_i) + \tau_2 (A_i c_j + A_j c_i) \\
& + 2\tau_3 c_p A_p a_i a_j + 2\tau_4 c_p A_p c_i c_j,
\end{aligned} \tag{2.43}$$

whilst the skew-symmetric part $\tilde{t}^{ss}_{ij}$ is given by

$$\begin{aligned}
\tilde{t}^{ss}_{ij} \;=\; & \lambda_1 (D^a_j a_i - D^a_i a_j) + \lambda_2 (D^c_j c_i - D^c_i c_j) + \lambda_3 c_p D^a_p (a_i c_j - a_j c_i) \\
& + \lambda_4 (A_j a_i - A_i a_j) + \lambda_5 (C_j c_i - C_i c_j) + \lambda_6 c_p A_p (a_i c_j - a_j c_i) \\
& + \tau_1 (D^a_j c_i - D^a_i c_j) + \tau_2 (D^c_j a_i - D^c_i a_j) + \tau_3 a_p D^a_p (a_i c_j - a_j c_i) \\
& + \tau_4 c_p D^c_p (a_i c_j - a_j c_i) + \tau_5 (A_j c_i - A_i c_j + C_j a_i - C_i a_j).
\end{aligned} \tag{2.44}$$

2.4 Elastic, electric and polarisation energies

The energy density for a sample of smectic C* liquid crystal under the influence of an electric field $\mathbf{E}$ is from [4, p.311]

$$w^* = w_{elas} + w_{elec} + w_{pol}. \tag{2.45}$$

The elastic energy density w_{elas} described by Leslie, Stewart, Carlsson and Nakagawa [36] is given by the expression

$$\begin{aligned} w_{elas} \;=\; & \tfrac{1}{2}K_1(\nabla\cdot\mathbf{a})^2 + \tfrac{1}{2}K_2(\nabla\cdot\mathbf{c})^2 + \tfrac{1}{2}K_3(\mathbf{a}\cdot\nabla\times\mathbf{c})^2 + \tfrac{1}{2}K_4(\mathbf{c}\cdot\nabla\times\mathbf{c})^2 \\ & + \tfrac{1}{2}K_5(\mathbf{b}\cdot\nabla\times\mathbf{c})^2 + K_6(\nabla\cdot\mathbf{a})(\mathbf{b}\cdot\nabla\times\mathbf{c}) + K_7(\mathbf{a}\cdot\nabla\times\mathbf{c})(\mathbf{c}\cdot\nabla\times\mathbf{c}) \\ & + K_8(\nabla\cdot\mathbf{c})(\mathbf{b}\cdot\nabla\mathbf{c}) + K_9(\nabla\cdot\mathbf{a})(\nabla\cdot\mathbf{c}). \end{aligned} \tag{2.46}$$

The electric energy contribution w_{elec} from [4, p.258] is given by

$$w_{elec} = -\tfrac{1}{2}\epsilon_0\epsilon_a\left(\mathbf{a}\cdot\mathbf{E}\cos\theta + \mathbf{c}\cdot\mathbf{E}\sin\theta\right)^2, \tag{2.47}$$

whilst the polarisation energy from [4, p.310] is given simply by

$$w_{pol} = -\mathbf{P}\cdot\mathbf{E}. \tag{2.48}$$

For convenience we define the following expressions

$$\Pi_i^a = \left(\frac{\partial w^*}{\partial a_{i,j}}\right)_{,j} - \frac{\partial w^*}{\partial a_i}, \tag{2.49}$$

$$\Pi_i^c = \left(\frac{\partial w^*}{\partial c_{i,j}}\right)_{,j} - \frac{\partial w^*}{\partial c_i}, \tag{2.50}$$

The contribution to $\mathbf{\Pi^c}$ and $\mathbf{\Pi^a}$ due to the polarisation term w_{pol} shall be dealt with first. The polarisation vector (2.6) allows us to write

$$w_{pol} = -P_0\mathbf{b}\cdot\mathbf{E} = -P_0\mathbf{E}\cdot(\mathbf{a}\times\mathbf{c}). \tag{2.51}$$

And from this we find that

$$\begin{aligned}\left(\frac{\partial w_{pol}}{\partial c_{i,j}}\right)_{,j} - \frac{\partial w_{pol}}{\partial c_i} &= -\frac{\partial}{\partial c_i}\left(-P_0 E_p \epsilon_{pqr} a_q c_r\right) \\ &= P_0 E_p \epsilon_{pqr} a_q \frac{\partial c_r}{\partial c_i} \\ &= P_0 E_p \epsilon_{pqr} a_q \delta_{ri} \\ &= P_0 E_p \epsilon_{pqi} a_q \\ &= P_0 \epsilon_{ipq} E_p a_q \end{aligned} \tag{2.52}$$

So the contribution from w_{pol} to $\mathbf{\Pi^c}$ which we shall denote by ${\mathbf{\Pi^c}}_{pol}$ is

$${\mathbf{\Pi^c}}_{pol} = P_0 \mathbf{E} \times \mathbf{a}. \tag{2.53}$$

A similar argument yields the contribution from w_{pol} to $\mathbf{\Pi^a}$ and in this case the contribution is

$${\mathbf{\Pi^a}}_{pol} = -P_0 \mathbf{E} \times \mathbf{c}. \tag{2.54}$$

Next, we quote the contributions to $\mathbf{\Pi^a}$ and $\mathbf{\Pi^c}$ resulting from the elastic (2.46) and electric (2.47) energy density expressions. First the contributions made to $\mathbf{\Pi^a}$ and $\mathbf{\Pi^c}$ due to w_{elas}

$$\begin{aligned}{\mathbf{\Pi^a}}_{elas} &= K_1 \nabla(\nabla \cdot \mathbf{a}) - K_3(\mathbf{a} \cdot \nabla \times \mathbf{c})(\nabla \times \mathbf{c}) - K_5(\mathbf{b} \cdot \nabla \times \mathbf{c})(\mathbf{c} \times \nabla \times \mathbf{c}) \\ &\quad + K_6\left\{\nabla(\mathbf{b} \cdot \nabla \times \mathbf{c}) - (\nabla \cdot \mathbf{a})(\mathbf{c} \times \nabla \times \mathbf{c})\right\} \\ &\quad - K_7(\mathbf{c} \cdot \nabla \times \mathbf{c})(\nabla \times \mathbf{c}) - K_8(\nabla \cdot \mathbf{c})(\mathbf{c} \times \nabla \times \mathbf{c}) \\ &\quad + K_9 \nabla(\nabla \cdot \mathbf{c}), \end{aligned} \tag{2.55}$$

$$\begin{aligned}{\mathbf{\Pi^c}}_{elas} &= K_2 \nabla(\nabla \cdot \mathbf{c}) - K_3 \nabla \times \{(\mathbf{a} \cdot \nabla \times \mathbf{c})\mathbf{a}\} \\ &\quad - K_4\{\nabla \times \{(\mathbf{c} \cdot \nabla \times \mathbf{c})\mathbf{c}\} + (\mathbf{c} \cdot \nabla \times \mathbf{c})(\nabla \times \mathbf{c})\} \\ &\quad + K_5\{(\mathbf{b} \cdot \nabla \times \mathbf{c})(\mathbf{a} \times \nabla \times \mathbf{c}) - \nabla \times \{(\mathbf{b} \cdot \nabla \times \mathbf{c})\mathbf{b}\}\} \\ &\quad + K_6\{(\nabla \cdot \mathbf{a})(\mathbf{a} \times \nabla \times \mathbf{c}) - \nabla \times \{(\nabla \cdot \mathbf{a})\mathbf{b}\}\}\end{aligned}$$

$$-K_7\{\nabla\times\{(\mathbf{a}\cdot\nabla\times\mathbf{c})\mathbf{c}+(\mathbf{c}\cdot\nabla\times\mathbf{c})\mathbf{a}\}+(\mathbf{a}\cdot\nabla\times\mathbf{c})(\nabla\times\mathbf{c})\}$$
$$+K_8\{\nabla(\mathbf{b}\cdot\nabla\times\mathbf{c})-\nabla\times\{(\nabla\cdot\mathbf{c})\mathbf{b}\}+(\nabla\cdot\mathbf{c})(\mathbf{a}\times\nabla\times\mathbf{c})\}$$
$$+K_9\nabla(\nabla\cdot\mathbf{a}). \tag{2.56}$$

Next, the contributions made to $\mathbf{\Pi^a}$ and $\mathbf{\Pi^c}$ due to w_{elec}

$$\mathbf{\Pi^a}_{elec}=\epsilon_0\epsilon_a\cos\theta\{(\mathbf{a}\cdot\mathbf{E})\cos\theta+(\mathbf{c}\cdot\mathbf{E})\sin\theta\}\mathbf{E}, \tag{2.57}$$

$$\mathbf{\Pi^c}_{elec}=\epsilon_0\epsilon_a\sin\theta\{(\mathbf{a}\cdot\mathbf{E})\cos\theta+(\mathbf{c}\cdot\mathbf{E})\sin\theta\}\mathbf{E}. \tag{2.58}$$

The contributions made by (2.53),(2.56) and (2.58) to $\mathbf{\Pi^c}$ are then

$$\mathbf{\Pi^c}=\mathbf{\Pi^c}_{elas}+\mathbf{\Pi^c}_{elec}+\mathbf{\Pi^c}_{pol}, \tag{2.59}$$

In a similar fashion we identify the contributions made to the vector $\mathbf{\Pi^a}$ by (2.54), (2.55) and (2.57) as

$$\mathbf{\Pi^a}=\mathbf{\Pi^a}_{elas}+\mathbf{\Pi^a}_{elec}+\mathbf{\Pi^a}_{pol}. \tag{2.60}$$

We show in Appendix B how one of the terms in the vector identities given by (2.49) and (2.50) is derived. All of the equations identified above will be of help as we construct the continuum equations governing the model we described vectorially from (2.3) to (2.7) along with the definitions (2.68) and (2.17). We shall begin our analysis by making clear what it is we aim to achieve. We have the framework for a model which we have outlined above. In the simple no-flow case we can construct a dynamical equation (2.8) which governs the orientation of the projection of the director $\mathbf{n}$ onto the smectic planes. For the special case noted above where the angle of inclination α of the electric field $\mathbf{E}$ is zero, the dynamical equation reduces to (2.9) and yields an exact solution (2.10) which represents a *travelling wave solution* (TWS) of wavefront type [59, p.235]. In other words for (2.9) we may express the solution (2.10) in the form

$$\phi_0(\tau)=\phi(x,t),\ \text{ where }\ \tau=x-ct, \tag{2.61}$$

where c is a positive constant. Next, we imagine perturbing our TWS and we suppose that this perturbation is brought about by the imposition of some infinitesimal flow. We then have the task of showing that the perturbation is *asymptotically stable*. That is, as $t \to \infty$, the perturbation decays to zero and our system returns to it's original state. We analyse this problem in a moving co-ordinate frame using the transformations

$$\bar{\phi}(\tau, t) = \phi(x, t), \quad t = t, \quad \tau = x - ct. \tag{2.62}$$

Then the space and time derivatives of $\phi(x, t)$ after the change of variables in the moving co-ordinate frame are given by

$$\frac{\partial \phi}{\partial x} = \frac{\partial \bar{\phi}}{\partial \tau}, \tag{2.63}$$

$$\frac{\partial^2 \phi}{\partial x^2} = \frac{\partial^2 \bar{\phi}}{\partial \tau^2}, \tag{2.64}$$

$$\frac{\partial \phi}{\partial t} = \frac{\partial \bar{\phi}}{\partial t} - c\frac{\partial \bar{\phi}}{\partial \tau}. \tag{2.65}$$

For convenience, in all further work we shall rename $\bar{\phi} \to \phi$. Using this transformation the projection of the director onto the smectic planes given by $\mathbf{c}$ in (2.4) and the associated vector $\mathbf{b}$ given by (2.5) are now dependent on τ and t so that

$$\mathbf{c} = (\cos(\phi(\tau, t)), \sin(\phi(\tau, t)), 0), \tag{2.66}$$

$$\mathbf{b} = (-\sin(\phi(\tau, t)), \cos(\phi(\tau, t)), 0). \tag{2.67}$$

We shall be considering flow effects in the moving co-ordinate frame. The flow velocity defined in the moving co-ordinate frame is given by

$$\mathbf{v}(\tau, t) = (u(\tau, t), v(\tau, t), w(\tau, t)). \tag{2.68}$$

In addition we regard the components of the flow velocity u, v and w to be infinitesimally small so that $|u(\tau, t)| \ll 1$, $|v(\tau, t)| \ll 1$ and $|w(\tau, t)| \ll 1$. With

the velocity vector defined, we shall set about the task of constructing the continuum equations for our model. We start by using (2.63), (2.64) and (2.56) along with the definitions (2.3), (2.5) and (2.4), all transformed appropriately with (2.62), to construct the vector $\mathbf{\Pi^c}$. We shall comment on $\mathbf{\Pi^a}$ at a later stage. First then the expression for the vector $\mathbf{\Pi^c}$ in component form is

$$\begin{aligned}
\Pi_1^c &= \epsilon_0\epsilon_a \sin\theta E^2(\sin\alpha\cos\alpha\cos\theta + \cos^2\alpha\sin\theta\cos\phi) \\
&\quad - K_2(\phi_{,\tau\tau}\sin\phi + \phi_{,\tau}^2\cos\phi), \qquad (2.69)\\
\Pi_2^c &= K_3(\phi_{,\tau\tau}\cos\phi - \phi_{,\tau}^2\sin\phi) - P_0 E\cos\alpha, \qquad (2.70)\\
\Pi_3^c &= K_8(\phi_{,\tau\tau}\sin\phi\cos\phi + \phi_{,\tau}^2\cos 2\phi) \\
&\quad - K_7(\phi_{,\tau\tau}\sin\phi\cos\phi + \phi_{,\tau}^2(\cos 2\phi + \cos^2\phi)) \\
&\quad + \epsilon_0\epsilon_a \sin\theta E^2(\sin^2\alpha\cos\theta + \sin\alpha\cos\alpha\sin\theta\cos\phi). \qquad (2.71)
\end{aligned}$$

Next, we construct the rate of strain tensor using (2.31) and find that the only non-zero components of D are

$$D_{11} = u_{,\tau}, \;\; D_{12} = D_{21} = \tfrac{1}{2}v_{,\tau}, \;\; D_{13} = D_{31} = \tfrac{1}{2}w_{,\tau}. \qquad (2.72)$$

Similarly, the vorticity tensor W has the following non-zero components

$$W_{12} = -\tfrac{1}{2}v_{,\tau}, \;\; W_{13} = -\tfrac{1}{2}w_{,\tau}, \;\; W_{21} = \tfrac{1}{2}v_{,\tau}, \;\; W_{31} = \tfrac{1}{2}w_{,\tau}. \qquad (2.73)$$

The co-rotational time fluxes $\mathbf{A}$ and $\mathbf{C}$ are given in component form below. We illustrate the derivation of these vectors by considering the calculation of C_1 in detail, the remaining terms are computed in a similar manner. For C_1 then we have that

$$C_1 = \dot{c}_1 - (W_{11}c_1 + W_{12}c_2 + W_{13}c_3). \qquad (2.74)$$

Now

$$\begin{aligned}
\dot{c}_1 &= \left(\frac{\partial}{\partial t} + v_1\frac{\partial}{\partial\tau}\right)\cos\phi, \\
&= -\left(\frac{\partial\phi}{\partial t} - c\frac{\partial\phi}{\partial\tau}\right)\sin\phi - u\frac{\partial\phi}{\partial\tau}\sin\phi, \qquad (2.75)
\end{aligned}$$

where $v_1 = u$ from (2.68) and

$$W_{11}c_1 + W_{12}c_2 + W_{13}c_3 = -\tfrac{1}{2}v_{,\tau}\sin\phi. \tag{2.76}$$

Which means that the C_1 component of the co-rotational time flux $\mathbf{C}$ (along with C_2 and C_3) is given by

$$\begin{aligned} C_1 &= ((c-u)\phi_{,\tau} - \phi_{,t})\sin\phi + \tfrac{1}{2}v_{,\tau}\sin\phi. \\ C_2 &= ((u-c)\phi_{,\tau} + \phi_{,t})\cos\phi - \tfrac{1}{2}v_{,\tau}\cos\phi, \\ C_3 &= -\tfrac{1}{2}w_{,\tau}\cos\phi. \end{aligned} \tag{2.77}$$

The co-rotational time flux $\mathbf{A}$ is found to have only one non-zero component

$$A_1 = \tfrac{1}{2}w_{,\tau}. \tag{2.78}$$

Using (2.72) we have that the vectors $\mathbf{D^a}$ and $\mathbf{D^c}$ are determined by (2.25) and (2.26) respectively. The only non-zero component of $\mathbf{D^a}$ is found to be

$$D_1^a = \tfrac{1}{2}w_{,\tau}, \tag{2.79}$$

whilst the vector $\mathbf{D^c}$ has components given by

$$\begin{aligned} D_1^c &= u_{,\tau}\cos\phi + \tfrac{1}{2}v_{,\tau}\sin\phi, \\ D_2^c &= \tfrac{1}{2}v_{,\tau}\cos\phi, \\ D_3^c &= \tfrac{1}{2}w_{,\tau}\cos\phi. \end{aligned} \tag{2.80}$$

Next we compute the vector $\tilde{\mathbf{g}}^{\mathbf{c}}$ using (2.24) and (2.77), (2.78), (2.79) and (2.80)

$$\begin{aligned} \tilde{g}_1^c &= -2(\lambda_2(u_{,\tau}\cos\phi + \tfrac{1}{2}v_{,\tau}\sin\phi) + \lambda_5[((c-u)\phi_{,\tau} - \phi_{,t})\sin\phi + \tfrac{1}{2}v_{,\tau}\sin\phi] \\ &\quad + \tfrac{1}{2}(\tau_1 + \tau_5)w_{,\tau}), \end{aligned} \tag{2.81}$$

$$\tilde{g}_2^c = -2(\tfrac{1}{2}\lambda_2 v_{,\tau}\cos\phi + \lambda_5[((u-c)\phi_{,\tau} + \phi_{,t})\cos\phi - \tfrac{1}{2}v_{,\tau}\cos\phi]), \tag{2.82}$$

$$\tilde{g}_3^c = -2(\tfrac{1}{2}(\lambda_2 - \lambda_5)w_{,\tau}\cos\phi + \tfrac{1}{2}(\tau_1 + \tau_5)w_{,\tau}). \tag{2.83}$$

Now, returning to the balance of angular momentum and considering (2.22) and the identity (2.50) we may re-write (2.22) as follows

$$\Pi_i^c + G_i^c + \tilde{g}_i^c + \tau c_i + \mu a_i = 0. \tag{2.84}$$

If we consider generalised external body forces to be zero, so that $G_i^c = 0$, we find on taking the scalar product of (2.84) with c_i and a_i respectively we get

$$\begin{aligned} c_i\Pi_i^c + c_i\tilde{g}_i^c + \tau c_i c_i &= 0 \\ a_i\Pi_i^c + a_i\tilde{g}_i^c + \mu a_i a_i &= 0. \end{aligned} \tag{2.85}$$

Consequently the Lagrange multiplier $\mu(\tau, t)$ is found from (2.85) to be

$$\mu(\tau, t) = -\Pi_3^c - \tilde{g}_3^c. \tag{2.86}$$

Whereas for the Lagrange multiplier $\tau(\tau, t)$ we have that

$$\tau(\tau, t) = -\Pi_1^c \cos\phi - \tilde{g}_1^c \cos\phi - \Pi_2^c \sin\phi - \tilde{g}_2^c \sin\phi \tag{2.87}$$

Now, equation (2.84) yields the following expressions

$$\Pi_1^c + \tilde{g}_1^c + \tau\cos\phi = 0, \tag{2.88}$$

$$\Pi_2^c + \tilde{g}_2^c + \tau\sin\phi = 0. \tag{2.89}$$

Multiplying (2.88) by $\sin\phi$ and (2.89) by $\cos\phi$ and subtracting we find that we are left with the following dynamical equation

$$\Pi_1^c \sin\phi - \Pi_2^c \cos\phi + \tilde{g}_1^c \sin\phi - \tilde{g}_2^c \cos\phi = 0, \tag{2.90}$$

which is valid so long as we can find the Lagrange multipliers γ and $\boldsymbol{\beta}$ that allow the a-equations to be satisfied.

2.5 The Lagrange multipliers γ and $\boldsymbol{\beta}$

In order to determine the Lagrange multipliers γ and $\boldsymbol{\beta}$, we follow the procedure outlined by Stewart [4, p.266-7]. Substituting (2.49) into (2.21) and assuming

that external body forces are absent so that $G_i^a = 0$, we write (2.21) as

$$\Pi_i^a + \tilde{g}_i^a + \gamma a_i + \mu c_i + \epsilon_{ijk}\beta_{k,j} = 0. \tag{2.91}$$

Taking the divergence of (2.91), noting that $\nabla \cdot (\nabla \times \boldsymbol{\beta}) = 0$ and substituting for μ from (2.86), the expression (2.91) reduces to

$$\frac{\partial \gamma}{\partial z} + \frac{\partial}{\partial \tau}\left[\Pi_1^a + \tilde{g}_1^a - (\Pi_3^c + \tilde{g}_3^c)\cos\phi\right] = 0. \tag{2.92}$$

Then integrating (2.92) with respect to z gives the following expression for γ

$$\gamma(\tau, y, z, t) = -z\frac{\partial}{\partial \tau}\left[\Pi_1^a + \tilde{g}_1^a - (\Pi_3^c + \tilde{g}_3^c)\cos\phi\right] + f(\tau, y, t), \tag{2.93}$$

where $f(\tau, y, t)$ is taken to be an arbitrary function of τ, y and t. The solution for γ guarantees the existence of the vector $\boldsymbol{\beta}$. Then $\boldsymbol{\beta}$ is calculated from $\boldsymbol{\beta} = -\mathfrak{G}$, where $\mathfrak{G}$ is given by

$$\mathfrak{G} = \left(\int_{z_0}^{z} \mathcal{F}_2(\tau, y, \tilde{z}, t)\, d\tilde{z} - \int_{y_0}^{y} \mathcal{F}_3(\tau, \tilde{y}, z_0, t)\, d\tilde{y}, - \int_{z_0}^{z} \mathcal{F}_1(\tau, y, \tilde{z}, t)\, d\tilde{z}, 0\right). \tag{2.94}$$

and $\boldsymbol{\mathcal{F}}$ is given by

$$\boldsymbol{\mathcal{F}} = \boldsymbol{\Pi}^a + \tilde{\mathbf{g}}^a + \gamma \mathbf{a} + \mu \mathbf{c}, \tag{2.95}$$

meaning that $\mathcal{F}_1$, $\mathcal{F}_2$ and $\mathcal{F}_3$ may be expressed as follows

$$\begin{aligned}
\mathcal{F}_1(\tau, y, z, t) &= \Pi_1^a(\tau, t) + \tilde{g}_1^a(\tau, t) - (\Pi_3^c(\tau, t) + \tilde{g}_3^c(\tau, t))\cos\phi(\tau, t), \\
\mathcal{F}_2(\tau, y, z, t) &= \Pi_2^a(\tau, t) + \tilde{g}_2^a(\tau, t) - (\Pi_3^c(\tau, t) + \tilde{g}_3^c(\tau, t))\sin\phi(\tau, t), \\
\mathcal{F}_3(\tau, y, z, t) &= \Pi_3^a(\tau, t) + \tilde{g}_3^a(\tau, t) - z\frac{\partial}{\partial \tau}\left[\Pi_1^a + \tilde{g}_1^a - (\Pi_3^c + \tilde{g}_3^c)\cos\phi\right] \\
&\quad + f(\tau, y, t).
\end{aligned}$$

Finally, letting $y_0 = z_0 = 0$ we find that

$$\begin{aligned}
\beta_1 &= \int_0^y f(\tau, \tilde{y}, t)\, d\tilde{y} + y\left(\Pi_3^a(\tau, t) + \tilde{g}_3^a(\tau, t)\right) \\
&\quad -z\left(\Pi_2^a(\tau, t) + \tilde{g}_2^a(\tau, t) - (\Pi_3^c(\tau, t) + \tilde{g}_3^c(\tau, t))\sin\phi(\tau, t)\right), \\
\beta_2 &= z\left(\Pi_1^a(\tau, t) + \tilde{g}_1^a(\tau, t) - (\Pi_3^c(\tau, t) + \tilde{g}_3^c(\tau, t))\cos\phi(\tau, t)\right), \\
\beta_3 &= 0.
\end{aligned}$$

At this point it is possible to construct the components of $\mathbf{\Pi}^a$ explicitly using (2.55) and appropriate values for **a** and **c**.

2.6 The Fully Nonlinear Problem

Now we are in a position to construct the full nonlinear problem. We start by noting that the divergence of the flow velocity **v** must be zero, a consequence of (2.18). Since all of the components of **v** are functions of t and τ only we can immediately write down a constraint on the u component of flow

$$\frac{\partial u}{\partial \tau} = 0. \tag{2.96}$$

Then, substituting (2.69), (2.70), (2.81) and (2.82) into (2.90), we arrive at the final expression for the conserved angular momentum, which were we to disregard the velocity field of the infinitesimal flow, would reduce to (2.8)

$$\begin{aligned}
&2\lambda_5((u-c)\phi_{,\tau} + \phi_{,t}) - 2\lambda_2 u_{,\tau}\sin\phi\cos\phi - (\tau_1+\tau_5)w_{,\tau}\sin\phi \\
&+ (\lambda_2\cos 2\phi - \lambda_5)v_{,\tau} \\
&= (K_2\sin^2\phi + K_3\cos^2\phi)\phi_{,\tau\tau} + (K_2-K_3)\phi_{,\tau}^2\sin\phi\cos\phi \\
&- \epsilon_0\epsilon_a E^2\sin\theta\cos\alpha(\cos\theta\sin\alpha\sin\phi + \sin\theta\cos\alpha\sin\phi\cos\phi) \\
&- P_0 E\cos\alpha\cos\phi.
\end{aligned} \tag{2.97}$$

Turning our attention to the equations governing the conservation of linear momentum (2.19) we assume that

$$F_i = 0, \tag{2.98}$$

$$G_k^a = G_k^c = 0, \tag{2.99}$$

where F_i represents the external body force per unit mass whilst G_k^a and G_k^c represent the generalised external body forces per unit volume related to **a** and

c. Then with our definitions of **a** and **c** given by (2.3) and (2.4) we find that

$$\tilde{g}^a_k a_{k,i} = 0, \quad \forall \ \ k, i, \tag{2.100}$$

$$\tilde{g}^c_k c_{k,2} = \tilde{g}^c_k c_{k,3} = 0, \quad \forall \ \ k. \tag{2.101}$$

and we are left to consider the following equations

$$\rho \dot{v}_1 = -\tilde{p}_{,1} + \tilde{g}^c_1 c_{1,1} + \tilde{g}^c_2 c_{2,1} + \tilde{t}_{11,1}, \tag{2.102}$$

$$\rho \dot{v}_2 = \tilde{t}_{21,1}, \tag{2.103}$$

$$\rho \dot{v}_3 = \tilde{t}_{31,1}. \tag{2.104}$$

where the superposed dot represents the usual material time derivative. The viscous stress tensor given by (2.42) is decomposed into symmetric $\tilde{t}^s_{ij}$ and skew-symmetric parts $\tilde{t}^{ss}_{ij}$ defined respectively by (2.43) and (2.44). Since our model is spatially dependent on τ but not y or z, we need only compute the components $\tilde{t}^s_{i1,1}$ and $\tilde{t}^{ss}_{i1,1}$. With this in mind we find that the symmetric components of the viscous stress tensor are given by

$$\begin{aligned}
\tilde{t}^s_{11} &= \mu_0 u_{,\tau} + \mu_3(u_{,\tau}\cos\phi + v_{,\tau}\sin\phi)\cos^3\phi \\
&\quad + 2\mu_4(u_{,\tau}\cos\phi + \tfrac{1}{2}v_{,\tau}\sin\phi)\cos\phi \\
&\quad + 2\lambda_2[((c-u)\phi_{,\tau} - \phi_{,t})\sin\phi + \tfrac{1}{2}v_{,\tau}\sin\phi]\cos\phi \\
&\quad + \kappa_1 w_{,\tau}\cos\phi + \kappa_3 w_{,\tau}\cos^3\phi + \tau_2 w_{,\tau}\cos\phi + \tau_4 w_{,\tau}\cos^3\phi, \qquad (2.105) \\
\tilde{t}^s_{21} &= \tfrac{1}{2}\mu_0 v_{,\tau} + \mu_3(u_{,\tau}\cos\phi + v_{,\tau}\sin\phi)\sin\phi\cos^2\phi \\
&\quad + \mu_4(v_{,\tau} + u_{,\tau}\cos\phi\sin\phi) + \lambda_2((u-c)\phi_{,\tau} + \phi_{,t}) - \tfrac{1}{2}v_{,\tau})\cos 2\phi \\
&\quad + \tfrac{1}{2}\kappa_1 w_{,\tau}\sin\phi + \kappa_3 w_{,\tau}\cos^2\phi\sin\phi \\
&\quad + \tfrac{1}{2}\tau_2 w_{,\tau}\sin\phi + \tau_4 w_{,\tau}\cos^2\phi\sin\phi, \qquad (2.106) \\
\tilde{t}^s_{31} &= \tfrac{1}{2}\mu_0 w_{,\tau} + \tfrac{1}{2}\mu_4 w_{,\tau}\cos^2\phi + \tfrac{1}{2}\mu_5 w_{,\tau}\cos^2\phi \\
&\quad + \tfrac{1}{2}\lambda_1 w_{,\tau} - \tfrac{1}{2}\lambda_2 w_{,\tau}\cos^2\phi + \tfrac{1}{2}\lambda_3 w_{,\tau}\cos^2\phi \\
&\quad + \kappa_1(u_{,\tau}\cos\phi + \tfrac{1}{2}v_{,\tau}\sin\phi)
\end{aligned}$$

$$+ \kappa_3(u_{,\tau}\cos\phi + v_{,\tau}\sin\phi)\cos^2\phi$$
$$+ \tau_1[((c-u)\phi_{,\tau} - \phi_{,t}) + \tfrac{1}{2}v_{,\tau}]\sin\phi. \tag{2.107}$$

Whereas the components of the skew-symmetric part of the viscous stress tensor are found to be

$$\tilde{t}^{ss}_{11} = 0, \tag{2.108}$$
$$\begin{aligned}\tilde{t}^{ss}_{21} &= \lambda_2(u_{,\tau}\sin\phi\cos\phi - \tfrac{1}{2}v_{,\tau}\cos 2\phi)\\ &\quad + \lambda_5((c-u)\phi_{,\tau} - \phi_{,t} + \tfrac{1}{2}v_{,\tau})\\ &\quad + \tfrac{1}{2}(\tau_1 w_{,\tau} + \tfrac{1}{2}\tau_5 w_{,\tau})\sin\phi,\end{aligned} \tag{2.109}$$
$$\begin{aligned}\tilde{t}^{ss}_{31} &= \tfrac{1}{2}\lambda_1 w_{,\tau} - \tfrac{1}{2}\lambda_2 w_{,\tau}\cos^2\phi + \tfrac{1}{2}\lambda_3 w_{,\tau}\cos^2\phi + \tfrac{1}{2}\lambda_4 w_{,\tau}\\ &\quad + \tfrac{1}{2}\lambda_5 w_{,\tau}\cos^2\phi + \tfrac{1}{2}\lambda_6 w_{,\tau}\cos^2\phi\\ &\quad + \tau_2(u_{,\tau}\cos\phi + \tfrac{1}{2}v_{,\tau}\sin\phi)\\ &\quad + \tau_4(u_{,\tau}\cos\phi + v_{,\tau}\sin\phi)\cos^2\phi\\ &\quad + \tau_5[((c-u)\phi_{,\tau} - \phi_{,t}) + \tfrac{1}{2}v_{,\tau}]\sin\phi.\end{aligned} \tag{2.110}$$

Then, using (2.3), (2.66), (2.81), (2.82), (2.105) and (2.108) in (2.102) we find that

$$\begin{aligned}\rho(u_{,t} + uu_{,\tau}) &= -\tilde{p}_{,\tau} + \phi_{,\tau}[\lambda_2(u_{,\tau}\sin 2\phi - v_{,\tau}\cos 2\phi) + (\tau_1+\tau_5)w_{,\tau}\sin\phi\\ &\quad + \lambda_5(v_{,\tau} + 2((c-u)\phi_{,\tau} - \phi_{,t}))]\\ &\quad + \frac{\partial}{\partial\tau}\Big[\mu_0 u_{,\tau} + \mu_3(u_{,\tau}\cos\phi + v_{,\tau}\sin\phi)\cos^3\phi\\ &\quad + 2\mu_4(u_{,\tau}\cos\phi + \tfrac{1}{2}v_{,\tau})\cos\phi\\ &\quad + \lambda_2(((c-u)\phi_{,\tau} - \phi_{,t}) + \tfrac{1}{2}v_{,\tau})\sin 2\phi\\ &\quad + (\kappa_1 + \tau_2 + (\kappa_3+\tau_4)\cos^2\phi)w_{,\tau}\cos\phi\Big],\end{aligned} \tag{2.111}$$
$$\begin{aligned}\rho(v_{,t} + uv_{,\tau}) &= \frac{\partial}{\partial\tau}\Big[\tfrac{1}{2}\mu_0 v_{,\tau} + \mu_3(u_{,\tau}\cos\phi + v_{,\tau}\sin\phi)\sin\phi\cos^2\phi\\ &\quad + \mu_4(u_{,\tau}\sin\phi\cos\phi + \tfrac{1}{2}v_{,\tau})\\ &\quad + \lambda_2(u_{,\tau}\sin\phi\cos\phi + [((u-c)\phi_{,\tau} + \phi_{,t}) - v_{,\tau}]\cos 2\phi)\end{aligned}$$

$$
\begin{aligned}
& - \lambda_5[((u-c)\phi_{,\tau} + \phi_{,t}) - \tfrac{1}{2}v_{,\tau}] \\
& + \tfrac{1}{2}(\kappa_1 + \tau_1 + \tau_2 + \tau_5 + 2(\kappa_3 + \tau_4)\cos^2\phi)w_{,\tau}\sin\phi\Big], \qquad (2.112)
\end{aligned}
$$

$$
\begin{aligned}
\rho(w_{,t} + uw_{,\tau}) \;=\; & \frac{\partial}{\partial\tau}\Big[\tfrac{1}{2}(\mu_0 + \mu_2 + 2\lambda_1 + \lambda_4 + (\mu_4 + \mu_5 \\
& - 2\lambda_2 + 2\lambda_3 + \lambda_5 + \lambda_6)\cos^2\phi)w_{,\tau} \\
& + (\kappa_1 + \tau_2)(u_{,\tau}\cos\phi + \tfrac{1}{2}v_{,\tau}\sin\phi) \\
& + (\kappa_3 + \tau_4)(u_{,\tau}\cos\phi + v_{,\tau}\sin\phi)\cos^2\phi \\
& + (\tau_1 + \tau_5)[((c-u)\phi_{,\tau} - \phi_{,t}) + \tfrac{1}{2}v_{,\tau}]\sin\phi\Big]. \qquad (2.113)
\end{aligned}
$$

The equations (2.96), (2.97), (2.111), (2.112) and (2.113) constitute the fully non-linear system of equations in five unknowns ϕ, u, v, w and p.

2.7 Discussion

The principal aim of this chapter was to construct a set of fully nonlinear continuum equations incorporating flow for the type of problem discussed by Stewart and Momoniat in [54], namely an infinite sample of ferroelectric smectic C liquid crystal in a planar layer geometry of depth less than the pitch length of the sample so that chirality of the sample is suppressed. We note from [53] that in thick samples of ferroelectric the rotation of the spontaneous polarisation **P** across the domain wall can modify the *local* electric field within the material a great deal. A fully featured model should take this field augmentation into account. However in choosing to model the sample as a thin film we are accepting the position that the polarisation plays a rôle in linearly interacting with the external electric field but it is assumed not to modify the local electric field strength within the material bulk. The travelling wave equation discussed by Stewart and Momoniat in [54] and incorporated into the model we have constructed assumes thin films and is perfectly adequate for the problem we are addressing.

We have generated the continuum equations by analysing our problem in

a moving co-ordinate frame using the transformations given at (2.62). Then by making the appropriate substitutions we were able to derive the continuum equations at (2.96), (2.97), (2.111), (2.112) and (2.113) for the unknowns ϕ, u, v, w and p. Needless to say the fully nonlinear problem cannot be solved analytically. The main thrust of the analysis in this chapter has been to derive equations which may then be subjected to infinitesimal perturbations. Typically this means taking a solution $\phi_0(\tau)$ and in our case we do have a known exact solution in the case of an in plane electric field and assuming that there is no flow. Then by introducing a small perturbation to all five of the unknowns we can go on to derive a full system of linear perturbation equations which we go on to do in Chapter 3.

The known solution is critical to the success of the subsequent analysis we shall be performing. Without it the perturbation equations once formulated would have to be expressed in terms of some unknown function $\phi_0(\tau)$. Because exact solutions are *not* available for the travelling wave problem when the field $\mathbf{E}$ is inclined, that is when $\alpha \neq 0$ we cannot reasonably use the equations we have developed here to study perturbations for systems with inclined fields. However useful work can be done when the electric field lies in the plane and the exact travelling wave solution will be of great value in helping to establish usable perturbation equations which we go on to develop in the next chapter.

Chapter 3

The Linearised Continuum Model

3.1 Introduction

In this chapter we shall be developing a system of linearised perturbation equations. By applying infinitesimal perturbations to the system of PDE's given by equations (2.111), (2.112), (2.113), (2.97) and (2.96), we shall reduce the PDE's to linear form. Once in this form we may begin the task of analysing the behaviour of the perturbed system and we shall examine an appropriate perturbation scheme in chapter 4.

Before proceeding it will prove helpful in the subsequent analysis to establish conventions for the naming of elastic constants and to make a number of simplifying assumptions. When dealing with elastic constants we shall adopt the convention used by Saupe [41]. Hence, from now onwards the elastic constants K_2 and K_3 appearing in (2.97) may be re-written as B_2 and B_1 respectively.

With regards to simplifying assumptions our first shall be that the elastic constants are taken to be equal, the so called one constant approximation. That is we shall assume $B_1 = B_2 = B$ following Stewart et al. [54].

Our second assumption is that the angle of incidence α of the electric field $\mathbf{E}$ is taken to be 0. This forces the electric field to lie parallel to the x-axis

and consequently the electric field vector is given by $\mathbf{E} = (E, 0, 0)$. Then if we suppose that $\phi = \phi_0(\tau)$ solves (2.9) and assume that $P_0 E < 0$, forcing us to take the negative sign for (2.10) as remarked upon by Stewart et al. [54], we have that

$$2\lambda_5 \frac{\partial \phi_0}{\partial t} = B\frac{\partial^2 \phi_0}{\partial x^2} - P_0 E \cos\phi_0 - \epsilon_0 \epsilon_a E^2 \sin^2\theta \sin\phi_0 \cos\phi_0, \tag{3.1}$$

where

$$\phi_0(\tau) = \frac{\pi}{2} - 2\arctan\left[\exp\left\{\sqrt{\frac{\beta}{B}}\tau\right\}\right], \tag{3.2}$$

and

$$\tau = x - ct. \tag{3.3}$$

This is a key assumption. We are going to suppose that (3.2) represents the solution about which we shall perform our perturbation analysis. In the unperturbed state we say that the system experiences no flow and we may approximate the director profile via (3.1).

Our third assumption is that there is no transverse flow. This means that for the moment we shall choose the y-component of the flow vector to be $v(\tau, t) = 0$. This means that we do not need to consider equation (2.112) for the remainder of this analysis.

3.2 Applying a perturbation to the non-linear system

With due regard to the assumptions outlined above, equations (2.96), (2.97), (2.111) and (2.113) reduce to the following system of PDE's.

$$\begin{aligned} B\phi_{,\tau\tau} &= 2\lambda_5((u-c)\phi_{,\tau} + \phi_{,t}) - 2\lambda_2 u_{,\tau}\sin\phi\cos\phi - (\tau_1+\tau_5)w_{,\tau}\sin\phi \\ &\quad + \epsilon_0\epsilon_a E^2 \sin^2\theta\cos^2\alpha\sin\phi\cos\phi + P_0 E\cos\alpha\cos\phi, \qquad (3.4) \\ \rho(u_{,t} + uu_{,\tau}) &= -\tilde{p}_{,\tau} + \phi_{,\tau}[\lambda_2 u_{,\tau}\sin 2\phi + (\tau_1+\tau_5)w_{,\tau}\sin\phi \\ &\quad + 2\lambda_5((c-u)\phi_{,\tau} - \phi_{,t}))] \end{aligned}$$

$$
\begin{aligned}
&+\frac{\partial}{\partial\tau}\Big[\left(\mu_0+\left(2\mu_4+\mu_3\cos^2\phi\right)\cos^2\phi\right)u_{,\tau}\\
&+\lambda_2((c-u)\phi_{,\tau}-\phi_{,t})\sin 2\phi\\
&+(\kappa_1+\tau_2+(\kappa_3+\tau_4)\cos^2\phi)w_{,\tau}\cos\phi\Big], \qquad (3.5)\\
\rho(w_{,t}+uw_{,\tau}) &= \frac{\partial}{\partial\tau}\Big[\tfrac{1}{2}(\mu_0+\mu_2+2\lambda_1+\lambda_4+(\mu_4+\mu_5\\
&-2\lambda_2+2\lambda_3+\lambda_5+\lambda_6)\cos^2\phi)w_{,\tau}\\
&+\left(\kappa_1+\tau_2+(\kappa_3+\tau_4)\cos^2\phi\right)u_{,\tau}\cos\phi\\
&+(\tau_1+\tau_5)((c-u)\phi_{,\tau}-\phi_{,t})\sin\phi\Big]. \qquad (3.6)\\
u_{,\tau} &= 0. \qquad (3.7)
\end{aligned}
$$

Our task now is to develop the linearised equations we shall use in subsequent stability analysis problems using (3.4), (3.5), (3.6) and (3.7). We begin by introducing perturbations of the following form

$$
\begin{aligned}
\phi(\tau,t) &= \phi_0(\tau)+\epsilon\bar{\phi}(\tau,t), \qquad (3.8)\\
u(\tau,t) &= u_0(\tau,t)+\epsilon\bar{u}(\tau,t), \qquad (3.9)\\
w(\tau,t) &= w_0(\tau,t)+\epsilon\bar{w}(\tau,t), \qquad (3.10)\\
p(\tau,t) &= p_0+\epsilon\bar{p}(\tau,t). \qquad (3.11)
\end{aligned}
$$

Here we note that the parameter ϵ is chosen so that $\epsilon \ll 1$. Note also that $u_0(\tau,t)=w_0(\tau,t)=0$, the unperturbed pressure p_0 is a constant and $\phi_0(\tau)$ is the solution given in (3.2). Essentially what we are doing is the following. We are supposing that without flow, setting $\mathbf{v}=\mathbf{0}$ is equivalent to setting $\epsilon=0$. Then (3.8), (3.9), (3.10) and (3.11) reduce to

$$
\begin{aligned}
\phi(\tau,t) &= \phi_0(\tau), \qquad (3.12)\\
u(\tau,t) &= 0, \qquad (3.13)\\
w(\tau,t) &= 0, \qquad (3.14)\\
p(\tau,t) &= p_0. \qquad (3.15)
\end{aligned}
$$

By making $0 < \epsilon \ll 1$ we are perturbing about a known state $\phi_0(\tau)$. From this we suppose that, however hydrodynamic flow is initially induced in the modelled system, the result is that the system is perturbed from its initial state (3.12)-(3.15) to its perturbed state (3.8)-(3.11). Our linearised equations will be functions of the perturbation terms $\bar{\phi}(\tau,t)$, $\bar{u}(\tau,t)$, $\bar{w}(\tau,t)$ and $\bar{p}(\tau,t)$ the initial state $\phi_0(\tau)$, and their derivatives.

Substituting (3.8), (3.9), (3.10) and (3.11) into our system of PDE's given by (3.4), (3.5), (3.6) and (3.7), discarding terms of $\mathcal{O}(\epsilon^2)$ and higher and handling the $\mathcal{O}(\epsilon^0)$ terms as discussed earlier by assuming they are approximately zero we arrive at the following expressions for the linearised perturbation equations. Firstly, the conserved angular momentum equation (3.4) yields

$$\begin{aligned} 2\lambda_5\left(\bar{\phi}_{,t} - c\bar{\phi}_{,\tau}\right) &= B\bar{\phi}_{,\tau\tau} + \lambda_2\bar{u}_{,\tau}\sin 2\phi_0 + (\tau_1+\tau_5)\bar{w}_{,\tau}\sin\phi_0 - 2\lambda_5\bar{u}\phi_{0,\tau} \\ &\quad - \left(\epsilon_0\epsilon_a E^2\sin^2\theta\cos 2\phi_0 - P_0 E\sin\phi_0\right)\bar{\phi}. \end{aligned} \tag{3.16}$$

As expected all of the perturbation terms appear to first order only. Next the conserved linear momentum equation (3.5) results in the following perturbation equation

$$\begin{aligned} &\bar{p}_{,\tau} + \rho\bar{u}_{,t} - \mu_0\bar{u}_{,\tau\tau} - 2\lambda_2 c\phi_{0,\tau}\bar{\phi}_{,\tau}\cos^2\phi_0 \\ &+ 2\lambda_2\left[c\sin 2\phi_0\phi_{0,\tau}\bar{\phi} - (c\bar{\phi}_{,\tau} - \phi_{0,\tau}\bar{u} - \bar{\phi}_{,t})\cos^2\phi_0\right]\phi_{0,\tau} \\ &- 2\lambda_2\sin\phi_0\cos\phi_0\bar{u}_{,\tau}\phi_{0,\tau} \\ &+ 2\lambda_2 c\sin^2\phi_0\phi_{0,\tau}\bar{\phi}_{,\tau} \\ &+ 2\lambda_2 c\sin^2\phi_0\bar{\phi}\phi_{0,\tau\tau} \\ &- 2\lambda_2\left[c\cos\phi_0\bar{\phi}\phi_{0,\tau\tau} + \left(c\bar{\phi}_{,\tau\tau} - \bar{\phi}_{,\tau t} - \phi_{0,\tau}\bar{u}_{,\tau} - \bar{u}\phi_{0,\tau\tau}\right)\sin\phi_0\right]\cos\phi_0 \\ &- 2\lambda_5 c\phi_{0,\tau}\bar{\phi}_{,\tau} \\ &+ 2\lambda_5\left[\phi_{0,\tau}\bar{u} + \bar{\phi}_{,t} - c\bar{\phi}_{,\tau}\right]\phi_{0,\tau} \\ &+ 2\mu_3\phi_{0,\tau}\bar{u}_{,\tau}\cos^3\phi_0\sin\phi_0 \end{aligned}$$

$$
\begin{aligned}
&- \left[2\mu_4 + \mu_3 \cos^2\phi_0\right]\left[\bar{u}_{,\tau}\phi_{0,\tau}\sin 2\phi_0 - \bar{u}_{,\tau\tau}\cos^2\phi_0\right] \\
&+ 2\left(\kappa_3+\tau_4\right)\phi_{0,\tau}\bar{w}_{,\tau}\cos^2\phi_0\sin\phi_0 \\
&+ \left[\kappa_1+\tau_2+\left(\kappa_3+\tau_4\right)\cos^2\phi_0\right]\sin\phi_0\phi_{0,\tau}\bar{w}_{,\tau} \\
&- \left(\tau_1+\tau_5\right)\sin\phi_0\bar{w}_{,\tau}\phi_{0,\tau} \\
&- \left[\kappa_1+\tau_2+\left(\kappa_3+\tau_4\right)\cos^2\phi_0\right]\cos\phi_0\bar{w}_{,\tau\tau} = 0,
\end{aligned} \tag{3.17}
$$

whilst equation (3.6) reduces to

$$
\begin{aligned}
&\rho\bar{w}_{,t} - \left(\tau_1+\tau_5\right)c\bar{\phi}\phi_{0,\tau\tau}\cos\phi_0 \\
&- \left(\tau_1+\tau_5\right)\left[c\bar{\phi}_{,\tau\tau} - \phi_{0,\tau}\bar{u}_{,\tau} - \bar{\phi}_{,\tau t} - \phi_{0,\tau\tau}\bar{u}\right]\sin\phi_0 \\
&- \left(\tau_1+\tau_5\right)c\phi_{0,\tau}\bar{\phi}_{,\tau}\cos\phi_0 \\
&- \left(\tau_1+\tau_5\right)\left[\left(c\bar{\phi}_{,\tau} - \phi_{0,\tau}\bar{u} - \bar{\phi}_{,t}\right)\cos\phi_0 - c\phi_{0,\tau}\bar{\phi}\sin\phi_0\right]\phi_{0,\tau} \\
&+ 2\left(\kappa_3+\tau_4\right)\phi_{0,\tau}\bar{u}_{,\tau}\cos^2\phi_0\sin\phi_0 \\
&- \tfrac{1}{2}\bar{w}_{,\tau\tau}\left[\mu_0+\mu_2+2\lambda_1+\lambda_4+\left(\mu_4+\mu_5-2\lambda_2+2\lambda_3+\lambda_6+\lambda_5\right)\cos^2\phi_0\right] \\
&+ \bar{w}_{,\tau}\left[\mu_4+\mu_5-2\lambda_2+2\lambda_3+\lambda_6+\lambda_5\right]\cos\phi_0\sin\phi_0\phi_{0,\tau} \\
&+ \left[\kappa_1+\tau_2+\left(\kappa_3+\tau_4\right)\cos^2\phi_0\right]\bar{u}_{,\tau}\phi_{0,\tau}\sin\phi_0 \\
&- \left[\kappa_1+\tau_2+\left(\kappa_3+\tau_4\right)\cos^2\phi_0\right]\bar{u}_{,\tau\tau}\cos\phi_0 = 0.
\end{aligned} \tag{3.18}
$$

Finally the linearised conserved mass equation maybe specified by

$$\bar{u}_{,\tau} = 0. \tag{3.19}$$

3.3 Expressing the linearised system in terms of hyperbolic functions

Note that with the exception of (3.19) all of the equations contain terms of the form $\phi_{0,\tau}$, $\phi_{0,\tau\tau}$, $\sin\phi_0$, $\cos\phi_0$, $\sin 2\phi_0$ and $\cos 2\phi_0$. Then using (3.2) we may write

$$\frac{d\phi_0}{d\tau} = -\zeta\,\mathrm{sech}(\zeta\tau), \tag{3.20}$$

$$\frac{d^2\phi_0}{d\tau^2} = \zeta^2 \mathrm{sech}(\zeta\tau)\tanh(\zeta\tau), \tag{3.21}$$

$$\sin\phi_0 = -\tanh(\zeta\tau), \tag{3.22}$$

$$\cos\phi_0 = \mathrm{sech}(\zeta\tau), \tag{3.23}$$

$$\sin 2\phi_0 = -2\tanh(\zeta\tau)\mathrm{sech}(\zeta\tau), \tag{3.24}$$

$$\cos 2\phi_0 = \mathrm{sech}^2(\zeta\tau) - \tanh^2(\zeta\tau). \tag{3.25}$$

where

$$\zeta = \sqrt{\frac{\beta}{B}}. \tag{3.26}$$

Consequently equations (3.16), (3.17), (3.18) and (3.19) may be expressed in terms of hyperbolic functions as follows

$$\begin{aligned} 2\lambda_5\left(\bar{\phi}_{,t} - c\bar{\phi}_{,\tau}\right) = {} & B\bar{\phi}_{,\tau\tau} - 2\lambda_2\tanh(\zeta\tau)\mathrm{sech}(\zeta\tau)\bar{u}_{,\tau} \\ & - (\tau_1+\tau_5)\tanh(\zeta\tau)\bar{w}_{,\tau} + 2\lambda_5\zeta\mathrm{sech}(\zeta\tau)\bar{u} \\ & - \left(\epsilon_0\epsilon_a E^2\sin^2\theta\left(\mathrm{sech}^2(\zeta\tau) - \tanh^2(\zeta\tau)\right)\right. \\ & \left. + P_0 E\tanh(\zeta\tau)\right)\bar{\phi}, \end{aligned} \tag{3.27}$$

$$\begin{aligned} & \bar{p}_{,\tau} + \rho\bar{u}_{,t} + 2\lambda_2 c\zeta\mathrm{sech}^3(\zeta\tau)\bar{\phi}_{,\tau} \\ & + 2\lambda_2\zeta[4c\tanh(\zeta\tau)\mathrm{sech}(\zeta\tau)\bar{\phi} \\ & + (c\bar{\phi}_{,\tau} + \zeta\mathrm{sech}(\zeta\tau)\bar{u} - \bar{\phi}_{,t})(\mathrm{sech}^2(\zeta\tau) - \tanh^2(\zeta\tau))]\mathrm{sech}(\zeta\tau) \\ & - 2\lambda_2\zeta\tanh(\zeta\tau)\mathrm{sech}^2(\zeta\tau)\bar{u}_{,\tau} \\ & + 2\lambda_2 c\zeta^2\tanh^3(\zeta\tau)\mathrm{sech}(\zeta\tau)\bar{\phi} \\ & - 2\lambda_2[c\zeta^2\mathrm{sech}^2(\zeta\tau)\tanh(\zeta\tau)\bar{\phi} \\ & - \left(c\bar{\phi}_{,\tau\tau} - \bar{\phi}_{,\tau t} + \zeta\mathrm{sech}(\zeta\tau)\bar{u}_{,\tau} - \zeta^2\mathrm{sech}(\zeta\tau)\tanh(\zeta\tau)\bar{u}\right)\tanh(\zeta\tau)]\mathrm{sech}(\zeta\tau) \\ & + 2\lambda_5 c\zeta\mathrm{sech}(\zeta\tau)\bar{\phi}_{,\tau} \\ & - 2\lambda_5\zeta\left[\bar{\phi}_{,t} - c\bar{\phi}_{,\tau} - \zeta\mathrm{sech}(\zeta\tau)\bar{u}\right]\mathrm{sech}(\tau\zeta) \\ & + 2\mu_3\zeta\mathrm{sech}^4(\zeta\tau)\tanh(\zeta\tau)\bar{u}_{,\tau} \end{aligned}$$

$$
\begin{aligned}
&- \left[2\mu_4 + \mu_3 \mathrm{sech}^2(\zeta\tau)\right] \left[2\zeta \tanh(\zeta\tau)\bar{u}_{,\tau} - \bar{u}_{,\tau\tau}\right] \mathrm{sech}^2(\zeta\tau) \\
&+ 2\left(\kappa_3 + \tau_4\right) \zeta \mathrm{sech}^3(\zeta\tau) \tanh(\zeta\tau)\bar{w}_{,\tau} \\
&+ \left[\kappa_1 + \tau_2 + \left(\kappa_3 + \tau_4\right) \mathrm{sech}^2(\zeta\tau)\right] \zeta \mathrm{sech}(\zeta\tau) \tanh(\zeta\tau)\bar{w}_{,\tau} \\
&- \left(\tau_1 + \tau_5\right) \zeta \mathrm{sech}(\zeta\tau) \tanh(\zeta\tau)\bar{w}_{,\tau} \\
&- \left[\kappa_1 + \tau_2 + \left(\kappa_3 + \tau_4\right) \mathrm{sech}^2(\zeta\tau)\right] \mathrm{sech}(\zeta\tau)\bar{w}_{,\tau\tau} \\
&- \mu_0 \bar{u}_{,\tau\tau} = 0,
\end{aligned} \tag{3.28}
$$

$$
\begin{aligned}
&\rho\bar{w}_{,t} \\
&- \left(\tau_1 + \tau_5\right) c\zeta^2 \mathrm{sech}^2(\zeta\tau) \tanh(\zeta\tau)\bar{\phi} \\
&+ \left(\tau_1 + \tau_5\right) \left[c\bar{\phi}_{,\tau\tau} + \zeta \mathrm{sech}(\zeta\tau)\bar{u}_{,\tau} - \bar{\phi}_{,\tau t} - \zeta^2 \mathrm{sech}(\zeta\tau) \tanh(\zeta\tau)\bar{u}\right] \tanh(\zeta\tau) \\
&+ \left(\tau_1 + \tau_5\right) c\zeta \, \mathrm{sech}^2(\zeta\tau)\bar{\phi}_{,\tau} \\
&+ \left(\tau_1 + \tau_5\right) \zeta \left[\left(c\bar{\phi}_{,\tau} + \zeta \mathrm{sech}(\zeta\tau)\bar{u} - \bar{\phi}_{,t}\right) \mathrm{sech}^2(\zeta\tau) - c\zeta \mathrm{sech}^2(\zeta\tau) \tanh(\zeta\tau)\bar{\phi}\right] \\
&+ 2\left(\kappa_3 + \tau_4\right) \zeta \mathrm{sech}^3(\zeta\tau) \tanh(\zeta\tau)\bar{u}_{,\tau} \\
&- \tfrac{1}{2}\bar{w}_{,\tau\tau} \left[\mu_0 + \mu_2 + 2\lambda_1 + \lambda_4 + \left(\mu_4 + \mu_5 - 2\lambda_2 + 2\lambda_3 + \lambda_6 + \lambda_5\right) \mathrm{sech}^2(\zeta\tau)\right] \\
&+ \bar{w}_{,\tau} \left[\mu_4 + \mu_5 - 2\lambda_2 + 2\lambda_3 + \lambda_6 + \lambda_5\right] \zeta \mathrm{sech}^2(\zeta\tau) \tanh(\zeta\tau) \\
&+ \left[\kappa_1 + \tau_2 + \left(\kappa_3 + \tau_4\right) \mathrm{sech}^2(\zeta\tau)\right] \zeta \mathrm{sech}(\zeta\tau) \tanh(\zeta\tau)\bar{u}_{,\tau} \\
&- \left(\kappa_1 + \tau_2 + \left(\kappa_3 + \tau_4\right) \mathrm{sech}^2(\zeta\tau)\right) \mathrm{sech}(\zeta\tau)\bar{u}_{,\tau\tau} = 0.
\end{aligned} \tag{3.29}
$$

3.4 Discussion

So, the problem we began with at (2.96), (2.97), (2.111), (2.112) and (2.113) for the unknowns ϕ, u, v, w and p has been linearised to give four perturbation equations. One of the key assumptions we made in this chapter was to assume the absence of transverse flow. Intuitively this is plausible since we have a travelling planar domain wall which we assume does not experience flow effects along the length of the wall itself. Consequently we only have four equations to concern ourselves with, a conserved mass perturbation equation (3.19), two perturba-

tion equations relating to the conserved linear momentum equation for flow in the x and z directions (3.28) and (3.29) and finally a perturbation equation for conserved angular momentum effects (3.27).

By imposing a one constant approximation we chose not to study anisotropic effects in the elastic constants, but since anisotropic effects are generally considered to be reasonably small we regard this as appropriate for an initial investigation [60]. We draw the readers attention once again to the decision to model a system where the electric field lies in the plane. The importance of this is drawn out where we are able to fully express the non-constant coefficients in our model in terms of the hyperbolic functions.

Notice also that the transformation to the co-moving frame employed in Chapter 2 implies that $P_0E < 0$. All further analysis will be performed with this in mind so that the polarisation P_0 and electric field E will be taken to be either $E < 0$ and $P_0 > 0$ or $E > 0$ and $P_0 < 0$. Note also the pressure in our model is initially taken to be a constant p_0 this is appropriate in a thin film model of an incompressible fluid.

We shall develop in the analysis that follows techniques for determining properties of the system through the use of Fourier mode analysis. This will allow us by the application of suitable perturbation forms, to construct differential eigenvalue problems which may be discretized and solved algebraically using standard linear algebra techniques. We shall begin investigating these methods in Chapter 4.

Chapter 4

Perturbation Analysis

4.1 Introduction

We turn now to the problem of perturbation analysis. In Chapter 3 we applied infinitesimal perturbations to the fully nonlinear system which left us with a series of linear perturbation equations. This linearised system forms the basis for the work which follows as we study the effect of perturbations on our continuum model.

In Chapter 3 we concentrated on developing a set of perturbation equations which briefly consist of five equations in total, one which captures the linear dynamics of the conserved angular momentum equation, three which describe the linear dynamics of the linear momentum equations and a perturbation equation modelling the linear response of the mass conservation equation.

With the linear equations developed the problem then boils down to choosing an appropriate ansatz for the form of the perturbation we wish to study. In [28] Stewart studies linearised continuum models of Smectic A materials subject to spatially periodic perturbations of the form $u \sim e^{\omega t + i\mathbf{q}\cdot\mathbf{x}}$. In principle we can perform a similar type of perturbation analysis. However in the analysis which follows we shall focus our efforts on analysing the perturbation models using perturbations of the form $u \sim \hat{u}(x)e^{-\omega t}$.

4.2 Non-Sinusoidal Perturbation on a Finite Interval

By treating the problem as a perturbation on some finite region in the scaled x direction called τ such that $|\tau| \leq \delta$ where $\delta \ll 1$ we may apply perturbations of the form proposed by Logan [59, p.240] and we seek solutions such that

$$\bar{\phi}(\tau, t) = \hat{\phi}(\tau)e^{-\omega t} \tag{4.1}$$

$$\bar{w}(\tau, t) = \hat{w}(\tau)e^{-\omega t} \tag{4.2}$$

$$\bar{u}(\tau, t) = \hat{u}(\tau)e^{-\omega t} \tag{4.3}$$

$$\bar{p}(\tau, t) = \hat{p}(\tau)e^{-\omega t}. \tag{4.4}$$

When we apply the ansatz (4.1)-(4.4) to the equations given at (3.19), (3.27), (3.28) and (3.29) we arrive at the following system of linear perturbation equations, the first being the perturbed conserved mass equation

$$\hat{u}_{,\tau} = 0, \tag{4.5}$$

along with the perturbation equation associated with the conservation of angular momentum equation

$$\begin{aligned} B\hat{\phi}_{,\tau\tau} &+ 2\lambda_5 c\hat{\phi}_{,\tau} - 2\lambda_2 \tanh(\zeta\tau)\mathrm{sech}(\zeta\tau)\hat{u}_{,\tau} \\ &-(\tau_1 + \tau_5)\tanh(\zeta\tau)\hat{w}_{,\tau} + 2\lambda_5\zeta\mathrm{sech}(\zeta\tau)\hat{u} \\ &-(P_0 E \tanh(\zeta\tau) - \epsilon_0\epsilon_a E^2 \sin^2\theta(1 - 2\,\mathrm{sech}^2(\zeta\tau)) - 2\lambda_5\omega)\,\hat{\phi} = 0, \end{aligned} \tag{4.6}$$

and a perturbation equation associated with the third conserved linear momentum equation

$$\begin{aligned} &-\rho\omega\hat{w} - (\tau_1 + \tau_5)\left[c\zeta^2\mathrm{sech}^2(\zeta\tau)\tanh(\zeta\tau)\hat{\phi} - c\zeta\mathrm{sech}^2(\zeta\tau)\hat{\phi}_{,\tau}\right] \\ &+(\tau_1 + \tau_5)\left[c\hat{\phi}_{,\tau\tau} + \zeta\mathrm{sech}(\zeta\tau)\hat{u}_{,\tau} + \omega\hat{\phi}_{,\tau} - \zeta^2\mathrm{sech}(\zeta\tau)\tanh(\zeta\tau)\hat{u}\right]\tanh(\zeta\tau) \\ &+(\tau_1 + \tau_5)\zeta\left[c\hat{\phi}_{,\tau} + \zeta\mathrm{sech}(\zeta\tau)\hat{u} + \omega\hat{\phi}_{,\tau} - c\zeta\tanh(\zeta\tau)\hat{\phi}\right]\mathrm{sech}^2(\zeta\tau) \end{aligned}$$

$$
\begin{aligned}
&+2(\kappa_3+\tau_4)\zeta\mathrm{sech}^3(\zeta\tau)\tanh(\zeta\tau)\hat{u}_{,\tau}\\
&-\tfrac{1}{2}\left[\mu_0+\mu_2+2\lambda_1+\lambda_4+(\mu_4+\mu_5-2\lambda_2+2\lambda_3+\lambda_6+\lambda_5)\mathrm{sech}^2(\zeta\tau)\right]\hat{w}_{,\tau\tau}\\
&+\left[\mu_4+\mu_5-2\lambda_2+2\lambda_3+\lambda_6+\lambda_5\right]\zeta\mathrm{sech}^2(\zeta\tau)\tanh(\zeta\tau)\hat{w}_{,\tau}\\
&+\left[\kappa_1+\tau_2+(\kappa_3+\tau_4)\mathrm{sech}^2(\zeta\tau)\right]\zeta\mathrm{sech}(\zeta\tau)\tanh(\zeta\tau)\hat{u}_{,\tau}\\
&-\left[\kappa_1+\tau_2+(\kappa_3+\tau_4)\mathrm{sech}^2(\zeta\tau)\right]\mathrm{sech}(\zeta\tau)\hat{u}_{,\tau\tau}=0. \qquad (4.7)
\end{aligned}
$$

Integrating the first of these equations gives

$$\hat{u}(\tau)=\kappa, \qquad (4.8)$$

where κ is a constant, which along with $\hat{u}_{,\tau}=0$ and $\hat{u}_{,\tau\tau}=0$ means that equations (4.6) and (4.7) maybe written as

$$
\begin{aligned}
&B\hat{\phi}_{,\tau\tau}+2\lambda_5 c\hat{\phi}_{,\tau}\\
&\quad-(\tau_1+\tau_5)\tanh(\zeta\tau)\hat{w}_{,\tau}+2\lambda_5\zeta\kappa\mathrm{sech}(\zeta\tau)\\
&\quad-(P_0E\tanh(\zeta\tau)-\epsilon_0\epsilon_a E^2\sin^2\theta(1-2\,\mathrm{sech}^2(\zeta\tau))-2\lambda_5\omega)\,\hat{\phi}=0, \qquad (4.9)
\end{aligned}
$$

and

$$
\begin{aligned}
&-\rho\omega\hat{w}-(\tau_1+\tau_5)\left[c\zeta^2\mathrm{sech}^2(\zeta\tau)\tanh(\zeta\tau)\hat{\phi}-c\zeta\mathrm{sech}^2(\zeta\tau)\hat{\phi}_{,\tau}\right]\\
&+(\tau_1+\tau_5)\left[c\hat{\phi}_{,\tau\tau}+\omega\hat{\phi}_{,\tau}-\kappa\zeta^2\mathrm{sech}(\zeta\tau)\tanh(\zeta\tau)\right]\tanh(\zeta\tau)\\
&+(\tau_1+\tau_5)\zeta\left[c\hat{\phi}_{,\tau}+\zeta\kappa\mathrm{sech}(\zeta\tau)+\omega\hat{\phi}_{,\tau}-c\zeta\tanh(\zeta\tau)\hat{\phi}\right]\mathrm{sech}^2(\zeta\tau)\\
&-\tfrac{1}{2}\left[\mu_0+\mu_2+2\lambda_1+\lambda_4+(\mu_4+\mu_5-2\lambda_2+2\lambda_3+\lambda_6+\lambda_5)\mathrm{sech}^2(\zeta\tau)\right]\hat{w}_{,\tau\tau}\\
&+\left[\mu_4+\mu_5-2\lambda_2+2\lambda_3+\lambda_6+\lambda_5\right]\zeta\mathrm{sech}^2(\zeta\tau)\tanh(\zeta\tau)\hat{w}_{,\tau}=0. \qquad (4.10)
\end{aligned}
$$

For convenience we shall assume that the only non-zero viscosities in the model are μ_0, λ_2, λ_5, τ_1 and τ_5. Furthermore we shall let $\kappa=0$ so that the flow velocity $\hat{u}(\tau)=0$. Taking this into account we find that the system collapses to two coupled linear second order ODE's

$$B\frac{d^2\hat{\phi}}{d\tau^2}+2\lambda_5 c\frac{d\hat{\phi}}{d\tau}-(\tau_1+\tau_5)\tanh(\zeta\tau)\frac{d\hat{w}}{d\tau}$$

$$-(P_0 E \tanh(\zeta\tau) - \epsilon_0\epsilon_a E^2 \sin^2\theta(1 - 2\,\mathrm{sech}^2(\zeta\tau)) - 2\lambda_5\omega)\,\hat{\phi} = 0, \tag{4.11}$$

$$\begin{aligned} c(\tau_1+\tau_5)\tanh(\zeta\tau)\frac{d^2\hat{\phi}}{d\tau^2} &+ \frac{1}{2}\left((2\lambda_2-\lambda_5)\,\mathrm{sech}^2(\zeta\tau) - \mu_0\right)\frac{d^2\hat{w}}{d\tau^2} \\ &+ (\tau_1+\tau_5)\left(2c\zeta\,\mathrm{sech}^2(\zeta\tau) + \omega\tanh(\zeta\tau)\right)\frac{d\hat{\phi}}{d\tau} \\ &- (2\lambda_2-\lambda_5)\,\zeta\,\mathrm{sech}^2(\zeta\tau)\tanh(\zeta\tau)\frac{d\hat{w}}{d\tau} \\ &+ (\tau_1+\tau_5)\left(\omega\zeta - 2c\zeta^2\tanh(\zeta\tau)\right)\mathrm{sech}^2(\zeta\tau)\hat{\phi} - \rho\omega\hat{w} = 0, \end{aligned} \tag{4.12}$$

with boundary conditions

$$\hat{\phi}(-\delta) = \hat{\phi}(\delta) = 0 \quad \text{and} \quad \hat{w}(-\delta) = \hat{w}(\delta) = 0, \tag{4.13}$$

where

$$\zeta = \sqrt{\frac{\beta}{B}}, \tag{4.14}$$

and

$$\beta = \epsilon_0|\epsilon_a|E^2\sin^2\theta. \tag{4.15}$$

4.2.1 The constant coefficient differential eigenvalue problem

The problem posed at (4.11), (4.12) and (4.13) is a coupled linear eigenvalue problem with non-constant coefficients. Needless to say the system is highly complex and as we shall see non-self-adjoint in nature. Inevitably we shall be forced to resort to approximation methods since closed form solutions do not exist. However the techniques we would normally apply in determining solutions are unavailable in this case because of the non-self-adjoint nature of the problem. With this in mind we shall in this section establish some of the mathematical machinery we shall use in later sections.

We start by simplifying (4.11), (4.12) and (4.13) and make a first attempt at analysing the problem. Suppose we are interested in the behaviour of the

perturbed system in the vicinity of the centre of the domain wall. Consider the coefficients in (4.11) and (4.12). We shall for convenience replace the coefficients $\tanh(\zeta\tau)$ and $\mathrm{sech}(\zeta\tau)$ with their values at $\tau = 0$. Furthermore, using the transformation

$$\hat{z}(\tau) = \rho\hat{w}(\tau) - \zeta(\tau_1 + \tau_5)\hat{\phi}(\tau), \tag{4.16}$$

and substituting for $\hat{w}(\tau)$ using (4.16) in (4.11) and (4.12), the problem reduces to the following system of equations

$$-\frac{B}{2\lambda_5}\frac{d^2\hat{\phi}}{d\tau^2} - c\frac{d\hat{\phi}}{d\tau} - \frac{\epsilon_0|\epsilon_a|E^2\sin^2\theta}{2\lambda_5}\hat{\phi} = \omega\hat{\phi}, \tag{4.17}$$

$$\frac{1}{2\rho}(2\lambda_2 - \lambda_5 - \mu_0)\left\{\frac{d^2\hat{z}}{d\tau^2} + \zeta(\tau_1 + \tau_5)\frac{d^2\hat{\phi}}{d\tau^2}\right\} + 2c\zeta(\tau_1 + \tau_5)\frac{d\hat{\phi}}{d\tau} = \omega\hat{z}. \tag{4.18}$$

Now with the equations in this form we have what is essentially an eigenvalue problem for ω. We proceed by defining the following constants

$$\tilde{a} = \frac{B}{2\lambda_5}, \quad \tilde{b} = c, \quad \tilde{c} = \frac{\epsilon_0|\epsilon_a|E^2\sin^2\theta}{2\lambda_5}, \tag{4.19}$$

$$\tilde{d} = -\frac{1}{2\rho}(2\lambda_2 - \lambda_5 - \mu_0), \quad \tilde{e} = \frac{\zeta}{2\rho}(2\lambda_2 - \lambda_5 - \mu_0)(\tau_1 + \tau_5). \tag{4.20}$$

$$\tilde{f} = 2c\zeta(\tau_1 + \tau_5). \tag{4.21}$$

Note that in the definition for $\tilde{d}$ we are assuming that $2\lambda_2 - \lambda_5 - \mu_0 < 0$. We justify this assumption by observing that as we approach the phase boundary between smectic and nematic, the viscosities λ_2 and λ_5 which are both temperature dependent approach zero since they are only present in the smectic phase. The Newtonian viscosity μ_0 is however always present and so at lower temperatures we expect $\tilde{d}$ to be positive. This allows us to re-write (4.17) and (4.18) as follows

$$-\tilde{a}\frac{d^2\hat{\phi}}{d\tau^2} - \tilde{b}\frac{d\hat{\phi}}{d\tau} - \tilde{c}\hat{\phi} = \omega\hat{\phi}, \tag{4.22}$$

$$-\tilde{d}\frac{d^2\hat{z}}{d\tau^2} + \tilde{e}\frac{d^2\hat{\phi}}{d\tau^2} + \tilde{f}\frac{d\hat{\phi}}{d\tau} = \omega\hat{z}. \tag{4.23}$$

Next we re-write (4.22) and (4.23) in operator form

$$\mathcal{L}\,\mathbf{x} = \omega\,\mathbf{x}, \tag{4.24}$$

where the linear differential operator $\mathcal{L}$ and vector $\mathbf{x}$ are given by

$$\mathcal{L} = \begin{bmatrix} \mathcal{L}_{11} & \mathcal{L}_{12} \\ \mathcal{L}_{21} & \mathcal{L}_{22} \end{bmatrix},\ \mathbf{x} = \begin{bmatrix} \hat{\phi} \\ \hat{z} \end{bmatrix}, \tag{4.25}$$

so that the operator elements $\mathcal{L}_{ij}$ are defined to be

$$\begin{aligned} \mathcal{L}_{11} &= -\tilde{a}\frac{d^2}{d\tau^2} - \tilde{b}\frac{d}{d\tau} - \tilde{c}, \\ \mathcal{L}_{12} &= 0, \\ \mathcal{L}_{21} &= \tilde{e}\frac{d^2}{d\tau^2} + \tilde{f}\frac{d}{d\tau}, \\ \mathcal{L}_{22} &= -\tilde{d}\frac{d^2}{d\tau^2}, \end{aligned} \tag{4.26}$$

along with the following homogeneous boundary conditions

$$\mathbf{x}(-\delta) = \mathbf{x}(\delta) = \mathbf{0}. \tag{4.27}$$

We shall return to the constant coefficient operator problem later in this chapter. Next however we shall explore the full perturbation problem as given in (4.11) and (4.12) and show how it too may be posed as an operator problem.

4.2.2 The generalised differential eigenvalue problem

The full system of perturbation equations is given in (4.11) and (4.12) along with boundary conditions given by (4.13) and parameters (4.14) and (4.15).

We shall begin by showing how the system may be written in the form of a generalised eigenvalue problem. As a start we shall assume we are at or near a phase transition, for example in the vicinity of a smectic C*-smectic A phase transition with a transition temperature T_{AC}. We assume that near the transition temperature the smectic cone angle is regarded as small and temperature

sensitive $\theta = \theta(T)$. As we increase the temperature the cone angle decreases, until finally, at the transition temperature T_{AC}, we find $\theta(T_{AC}) = 0$. This small cone angle assumption is reasonable and has been exploited to investigate the behaviour of ferroelectrics materials near transition temperatures by for example Lagerwall [30, p.177]. Then we may make the approximation $\sin\theta \approx \theta$. This means that the viscosities λ_2, λ_5, τ_2 and τ_5 may be replaced with the equivalent tilt angle expressions [4, 49]. We may treat the elastic constant B in the same manner replacing it with the equivalent tilt angle expression [49, 42]. For the viscosities we have that the tilt angle equivalents are given by

$$\tau_1 = \bar{\tau}_1\theta, \quad \tau_5 = \bar{\tau}_5\theta, \quad \lambda_2 = \bar{\lambda}_2\theta^2, \quad \lambda_5 = \bar{\lambda}_5\theta^2. \tag{4.28}$$

Similarly the elastic constant B was chosen in Chapter 2 to conform to the one constant approximation $B = B_1 = B_2$. This is the notation introduced by Saupe [41]. The tilt angle equivalent expressions for B_1 and B_2 are given by

$$B_1 = \bar{B}_1\theta^2, \quad B_2 = \bar{B}_2\theta^2. \tag{4.29}$$

With this in mind we shall use the following tilt angle equivalent expression

$$B = \bar{B}\theta^2, \tag{4.30}$$

where we make the association $\bar{B} = \bar{B}_1 = \bar{B}_2$. Then we may re-write equations (4.11) and (4.12) as

$$\begin{aligned}\bar{B}\theta^2\frac{d^2\hat{\phi}}{d\tau^2} + 2\bar{\lambda}_5\theta^2 c\frac{d\hat{\phi}}{d\tau} - (\bar{\tau}_1 + \bar{\tau}_5)\theta\tanh(\zeta\tau)\frac{d\hat{w}}{d\tau} \\ -(P_0 E\tanh(\zeta\tau) - \epsilon_0\epsilon_a E^2\theta^2(1 - 2\,\mathrm{sech}^{\,2}(\zeta\tau)) - 2\bar{\lambda}_5\theta^2\omega)\,\hat{\phi} = 0,\end{aligned} \tag{4.31}$$

$$\begin{aligned}c(\bar{\tau}_1 + \bar{\tau}_5)\theta\tanh(\zeta\tau)\frac{d^2\hat{\phi}}{d\tau^2} + \frac{1}{2}\left(\left(2\bar{\lambda}_2 - \bar{\lambda}_5\right)\theta^2\,\mathrm{sech}^{\,2}(\zeta\tau) - \mu_0\right)\frac{d^2\hat{w}}{d\tau^2} \\ + (\bar{\tau}_1 + \bar{\tau}_5)\,\theta\left(2c\zeta\,\mathrm{sech}^2(\zeta\tau) + \omega\tanh(\zeta\tau)\right)\frac{d\hat{\phi}}{d\tau}\end{aligned}$$

$$- \left(2\bar{\lambda}_2 - \bar{\lambda}_5\right) \theta^2 \zeta \,\mathrm{sech}^2\left(\zeta\tau\right) \tanh(\zeta\tau) \frac{d\hat{w}}{d\tau}$$
$$+ \left(\bar{\tau}_1 + \bar{\tau}_5\right) \theta \left(\omega\zeta - 2c\zeta^2 \tanh(\zeta\tau)\right) \,\mathrm{sech}^{\,2}(\zeta\tau)\hat{\phi} - \rho\omega\hat{w} = 0, \qquad (4.32)$$

with the same parameters (4.14) and (4.15) and boundary conditions (4.13) as before. The problem posed at (4.31) and (4.32) is essentially a linear operator problem and we may write it as follows

$$\mathcal{A}\mathbf{x} = \omega\mathcal{B}\mathbf{x}, \qquad (4.33)$$

where we define the operators $\mathcal{A}$ and $\mathcal{B}$ and the vector $\mathbf{x}$ to be

$$\mathcal{A} = \begin{bmatrix} \mathcal{A}_{11} & \mathcal{A}_{12} \\ \mathcal{A}_{21} & \mathcal{A}_{22} \end{bmatrix}, \; \mathcal{B} = \begin{bmatrix} \mathcal{B}_{11} & \mathcal{B}_{12} \\ \mathcal{B}_{21} & \mathcal{B}_{22} \end{bmatrix}, \; \mathbf{x} = \begin{bmatrix} \hat{\phi} \\ \hat{z} \end{bmatrix}. \qquad (4.34)$$

As before the boundary conditions for this problem are

$$\mathbf{x}(-\delta) = \mathbf{x}(\delta) = \mathbf{0}. \qquad (4.35)$$

Now the operator elements $\mathcal{A}$ and $\mathcal{B}$ may be written in the form

$$\begin{aligned}
\mathcal{A}_{11} &= \bar{B}\theta^2 \frac{d^2}{d\tau^2} + 2\bar{\lambda}_5\theta^2 c\frac{d}{d\tau} - (P_0 E \tanh(\zeta\tau) - \epsilon_0\epsilon_a E^2\theta^2(1 - 2\mathrm{sech}^2(\zeta\tau))), \\
\mathcal{A}_{12} &= -(\bar{\tau}_1 + \bar{\tau}_5)\theta\frac{d}{d\tau}, \\
\mathcal{A}_{21} &= (\bar{\tau}_1 + \bar{\tau}_5)\theta(c\tanh(\zeta\tau)\frac{d^2}{d\tau^2} + 2c\zeta\mathrm{sech}^2(\zeta\tau)\frac{d}{d\tau} - 2\zeta^2\tanh(\zeta\tau)\mathrm{sech}^2(\zeta\tau)), \\
\mathcal{A}_{22} &= \frac{1}{2}((2\bar{\lambda}_2 - \bar{\lambda}_5)\theta^2\mathrm{sech}^2(\zeta\tau) - \mu_0)\frac{d^2}{d\tau^2} - (2\bar{\lambda}_2 - \bar{\lambda}_5)\theta^2\zeta\mathrm{sech}^2(\zeta\tau)\tanh(\zeta\tau)\frac{d}{d\tau},
\end{aligned} \qquad (4.36)$$

and

$$\begin{aligned}
\mathcal{B}_{11} &= 2\bar{\lambda}_5\theta^2, \\
\mathcal{B}_{12} &= 0, \\
\mathcal{B}_{21} &= (\bar{\tau}_1 + \bar{\tau}_5)\theta(\tanh(\zeta\tau)\frac{d}{d\tau} + \zeta\mathrm{sech}^2(\zeta\tau)), \\
\mathcal{B}_{22} &= -\rho.
\end{aligned} \qquad (4.37)$$

And this allow us to write (4.33) in the form

$$(\mathcal{A} - \omega\mathcal{B})\mathbf{x} = \mathbf{0}. \tag{4.38}$$

Compare (4.38) with the constant coefficient differential eigenvalue problem (4.24) where the operator $\mathcal{B}$ is replaced with the identity operator. The equation (4.38) represents what is known as a *generalised differential eigenvalue problem.*

4.3 Stability analysis by weighted residual methods

In Appendix F we consider the conditions required to make an operator $\mathcal{L} \in \mathbb{R}^{2\times 2}$ self-adjoint. We can show using these conditions that the generalised differential eigenvalue problem (4.38) and the simplified differential eigenvalue problem (4.24) are both non-self-adjoint. In fact in order to ensure self-adjointness in the generalised differential eigenvalue problem given at (4.33) requires [61]

$$\int_a^b (u\mathcal{A}v - v\mathcal{A}u)\, dx = 0, \text{ and } \int_a^b (u\mathcal{B}v - v\mathcal{B}u)\, dx = 0,\ u, v \in u_{TF}, \tag{4.39}$$

where u_{TF} represents the set of admissible trial functions. Analysing the properties of non-self-adjoint operators [62] is notoriously difficult. In order to appreciate the problems involved in studying non-self-adjoint systems it pays to consider briefly the relative ease with which the spectral properties of a self-adjoint system may be determined.

Self-adjoint linear operators enjoy the distinct advantage of having an extensive and well researched canon of solution techniques provided by the *spectral theory.* Operator problems which are self-adjoint in character [63] are often approached using a variational method such as the Rayleigh-Ritz method or the assumed modes method [64].

Numerical techniques such as the Rayleigh-Ritz method are available for the determination the spectral properties of the eigenvalues of self-adjoint operator

problems. In a self-adjoint system, by exploiting the orthogonality of the basis functions which constrains the sum of the squares of the Fourier coefficients to be equal to one, and then establishing criteria which ensure that the operator is positive definite the eigenvalues of the operator are then guaranteed to be non-negative.

By applying the Ritz method, numerically computed approximations to the first eigenvalue provide an upper bound on the exact value of the first eigenvalue whose accuracy improves as the number of orthogonal functions satisfying the orthogonality condition is increased. This method is illustrated in [63]. Certainly in the case of [63] the value of the Rayleigh-Ritz scheme lies in the ability of the technique to determine perturbation response times since the dominant behaviour of the decaying perturbation is controlled by the first eigenvalue.

In order to tackle either of the non-self-adjoint problems discussed earlier in this chapter we are forced to use numerical approximations. The nature of the equations at (4.38) and (4.24) suggests the use of weighted residual methods as a method of solution. Broadly speaking weighted residual methods discussed in Appendix E utilise a weighting function which when applied to a residual gives an expression which when integrated should vanish identically, the so called orthogonality condition.

Schemes which fall under the scope of weighted residuals include among others [65, 64, 66, 67] the Galerkin method, the collocation method, the least squares method and the method of subdomains. The solution method we shall study here will be the method of Galerkin and we shall encounter the collocation method later in this chapter. We begin our analysis by considering the constant coefficient problem (4.24) and (4.25) along with the boundary conditions (4.27)

4.3.1 Analysis of the constant coefficient differential eigenvalue problem

In this section we shall concern ourselves with the analysis of (4.24) and (4.25) along with boundary conditions (4.27). As was demonstrated in sub-section (4.2.1) we may reduce the full differential eigenvalue problem to one which involves constant coefficients. Whilst this is *not* an accurate representation of the full differential eigenvalue problem, it is nonetheless accessible and it is possible to demonstrate in broad terms how the method of weighted residuals may be applied to a non-self-adjoint differential eigenvalue problem.

We shall concern ourselves with studying the Galerkin method as described in Appendix E. To begin with consider the problem as initially posed at (4.22) and (4.23). We begin by defining the vector $\mathbf{x}^n \in \mathbb{C}^{2\times 1}$ along with elements $\hat{\phi}^n$ and $\hat{z}^n$ thus

$$\mathbf{x}^n = \left[\begin{array}{c} \hat{\phi}^n \\ \hat{z}^n \end{array} \right], \ \hat{\phi}^n = \sum_{j=1}^{n} a_j \phi_j, \ \hat{z}^n = \sum_{j=n+1}^{2n} a_j \phi_j. \tag{4.40}$$

We assume here that $\phi_j \in C^2[-\delta, \delta]$ are trial functions chosen to satisfy the boundary conditions at $\tau = -\delta$ and $\tau = \delta$. We form the residuals $R_1(\mathbf{x}^n, \tau)$ and $R_2(\mathbf{x}^n, \tau)$ and write these as follows

$$\begin{aligned} R_1(\mathbf{x}^n, \tau) &= \mathcal{L}_{11}\hat{\phi}^n + \mathcal{L}_{12}\hat{z}^n - \omega\hat{\phi}^n \\ &= -\tilde{a}\sum_{j=1}^{n} a_j \phi_j'' - \tilde{b}\sum_{j=1}^{n} a_j \phi_j' - \tilde{c}\sum_{j=1}^{n} a_j \phi_j - \omega\sum_{j=1}^{n} a_j \phi_j, \qquad (4.41) \\ R_2(\mathbf{x}^n, \tau) &= \mathcal{L}_{21}\hat{\phi}^n + \mathcal{L}_{22}\hat{z}^n - \omega\hat{z}^n \\ &= -\tilde{d}\sum_{j=n+1}^{2n} a_j \phi_j'' + \tilde{e}\sum_{j=1}^{n} a_j \phi_j'' + \tilde{f}\sum_{j=1}^{n} a_j \phi_j' - \omega\sum_{j=n+1}^{2n} a_j \phi_j. \\ . \qquad (4.42) \end{aligned}$$

Next we multiply (4.41) by $\phi_i, \ i = 1, 2, \ldots, n$ and (4.42) by $\phi_i, \ i = n+1, n+2, \ldots, 2n$ giving

$$-\tilde{a}\sum_{j=1}^{n} a_j \phi_j'' \phi_i - \tilde{b}\sum_{j=1}^{n} a_j \phi_j' \phi_i - \tilde{c}\sum_{j=1}^{n} a_j \phi_j \phi_i = \omega\sum_{j=1}^{n} a_j \phi_j \phi_i, \ i = 1, 2, \ldots, n, \tag{4.43}$$

and

$$-\tilde{d}\sum_{j=n+1}^{2n} a_j\phi_j''\phi_i+\tilde{e}\sum_{j=1}^{n} a_j\phi_j''\phi_i+\tilde{f}\sum_{j=1}^{n} a_j\phi_j'\phi_i=\omega\sum_{j=n+1}^{2n} a_j\phi_j\phi_i,\ i=n+1,\ldots,2n.. \tag{4.44}$$

This step effectively discretizes the problem. Then integrating (4.43) and (4.44) with respect to τ over the interval $\tau \in [-\delta, \delta]$ we find that the problem reduces to one of the form

$$\sum_{j=1}^{2n} (p_{ij}a_j + q_{ij}a_j + r_{ij}a_j - \omega s_{ij}a_j) = 0,\ i = 1,\ldots,2n. \tag{4.45}$$

Now if we let

$$A_{ij} = p_{ij} + q_{ij} + r_{ij}, \tag{4.46}$$

and

$$B_{ij} = s_{ij}, \tag{4.47}$$

along with

$$\mathbf{a} = (a_1, a_2, \ldots, a_{2n})^T, \tag{4.48}$$

we may write (4.45) as the generalised eigenvalue problem

$$\mathsf{A}\mathbf{a} = \omega\mathsf{B}\mathbf{a}. \tag{4.49}$$

The differential eigenvalue problem has at this point been reduced to the form of an algebraic eigenvalue problem. The system represents $2n$ homogeneous linear simultaneous equations in $2n$ unknowns. The task now is to determine the discrete eigenvalue spectrum and we tackle this in the next section.

4.3.2 Derivation of the algebraic eigenvalue problem

We shall employ linear algebra solution techniques in order to determine the discrete eigenvalue spectrum. Referring to the algebraic problem posed at (4.45)

the matrix elements p_{ij}, q_{ij}, r_{ij} and s_{ij} may be written as follows. First of all the elements represented by p_{ij}

$$p_{ij} = -\tilde{a}\int_{-\delta}^{\delta}\phi_j''\phi_i d\tau = \tilde{a}\int_{-\delta}^{\delta}\phi_j'\phi_i' d\tau = p_{ji},\ i,j = 1,2,\ldots,n, \tag{4.50}$$

$$p_{ij} = p_{ji} = 0,\ i = 1,2,\ldots,n;\ j = n+1, n+2,\ldots,2n, \tag{4.51}$$

$$p_{ij} = -\tilde{e}\int_{-\delta}^{\delta}\phi_j''\phi_i d\tau = \tilde{e}\int_{-\delta}^{\delta}\phi_j'\phi_i' d\tau = p_{ji},\ i = n+1,\ldots,2n;\ j = 1,\ldots,n \tag{4.52}$$

$$p_{ij} = -\tilde{d}\int_{-\delta}^{\delta}\phi_j''\phi_i d\tau = \tilde{d}\int_{-\delta}^{\delta}\phi_j'\phi_i' d\tau = p_{ji},\ i,j = n+1,\ldots,2n. \tag{4.53}$$

Similarly for q_{ij} we find the following expressions

$$q_{ij} = -\tilde{b}\int_{-\delta}^{\delta}\phi_j'\phi_i d\tau,\ \ i,j = 1,2,\ldots,n, \tag{4.54}$$

$$q_{ij} = q_{ji} = 0,\ \ i = 1,2,\ldots,n;\ j = n+1, n+2,\ldots,2n, \tag{4.55}$$

$$q_{ij} = \tilde{f}\int_{-\delta}^{\delta}\phi_j'\phi_i d\tau,\ \ i = n+1,\ldots,2n;\ j = 1,\ldots,n, \tag{4.56}$$

$$q_{ij} = q_{ji} = 0,\ \ i,j = n+1,\ldots,2n. \tag{4.57}$$

In addition we find that r_{ij} maybe written in the form

$$r_{ij} = -\tilde{c}\int_{-\delta}^{\delta}\phi_j\phi_i d\tau = r_{ji},\ \ i,j = 1,2\ldots,n, \tag{4.58}$$

$$r_{ij} = r_{ji} = 0,\ \ i = 1,2,\ldots,n;\ j = n+1, n+2,\ldots,2n, \tag{4.59}$$

$$r_{ij} = r_{ji} = 0,\ \ i = n+1, n+2,\ldots,2n;\ j = 1,2,\ldots,n, \tag{4.60}$$

$$r_{ij} = r_{ji} = 0,\ \ i,j = n+1, n+2,\ldots,2n. \tag{4.61}$$

And finally, the matrix elements s_{ij} maybe written

$$s_{ij} = \int_{-\delta}^{\delta}\phi_i\phi_j d\tau = s_{ji},\ \ i,j = 1,2,\ldots,n, \tag{4.62}$$

$$s_{ij} = s_{ji} = 0,\ \ i = 1,2,\ldots,n; j = n+1,\ n+2,\ldots,2n, \tag{4.63}$$

$$s_{ij} = s_{ji} = 0,\ \ i = n+1, n+2,\ldots,2n;\ j = 1,2,\ldots,n, \tag{4.64}$$

$$s_{ij} = \int_{-\delta}^{\delta}\phi_i\phi_j d\tau = s_{ji},\ \ i,j = n+1, n+2,\ldots,2n. \tag{4.65}$$

It is worth noting a number of points at this stage. The first is that the matrices A and B which form our eigenvalue problem as posed at (4.49), are non-hermitian. This is to be expected given that the differential eigenvalue problem we began with was found to be non-self-adjoint. Of course this means that the eigenvalues for the system are generally complex so we expect that $\omega \in \mathbb{C}$.

Solving an algebraic eigenvalue problem such as this involves solving for the eigenvalue ω and the Fourier coefficients, the a_j's of the problem. This typically requires resorting to solution techniques such as those presented in [65, p.120-124]. Our principal aim here shall be to analyse the eigenvalue spectrum for this system and so we shall not pursue a more general study of the Fourier coefficients at this time.

The next point relates to the selection of trial functions, the ϕ_j's and z_j's in the problem. We need to select trial functions which satisfy the boundary conditions of our problem. In order to ensure rapid convergence of the eigenvalues, we would normally seek trial functions which represented good approximations to the actual eigenfunctions of the system under consideration.

Here, however for convenience we shall choose our trial functions so that they simply satisfy the boundary conditions specified by the problem. Although the rate of convergence is important our main concern is to demonstrate the method working.

So for our trial functions we may in principle use trigonometric or polynomial forms so long as they satisfy our boundary conditions. With this in mind we shall use polynomial trial functions of the following form

$$\phi_j(\tau) = (\tau - \delta)^j(\tau + \delta). \tag{4.66}$$

Then we may approximate our perturbation solutions in the form

$$\hat{\phi}^n(\tau) = \sum_{j=1}^{n} a_j(\tau - \delta)^j(\tau + \delta),\ \hat{z}^n(\tau) = \sum_{j=n+1}^{2n} a_j(\tau - \delta)^j(\tau + \delta). \tag{4.67}$$

Now, having specified the trial functions so that they exactly match the boundary conditions we investigate the eigenvalues of (4.49). We shall restrict our initial investigation to the case where $n = 2$. This gives an algebraic eigenvalue problem consisting of four homogeneous linear simultaneous equations in four unknowns. We write (4.49) in the form

$$(\mathsf{A} - \omega\mathsf{B})\,\mathbf{a} = \mathbf{0}. \tag{4.68}$$

Then letting

$$\mathsf{M} = \mathsf{A} - \omega\mathsf{B}, \tag{4.69}$$

we are left to solve the following system of equations

$$\mathsf{M}\mathbf{a} = \mathbf{0}. \tag{4.70}$$

The elements of M which we denote as m_{ij} may be determined straightforwardly using (4.69) and (4.50)-(4.62). The elements of M are given then by

$$\begin{aligned}
m_{11} &= \frac{8}{3}\tilde{a}\delta^3 - \frac{16}{15}\tilde{c}\delta^5 - \frac{16}{15}\omega\delta^5,\\
m_{12} &= \frac{16}{15}\tilde{c}\delta^6 + \frac{16}{15}\omega\delta^6 - \frac{8}{15}\tilde{b}\delta^5 - \frac{8}{3}\tilde{a}\delta^4,\\
m_{13} &= 0,\\
m_{14} &= 0,\\
m_{21} &= \frac{16}{15}\tilde{c}\delta^6 + \frac{16}{15}\omega\delta^6 + \frac{8}{15}\tilde{b}\delta^5 - \frac{8}{3}\tilde{a}\delta^4,\\
m_{22} &= \frac{64}{15}\tilde{a}\delta^5 - \frac{128}{105}\tilde{c}\delta^7 - \frac{128}{105}\omega\delta^7,\\
m_{23} &= 0,\\
m_{24} &= 0,\\
m_{31} &= \frac{16}{15}\tilde{f}\delta^6 - \frac{16}{5}\tilde{e}\delta^5,\\
m_{32} &= \frac{32}{5}\tilde{e}\delta^6 - \frac{64}{105}\tilde{f}\delta^7,\\
m_{33} &= \frac{384}{35}\tilde{d}\delta^7 - \frac{128}{63}\omega\delta^9,
\end{aligned}$$

$$
\begin{aligned}
m_{34} &= \frac{128}{45}\omega\delta^{10} - \frac{128}{7}\tilde{d}\delta^{8}, \\
m_{41} &= \frac{64}{15}\tilde{e}\delta^{6} - \frac{64}{35}\tilde{f}\delta^{7}, \\
m_{42} &= \frac{32}{21}\tilde{f}\delta^{8} - \frac{1024}{105}\tilde{e}\delta^{7}, \\
m_{43} &= \frac{128}{45}\omega\delta^{10} - \frac{128}{7}\tilde{d}\delta^{8}, \\
m_{44} &= \frac{2048}{63}\tilde{d}\delta^{9} - \frac{2048}{495}\omega\delta^{11}.
\end{aligned} \tag{4.71}
$$

Now in order to solve (4.70) we first must determine values of ω for which (4.70) has non-trivial solutions. In other words, borrowing notation from [68] and recalling (4.69), we seek a set of eigenvalues $\sigma(\mathsf{A},\mathsf{B})$ such that

$$\sigma(\mathsf{A},\mathsf{B}) = \{\omega \in \mathbb{C} : \det(\mathsf{A} - \omega\mathsf{B}) = 0\}. \tag{4.72}$$

We may calculate $\det(\mathsf{A} - \omega\mathsf{B}) = 0$ using a symbolic mathematics package such as MAPLE and we find that the set of eigenvalues $\sigma(\mathsf{A},\mathsf{B})$ satisfying (4.70) is given by

$$\sigma(\mathsf{A},\mathsf{B}) = \left(\tfrac{247}{21} \pm \tfrac{8\sqrt{466}}{21}\right)\tfrac{\tilde{d}}{\delta^2}, \tfrac{1}{2\delta^2}\left(13\tilde{a} - 2\delta^2\tilde{c} \pm \sqrt{64\tilde{a}^2 - 7\delta^2\tilde{b}^2}\right). \tag{4.73}$$

Note that the first two eigenvalues are *always* real and positive since

$$\tfrac{247}{21} - \tfrac{8\sqrt{466}}{21} \approx 3.538 > 0 \ \text{ and } \ \tfrac{\tilde{d}}{\delta^2} > 0. \tag{4.74}$$

because as we noted earlier $\tilde{d} > 0$. Note also that the remaining roots are real if

$$64\tilde{a}^2 - 7\delta^2\tilde{b}^2 = 0, \tag{4.75}$$

imaginary if

$$64\tilde{a}^2 - 7\delta^2\tilde{b}^2 < 0 \ \text{ and } \ 13\tilde{a} - 2\delta^2\tilde{c} = 0, \tag{4.76}$$

and complex if

$$64\tilde{a}^2 - 7\delta^2\tilde{b}^2 < 0 \ \text{ and } \ 13\tilde{a} - 2\delta^2\tilde{c} \neq 0, \tag{4.77}$$

In order to get a quantitative feel for how the Galerkin method behaves when applied to the model problem we have been considering we shall perform a

numerical analysis using appropriate physical parameters. First of all referring to Carlsson et. al. and Stewart [49, 4] we may construct a table of values which reflect typical values for viscosity, elastic constants, material density and dielectric and polarisation terms. We must be mindful however of the fact that the matrix M is structured in such a way that terms containing τ_1 and τ_5 do not generally appear in the characteristic equation and consequently play no role in determining the eigenvalue response of this particular system.

We begin by defining the viscous terms we shall be employing. Recalling that the viscous terms λ_5 and λ_2 are temperature dependent whereas μ_0 is not we list in Table 4.1 the values μ_0, $\bar{\lambda}_5$ and $\bar{\lambda}_2$. Referring to [4] we determine the

Parameter	Symbol	Value
Isotropic viscosity	μ_0	0.2 Pa s
Nematic-like viscosities	$\bar{\lambda}_2$	-0.12 Pa s
	$\bar{\lambda}_5$	0.1 Pa s

Table 4.1: Isotropic and nematic-like viscosities

value of θ for this problem by supposing that the relationship between λ_5 and λ_2 is given by the expression

$$\lambda_5 - \lambda_2 = \left(\bar{\lambda}_5 - \bar{\lambda}_2\right)\theta^2 = \frac{13}{400}. \tag{4.78}$$

Then we may express the smectic cone angle θ as

$$\theta = \pm\frac{\sqrt{13}}{20}\left\{\bar{\lambda}_5 - \bar{\lambda}_2\right\}^{-\frac{1}{2}}. \tag{4.79}$$

Now with B expressed in its θ dependent form as given at (4.30) we define the remaining physical parameters in Table 4.2. We note here that the soliton model adopted throughout this analysis assumes a negative dielectric anisotropy. This is regarded as a reasonable assumption since many smectic C* materials possess negative dielectric anisotropy. For instance Müller and Jayaraman [69] studied

the dielectric properties of ferroelectric compounds 80SI and FeC8 and found the dielectric anisotropy to be negative over large temperature ranges in both materials. Other smectic C* materials reported as having negative dielectric anisotropy include SCE3 [4, p. 313] which at 15°C has a dielectric anisotropy of $\epsilon_a = -1.94$ as reported by MacGregor [70]. The manufacturer Merck remarks in its handbook on liquid crystal mixtures [71] that it is desirable for ferroelectric materials to possess negative dielectric anisotropy specifically in order to obtain dielectric stabilization during the switching process in SSFLC devices. Stabilization via an a.c. field is explored in detail by Gouda et. al. [33]. Using

Parameter	Symbol	Value
Smectic cone angle	θ	0.384 rad
Elastic constant	$\bar{B}$	1×10^{-11} N
Polarisation constant	P_0	-100μC m^{-2}
Electric field	E	0.1 V μm^{-1}
Permittivity of free space	ϵ_0	8.854×10^{-12} F m^{-1}
Dielectric anisotropy	ϵ_a	-2
Density	ρ	1000 kg m^{-3}

Table 4.2: Smectic cone angle, elastic, dielectric and material density parameters

the parameter values tabulated in Tables 4.1 and 4.2 we choose values of n such that $n \in [2, 6]$. Then starting at $n = 2$ we form the characteristic equation corresponding to the set of eigenvalues specified at (4.72), and form successively higher order approximations by considering larger values of n. As we increase the number of terms we use in the perturbation expansions we refine the eigenvalue approximations.

For $n = 2$ with the parameters given above we find that there are four eigenvalues in total, two real and two complex conjugate. When $n = 4$ we find that there are eight eigenvalues four real and four complex. By selecting the first pair of real roots generated when $n = 2$ and tracking these eigenvalues for successively larger values of n we may show numerically that in the case

of the first eigenmodes the eigenvalues demonstrate convergent behaviour. We track the first two real positive eigenvalues for our algebraic eigenvalue problem and plot the results in Figure 4.1. We plot the eigenvalues up to $n = 12$ so that

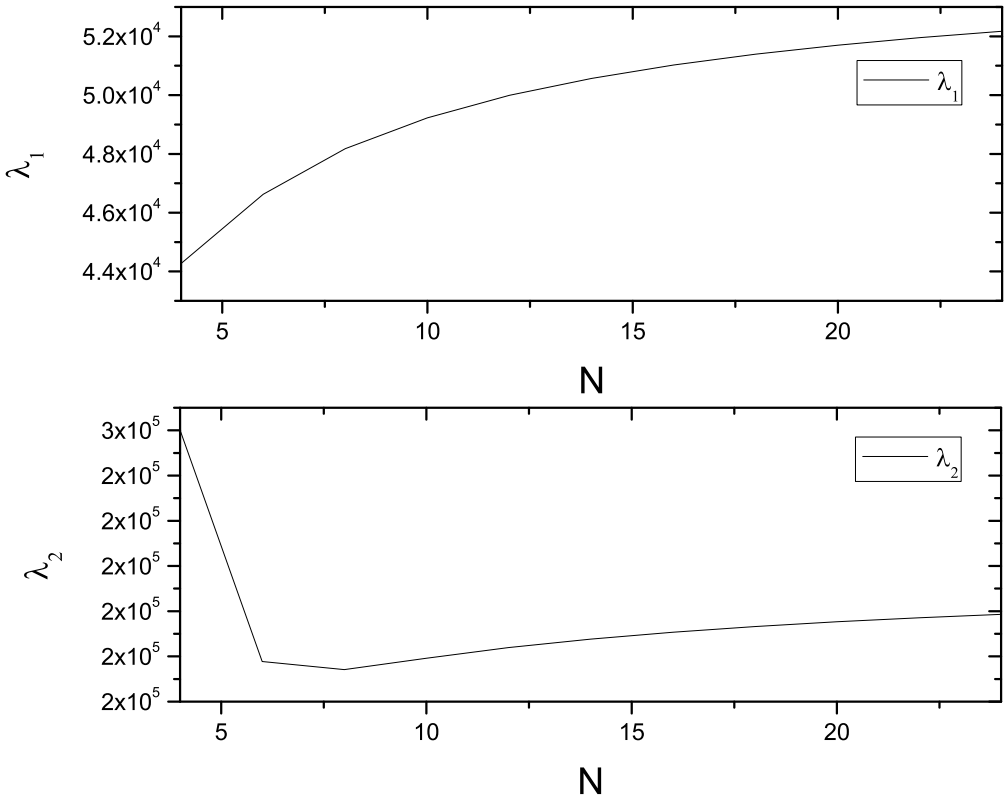

Figure 4.1: Plots of the first two real eigenvalues λ_1 and λ_2 versus the total number of trial functions N used in the approximations. The interval width used to compute these values was 200μm. The time taken to generate the data for $N = 24$ was of the order of four days.

$N = 2n = 24$ in the figures. Fundamentally what this means is that we are using at most 12 summed trial functions for each of the perturbation terms giving 24 in total. As noted in the figure, the time taken to compute the eigenmodes when $N = 24$ (that is when $n = 12$) was approximately four days using the symbolic mathematics package MAPLE. In order to resolve all 24 roots 120 digits of precision were required. This may seem excessive but the precision had to be set high in order that the root finding function could successfully identify the roots. Setting the number of digits of precision lower introduced numerical

errors and resulted in the Newton solver becoming unstable.

The graphs shown in Figure 4.1 indicate that the first two eigenvalues appear to be converging to finite values as expected. This does not of course constitute a proof. However it strongly suggests that the Galerkin method is finding appropriate eigenvalues given the trial functions we are assuming. In order to back this up we show in Figure 4.2 the absolute error between consecutive calculations of the first and second real eigenvalues λ_1 and λ_2. We shall extend the

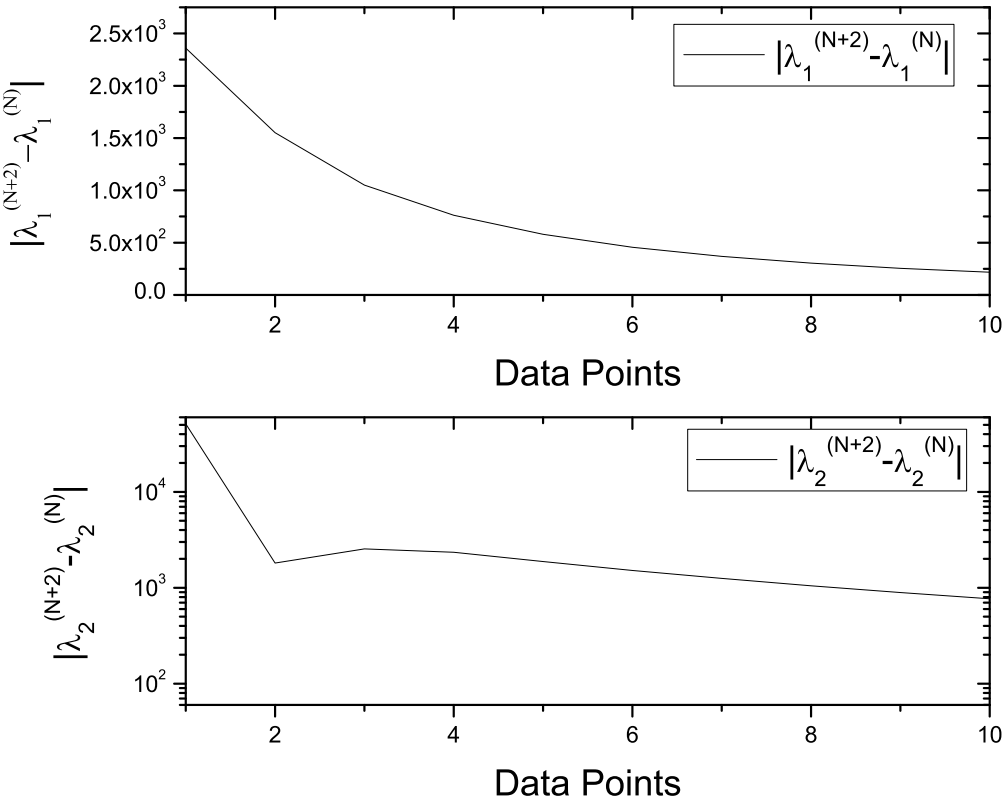

Figure 4.2: Plots of $|\lambda_1^{(N+2)} - \lambda_1^{(N)}|$ and $\log|\lambda_2^{(N+2)} - \lambda_2^{(N)}|$.

method we have outlined here to examine the very much more complex problem represented by (4.38), (4.37), (4.36) and (4.35) in the next section where we study the operator problem in full.

4.3.3 Analysis of the generalised differential eigenvalue problem

We shall in this section investigate the full differential eigenvalue problem using the ideas we developed in the previous section. In particular we aim to develop a physical understanding of the behaviour of the system specified at (4.38), (4.37), (4.36) and (4.35) and we shall rely heavily on numerical techniques as we do so.

Because of the general complexity of the full non-self-adjoint problem we shall not be delving too deeply into the mathematical details of the weighted residual method used to investigate the system. The techniques employed are much the same as those used for the constant coefficient eigenvalue problem and the general method of implementation has already been discussed.

Of principal concern shall be the investigation of the stability properties of the system. Throughout this section we shall concentrate on a relatively simple model where each of the perturbation terms is approximated by two trial functions. Whilst two terms per approximation does not represent the height of accuracy, it does give quantitatively useful results.

We shall later in this study, make use of the notion of marginal stability. It is clear from numerical work that frequently, in the models we intend to investigate, the first four eigenvalues tend to occur in the form of two real positive eigenvalues and two complex conjugate eigenvalues all of which are nonlinearly dependent on the electric field strength E.

Typically we might expect these eigenvalues to represent the dominant eigenmodes in the spectrum for the problem in hand. In particular so far as stability is concerned, given the form we have assumed for exponential decay any eigenvalue with $\Re(\omega) > 0$ represents a stable perturbation. Of course the eigenvalue ω is strongly E field dependent so that generally $\omega = \omega(E)$. Then as we vary E the eigenvalue can in principle cross from positive to negative or negative

to positive. As an example consider the graphs in Figure 4.3. Note first that

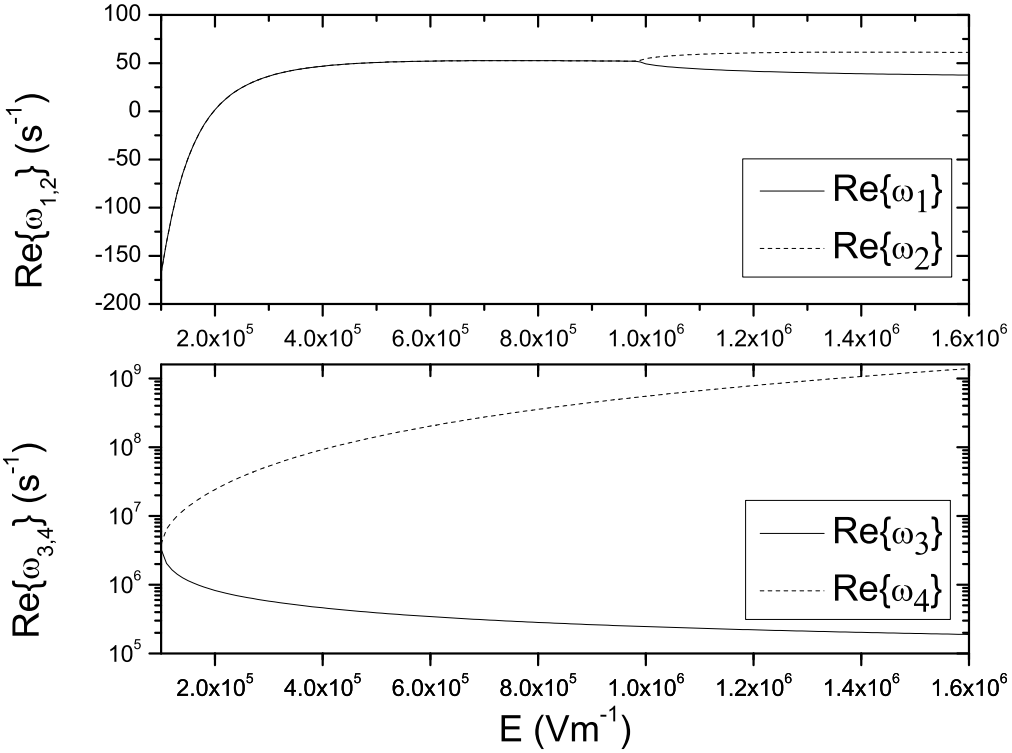

Figure 4.3: Plot of the first four eigenvalues for the problem as described at (4.38), (4.37), (4.36) and (4.35) with varying E field. The data presented in Table's 4.1 and 4.2 were used along with $\bar{\tau}_5 = 0.01$. Then $\bar{\tau}_1$ is determined from $\bar{\tau}_1 = \bar{\tau}_5 - 0.0273\ \theta^{-1}$. To plot the figures we set $n = 2$ and used 20 significant digits to perform the calculations. The interval width used to compute these values was taken to be 200μm wide, so $\delta = 100\mu$m.

there are four eigenvalues ω_1, ω_2, ω_3 and ω_4. Two of the eigenvalues ω_3 and ω_4 are generally real and positive. The other eigenvalues ω_1 and ω_2 are generally complex conjugate up to a field strength of $E \approx 1 \times 10^6 Vm^{-1}$. Beyond this value of E we find that ω_1 and ω_2 become generally real and this is indicated by the bifurcation point beyond which $\Re(\omega_1) \neq \Re(\omega_2)$. When the electric field strength is of the order of $1 \times 10^{-5} Vm^{-1}$ we notice that the real parts of ω_1 and ω_2 change sign and we denote the value of E at which this takes place by E_c. When $E < E_c$ we find that $\Re(\omega_1) < 0$ and $\Re(\omega_2) < 0$. Similarly when $E > E_c$ we find that $\Re(\omega_1) > 0$ and $\Re(\omega_2) > 0$. The point at which the real parts of $\omega_{1,2}$

cross the E axis represent a transition from an *unstable* to a *stable* state.

We choose to interpret this stability transition in the following way. Consider equation (2.9). We know that this equation has an exact solution given by (2.10) along with (2.11) and (2.12). This solution predicts the existence of a travelling wave for all values of the electric field E. However it is known from experiment that travelling wave phenomena do not occur at all field strengths from $E > 0$. In fact it is generally the case that fields of the order of $1 \times 10^5 - 1 \times 10^7$ Vm^{-1} are required in order to initiate propagating soliton-like behaviour.

Remember however that equation (2.9) represents an approximation. In order to fully determine the physical behaviour of the system under investigation we must consider the conserved linear momentum and mass equations. The resultant perturbation problem which we are in the process of analysing breaks down for values of E much less than approximately 1×10^5 Vm^{-1}, but in the field regime we are studying the eigenvalue data may be expected to offer a reasonable representation of what the physical system is doing at physically plausible field strengths. At the critical field strength E_c our hypothesis is that the field is sufficiently energetic that a travelling wave might be expected to manifest itself in a material sample subject to the same physical conditions as the model.

In principle and in fact applying the Galerkin method to the linear differential operator problem we constructed at (4.36), (4.37) and (4.38) involves a straightforward extension of the weighted residual method presented at (4.40), (4.41) and (4.42). The graphs at Figure 4.3 were both constructed using this method. We construct the residuals as before and incorporate the differential operator $\mathcal{B}$, then

$$\begin{aligned} R_1(\mathbf{x}^n, \tau) &= \mathcal{A}_{11}\hat{\phi}^n + \mathcal{A}_{12}\hat{z}^n - \omega\left(\mathcal{B}_{11}\hat{\phi}^n + \mathcal{B}_{12}\hat{z}^n\right) \\ &= \mathcal{A}_{11}\sum_{j=1}^{n} a_j\phi_j + \mathcal{A}_{12}\sum_{j=n+1}^{2n} a_j\phi_j - \omega\left(\mathcal{B}_{11}\sum_{j=1}^{n} a_j\phi_j + \mathcal{B}_{12}\sum_{j=n+1}^{2n} a_j\phi_j\right), \end{aligned}$$

(4.80)

and

$$\begin{aligned} R_2(\mathbf{x}^n,\tau) &= \mathcal{A}_{21}\hat{\phi}^n + \mathcal{A}_{22}\hat{z}^n - \omega\left(\mathcal{B}_{21}\hat{\phi}^n + \mathcal{B}_{22}\hat{z}^n\right) \\ &= \mathcal{A}_{21}\sum_{j=1}^{n} a_j\phi_j + \mathcal{A}_{22}\sum_{j=n+1}^{2n} a_j\phi_j - \omega\left(\mathcal{B}_{21}\sum_{j=1}^{n} a_j\phi_j + \mathcal{B}_{22}\sum_{j=n+1}^{2n} a_j\phi_j\right). \end{aligned} \tag{4.81}$$

Now we multiply (4.80) by $\phi_i,\ i = 1, 2, \cdots, n$ and (4.81) by $\phi_i,\ i = n+1, n+2, \cdots, 2n$ and integrate with respect to τ over the $\tau \in [-\delta, \delta]$ to get

$$\begin{aligned} \int_{-\delta}^{\delta} \phi_i R_1\, d\tau &= \int_{-\delta}^{\delta} \sum_{j=1}^{n} a_j\phi_i\mathcal{A}_{11}\phi_j\, d\tau + \int_{-\delta}^{\delta} \sum_{j=n+1}^{2n} a_j\phi_i\mathcal{A}_{12}\phi_j\, d\tau \\ &\quad - \omega\left(\int_{-\delta}^{\delta} \sum_{j=1}^{n} a_j\phi_i\mathcal{B}_{11}\phi_j\, d\tau + \int_{-\delta}^{\delta} \sum_{j=n+1}^{2n} a_j\phi_i\mathcal{B}_{12}\phi_j\right) d\tau. \\ &\quad i = 1, 2, \ldots, n, \end{aligned} \tag{4.82}$$

and

$$\begin{aligned} \int_{-\delta}^{\delta} \phi_i R_2\, d\tau &= \int_{-\delta}^{\delta} \sum_{j=1}^{n} a_j\phi_i\mathcal{A}_{21}\phi_j\, d\tau + \int_{-\delta}^{\delta} \sum_{j=n+1}^{2n} a_j\phi_i\mathcal{A}_{22}\phi_j\, d\tau \\ &\quad - \omega\left(\int_{-\delta}^{\delta} \sum_{j=1}^{n} a_j\phi_i\mathcal{B}_{21}\phi_j\, d\tau + \int_{-\delta}^{\delta} \sum_{j=n+1}^{2n} a_j\phi_i\mathcal{B}_{22}\phi_j\right) d\tau. \\ &\quad i = n+1, n+2, \ldots, 2n. \end{aligned} \tag{4.83}$$

Now both (4.82) and (4.83) may be expressed as

$$\begin{aligned} \int_{-\delta}^{\delta} \phi_i R_1\, d\tau &= \sum_{j=1}^{n} a_j(\phi_i, \mathcal{A}_{11}\phi_j) + \sum_{j=n+1}^{2n} a_j(\phi_i, \mathcal{A}_{12}\phi_j) \\ &\quad - \omega\left(\sum_{j=1}^{n} a_j(\phi_i, \mathcal{B}_{11}\phi_j) + \sum_{j=n+1}^{2n} a_j(\phi_i, \mathcal{B}_{12}\phi_j)\right) \\ &\quad i = 1, 2, \ldots, n, \end{aligned} \tag{4.84}$$

and

$$\int_{-\delta}^{\delta} \phi_i R_2\, d\tau = \sum_{j=1}^{n} a_j(\phi_i, \mathcal{A}_{21}\phi_j) + \sum_{j=n+1}^{2n} a_j(\phi_i, \mathcal{A}_{22}\phi_j)$$

$$- \omega \left(\sum_{j=1}^{n} a_j(\phi_i, \mathcal{B}_{21}\phi_j) + \sum_{j=n+1}^{2n} a_j(\phi_i, \mathcal{B}_{22}\phi_j) \right)$$
$$i = n+1, n+2, \ldots, 2n, \tag{4.85}$$

where we define the inner products

$$(\phi_i, \mathcal{A}_{rs}\phi_j) = \int_{-\delta}^{\delta} \phi_i \mathcal{A}_{rs}\phi_j \; d\tau, \tag{4.86}$$

and

$$(\phi_i, \mathcal{B}_{rs}\phi_j) = \int_{-\delta}^{\delta} \phi_i \mathcal{B}_{rs}\phi_j \; d\tau. \tag{4.87}$$

This allows us to express the problem in terms of block matrices as follows

$$\mathsf{A} = \left[\begin{array}{c|c} A_{11} & A_{12} \\ \hline A_{21} & A_{22} \end{array}\right] \quad \text{and} \quad \mathsf{B} = \left[\begin{array}{c|c} B_{11} & B_{12} \\ \hline B_{21} & B_{22} \end{array}\right], \tag{4.88}$$

where we define the block matrix elements as

$$A_{11} = (\phi_i, \mathcal{A}_{11}\phi_j), \quad i,j = 1,2,\ldots,n, \tag{4.89}$$
$$A_{12} = (\phi_i, \mathcal{A}_{12}\phi_j), \quad i = 1,2,\ldots,n;\ j = n+1, n+2, \ldots, 2n, \tag{4.90}$$
$$A_{21} = (\phi_i, \mathcal{A}_{21}\phi_j), \quad i = n+1, n+2, \ldots, 2n;\ j = 1,2,\ldots,2n, \tag{4.91}$$
$$A_{22} = (\phi_i, \mathcal{A}_{22}\phi_j), \quad i,j = n+1, n+2, \ldots, 2n, \tag{4.92}$$

and

$$B_{11} = (\phi_i, \mathcal{B}_{11}\phi_j), \quad i,j = 1,2,\ldots,n, \tag{4.93}$$
$$B_{12} = (\phi_i, \mathcal{B}_{12}\phi_j), \quad i = 1,2,\ldots,n;\ j = n+1, n+2, \ldots, 2n, \tag{4.94}$$
$$B_{21} = (\phi_i, \mathcal{B}_{21}\phi_j), \quad i = n+1, n+2, \ldots, 2n;\ j = 1,2,\ldots,2n, \tag{4.95}$$
$$B_{22} = (\phi_i, \mathcal{B}_{22}\phi_j), \quad i,j = n+1, n+2, \ldots, 2n, \tag{4.96}$$

with the Fourier coefficients expressed as a vector

$$\mathbf{a} = \left[\begin{array}{cccc|ccc} a_1 & a_2 & \cdots & a_n & a_{n+1} & a_{n+2} & \cdots & a_{2n} \end{array}\right]^T. \tag{4.97}$$

Finally we may write our system in the form of an algebraic eigenvalue problem, so that

$$(\mathsf{A} - \omega\mathsf{B})\mathbf{a} = \mathbf{0}. \tag{4.98}$$

Once in the form (4.98), we proceed to investigate the eigenvalue properties of this system. Using as before the method of Galerkin as a solution technique, we explore the behaviour of the system by choosing appropriate trial and weighting functions, in the discussion above these are the ϕ_j's and ϕ_i's respectively. We again choose trial and weighting functions which satisfy our boundary conditions. With this in mind we use the polynomial form employed previously at (4.66). Since we are implementing a Galerkin type method the weighting functions exactly coincide with the trial functions.

The Galerkin method as described here was infact used to generate the graphs in Figure 4.3. By setting $n = 2$ and varying the electric field E we generated four eigenvalues using two trial functions per perturbation.

4.3.4 Parameter variation and electric field strength

An obvious question to ask is how parameter variation affects the critical electric field strength E_c. We can investigate this quite straightforwardly by using the numerical scheme we discussed in the previous section and adapting it slightly. For instance we may want to investigate the critical field response to variation of the smectic cone angle θ. To do this we need to track the position of the critical field, that is the point at which the real part of the complex eigenvalues change sign, as we vary θ.

We set out to explore this and did so by setting the problem so that $n = 2$, giving again a total of four eigenvalues two of which are generally real and positive and two of which are generally complex conjugate. The method involves choosing a parameter to vary, selecting upper and lower limits for the parameter,

determining a step size and looping from the low value to the high value using the chosen step size. Then at each parameter value we look for the critical electric field that is characteristic for the model. The electric field is swept from a minimum value $E_{min} = 0.1$ V μm^{-1} to maximum value $E_{max} = 0.6$ V μm^{-1} using a step size of 0.01 V μm^{-1}.

Over this range we expect to see the real part of the complex conjugate roots pass through zero indicating a sign change. To detect the sign change in the array of real eigenvalue data we simply scan through a list of eigenvalue/electric field strength pairs until we locate a transition from negative to positive as the field strength increases. Then at the point where we detect a zero we select three points either side for a total of six data points.

To determine the critical field strength we use the six data points clustered around the zero to construct a polynomial interpolant using the MAPLE function `PolynomialInterpolant(Z,x)` which takes a list of N data points in `Z` and from this constructs a polynomial interpolant of order $N - 1$. We could improve the accuracy by increasing the number of data points chosen for the interpolant either side of the field axis but settled for six because it yields a perfectly acceptable approximation.

Then employing a suitable root solver (see Appendix H) and using the two closest electric field strengths either side of the location of the zero we refine the field strength up to a predetermined level of accuracy. Collecting the field strengths as we vary our parameter we then plot the parameter as it varies against critical field strength. Consider for example Figures 4.4 and 4.5.

In Figure 4.4 we chart the relationship between the electric field strength E_c and the rotational viscosity λ_5. The range of values of λ_5 varies from a minimum of $\lambda_5^{min} = 0.015$ Pa s to a maximum value of $\lambda_5^{max} = 0.023$ Pa s. Similarly Figure 4.5 relates the critical field strength E_c to the viscosity λ_2. In

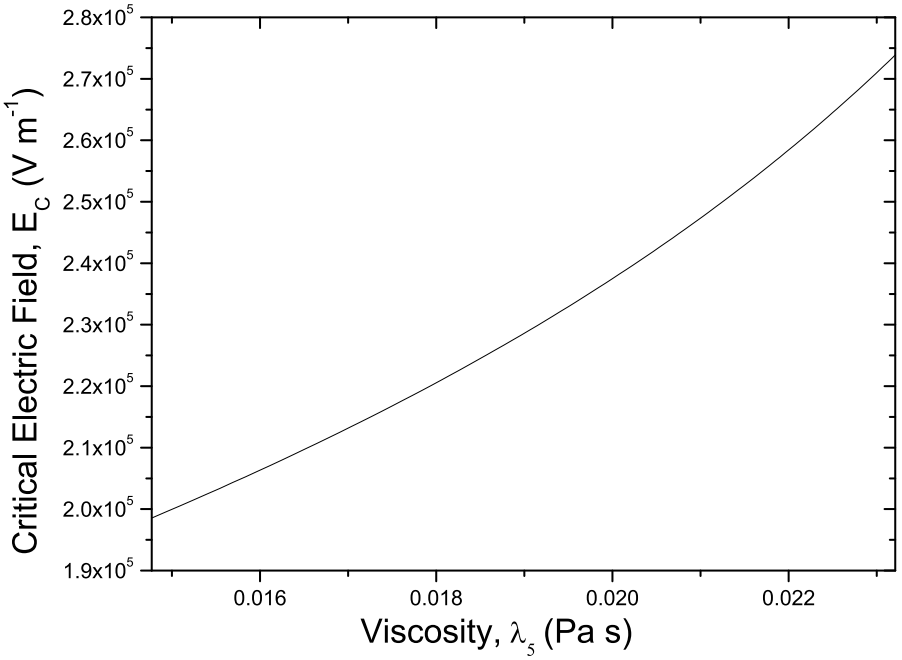

Figure 4.4: Rotational viscosity λ_5 versus critical electric field strength E_c. The interval size is 200μm, giving a value of $\delta = 100\mu$m. Note the nonlinear nature of the field response to increasing viscosity

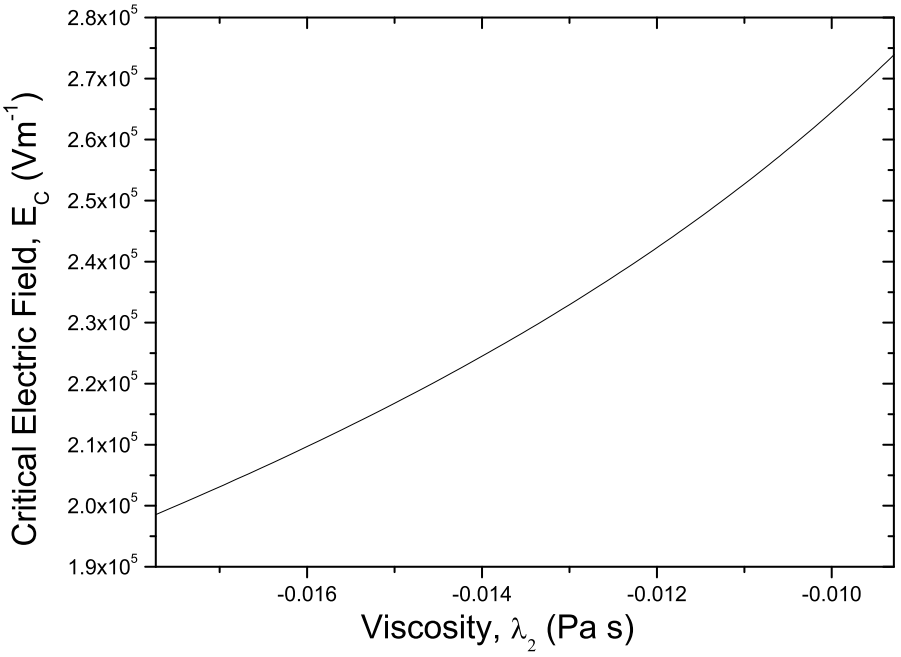

Figure 4.5: Rotational viscosity λ_2 versus critical electric field strength E_c. The interval size is 200μm, giving a value of $\delta = 100\mu$m.

this case the graph was plotted between a minimum value of $\lambda_2^{min} = -0.018$ Pa s and a maximum value of $\lambda_2^{max} = -0.009$ Pa s.

Notice in particular the nonlinear relationship between λ_5 and the critical field strength E_c. As the rotational viscosity λ_5 is increased the energy we need to impart into the system via the electric field increases at a nonlinear rate. We might expect this to be the case since we are studying a non-Newtonian fluid. The results suggest that as we lower the temperature (which is equivalent to increasing the smectic cone angle and therefore increasing the viscosity) the electric field strength required to drive a soliton increases in response. In otherwords, the electric field must do more work on the liquid crystal sample in order to overcome viscous effects and initiate a travelling wave.

Next we study the effect of τ_1 and τ_5 in the model. In Figure 4.6 we demonstrate the relationship between one of the *ac-coupling* coefficients τ_5 and the critical field E_c. In this case the range of values of τ_5 used to construct the graph varied from a minimum of $\tau_5^{min} = 0.028$ Pa s to a maximum of $\tau_5^{max} = 0.038$ Pa s. For the graph depicted in Figure 4.7 we measure the critical field response to another of the ac-coupling coefficients and note that the minimum and maximum values of τ_1 are given by $\tau_1^{min} = 0.001$ Pa s and $\tau_1^{max} = 0.011$ Pa s. This time the field strength dependency E_c appears to vary inversely with increasing coupling viscosity for both τ_1 and τ_5. This behaviour is somewhat counter-intuitive. We noted above for λ_5 that as we increase the viscosity, we increase the electric field threshold at which we observe travelling waves. With the τ_1 and τ_5 graphs the opposite appears to be the case. Quite why this is remains unclear.

The linearised model we are studying has been adapted to use a restricted number of viscosities namely μ_0, λ_2, λ_5, τ_1 and τ_5. For a fuller picture we could have incorporated other viscous coefficients but due to limited experimental data chose to restrict the choice to the 5 viscosity coefficients previously mentioned.

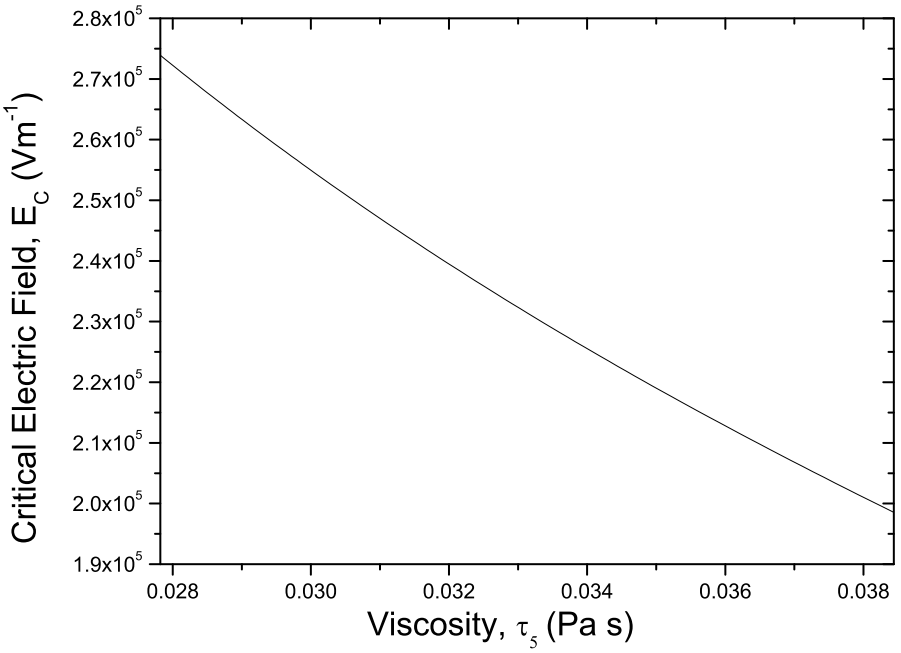

Figure 4.6: Coupling viscosity τ_5 versus critical electric field strength E_c. The interval size is 200μm, giving a value of $\delta = 100\mu$m. Once again notice the nonlinear nature of the field response to increasing viscosity.

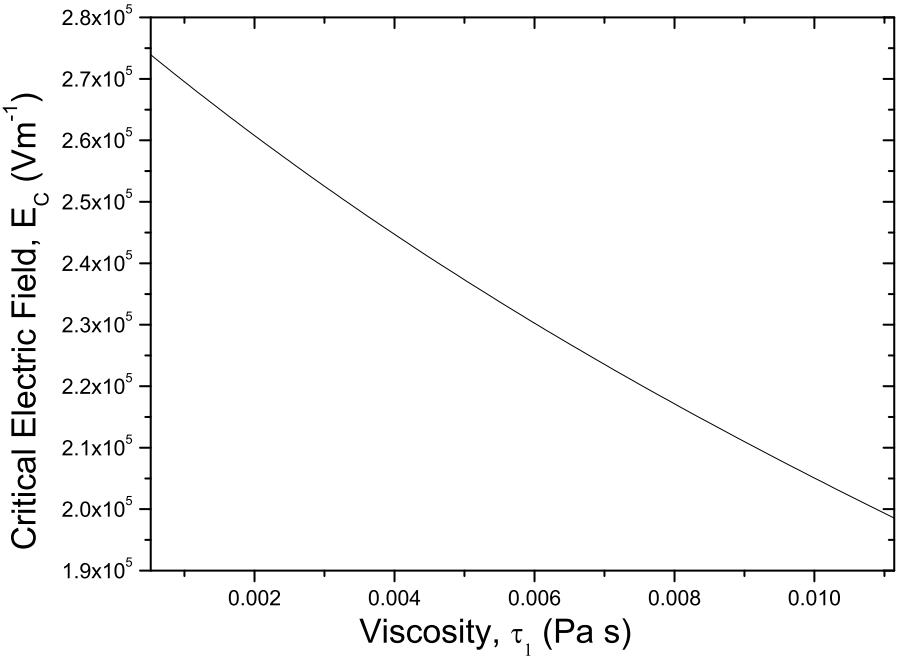

Figure 4.7: Coupling viscosity τ_1 versus critical electric field strength E_c. The interval size is 200μm, giving a value of $\delta = 100\mu$m. Once again notice the nonlinear nature of the field response to increasing viscosity.

4.3.5 Best fit curves

We can of course extend the techniques we have been discussing to study material parameter effects on different interval widths. Throughout the previous section we set $\delta = 100\mu$m. Consider now Figure 4.8 The curves in Figure 4.8 were gener-

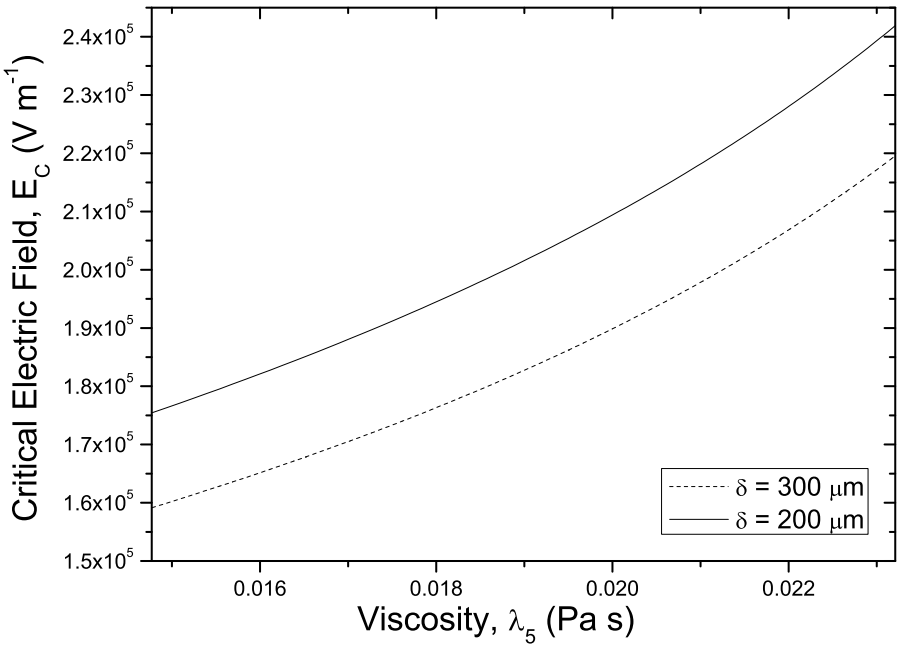

Figure 4.8: Critical electric field strength E_c versus rotational viscosity λ_5 for $\delta = 200$ μm and $\delta = 300$ μm.

ated using different interval widths of $\delta = 200\mu$m and $\delta = 300\mu$m corresponding to intervals of 400 μm and 600 μm respectively. Both curves are non-linear in nature. Note in particular the fact that the lower curve (dashed line) represents the field response against viscosity for an interval width of $\delta = 300\mu$m. The upper curve (solid line) represents the smaller interval width of $\delta = 200$ μm.

Interpreting these curves we note that each identifies a boundary analogous to a Freedericksz transition. At each point on the curves we are identifying thresholds at which travelling waves are initiated in response to an applied electric field. The data suggests that for a larger interval the field strength E_c required to shift the system from an unstable to a stable state is generally lower given

the parameters we have chosen than would be the case in a smaller interval.

We conclude that the field required to initiate travelling waves in the system in the smaller region is greater than that for the larger interval. We suggest that this comes about as a result of the fact that in a thinner sample the molecules in the bulk experience a greater degree of influence from molecules at the boundary than do molecules in a sample with a larger interval width. The electric field has to do more work to overcome elastic and viscous effects in a thinner sample than in a thicker sample.

To get a quantitative understanding of the nonlinear behaviour of the two curves given in Figure 4.8 we conducted a simple curve fitting exercise using the graphing software package Origin. We use the best fit exponential decay function `ExpDec1` which determines a best fit of the form

$$y(x) = A_1 e^{-\frac{x}{t_1}} + y_0. \tag{4.99}$$

The model data is arranged so that the best fit exponential curve is actually modelling E as a function of λ_5 then the exponential best fit really represents the function

$$E(\lambda_5) = E_1 e^{-\frac{\lambda_5}{\lambda}} + E_0. \tag{4.100}$$

A straightforward comparison establishes the fact that E_1 corresponds to A_1, λ corresponds to t_1 and E_0 corresponds to y_0. We set out to establish values for the constants A_1, t_1 and y_0 in the cases where $\delta = 200$ μm and $\delta = 300$ μm. We used Origin to determine the best exponential fit for the coefficients corresponding to the $\delta = 200$ μm case and the results are given in Table 4.3. We note here that using Table 4.3 we may determine the approximate values of the electric field strength E_c at the extremal points using the exact values for λ_5. We list extremal values for $\delta = 200$ μm in Table 4.4. Note that we determine the percentage error

Constant	Value
y_0	131 $\mathrm{kVm^{-1}}$
A_1	9.17 $\mathrm{kVm^{-1}}$
t_1	-9.32 $\mathrm{mPa^{-1}s^{-1}}$

Table 4.3: Best fit data for $\delta = 200$ μm.

λ_5 (Pa s)	E_c^{exact} ($\mathrm{kVm^{-1}}$)	E_c^{approx} ($\mathrm{kVm^{-1}}$)	Δ_{err} (%)
0.01477	175.4	175.9	0.29
0.02321	242.0	241.7	0.12

Table 4.4: Extremal values for $\delta = 200$ μm using the data given in Table 4.3.

Δ_{err} using the formula given in (4.101)

$$\Delta_{err} = \frac{|E_c^{exact} - E_c^{approx}|}{|E_c^{exact}|} \times 100. \tag{4.101}$$

Next, in Table 4.5, we list the best fit data determined once again using Origin, in the case where $\delta = 300$ μm. We list extremal values for $\delta = 300$ μm

Constant	Value
y_0	120 $\mathrm{kVm^{-1}}$
A_1	7.73 $\mathrm{kVm^{-1}}$
t_1	-9.11 $\mathrm{mPa^{-1}s^{-1}}$

Table 4.5: Best fit data for $\delta = 300$ μm.

in Table 4.6. The percentage error Δ_{err} indicates that in both the $\delta = 200$ μm

λ_5 (Pa s)	E_c^{exact} ($\mathrm{kVm^{-1}}$)	E_c^{approx} ($\mathrm{kVm^{-1}}$)	Δ_{err} (%)
0.01477	159.2	159.5	0.19
0.02321	219.6	219.2	0.18

Table 4.6: Extremal values for $\delta = 300$ μm using the data given in Table 4.5.

case and the $\delta = 300$ μm the exponential fit at the extremal values deviates from the numerically computed value by no more than about ± 400 $\mathrm{Vm^{-1}}$ so the best

fit curve is a reasonable measure of the quantitative behaviour of the numerical data generated via the Galerkin scheme.

4.3.6 Determination of power law relationships

A question of great importance concerns the existence of power law relationships. For example we might ask the question *if we vary the physical parameter B say, how does the critical field E_c strength vary in response?* Previously we attempted to find best fit curves to match the data. Now we shall attempt to establish whether or not there are specific power law relationships governing the response of the critical field strength to varying parameters. We shall follow the approach adopted by Stewart and Stewart [72] as they investigated shear flow in smectic A liquid crystals.

We start by exploring the variation of the critical field strength E_c with respect to the elastic constant B. It is generally easier to control the properties of the material with regard to the elastic constants and so qualitatively the data and graphs presented here are perhaps the most pertinent in terms of physically measurable quantities. Our aim here is to establish power law relationships, if indeed such relationships exist, between B and E_c. Consider the graph in Figure 4.9. It is clear from this figure that by increasing the interval width we lower the threshold at which the stable region is encountered. Note also the non-linear dependency on δ. Let us focus in on the the curve corresponding to an interval width of $\delta = 100$ μm. We show the curve in Figure 4.10. The curve of the raw data is clearly non-linear. However, in the inset graph we have plotted the curve of $\log_{10} B$ against $\log_{10} E_c$. This suggests a linear relationship of the form

$$\log_{10} E_c = \log_{10} \kappa + m \log_{10} B. \tag{4.102}$$

Once again using the package Origin we computed a linear best fit curve for the

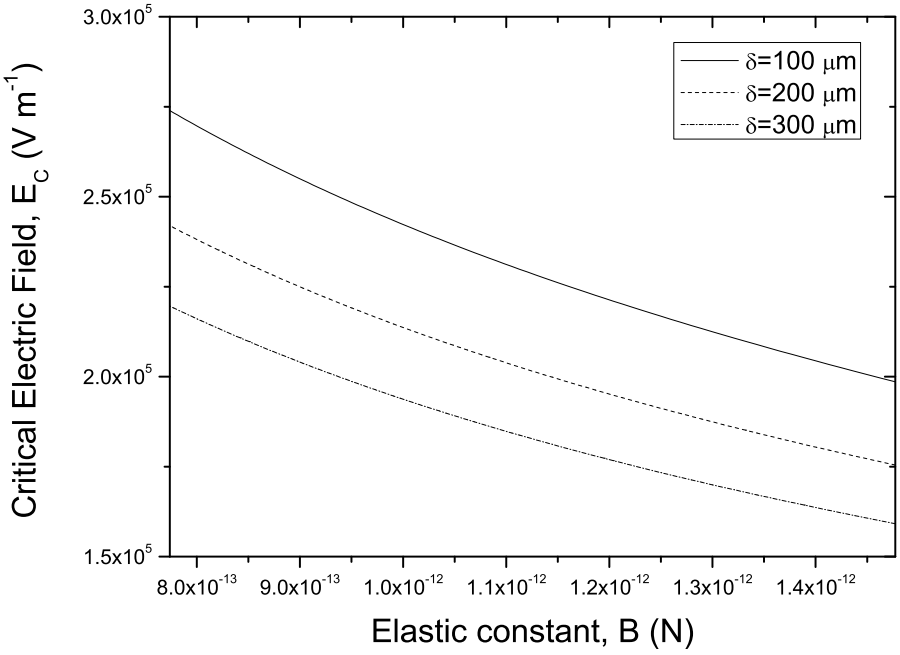

Figure 4.9: Critical electric field strength E_c versus elastic constant B for three different interval widths. Notice the distinctly non-linear dependence on δ.

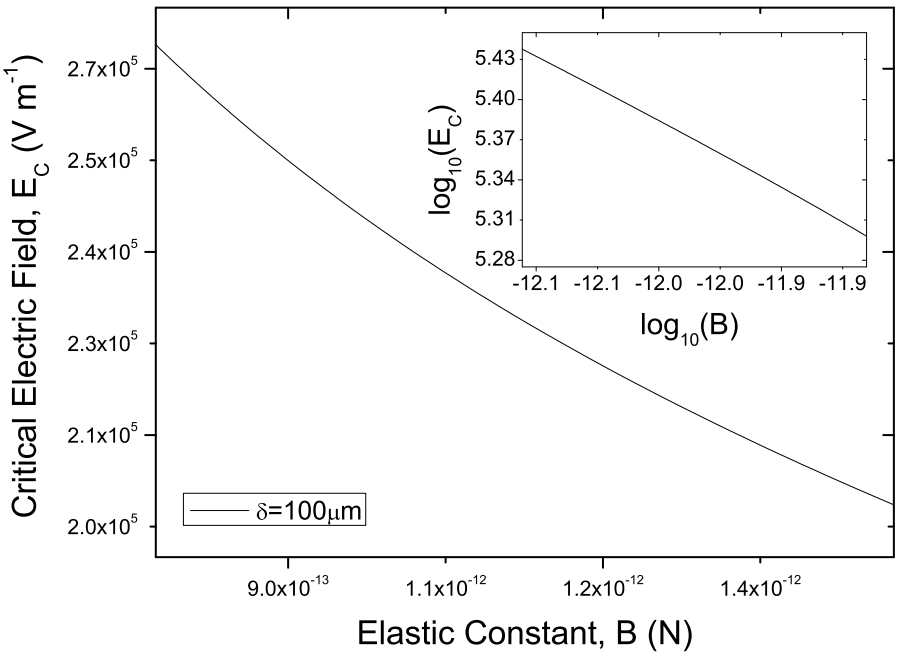

Figure 4.10: Critical electric field strength E_c versus elastic constant B for $\delta = 100$ μm. Notice the distinctly non-linear dependence of E_c against B. Note however that when we plot $\log_{10} E_c$ against $\log_{10} B$ we find a relationship which is generally linear in nature.

data used to generate the log-log graph. We found using this best fit method that the slope m and intercept $\log_{10}\kappa$ were given approximately by the data in Table 4.7. Using (4.102) the critical field and elastic constant may then be

Constant	Value
$\log_{10}\kappa$	-0.5509
κ	0.2813
m	-0.4946

Table 4.7: Linear best fit data for $\log_{10} E_c = \log_{10}\kappa + m\log_{10} B$, with $\delta = 100\ \mu$m.

related by a power law of the form

$$E_c = \kappa B^m \tag{4.103}$$

The values tabulated mean that in this case for $\delta = 100\ \mu$m the relationship between the critical field E_c and B is approximately of the form

$$E_c \propto \frac{1}{\sqrt{B}} \tag{4.104}$$

Now consider the graph in Figure 4.11. Here we find that a linear response is obtained by plotting the parameter τ_1 against $\ln E_c$. By considering a linear fit of the form

$$\ln E_c = c + m\tau_1, \tag{4.105}$$

we have that the power law relationship in this case may be written as

$$E_c = e^{c+m\tau_1} = \kappa e^{m\tau_1} \tag{4.106}$$

Then by constructing a linear fit using Origin, we may determine values for c, m and we list these in Table 4.8. Then we find that the value of κ is given straightforwardly as $\kappa = 276.9\ \text{kVm}^{-1}$. It should be noted that a log-log fit of τ_1 against E_c yields a nonlinear curve hence the decision to plot a linear-log fit for τ_1 and E_c.

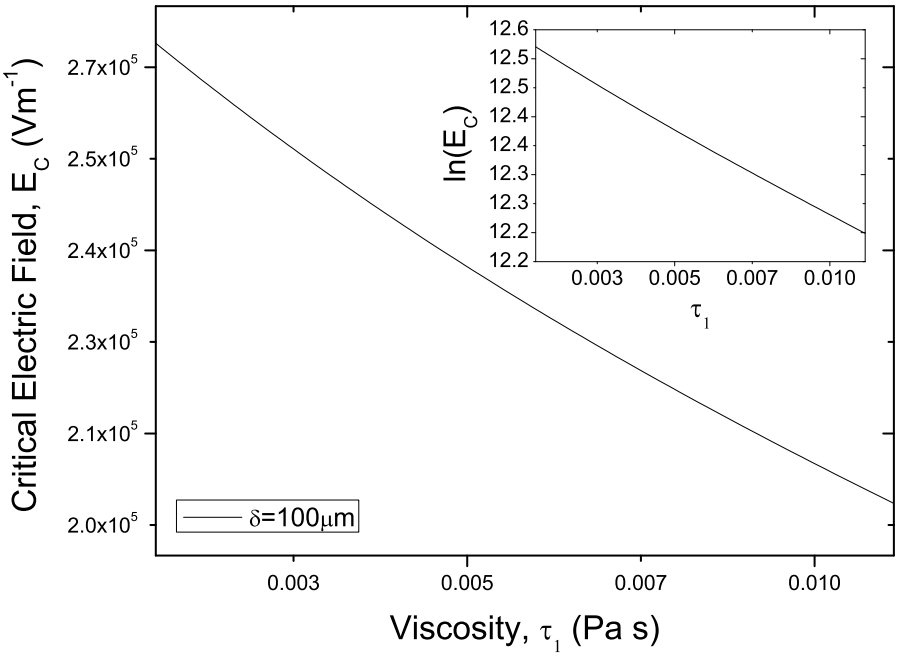

Figure 4.11: Critical electric field strength E_c versus elastic constant τ_1 for $\delta = 100$ μm. The inset graph is the linear response found by plotting τ_1 against $\ln E_c$.

Constant	Value
c	12.5315
m	-30.335

Table 4.8: Linear best fit data for $\ln E_c = c + m\tau_1$, with $\delta = 100$ μm.

The parameter λ_5 is plotted against E_c in Figure 4.12. This yields a nonlinear curve and we again plot a log-log graph as an inset. Plotting λ_5 against $log_{10}E_c$ also yields a non-linear curve. This leads us to speculate that the power law governing the response of the electric field to variations in λ_5 is non-linear in nature. As yet we have not determined the form of this more complicated interaction.

Moving on from here we investigated the power law form governing field response involving the parameter τ_5. Once again we graph the critical field response E_c against τ_5 and display the result in Figure 4.13. Note that the inset log-log graph indicates that an appropriate fit for this data is a linear fit, as

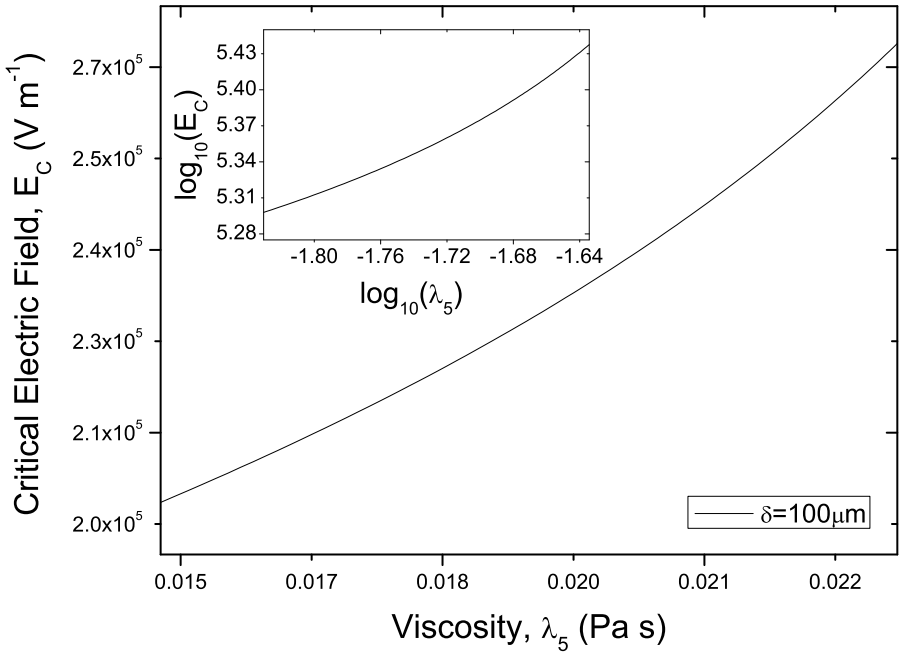

Figure 4.12: Critical electric field strength E_c versus elastic constant λ_5 for $\delta = 100$ μm. The inset graph is the linear response found by plotting λ_5 against $\ln E_c$. Note the log-log response is non-linear.

was the case with B against E_c in (4.102). Performing a linear best fit on the

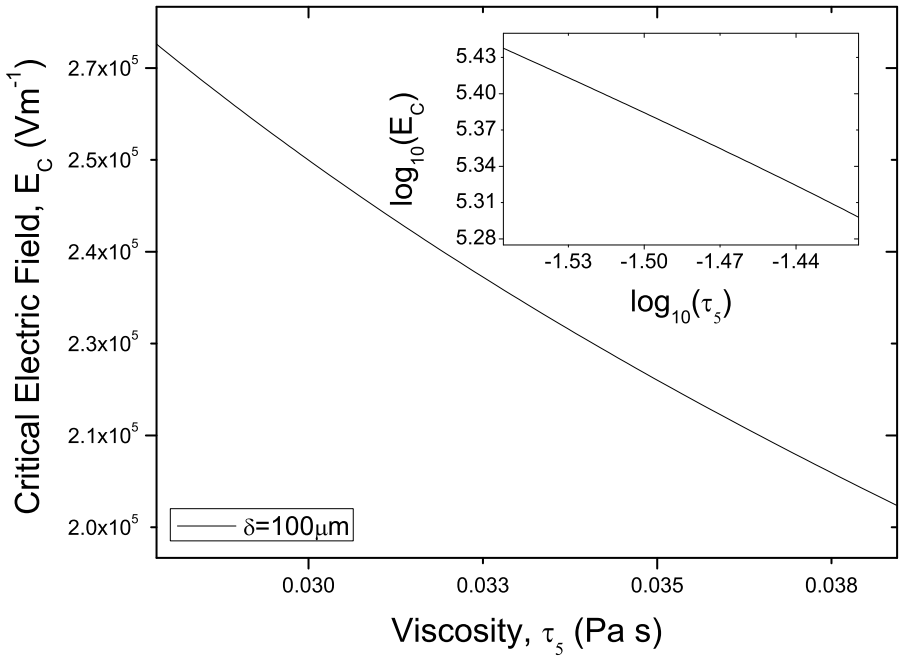

Figure 4.13: Critical electric field strength E_c versus elastic constant τ_5 for $\delta = 100$ μm. The inset graph is the linear response found by plotting $\log_{10} \tau_5$ against $\log_{10} E_c$.

log-log graph yields the best fit data given in Table 4.9. Notice that the slope on

Constant	Value
$\log_{10}\kappa$	3.9
κ	7.944×10^3
m	-0.9891

Table 4.9: Linear best fit data for $\log_{10} E_c = \log_{10}\kappa + m\log_{10}\tau_5$, with $\delta = 100\ \mu$m.

this curve indicates that the relationship between E_c and τ_5 appears to follow a reciprocal law so that

$$E_c \propto \frac{1}{\tau_5}. \tag{4.107}$$

4.4 Discussion

We started this chapter with a set of four linear perturbation equations. By assuming time decaying spatially dependent perturbation solutions we constructed a pair of perturbation equations. We achieved this by determining that the flow in the x direction was constant. This meant we were in a position to concentrate solely on the perturbation equations for the conserved angular momentum equation and the third conserved linear momentum equation.

Then by deciding to limit the number of viscosity terms to five, these being μ_0, λ_2, λ_5, τ_1 and τ_5, assuming that the non-constant coefficients may be assumed to be constant in the vicinity of $\tau = 0$ and that by making a suitable transformation we could reduce the problem to a non-self-adjoint differential eigenvalue problem. In a similar manner we constructed a generalised non-self-adjoint differential eigenvalue problem using the full equations but again limiting the number of viscosity terms to five as listed above.

By applying a suitable weighted residual method namely the method of Galerkin we were able to demonstrate for a suitable choice of parameters that in

the constant coefficient system the first two real eigenvalues could be computed to an arbitrary degree of accuracy by choosing an appropriate number of terms in the polynomial expansions. Although computational limitations meant that the number of Fourier terms we considered had to be truncated at approximately twelve per function we were able to demonstrate that by increasing the number of terms we were able to achieve a degree of convergence which we corroborated by plotting the difference between successive approximations of the two eigenvalues.

When we came to consider the full system our goal then was to determine critical field strengths once again using a Galerkin type method. This time calculating four eigenvalues at a time for suitable material parameters over a range of plausible electric field strengths we were able to determine numerically the point at which the system went from an unstable to a stable steady state and by tracking and recording the field strengths at which the transitions took place we were in a position to determine critical field strengths versus parameter values from which we made a first attempt at analysis using power law methods.

Whilst the results we have generated rely on approximations, the critical field strengths we have determined are of the order of $100 \sim 200$ kV m^{-1} and these seem to be roughly in agreement with the field strengths at which travelling waves appear. For instance Stannarius and Langer [53], report the existence of propagating wave fronts in thin film ferroelectric smectic C* samples at field strengths of approximately 120 kV m^{-1} so the numerically determined results are broadly in agreement.

Its worth noting at this point that our starting assumption, of director reorientation in a ferroelectric sample under the influence of a non-inclined electric field without flow, gives rise to an exact solution which exists for *all* electric field strengths E. The result of the linear perturbation analysis presented above how-

ever demonstrates that there exists a physical regime, which is bounded above by an electric field of magnitude E_c, where travelling waves are *not* observed. In other words the results given here establish the minimum field strength required in order that the travelling waves (2.10) predicted by (2.9) exist. Then solution (2.10) must be re-written as

$$\phi(x,t) = \begin{cases} \frac{\pi}{2} - 2\arctan\left[\exp\left\{\sqrt{\frac{\beta}{B}}\,(x-ct)\right\}\right], & \text{for } E > E_c, \\ -\frac{\pi}{2}, & \text{for } E \leq E_c. \end{cases} \tag{4.108}$$

Once again β and c are given by (2.11) and (2.12) respectively.

No doubt the polynomial forms we chose to match the boundary condition of our problem could be improved on. The polynomials used here were very simple forms. Other researchers for instance Hill and Straughan [73] have used a Legendre spectral element method for eigenvalues in hydrodynamic stability problems. Seeking faster convergence and greater accuracy using a more sophisticated approximation method such as [73] is one possible avenue for future research.

From here we proceed in Chapter 5 to examine a problem inspired by work conducted by Stewart and Wigham [72] on the analysis of cylindrical wave fronts in smectic C liquid crystals. We shall construct a method using ideas from [72] to construct solutions to approximate wave front domain wall profiles for ferroelectric samples in inclined electric fields.

Chapter 5

Travelling Domain Walls

5.1 Introduction

In this chapter we shall investigate a method for approximating the wavefront profile of a travelling plane wave in a sample of smectic C* under the influence of an inclined electric field of the kind described by Stewart and Momoniat [54]. The governing equations for this problem were given at (2.8) and (2.9) along with the exact solution to (2.9) which we presented at (2.10). Inspiration for this work comes principally from the paper by Stewart and Wigham [7], which itself had its roots in the work of Stelzer and Arodź [74] and Arodź and Larsen [75]. In all three papers the authors discuss the time and space evolution of a cylindrical domain wall.

In [7, 74] the problems relate to domain wall evolution in samples of smectic C and nematic materials respectively. By contrast Arodź and Larsen [75] looked at the problem of domain wall evolution and growth in relation to cosmological expansion problems. It is thought that phase transitions in the early universe gave rise to topologically stable defects including vacuum domain walls, cosmological strings and walls bounded by strings [76]. Arodź and Larsens work was motivated by a desire to investigate the physical behaviour of these cosmological walls.

Regardless of the problem being studied, circular domain wall evolution is

tackled in all three cases by transforming to a co-moving frame of reference whose origin lies at the centre of the moving domain wall. Performing a transformation to a co-moving frame permits closer study of the problems. In particular, insofar as liquid crystals are concerned, such a transformation yields information about the radial propagation of the domain wall, the evolution of the domain wall width and an approximate solution for the director orientation.

Here we shall attempt to apply the techniques used to study circular domain wall problems to a problem with a planar geometry. The exact solution (2.10) to (2.9) is a soliton. One of its key features is the presence of a *domain wall* connecting two constant states. The domain wall has finite width and is persistent, that is to say the theoretical solution maintains a constant wave profile at all times.

5.2 A review of the dynamics of cylindrical domain walls

Briefly, in [7] Stewart and Wigham consider a sample of smectic C liquid crystal under the influence of a circular magnetic field. An electrical current flows through a long thin wire of circular cross section passing through the sample, as shown in Figure 5.1 where the current carrying wire is represented by the dark region at the centre of the diagram. This current induces a concentric magnetic field $\mathbf{B}$ about the wire given by

$$\mathbf{B} = \frac{\mu_0}{2\pi}\frac{I}{\rho(t)+\xi}\hat{\boldsymbol{\alpha}}, \tag{5.1}$$

which in turn gives rise to a travelling circular domain wall of finite width concentric about the wire.

Either side of the domain wall the projection $\mathbf{c}$ of the smectic director $\mathbf{n}$ onto the planar layers reorients through an angle $|\phi_1 - \phi_0|$. This means that in the radial direction between the wire and the trailing edge (inner edge) of the

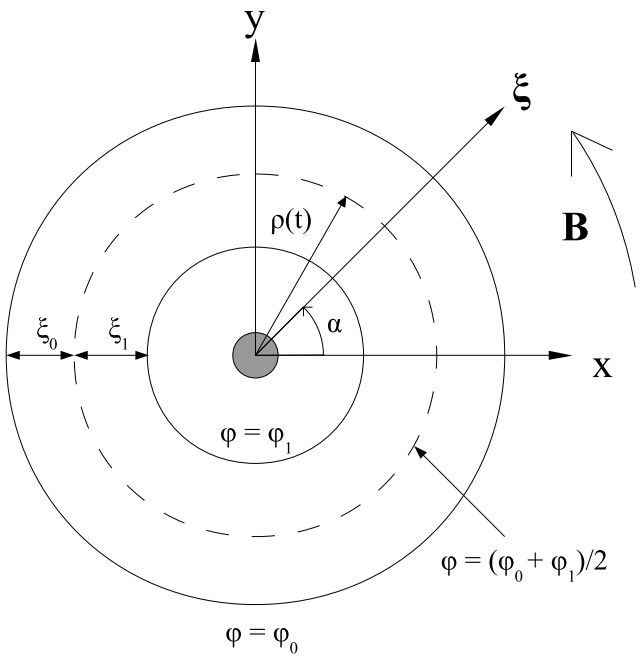

Figure 5.1: Schematic representation of the travelling domain wall discussed in [7]. A current carrying wire (grey circle) generates a concentric magnetic field **B**. The projection **c** of the smectic director **n** in the smectic planes re-orients through an angle ϕ between the trailing and leading edges of the domain wall. The centre of the domain wall is time varying and has position $\rho(t)$ relative to the origin of the cartesian co-ordinate system. The wall width is given by $\xi_0+\xi_1$, and the angular orientation of the the projection **c** at the centre of the domain wall it is assumed to be $\frac{1}{2}(\phi_0 + \phi_1)$.

domain wall, the angular orientation of **c** is fixed at $\phi = \phi_1$. Beyond the leading edge (outer edge) of the domain wall to infinity the angular orientation is fixed at $\phi = \phi_0$. In this model the orientation of the projection of the director onto the smectic planes is given by $\mathbf{c} = \hat{\boldsymbol{\xi}} \sin\phi(\xi, t) + \hat{\boldsymbol{\alpha}} \cos\phi(\xi, t)$. By describing the problem in a co-moving coordinate frame, Stewart and Wigham were able to develop a dynamic equation for the reorientation of ϕ.

5.3 The geometry of the planar domain wall

We begin our analysis by considering Figure 5.2. We assume that when looking along the z-axis towards the origin, the travelling wave may be represented by a moving domain wall of finite width. Beyond the leading and trailing edges of the domain wall we assume that the director **c** is fixed. This means that to the left of the trailing edge of the domain wall the projection of **c** onto the smectic planes is oriented at the constant angle ϕ_0. Similarly to the right of the leading edge the director **c** is oriented at the constant angle ϕ_1. These competing boundary conditions give rise to a domain wall. Throughout the full depth of the domain wall the director reorients from one fixed state to another.

Half way between the leading and trailing edges at the centre of the domain wall, indicated by the dotted line in Figure 5.2, the director **c** is assumed to

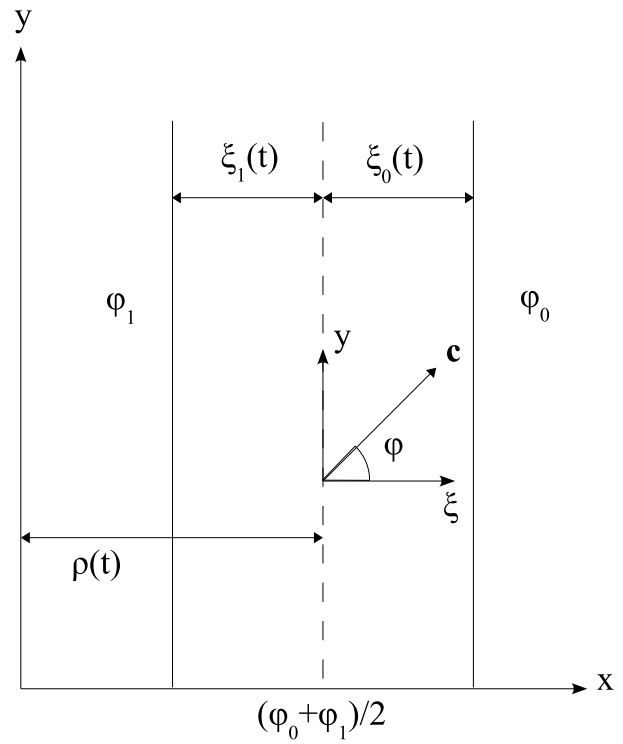

Figure 5.2: The geometry of the planar wave problem and associated co-moving coordinate system

have undergone a rotation of $\frac{1}{2}(\phi_1 + \phi_0)$. Across the domain wall as a whole the director reorients itself through an angle of $|\phi_1 - \phi_0|$.

The position of the centre of the domain wall from the origin of the untransformed Cartesian system is measured by the time dependent variable $\rho(t)$. The coordinate ξ measures the *outwards* linear distance in the transformed system from $\rho(t)$. At anytime t the leading and trailing edges of the domain wall are at positions $\rho(t) + \xi_1(t)$ and $\rho(t) - \xi_0(t)$ respectively. Note that $\xi_0(t)$ and $\xi_1(t)$ are time dependent and denote the distance from the wall core at position $\rho(t)$ to the leading and trailing edges of the domain wall.

Then following Stelzer and Arodź [74] and Stewart and Wigham [7] we transform the problem to a co-moving frame of reference with coordinates ξ, y and z and basis vectors given by $\hat{\boldsymbol{\xi}}$, $\hat{\mathbf{y}}$, $\hat{\mathbf{z}}$. That is we transform to a frame of reference coincident with the centre of the domain wall as shown in Figure 5.2. These basis vectors are related to their Cartesian counterparts via the expressions

$$x = \rho(t) + \xi, \quad y = y, \quad z = z. \tag{5.2}$$

Consequently we find that the scale factors are straightforwardly written

$$h_1 = 1, \quad h_2 = 1, \quad h_3 = 1. \tag{5.3}$$

and in terms of the new basis vectors we find that the expressions for the smectic C* layer normal $\mathbf{a}$ and the projection of the director onto the smectic plane $\mathbf{c}$ become

$$\mathbf{a} = \hat{\mathbf{z}}, \quad \mathbf{c} = \hat{\boldsymbol{\xi}}\cos\phi + \hat{\mathbf{y}}\sin\phi, \quad \text{where} \quad \phi = \phi(\xi, t). \tag{5.4}$$

In addition the polarisation $\mathbf{P}$ is given by the expression $\mathbf{P} = P_0\mathbf{b}$ where $\mathbf{b}$ is given by

$$\mathbf{b} = -\hat{\boldsymbol{\xi}}\sin\phi + \hat{\mathbf{y}}\cos\phi. \tag{5.5}$$

Similarly the electric field is defined in the new coordinate system to be

$$\mathbf{E} = E(\hat{\boldsymbol{\xi}}\cos\alpha + \hat{\mathbf{z}}\sin\alpha), \tag{5.6}$$

and we assume that the angle of incidence of the field with the sample α is constrained by the condition $0 \leq \alpha < \frac{\pi}{2}$.

Using standard results [77] the gradient operator ∇ in the transformed frame of reference is given by the expression

$$\nabla = \hat{\boldsymbol{\xi}}\frac{\partial}{\partial \xi} + \hat{\mathbf{y}}\frac{\partial}{\partial y} + \hat{\mathbf{z}}\frac{\partial}{\partial z}, \tag{5.7}$$

whilst the material time derivative with respect to the co-moving frame in terms of the co-moving coordinates [7] is given by the expression

$$\frac{\mathrm{D}}{\mathrm{D}t} = \frac{\partial}{\partial t} + \mathbf{v}\cdot\nabla - \frac{\mathrm{d}\mathbf{r}}{\mathrm{d}t}\cdot\nabla. \tag{5.8}$$

Here the vector $\mathbf{r}(t)$ is taken to be the position vector of the origin of the co-moving frame at time t relative to the fixed Cartesian frame. The vector $\mathbf{v}$ represents the velocity of a material element. Both $\mathbf{r}(t)$ and $\mathbf{v}$ are expressed in terms of co-moving coordinates. In this model we shall assume that there is negligible hydrodynamic flow so we may write $\mathbf{v} = 0$, whereas the position of the origin in co-moving coordinates is given by $\mathbf{r}(t) = \rho(t)\hat{\boldsymbol{\xi}}$.

Applying these definitions to the expression for the material time derivative we find that (5.8) reduces to

$$\frac{\mathrm{D}}{\mathrm{D}t} = \frac{\partial}{\partial t} - \frac{\mathrm{d}\rho}{\mathrm{d}t}\frac{\partial}{\partial \xi}. \tag{5.9}$$

With these definitions in place we shall now look at the continuum theory required to further analyse the planar domain wall problem

5.4 Smectic C* continuum theory for the planar domain wall

In order to proceed with the analysis of the problem we must construct a continuum model to describe the dynamic evolution of the director in time and space. To achieve this we shall appeal to many of the equations and expressions used

in Chapter 2. We shall recap the relevant parts of the theory where necessary. However, the intention here is to keep details to a minimum where it is clear that the material has already been covered elsewhere in the text.

The vectors **a** and **c** are subject to the constraints detailed at (2.17). We have already assumed no hydrodynamic flow is present so the dynamic equations arising from the balance of linear momentum may be disregarded. Instead the governing dynamic equations for this system are those that arise whilst considering the balance of angular momentum. The two equations which form the backbone of subsequent analysis were introduced at (2.21) and (2.22). We restate them here in a slightly different form in order to emphasise the role of the generalised body forces $\mathbf{G^a}$ and $\mathbf{G^c}$

$$\left(\frac{\partial w}{\partial a_{i,j}}\right)_{,j} - \frac{\partial w}{\partial a_i} + G_i^a + \tilde{g}_i^a + \gamma a_i + \mu c_i + \epsilon_{ijk}\beta_{k,j} = 0, \tag{5.10}$$

$$\left(\frac{\partial w}{\partial c_{i,j}}\right)_{,j} - \frac{\partial w}{\partial c_i} + G_i^c + \tilde{g}_i^c + \tau c_i + \mu a_i = 0, \tag{5.11}$$

Whereas previously in (2.21) and (2.22) we posed the problem in terms of the total energy density w^*, here we shall take the dielectric and polarisation energy densities and treat them separately from the elastic energy in the bulk. We shall consider an electric energy density w_E defined to be the sum of the polarisation and dielectric energy densities so that

$$w_E = w_{elec} + w_{pol}. \tag{5.12}$$

Then using the definition of the electric energy density from [4, p.28] we write

$$w_{elec} = -\tfrac{1}{2}\epsilon_0\epsilon_a \left(\mathbf{n}\cdot\mathbf{E}\right)^2, \tag{5.13}$$

and

$$w_{pol} = -\mathbf{P}\cdot\mathbf{E}, \tag{5.14}$$

so that the electric energy density is given by

$$w_E = -\tfrac{1}{2}\epsilon_0\epsilon_a \left(\mathbf{n}\cdot\mathbf{E}\right)^2 - \mathbf{P}\cdot\mathbf{E}. \tag{5.15}$$

Now from [4, p.28] the electric energy potential ψ_E is the negative of the electric energy density so that

$$\psi_E = \tfrac{1}{2}\epsilon_0\epsilon_a \left(\mathbf{n}\cdot\mathbf{E}\right)^2 + \mathbf{P}\cdot\mathbf{E}. \tag{5.16}$$

Then recalling the definition for the director $\mathbf{n}$ at (2.1) and the expression for the polarisation $\mathbf{P} = P_0\mathbf{E}\cdot\mathbf{b}$ with $\mathbf{b}$ given by the expression at (2.2) we may write (5.16) in terms of $\mathbf{a}$, $\mathbf{c}$ and $\mathbf{E}$ as follows

$$\psi_E = \tfrac{1}{2}\epsilon_0\epsilon_a \left(\mathbf{a}\cdot\mathbf{E}\cos\theta + \mathbf{c}\cdot\mathbf{E}\sin\theta\right)^2 + P_0\mathbf{E}\cdot\left(\mathbf{a}\times\mathbf{c}\right). \tag{5.17}$$

This means the electric energy potential for a sample of ferroelectric smectic C may be written in Cartesians as

$$\psi_E = \tfrac{1}{2}\epsilon_0\epsilon_a \left(a_iE_i\cos\theta + c_iE_i\sin\theta\right)^2 + P_0E_p\epsilon_{pqr}a_qc_r. \tag{5.18}$$

Then referring to [4, p.263], the generalised body forces are written

$$G_i^a = \frac{\partial\psi_E}{\partial a_i}, \quad G_i^c = \frac{\partial\psi_E}{\partial c_i}. \tag{5.19}$$

This in turn allows us to express the vector components G_i^a and G_i^c as

$$G_i^a = \epsilon_0\epsilon_a(\mathbf{n}\cdot\mathbf{E})E_i\cos\theta - P_0[\mathbf{E}\times\mathbf{c}]_i, \tag{5.20}$$

$$G_i^c = \epsilon_0\epsilon_a(\mathbf{n}\cdot\mathbf{E})E_i\sin\theta + P_0[\mathbf{E}\times\mathbf{a}]_i. \tag{5.21}$$

Time dependent effects are introduced through the quantities $\tilde{g}_i^a$ and $\tilde{g}_i^c$. Whereas at (2.23) and (2.24) we were modelling the effects of flow, now we are assuming negligible flow so $\tilde{g}_i^a$ and $\tilde{g}_i^c$ assume the form

$$\tilde{g}_i^a = -2(\lambda_4\dot{a}_i + \lambda_6c_ic_p\dot{a}_p + \tau_5\dot{c}_i), \tag{5.22}$$

$$\tilde{g}_i^c = -2(\lambda_5\dot{c}_i + \tau_5\dot{a}_i). \tag{5.23}$$

where λ_4, λ_6, λ_5 and τ_5 are dynamic viscosity coefficients whilst the superposed dot represents the material time derivative. In addition the notation adopted

in [7] and employed in Chapter 2 is used here so that we define for convenience the expressions

$$\Pi_i^a = \left(\frac{\partial w}{\partial a_{i,j}}\right)_{,j} - \frac{\partial w}{\partial a_i}, \tag{5.24}$$

$$\Pi_i^c = \left(\frac{\partial w}{\partial c_{i,j}}\right)_{,j} - \frac{\partial w}{\partial c_i}. \tag{5.25}$$

The elastic energy density is given by the expression at (2.46)and we make the following assignment

$$w = w_{elas}. \tag{5.26}$$

5.5 Governing dynamic equation for the planar problem

The previous section encapsulates the theory needed to construct the dynamic equations we shall be concerned with. We start by noting the following identities

$$\nabla \cdot \mathbf{a} = 0, \tag{5.27}$$

$$\nabla \cdot \mathbf{c} = -\frac{\partial \phi}{\partial \xi} \sin\phi, \tag{5.28}$$

$$\nabla \times \mathbf{c} = \frac{\partial \phi}{\partial \xi} \cos\phi \, \hat{\mathbf{z}}, \tag{5.29}$$

$$\mathbf{a} \cdot \nabla \times \mathbf{c} = \frac{\partial \phi}{\partial \xi} \cos\phi, \tag{5.30}$$

$$\mathbf{c} \cdot \nabla \times \mathbf{c} = 0, \tag{5.31}$$

$$\mathbf{b} \cdot \nabla \times \mathbf{c} = 0. \tag{5.32}$$

We find after taking account of expressions (5.27) to (5.32) and applying (5.24) and (5.25) to (5.26) that the vectors $\mathbf{\Pi^a}$ and $\mathbf{\Pi^c}$ take essentially the same form as the equivalent expressions in [7]

$$\begin{aligned} \mathbf{\Pi^a} &= -K_3(\mathbf{a} \cdot \nabla \times c)(\nabla \times \mathbf{c}) - K_8(\nabla \cdot \mathbf{c})(\mathbf{c} \times \nabla \times \mathbf{c}) \\ &\quad + K_9 \nabla(\nabla \cdot \mathbf{c}), \qquad (5.33) \\ \mathbf{\Pi^c} &= K_2 \nabla(\nabla \cdot \mathbf{c}) - K_3 \nabla \times \{(\mathbf{a} \cdot \nabla \times \mathbf{c})\mathbf{a}\} \end{aligned}$$

$$-K_7[\nabla \times \{(\mathbf{a}\cdot\nabla\times\mathbf{c})\mathbf{c}\} + (\mathbf{a}\cdot\nabla\times\mathbf{c})(\nabla\times\mathbf{c})]$$
$$-K_8\nabla\times\{(\nabla\cdot\mathbf{c})\mathbf{b}\}. \tag{5.34}$$

We note here that the vector identities in (5.34) may be written as follows

$$\nabla(\nabla\cdot\mathbf{c}) = -\left[\frac{\partial^2\phi}{\partial\xi^2}\sin\phi + \left(\frac{\partial\phi}{\partial\xi}\right)^2\cos\phi\right]\hat{\boldsymbol{\xi}}, \tag{5.35}$$

$$\nabla\times\{(\mathbf{a}\cdot\nabla\times\mathbf{c})\mathbf{a}\} = -\left[\frac{\partial^2\phi}{\partial\xi^2}\cos\phi - \left(\frac{\partial\phi}{\partial\xi}\right)^2\sin\phi\right]\hat{\mathbf{y}}, \tag{5.36}$$

$$\nabla\times(\mathbf{a}\cdot\nabla\times\mathbf{c})\,\mathbf{c} = \frac{\partial}{\partial\xi}\left[\frac{\partial\phi}{\partial\xi}\sin\phi\cos\phi\right]\hat{\mathbf{z}}, \tag{5.37}$$

$$(\mathbf{a}\cdot\nabla\times\mathbf{c})\,(\nabla\times\mathbf{c}) = \left(\frac{\partial\phi}{\partial\xi}\right)^2\cos^2\phi\,\hat{\mathbf{z}}, \tag{5.38}$$

$$\nabla\times\{(\nabla\cdot\mathbf{c})\,\mathbf{b}\} = \frac{\partial}{\partial\xi}\left[\frac{\partial\phi}{\partial\xi}\sin\phi\cos\phi\right]\hat{\mathbf{z}}. \tag{5.39}$$

This means that the vector contributions relating to K_7 and K_8 contain components in the $\hat{\mathbf{z}}$ direction only. The expressions (5.35)-(5.36) mean that we may write $\mathbf{\Pi}^c$ as

$$\Pi_1^c = -K_2\left[\frac{\partial^2\phi}{\partial\xi^2}\sin\phi + \left(\frac{\partial\phi}{\partial\xi}\right)^2\cos\phi\right], \tag{5.40}$$

$$\Pi_2^c = K_3\left[\frac{\partial^2\phi}{\partial\xi^2}\cos\phi - \left(\frac{\partial\phi}{\partial\xi}\right)^2\sin\phi\right], \tag{5.41}$$

$$\Pi_3^c = -\left(K_7+K_8\right)\frac{\partial}{\partial\xi}\left[\frac{\partial\phi}{\partial\xi}\sin\phi\cos\phi\right] - K_7\left(\frac{\partial\phi}{\partial\xi}\right)^2\cos^2\phi. \tag{5.42}$$

Next, using equations (5.4) and (5.6) we may write G_i^a in the following form

$$G_1^a = D(\xi,t)\cos\alpha\cos\theta - P_0E\sin\alpha\sin\phi, \tag{5.43}$$

$$G_2^a = P_0E\sin\alpha\cos\phi, \tag{5.44}$$

$$G_3^a = D(\xi,t)\sin\alpha\cos\theta - P_0E\cos\alpha\sin\phi, \tag{5.45}$$

whilst G_i^c may be written as

$$G_1^c = D(\xi,t)\cos\alpha\sin\theta, \tag{5.46}$$

$$G_2^c = -P_0E\cos\alpha, \tag{5.47}$$

$$G_3^c = D(\xi,t)\sin\alpha\sin\theta, \tag{5.48}$$

and we define $D(\xi, t)$ to be

$$D(\xi, t) = \epsilon_0 \epsilon_a E^2 (\cos\phi \sin\theta \cos\alpha + \cos\theta \sin\alpha). \tag{5.49}$$

Then finally using the expression for the material time derivative at (5.8) we may express (5.22) and (5.23) as

$$\tilde{\mathbf{g}}^a = -2\tau_5 \dot{\mathbf{c}}, \tag{5.50}$$

$$\tilde{\mathbf{g}}^c = -2\lambda_5 \dot{\mathbf{c}}, \tag{5.51}$$

where

$$\dot{c}_1 = -\sin\phi \left(\frac{\partial \phi}{\partial t} - \frac{\mathrm{d}\rho}{\mathrm{d}t} \frac{\partial \phi}{\partial \xi} \right), \tag{5.52}$$

$$\dot{c}_2 = \cos\phi \left(\frac{\partial \phi}{\partial t} - \frac{\mathrm{d}\rho}{\mathrm{d}t} \frac{\partial \phi}{\partial \xi} \right), \tag{5.53}$$

$$\dot{c}_3 = 0. \tag{5.54}$$

5.6 The c-equations

As Stewart and Wigham showed in [7, eq 2.40], once the geometry of the problem has been established, a suitable frame of reference chosen and the appropriate portions of the continuum theory relating to ferroelectric liquid crystals chosen we may then construct a governing equation which models the director dynamics.

We begin by considering the c-equation. Using (5.25) we may rewrite (5.11) as

$$\Pi_i^c + G_i^c + \tilde{g}_i^c + \tau c_i + \mu a_i = 0. \tag{5.55}$$

Then taking the scalar product of (5.55) with c_i and a_i respectively we find that

$$c_i \Pi_i^c + c_i G_i^c + c_i \tilde{g}_i^c + \tau c_i c_i = 0, \tag{5.56}$$

$$a_i \Pi_i^c + a_i G_i^c + a_i \tilde{g}_i^c + \mu a_i a_i = 0. \tag{5.57}$$

Then from (5.57) we find that the Lagrange multiplier $\mu(\xi, t)$ may be expressed as

$$\mu(\xi, t) = -\Pi_3^c - G_3^c - \tilde{g}_3^c. \tag{5.58}$$

Conversely, the Lagrange multiplier $\tau(\xi, t)$ is expressed as follows

$$\tau(\xi,t) = -\Pi_1^c \cos\phi - G_1^c \cos\phi - \tilde{g}_1^c \cos\phi - \Pi_2^c \sin\phi - G_2^c \sin\phi - \tilde{g}_2^c \sin\phi. \quad (5.59)$$

Then from (5.55) we have that

$$\Pi_1^c + G_1^c + \tilde{g}_1^c + \tau\cos\phi = 0, \quad (5.60)$$

$$\Pi_2^c + G_2^c + \tilde{g}_2^c + \tau\sin\phi = 0. \quad (5.61)$$

Multiplying (5.60) by $\sin\phi$ and (5.61) by $\cos\phi$ and subtracting we find that

$$\Pi_1^c \sin\phi - \Pi_2^c \cos\phi + G_1^c \sin\phi - G_2^c \cos\phi + \tilde{g}_1^c \sin\phi - \tilde{g}_2^c \cos\phi = 0. \quad (5.62)$$

Then substituting (5.46), (5.47), (5.40), (5.41) along with (5.51), (5.52), (5.53) into (5.62) we get the following dynamic equation

$$\begin{aligned} 2\lambda_5 \left(\frac{\partial\phi}{\partial t} - \frac{\mathrm{d}\rho}{\mathrm{d}t}\frac{\partial\phi}{\partial\xi}\right) &= \left(K_2 \sin^2\phi + K_3\cos^2\phi\right)\frac{\partial^2\phi}{\partial\xi^2} + (K_2 - K_3)\left(\frac{\partial\phi}{\partial\xi}\right)^2 \sin\phi\cos\phi \\ &\quad - D(\xi,t)\cos\alpha\sin\theta\sin\phi - P_0 E\cos\alpha\cos\phi. \end{aligned} \quad (5.63)$$

We note briefly that the elastic constants K_2 and K_3 correspond to the Orsay constants B_2 and B_1 respectively and are positive as described in [37, 4]. Also $\lambda_5 > 0$ as noted in [22]. The equation (5.63) forms the basis for subsequent work on this problem. Compared to its equivalent in [7, eq. 2.40], (5.63) possess similar features and is certainly non-linear in nature. The polynomial approximation method as described in [7] may be employed to develop a solution for the wavefront described by $\phi(\xi, t)$.

5.7 Using polynomial approximations to solve the nonlinear system

The equation at (5.63) cannot be solved exactly. Instead, following the method of polynomial expansions presented in [7], we shall derive a pair of coupled

nonlinear equations. Our goal is to use the solutions to these equations to construct an approximating polynomial which captures the behaviour of the planar wavefront as it travels. As a bonus the half wall width information can also be used to approximate the wall width of the domain wall.

As discussed by Stewart and Wigham [7] the aim is to construct a Taylor-expansion with respect to the wall distance. The expansion is performed about the wall core value at $\xi = 0$. Then referring to Figure 5.2 we see that at the wall core when $\xi = 0$ we have that

$$\phi(0,t) = \tfrac{1}{2}\left(\phi_0 + \phi_1\right) \text{ for all } t \geq 0. \tag{5.64}$$

Taylor expanding about $\xi = 0$ to third order in ξ with time dependent coefficients allows us to express $\phi(\xi, t)$ as a polynomial approximation

$$\phi(\xi,t) = \tfrac{1}{2}\left(\phi_0 + \phi_1\right) + a(t)\xi + \tfrac{1}{2}b(t)\xi^2 + \tfrac{1}{6}c(t)\xi^3. \tag{5.65}$$

Then referring to Figure 5.2 once more we define the boundary conditions of our problem in the following manner

$$\phi(\xi_0,t) = \phi_0, \quad \phi(-\xi_1,t) = \phi_1, \tag{5.66}$$

$$\frac{\partial}{\partial\xi}\phi(\xi_0,t) = 0, \quad \frac{\partial}{\partial\xi}\phi(-\xi_1,t) = 0. \tag{5.67}$$

With the boundary conditions stated above we find on substituting (5.65) into (5.66) and (5.67) the following system of four simultaneous linear equations in three unknowns $a(t)$, $b(t)$ and $c(t)$

$$a(t)\xi_0 + \tfrac{1}{2}b(t)\xi_0^2 + \tfrac{1}{6}c(t)\xi_0^3 = \tfrac{1}{2}\left(\phi_0 - \phi_1\right), \tag{5.68}$$

$$a(t)\xi_1 - \tfrac{1}{2}b(t)\xi_1^2 + \tfrac{1}{6}c(t)\xi_1^3 = \tfrac{1}{2}\left(\phi_0 - \phi_1\right), \tag{5.69}$$

$$a(t) + b(t)\xi_0 + \tfrac{1}{2}c(t)\xi_0^2 = 0, \tag{5.70}$$

$$a(t) - b(t)\xi_1 + \tfrac{1}{2}c(t)\xi_1^2 = 0. \tag{5.71}$$

This system of equations may be solved using Gaussian elimination and full details are given in Appendix (D). For now we simply state that on solving (5.68)-(5.71) we are lead to conclude that $\xi_0(t) = \xi_1(t)$ and $b(t) = 0$. Furthermore we find that $a(t)$ and $c(t)$ are related to the half wall width $\xi_0(t)$ via the following expressions

$$a(t) = -\frac{\xi_0^2(t)}{2}c(t) = \frac{3}{4}\frac{(\phi_0 - \phi_1)}{\xi_0(t)}, \tag{5.72}$$

$$c(t) = -\frac{3}{2}\frac{(\phi_0 - \phi_1)}{\xi_0^3}. \tag{5.73}$$

In addition we may express $c(t)$ in terms of $a(t)$ via (5.72) and (5.73) where we find

$$c(t) = -\frac{32}{9}\frac{1}{(\phi_0 - \phi_1)^2}a^3(t). \tag{5.74}$$

We note that we may express the solution $\phi(\xi, t)$ in terms of $a(t)$, ξ, ϕ_0 and ϕ_1 as follows

$$\phi(\xi,t) = \begin{cases} \phi_1, & \text{for } \xi \leq -\xi_0(t), \\ \frac{1}{2}(\phi_0 + \phi_1) + a(t)\xi - \frac{16}{27}\frac{1}{(\phi_0-\phi_1)^2}a^3(t)\xi^3, & \text{for } -\xi_0(t) < \xi < \xi_0(t), \\ \phi_0, & \text{for } \xi \geq \xi_0(t). \end{cases} \tag{5.75}$$

Now with (5.7) we proceed to develop a pair of coupled nonlinear differential equations in terms of $a(t)$ and $\rho(t)$. In order to achieve this we begin by expanding the trigonometric terms in (5.63) up to third order in ξ so that the cosine terms take the form

$$\begin{aligned} \cos\phi &= \cos\left(\tfrac{1}{2}(\phi_0 + \phi_1)\right) - \sin\left(\tfrac{1}{2}(\phi_0 + \phi_1)\right)a(t)\xi - \frac{1}{2}\cos\left(\tfrac{1}{2}(\phi_0 + \phi_1)\right)a^2(t)\xi^2 \\ &\quad + \sin\left(\tfrac{1}{2}(\phi_0 + \phi_1)\right)\left(\tfrac{16}{27}\frac{1}{(\phi_0-\phi_1)^2} + \tfrac{1}{6}\right)a^3(t)\xi^3 + O(\xi^4), \end{aligned} \tag{5.76}$$

and the sine terms are expressed as

$$\begin{aligned} \sin\phi &= \sin\left(\tfrac{1}{2}(\phi_0 + \phi_1)\right) + \cos\left(\tfrac{1}{2}(\phi_0 + \phi_1)\right)a(t)\xi - \frac{1}{2}\sin\left(\tfrac{1}{2}(\phi_0 + \phi_1)\right)a^2(t)\xi^2 \\ &\quad - \cos\left(\tfrac{1}{2}(\phi_0 + \phi_1)\right)\left(\tfrac{16}{27}\frac{1}{(\phi_0-\phi_1)^2} + \tfrac{1}{6}\right)a^3(t)\xi^3 + O(\xi^4). \end{aligned} \tag{5.77}$$

Then using (5.76) and (5.77) and defining

$$\Phi_- = \phi_0 - \phi_1, \tag{5.78}$$

$$\Phi_+ = \phi_0 + \phi_1. \tag{5.79}$$

we find that the differential equation given at (5.63) may be expressed up to third order in ξ by the following

$$\begin{aligned}
&2\lambda_5 \left(\frac{\mathrm{d}a}{\mathrm{d}t} \left[\xi - \frac{16}{9} \frac{1}{\Phi_-^2} a^2 \xi^2 \right] - \frac{\mathrm{d}\rho}{\mathrm{d}t} \left[a - \frac{16}{9} \frac{1}{\Phi_-^2} a^3 \xi^2 \right] \right) = \\
&- \frac{32}{9} K_2 \left(\sin^2 \frac{\Phi_+}{2} \frac{1}{\Phi_-^2} a^3 \xi + \sin \Phi_+ \frac{1}{\Phi_-^2} a^4 \xi^2 + \cos \Phi_+ \frac{1}{\Phi_-^2} a^5 \xi^3 \right) \\
&- \frac{32}{9} K_3 \left(\cos^2 \frac{\Phi_+}{2} \frac{1}{\Phi_-^2} a^3 \xi - \sin \Phi_+ \frac{1}{\Phi_-^2} a^4 \xi^2 - \cos \Phi_+ \frac{1}{\Phi_-^2} a^5 \xi^3 \right) \\
&+ (K_2 - K_3) \left(\frac{1}{2} \sin \Phi_+ a^2 + \left(\cos \Phi_+ - \frac{16}{9} \sin \Phi_+ \frac{1}{\Phi_-^2} \right) a^3 \xi - \sin \Phi_+ a^4 \xi^2 \right) \\
&- (K_2 - K_3) \left(\cos \Phi_+ \left(\frac{16}{27} \frac{1}{\Phi_-^2} + \frac{1}{6} \right) a^5 + \frac{1}{2} \cos \Phi_+ a^5 + \frac{32}{9} \cos \Phi_+ \frac{1}{\Phi_-^2} a^4 \right) \xi^3 \\
&- A(\theta, \alpha) \left(\sin \frac{\Phi_+}{2} + \cos \frac{\Phi_+}{2} a\xi - \frac{1}{2} \sin \frac{\Phi_+}{2} a^2 \xi^2 - \cos \frac{\Phi_+}{2} \left(\frac{16}{27} \frac{1}{\Phi_-^2} + \frac{1}{6} \right) a^3 \xi^3 \right) \\
&- B(\theta, \alpha) \left(\frac{1}{2} \sin \Phi_+ + \cos \Phi_+ a\xi - \sin \Phi_+ a^2 \xi^2 - \left(\frac{2}{3} + \frac{16}{27} \frac{1}{\Phi_-^2} \right) \cos \Phi_+ a^3 \xi^3 \right) \\
&- C(\alpha) \left(\cos \frac{\Phi_+}{2} - \sin \frac{\Phi_+}{2} a\xi - \frac{1}{2} \cos \frac{\Phi_+}{2} a^2 \xi^2 + \sin \frac{\Phi_+}{2} \left(\frac{16}{27} \frac{1}{\Phi_-^2} + \frac{1}{6} \right) a^3 \xi^3 \right) \\
&+ O(\xi^4),
\end{aligned} \tag{5.80}$$

where we define $A(\theta, \alpha)$, $B(\theta, \alpha)$ and $C(\alpha)$ to be

$$A(\theta, \alpha) = \epsilon_0 \epsilon_a E^2 \sin\theta \cos\alpha \sin\alpha \cos\theta, \tag{5.81}$$

$$B(\theta, \alpha) = \epsilon_0 \epsilon_a E^2 \sin^2\theta \cos^2\alpha, \tag{5.82}$$

$$C(\alpha) = P_0 E \cos\alpha. \tag{5.83}$$

Finally by setting the coefficients of the zeroth and first order powers of ξ to zero we are left with a pair of coupled nonlinear differential equations. The first equation results from considering the coefficient of the zeroth order power of ξ

$$-2\lambda_5 a \frac{\mathrm{d}\rho}{\mathrm{d}t} = \frac{1}{2} (K_2 - K_3) \sin \Phi_+ a^2 - A(\theta, \alpha) \sin \frac{\Phi_+}{2}$$

$$- B(\theta,\alpha)\sin\Phi_+ - C(\alpha)\cos\frac{\Phi_+}{2}. \tag{5.84}$$

The second equation is derived by considering the coefficient of the first order power of ξ

$$\begin{aligned} 2\lambda_5\frac{\mathrm{d}a}{\mathrm{d}t} &= -\frac{32}{9}\left(K_2\sin^2\frac{\Phi_+}{2}+K_3\cos^2\frac{\Phi_+}{2}\right)\frac{1}{\Phi_-^2}a^3 \\ &\quad + (K_2-K_3)\left(\cos\Phi_+ - \frac{16}{9}\sin\Phi_+\frac{1}{\Phi_-^2}\right)a^3 \\ &\quad - \left(A(\theta,\alpha)\cos\frac{\Phi_+}{2} + B(\theta,\alpha)\cos\Phi_+ - C(\alpha)\sin\frac{\Phi_+}{2}\right)a. \end{aligned} \tag{5.85}$$

Taken together (5.84) and (5.85) along with boundary conditions which we assume to be $\rho(0)=\rho_0$ and $a(0)=a_0$ may be studied for different values of ϕ_0, ϕ_1, ρ_0 and a_0. In the case of the π-wall which comes about as a result of studying the planar geometry of the problem with an in plane electric field (that is one where the field angle α is zero), we may solve (5.84) and (5.85) exactly. Using the solution to (5.85) we may construct a solution for $\phi(\xi,t)$ and we shall explore this in the next section.

5.8 The π-wall

In this section we shall explore the solutions of (5.84) and (5.85) when confronted with an electric field inclined at an angle $\alpha=0$. We saw in Chapter 2 that the reaction-diffusion equation (2.9) corresponding to the problem we are investigating here does have an exact solution (2.10) and the resulting wave travels with a speed given by (2.12). The intention here is to use the known solution to the exactly solvable problem as a yardstick against which we can compare the approximate solution $\phi(\xi,t)$.

As we have already established, the travelling wave (2.9) travels between two known states ϕ_0 and ϕ_1 at a constant speed. As a matter of convenience we shall plot the negative of the known solution. If we plot the negative wave at time

$t = 1$ and assume the negative sign in the solution at (2.10) with the remaining constants set to 1 we see the graph displayed in Figure 5.3. Examining the

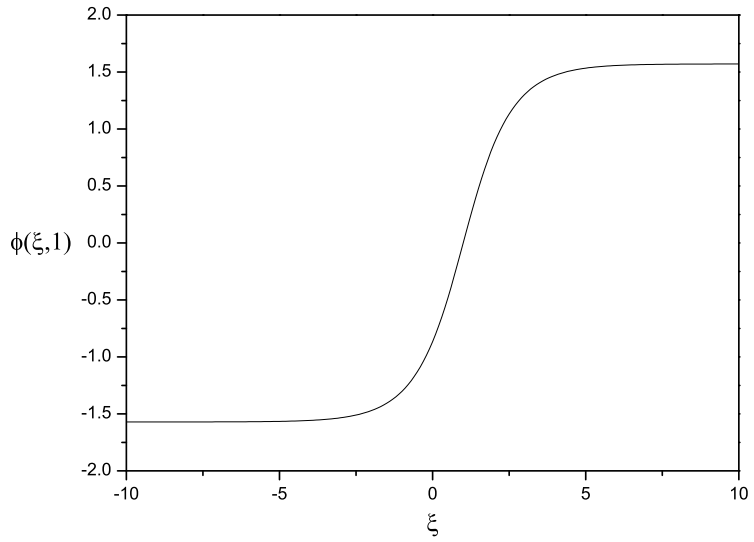

Figure 5.3: Travelling wave at $t = 1$ with negative addition of νt

travelling wave we see that the $-\frac{\pi}{2}$ region is growing at the expense of the $\frac{\pi}{2}$ region. In the model we have just constructed we shall assume that the region denoted by ϕ_1 corresponds to the $-\frac{\pi}{2}$ state so that $\phi_1 = -\frac{\pi}{2}$. Similarly we assume that the region denoted by ϕ_0 corresponds to the $\frac{\pi}{2}$ state so that we choose $\phi_0 = \frac{\pi}{2}$.

Now choosing these values for ϕ_0 and ϕ_1 and additionally assuming that $K_2 = K_3 \equiv B$ and $\epsilon_a = -|\epsilon_a|$, we may re-write (5.84) and (5.85) in the following forms

$$2\lambda_5 \frac{\mathrm{d}\rho}{\mathrm{d}t} = \frac{P_0 E}{a}, \tag{5.86}$$

$$2\lambda_5 \frac{\mathrm{d}a}{\mathrm{d}t} = -\frac{32B}{9\pi^2} a^3 + \epsilon_0 |\epsilon_a| E^2 \sin^2\theta a. \tag{5.87}$$

Equation (5.87) is a Bernouilli equation which we can solve. We follow [7] and

begin by making the following definitions

$$\beta_0 = \frac{\epsilon_0|\epsilon_a|E^2\sin^2\theta}{2\lambda_5}, \quad \beta_1 = \frac{16B}{9\lambda_5\pi^2}, \tag{5.88}$$

which means that (5.87) may be written more succinctly as follows

$$\frac{\mathrm{d}a}{\mathrm{d}t} = \beta_0 a - \beta_1 a^3. \tag{5.89}$$

We then make the substitution

$$a(t) = \frac{1}{\sqrt{v(t)}} = v^{-\frac{1}{2}}(t), \tag{5.90}$$

which means that the derivative in (5.89) may be written in the form

$$\frac{\mathrm{d}a}{\mathrm{d}t} = -\frac{1}{2}v^{-\frac{3}{2}}\frac{\mathrm{d}v}{\mathrm{d}t}. \tag{5.91}$$

This in turn allows us to express (5.89) in terms of $v(t)$

$$-\frac{1}{2}v^{-\frac{3}{2}}\frac{\mathrm{d}v}{\mathrm{d}t} = \beta_0 v^{-\frac{1}{2}} - \beta_1 v^{-\frac{3}{2}}, \tag{5.92}$$

giving the following equation

$$\frac{\mathrm{d}v}{\mathrm{d}t} + 2\beta_0 v = 2\beta_1. \tag{5.93}$$

An integrating factor for this is $e^{2\beta_0 t}$ which leads to

$$\frac{\mathrm{d}}{\mathrm{d}t}\left[e^{2\beta_0 t}v\right] = 2\beta_1 e^{2\beta_0 t}. \tag{5.94}$$

Integrating we find

$$\begin{aligned} e^{2\beta_0 t}v(t) &= 2\beta\int e^{2\beta_0 t}dt + C, \\ \Rightarrow v(t) &= \frac{\beta_1}{\beta_0} + Ce^{-2\beta_0 t}. \end{aligned} \tag{5.95}$$

Letting $v(0) = v_0$ we find that at $t = 0$

$$C = v_0 - \frac{\beta_1}{\beta_0}. \tag{5.96}$$

So we arrive at the final expression for $v(t)$ which is

$$v(t) = \frac{\beta_1}{\beta_0}\left(1 - e^{-2\beta_0 t}\right) + v_0 e^{-2\beta_0 t} \tag{5.97}$$

Then using the expression for $a(t)$ given at (5.90) we see immediately that

$$a(t) = \left\{\frac{\beta_1}{\beta_0}\left(1 - e^{-2\beta_0 t}\right) + \frac{1}{a_0^2}e^{-2\beta_0 t}\right\}^{-\frac{1}{2}}, \tag{5.98}$$

where we have used the fact that $a(0) = a_0$ so that

$$a(0) = \frac{1}{\sqrt{v(0)}} = \frac{1}{\sqrt{v_0}} = a_0, \tag{5.99}$$

meaning that $v_0 = \frac{1}{a_0^2}$. Now we established in (5.72) that $a(t)$ and $\xi_0(t)$ were related via

$$\xi_0(t) = \frac{3\left(\phi_0 - \phi_1\right)}{4a(t)}, \tag{5.100}$$

which together with our choices of $\phi_0 = \frac{\pi}{2}$ and $\phi_1 = -\frac{\pi}{2}$ lead to the following expression for the half-wall width

$$\xi_0(t) = \frac{3\pi}{4a(t)}. \tag{5.101}$$

Then when $t = 0$ we find that the initial value of $\xi_0(t)$ is

$$\xi_0(0) = \frac{3\pi}{4a(0)} = \frac{3\pi}{4a_0}. \tag{5.102}$$

Now, using the relationship at (5.101) the expression for $a(t)$ given at (5.98) and the initial condition (5.102) we may write down the half-wall width as a function of t as follows

$$\xi_0(t) = \frac{3\pi}{4}\left\{\frac{\beta_1}{\beta_0}\left(1 - e^{-2\beta_0 t}\right) + \frac{16\xi_0^2(0)}{9\pi^2}e^{-2\beta_0 t}\right\}^{\frac{1}{2}}, \tag{5.103}$$

Pausing briefly we consider the long term behaviour of the half-wall width which is

$$\lim_{t\to\infty} \xi_0(t) = \frac{3\pi}{4}\sqrt{\frac{\beta_1}{\beta_0}} \tag{5.104}$$

Finally, returning to the differential equation for the position of the wall core at time t given by (5.86) and using the expression for $a(t)$ we found at (5.90), we see that the time rate of change of the wall core is given by

$$\frac{\mathrm{d}\rho}{\mathrm{d}t} = \frac{P_0 E}{2\lambda_5}\left\{\frac{\beta_1}{\beta_0}\left(1 - e^{-2\beta_0 t}\right) + \frac{1}{a_0^2}e^{-2\beta_0 t}\right\}^{\frac{1}{2}}. \tag{5.105}$$

The time rate of change of the wall core represents the speed or velocity of the travelling wave. Recall from Chapter 2 that the wave speed ν for a travelling wave under the influence of an in plane electric field given by (2.12) is

$$\nu = \frac{|P_0 E|}{2\lambda_5}\sqrt{\frac{B}{\beta}}, \tag{5.106}$$

where β is given by (2.11). At time $t = 0$ and assuming $P_0 E > 0$ the time rate of change of the core of the domain wall is given by

$$\frac{\mathrm{d}\rho}{\mathrm{d}t} = \frac{P_0 E}{2\lambda_5}\frac{1}{a_0}. \tag{5.107}$$

Equating (5.107) to (5.106) and solving for a_0 we find that the initial condition for a_0 may be written as

$$a_0 = \sqrt{\frac{\beta}{B}}, \tag{5.108}$$

and this in turn can be used to establish an approximate condition for the initial half-wall width from (5.102)

$$\xi_0(0) = \frac{3\pi}{4}\sqrt{\frac{B}{\beta}}. \tag{5.109}$$

Then using (5.109) we find that the expression for the half-wall width (5.103) reduces to the following

$$\xi_0(t) = \frac{3\pi}{4}\sqrt{\frac{B}{\beta}}\left\{\frac{32}{9\pi^2} + \left(1 - \frac{32}{9\pi^2}e^{-2\beta_0 t}\right)\right\}^{\frac{1}{2}}. \tag{5.110}$$

Then using the final result (5.110) we may find an approximate solution for the negative of the wavefront at time $t = 0$ given the expression for $\phi(\xi, t)$ at (5.7)

and the expression for $a(t)$ at (5.98). We shall employ physical parameters for a well known material specifically SCE13 taken from ([4, p.312]). We tabulate the relevant quantities in Table 5.1. The rotational viscosity and permittivity

Parameter	Symbol	Value
Smectic cone angle	θ	25.5°
Spontaneous polarisation	P_0	$135\ \mu\text{C m}^{-2}$
Dielectric constant	ϵ_a	-0.72
Elastic constant	B	1.41×10^{-12} N
Ancillary data		
Rotational viscosity	λ_5	0.025 Pa s
Permittivity of free space	ϵ_0	$\epsilon_0 = 8.854^{-12}\ \text{Fm}^{-1}$

Table 5.1: Material parameters and ancillary data for SCE13 at 52.5°C

values given here are taken from ([4, p.317 and p.329]).We have chosen a field strength of $E = 1 \times 10^8$ V m^{-1}. A plot of the exact solution against the approximate solution is given in Figure 5.4. As Figure 5.4 shows the domain wall is of the order of 40nm in width. Features this size are needless to say too small to be detected optically. The approximate solution at $t = 0$ represents a very close approximation to the known exact solution calculated with the same physical parameters and field strength values. In particular the approximate wavefront solution is a very close approximation to the exact solution over a range of approximately 20nm. At longer timescales the wavefront settles to a width of approximately 30nm so at large times the approximate solution is qualitatively less accurate.

5.9 Discussion

The work presented in this chapter was as we remarked upon earlier an attempt to adapt an existing method namely that of Stewart and Wigham [7] for approximating the wave front of a travelling domain wall in a sample of smectic

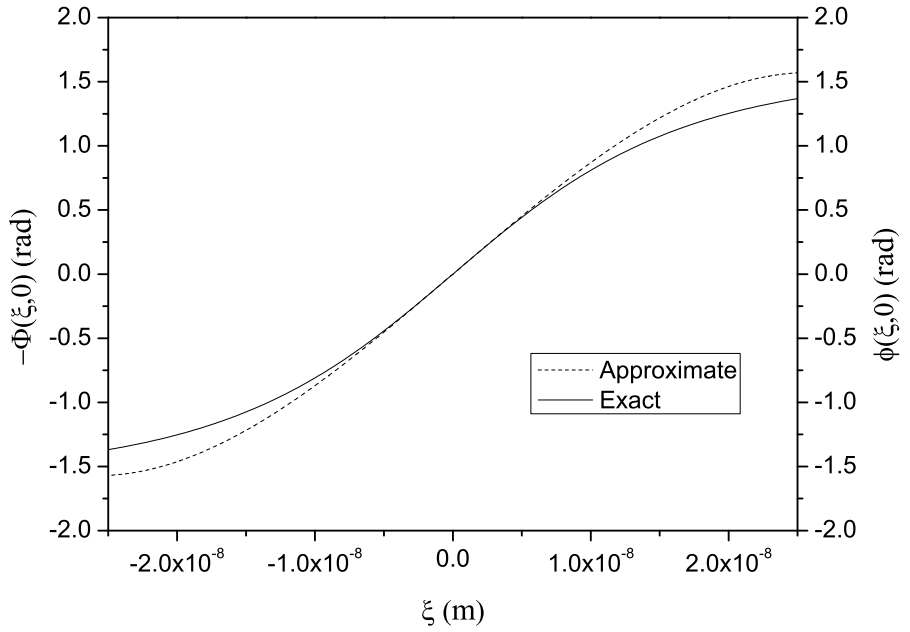

Figure 5.4: Approximate solution and the exact solution for comparison plotted at $t = 0$ with a field strength of $E = 1 \times 10^8$ V m^{-1} and physical parameters taken from Table 5.1.

C liquid crystal. In our case the domain wall is planar and the material ferroelectric. The planar nature of the problem makes the problem slightly easier to pose than in the cylindrical case, but nonetheless we were able to derive a wave profile which is in good agreement with the wave profile for the π-wall.

We can in principal extend this technique to determine wave shapes for domain wall where the boundary conditions are not exact multiples of π and this would be a relatively straightforward procedure. We simply identify the boundary conditions from the nonlinear reaction term in the dynamic equation and use these as boundary conditions instead of $\pm\frac{\pi}{2}$ as in the exact case.

Another benefit of employing the technique is that it provides an insight into the development of the wave front in terms of speed and position although the positional information is perhaps not as useful as the wavespeed information. In addition it is possible to analytically derive an approximation for wall width.

From here we proceed in the final chapter to present a numerical algorithm which may be used to determine wavespeeds in travelling domain walls with a particular focus on the domain walls we have been investigating throughout this thesis. In fact the method is quite general and may be applied to any reaction-diffusion system with an appropriate nonlinear kinetic term.

Chapter 6

Computing the wave speed of soliton-like solutions in Smectic C* liquid crystals

6.1 Introduction

In this chapter we consider the problem of determining the wave speed of travelling wave solutions satisfying parabolic PDE's of the form

$$\frac{\partial \phi}{\partial t} = \frac{\partial^2 \phi}{\partial x^2} - i\left(\phi\right), \tag{6.1}$$

where $i(\phi)$ represents a nonlinear reaction term. Nonlinear parabolic PDE's of the form (6.1), known commonly as reaction-diffusion or evolution equations, occur often in many branches of mathematics, engineering, chemistry and biology. Examples of nonlinear reaction diffusion equations include the Fisher model [59, p.234-5] modeling species diffusion, the Nagumo model of the propogation of nerve signals through a nerve axon [59, p.242] and in electronic engineering the study of bistable transmission lines [78] leads to nonlinear reaction diffusion type problems. Nonlinear parabolic PDE's of the type we shall be concerning ourselves with typically yield solitary wave solutions which typically travel between two states. For example in earlier chapters we studied the effect of perturbing

solutions to equation (6.2) in the special case where $\alpha = 0$

$$2\lambda_5 \frac{\partial \phi}{\partial t} = B\frac{\partial^2 \phi}{\partial x^2} - P_0 E \cos\alpha \cos\phi \\ -\epsilon_0 \epsilon_a E^2 \left(\frac{1}{4} \sin 2\alpha \sin 2\theta \sin\phi + \frac{1}{2} \cos^2\alpha \sin^2\theta \sin 2\phi \right). \quad (6.2)$$

Equation (6.2) which appears in [54], governs the temporal and spatial development of the usual c-director orientation angle $\phi(x,t)$ in a sample of smectic C* in the planar layer arrangement of Fig. 6.1(a), under the influence of an external electric field $\mathbf{E}$ at an angle of α to the plane of the sample, as shown in Fig. 6.1(c). To recap, we note that P_0 represents the polarisation, B is an elastic constant, E the magnitude of the electric field, λ_5 is a rotational viscosity, ϵ_0 is the permittivity of free space, ϵ_a is the (unitless) measure of the dielectric anisotropy and θ is the (fixed) angle the director $\mathbf{n}$ makes with the layer normal $\mathbf{a}$. In [54]

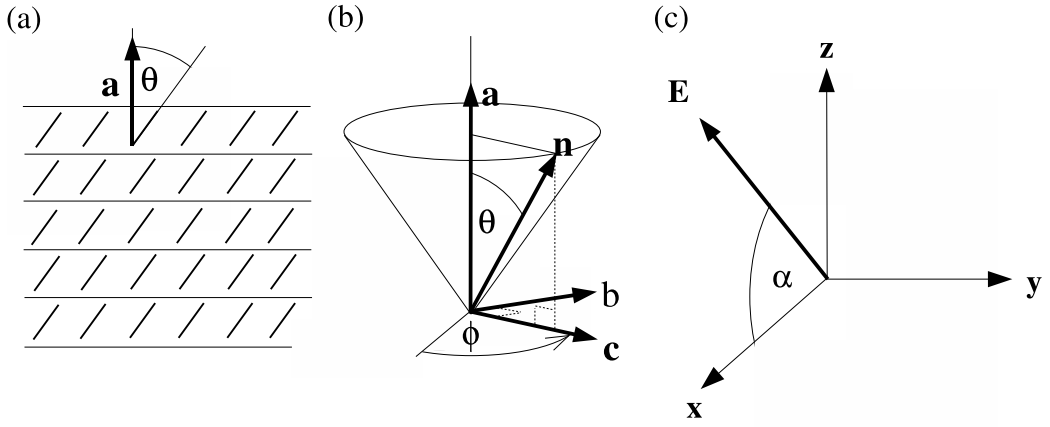

Figure 6.1: (a) The planar layer arrangement of the liquid crystal sample being considered. The molecules are tilted at a fixed angle θ to the layer normal $\mathbf{a}$ which is aligned with the z-axis. (b) The average molecular alignment is denoted by the unit vector $\mathbf{n}$, called the director. The vector $\mathbf{c}$ is the unit orthogonal projection of $\mathbf{n}$ onto the smectic planes. The orientation angle of the c-director is ϕ. Note also that smectic C* has a spontaneous polarisation which lies along the vector $\mathbf{b}$ and is denoted by $\mathbf{P} = P_0\mathbf{b}$ where $\mathbf{b} = \mathbf{a} \times \mathbf{c}$. (c) The electric field $\mathbf{E}$ at an angle of incline $\alpha \geq 0$ with respect to the smectic layers in the xy-plane [8].

Stewart and Momoniat examine in some detail the characteristic features of the *electric energy density* used to construct (6.2). In this case the electric energy

density defines the energy states between which travelling wave solutions satisfying (6.2) propagate. By non-dimensionalising and rescaling they study the effect of varying the angle of the field E on the electric energy density. We shall briefly review the energy density function and the associated equilibrium states before going on to consider the wave speed problem in detail.

6.2 Electric Energy Density

We shall follow [54] as we explore the electric energy density and its connection to equilibrium states. We begin by considering equation (6.2). This has a non-linear *kinetic* term given by

$$i(\phi) = P_0 E \cos\alpha \cos\phi + \epsilon_0 \epsilon_a E^2 \left(\frac{1}{4} \sin 2\alpha \sin 2\theta \sin\phi + \frac{1}{2} \cos^2\alpha \sin^2\theta \sin 2\phi \right). \tag{6.3}$$

Here the function $i(\phi)$ is actually the derivative of the electric energy density which we denote by w_{elec}. This means we may re-write (6.2) as

$$2\lambda_5 \frac{\partial \phi}{\partial t} = B \frac{\partial^2 \phi}{\partial x^2} - \frac{\partial w_{elec}}{\partial \phi}, \tag{6.4}$$

and we make the association

$$i(\phi) = \frac{\partial w_{elec}}{\partial \phi}. \tag{6.5}$$

Then, on integrating (6.5) we recover the total electric energy density w_{elec}, which is given by the expression

$$w_{elec} = P_0 E \cos\alpha \sin\phi - \frac{1}{2} \epsilon_0 \epsilon_a E^2 \left(\sin\alpha \cos\theta + \cos\alpha \sin\theta \cos\phi \right)^2. \tag{6.6}$$

By introducing suitable dimensionless parameters χ and σ defined by

$$\chi = 2P_0 (\epsilon_0 \epsilon_a E \cos\alpha \sin^2\theta)^{-1}, \tag{6.7}$$

$$\sigma = \tan\alpha \cot\theta, \tag{6.8}$$

we may write the electric energy density (6.6) as

$$w_{elec} = \frac{1}{2}\epsilon_0\epsilon_a E^2 \cos^2\alpha \sin^2\theta \; \bar{w}_{elec}, \tag{6.9}$$

where $\bar{w}_{elec}$ is the dimensionless quantity given by

$$\bar{w}_{elec} = \chi \sin\phi - (\sigma + \cos\phi)^2 . \tag{6.10}$$

The behaviour of the electric energy density w_{elec} may be described completely by considering the expression (6.10). If we reverse the sign of the electric field we change the sign of χ. In addition changing the signs of the dielectric anisotropy ϵ_a and electric field E simultaneously corresponds to changing the sign of w_{elec}. This means that we can characterise all possibilities by considering $\bar{w}_{elec}$ only.

Notice that the parameter σ is a measure of the tilt of the electric field with respect to the plane in which the sample lies. If the electric field lies in the plane of the sample $\alpha = 0$ and $\sigma = 0$. Since we choose to make $0 < \theta < \frac{\pi}{2}$ and $0 \leq \alpha < \frac{\pi}{2}$ we need only consider cases where $\sigma \geq 0$. The parameter χ is a measure of the ratio of the spontaneous polarisation P_0 to the magnitude of the electric field $\mathbf{E}$. Note that since $\chi \propto \frac{1}{E}$ we expect $|\chi|$ to decrease as $|E|$ increases. In the presence of smaller magnitude fields and small electric field inclination angles α we generally expect $\sigma < |\chi|$ [54].

Consider the graphs shown in Figure 6.2. The graph in Figure 6.2(a) charts the number of equilibrium states and the position of those equilibrium states as we vary the parameter χ. In this figure σ is fixed and has a value of $\sigma = 0.001$. As χ increases, that is as $\mathbf{E}$ decreases in magnitude, the number of equilibria goes from four to two as we pass through some critical value χ_c. In the case of Figure 6.2 the critical value of χ is given approximately by $\chi_c \approx 1.9$. When $\chi < \chi_c$ four equilibria become available. Above this critical value when $\chi > \chi_c$ only two equilibria are available. In otherwords at fixed σ and with $\chi = \chi(E)$ where χ is a function only of the field strength E, we find that as we lower the

field E we eventually pass through a critical point on the $\chi - \phi$ plane into a region where only two equilibria are available.

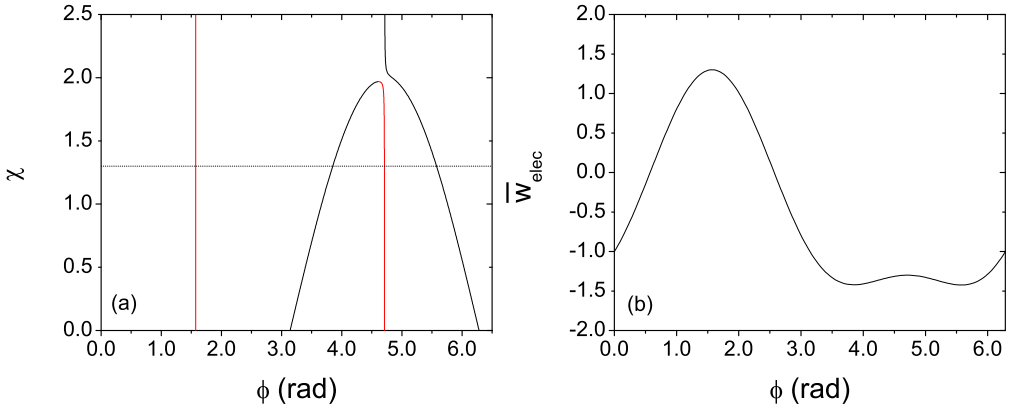

Figure 6.2: For fixed $\sigma = 0.001$ the graphs show (a) the equilibrium states as χ varies with unstable equilibria (red lines) and stable equilibria (black lines), and (b) the electric energy density at fixed $\sigma = 0.001$ corresponding to the dotted line through $\chi = 1.3$ in (a).

The equilibrium states are determined for each value of χ by considering the positions of the local minima and local maxima given by the electric energy density function $\bar{w}_{elec}$. Consider now the dotted horizontal line corresponding to $\chi = 1.3$ in Figure 6.2(a). With σ fixed at $\sigma = 0.001$ it is a straightforward exercise to plot the dimensionless energy $\bar{w}_{elec}$ and the result is shown in Figure 6.2(b). Notice that for $\chi = 1.3$ when $\sigma = 0.001$ there are 4 equilibria, and furthermore notice that two of the equilibria are *asymptotically stable* (black lines) whilst two are *unstable* (red lines). In terms of the dimensionless energy density, asymptotically stable and unstable equilibria occur at local minima and local maxima respectively.

Consider now the graphs show in Figure 6.3. This time we have chosen a value of $\sigma = 0.217$ in order to illustrate the qualitative differences in behaviour of the electric energy density as we increase the field inclination. As was the case in Figure 6.2 we have chosen to consider the electric energy density $\bar{w}_{elec}$ at the point where the $\chi = 1.3$. We observe, by comparing Figure 6.2(a) and

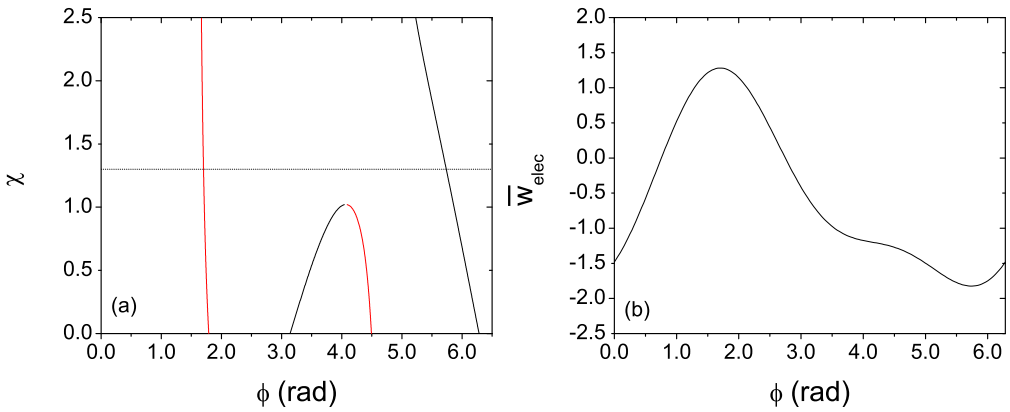

Figure 6.3: For fixed $\sigma = 0.217$ the graphs show (a) the equilibrium states as χ varies with unstable equilibria (red lines) and stable equilibria (black lines), and (b) the electric energy density at fixed $\sigma = 0.217$ corresponding to the dotted line through $\chi = 1.3$ in (a).

Figure 6.3(a), that at steeper inclinations of the electric field when we fix χ the number of equilibria drops from four to two. In Figure 6.3 the critical value of χ occurs at approximately $\chi_c \approx 1.1$. In effect there are two sets of critical values, a critical value χ_c which determines the threshold between two equilibria and four equilibria based on electric field strength E, and a critical value σ_c which determines the threshold between two and four equilibria by electric field inclination α.

Next we consider only values of $\chi < 0$ and determine equilibria by studying $-\bar{w}_{elec}$. First we present graphs corresponding to equilibrium states for $\sigma = 0.001$ and $\sigma = 0.217$ while we vary χ such that $-2.5 \leq \chi < 0$ and plot the results in Figures 6.4 and 6.5. Once again we have chosen a fixed value for χ of $\chi = -1.3$. Notice that now we expect the number of equilibria to undergo a bifurcation from four to two at some critical value of χ as we make χ more *negative*. Again fixing σ allows us to determine approximate critical values. For instance in Figure 6.4 the critical value χ_c is given approximately by $\chi_c \approx -1.9$. In addition we make the observation that by fixing χ and varying σ we can in principle record σ_c the critical value of σ in a like manner.

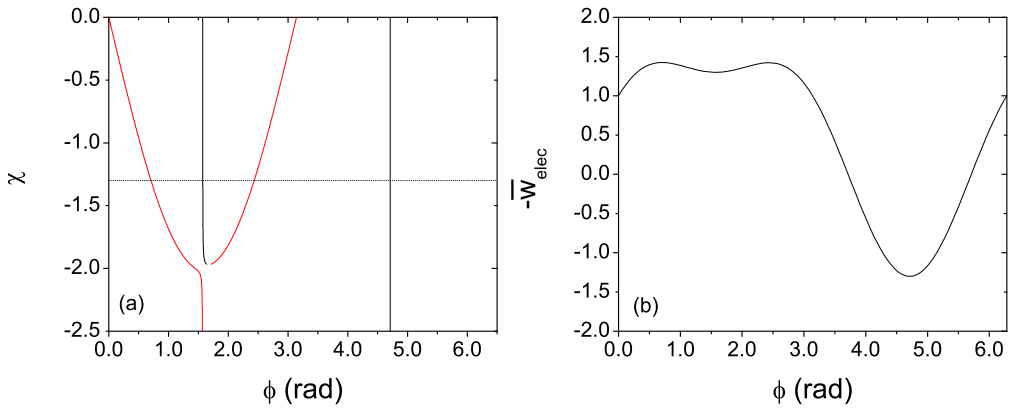

Figure 6.4: For fixed $\sigma = 0.001$ the graphs show (a) the equilibrium states as χ varies with unstable equilibria (red lines) and stable equilibria (black lines), and (b) the electric energy density at fixed $\sigma = 0.001$ corresponding to the dotted line through $\chi = -1.3$ in (a).

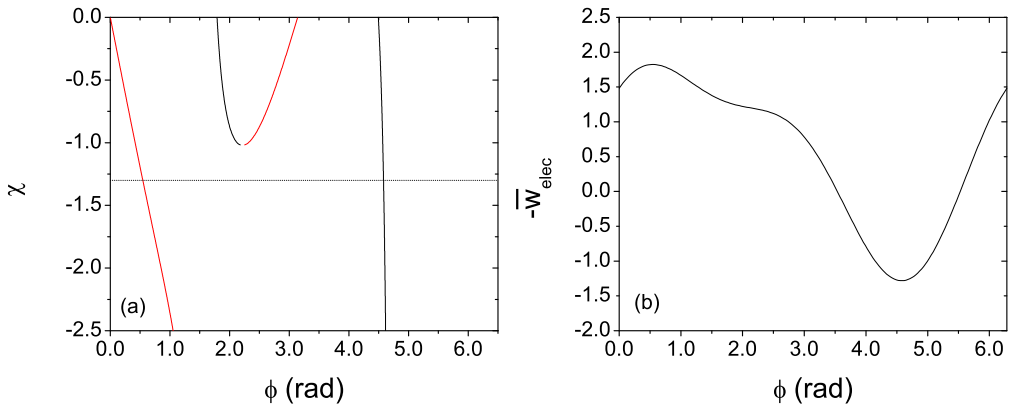

Figure 6.5: For fixed $\sigma = 0.217$ the graphs show (a) the equilibrium states as χ varies with unstable equilibria (red lines) and stable equilibria (black lines), and (b) the electric energy density at fixed $\sigma = 0.217$ corresponding to the dotted line through $\chi = -1.3$ in (a).

Throughout the remainder of this chapter we shall be concerned with determining wave speeds of travelling waves connecting equilibrium states. For the most part our principal aim shall be to determine wave speed *magnitudes* rather than the relative direction of travel of the wave and we begin exploring these topics in the next and following sections.

6.3 Scaling the dynamical equation

Consider the scaled variables T and X

$$T = \frac{1}{4}t(2\lambda_5)^{-1}\epsilon_0 \left|\epsilon_a\right| E^2 \cos^2\alpha \sin^2\theta, \tag{6.11}$$

$$X = \frac{1}{2}xB^{\frac{1}{2}}\left(\epsilon_0 \left|\epsilon_a\right| E^2 \cos^2\alpha \sin^2\theta\right)^{\frac{1}{2}}. \tag{6.12}$$

and the transformation

$$\hat{\phi}(X,T) = 2\phi(X,T) - \pi. \tag{6.13}$$

This permits (6.2) to be expressed as

$$\frac{\partial\hat{\phi}}{\partial T} = \frac{\partial^2\hat{\phi}}{\partial X^2} - 4\chi\sin\frac{\hat{\phi}}{2} - 4\sin\hat{\phi} + 8\sigma\cos\frac{\hat{\phi}}{2}, \tag{6.14}$$

and is typical of the type of equation we shall study in the remainder of this chapter. If $\sigma \neq 0$ then no closed form solutions are known and therefore to solve such an equation we must resort to numerical methods. If, on the other hand, $\sigma = 0$, then (6.14) becomes

$$\frac{\partial\hat{\phi}}{\partial T} = \frac{\partial^2\hat{\phi}}{\partial X^2} - 4\chi\sin\frac{\hat{\phi}}{2} - 4\sin\hat{\phi}, \tag{6.15}$$

which admits the travelling wave solution [4, 79, 80]

$$\hat{\phi}(X,T) = 4\arctan\left\{\exp\left[\mp 2\left(X + \nu T + c\right)\right]\right\}, \quad \nu = \pm\chi, \tag{6.16}$$

where c is an arbitrary constant. Note that for (6.15) the wave velocity is exactly $\nu = \pm\chi$ and that $\hat{\phi} \to 0$ as $X \to \infty$ while $\hat{\phi} \to 2\pi$ as $X \to -\infty$. Given this special solution for $\sigma = 0$, we conjecture that when $\sigma \neq 0$, (6.14) admits travelling wave solutions of the form

$$\psi(z) = \hat{\phi}(X,T), \quad z = X + \nu T, \tag{6.17}$$

where ν now represents a dimensionless wave speed. Justification for this stems from experimental observations, for example the work of Abdulhalim *et al.* [81].

By considering equation (6.1) we develop a simple numerical scheme which will, assuming the equation admits travelling wave solutions, allow us to compute the wave speed directly. We will demonstrate the technique by considering equation (6.15) (where $\sigma \neq 0$) and exploit the fact that it has the well-known solution and wave speed stated in equation (6.16) in order to demonstrate that the new method converges numerically and finds the known exact solution. We will then briefly examine the method applied to the full three term problem in (6.14) when $\sigma \neq 0$.

6.4 Theory

We begin by considering (6.1). We shall employ a technique motivated by, but distinct in nature from, iterative integral methods introduced by Chernyak [82]. Our aim is to express the PDE as an integral equation. Then we may apply boundary conditions and treat the problem approximately using discrete rather than continuous methods. The first step is to recast (6.1) using the transformation

$$\psi(z) = \phi(x,t)\,, \quad z = x + \nu t\,, \tag{6.18}$$

to obtain the equivalent expression

$$\frac{d^2\psi}{dz^2} - \nu\frac{d\psi}{dz} - i\,(\psi) = 0\,. \tag{6.19}$$

By making the substitution

$$p(\psi) = \frac{d\psi}{dz}\,, \tag{6.20}$$

we can transform (6.19) to $p-\psi$ phase space by noting that

$$\frac{d^2\psi}{dz^2} = \frac{dp}{dz} = \frac{d\psi}{dz}\frac{dp}{d\psi} = p\frac{dp}{d\psi}\,. \tag{6.21}$$

Then equation (6.19) becomes

$$p\frac{dp}{d\psi} - \nu p - i\,(\psi) = 0. \tag{6.22}$$

Now, we seek solutions for $\psi(z)$ connecting two constant states a and b say, such that the solution satisfies the boundary conditions

$$\lim_{z\to-\infty}\psi(z)=a,\quad \lim_{z\to\infty}\psi(z)=b. \tag{6.23}$$

Since the solution $\psi(z)$ approaches constant values for large $|z|$ we expect

$$p(a)=\lim_{z\to-\infty}\psi'(z)=0,\quad p(b)=\lim_{z\to\infty}\psi'(z)=0, \tag{6.24}$$

where the prime denotes differentiation with respect to z. Integrating with respect to ψ and noting that $p(a)=0$ and $p(b)=0$, we find that (6.22) may be written in the form of an integral equation.

$$p^2(\psi)-\lambda\int_{t=a}^{\psi}p(t)dt=f(\psi)\,, \tag{6.25}$$

where $\lambda=2\nu$ and

$$f(\psi)=2\int_{t=a}^{\psi}i(t)\,dt\,. \tag{6.26}$$

Equation (6.25) is known as an exceptional nonlinear Volterra-type equation of the second kind [83]. Our aim is to use (6.25) to determine the wave speed ν of the travelling wave connecting the steady states obtained by considering zeros of the nonlinear term $i(\psi)$. To solve (6.25) we assume that for $\psi<a$ and $\psi>b$, $p(\psi)=0$, whereas we expect $p(\psi)\neq 0$ in the interval $a\leq\psi\leq b$. Based on this assumption, and using the fact that $p(a)=p(b)=0$, we shall construct a numerical scheme for the solution $p(\psi)$ using a simple trapezoidal quadrature rule in place of the integral. This in turn will lead us to an iterative procedure which we shall use to numerically calculate an accurate approximation to the actual wave speed ν.

6.5 Numerical method

We proceed as follows. Firstly, suppose that between $\psi = a$ and $\psi = b$ we divide the interval into $N-1$ equally spaced strips of width

$$h^{(N)} = \frac{b-a}{N-1}, \tag{6.27}$$

where $h^{(N)}$ denotes the strip width for an interval with N node points. The variable ψ is defined discretely as

$$\psi_i = a + ih^{(N)},\ i = 0, \ldots, N-1. \tag{6.28}$$

Then we can compute the discrete solution p_i at N points giving the set of solutions

$$p_i = p(\psi_i),\ i = 0, \ldots, N-1. \tag{6.29}$$

Denoting $f(\psi_i)$ by f_i and using (6.25) to generate our N solutions for p_i at equally spaced values of ψ between a and b via

$$p^2(\psi_j) - \lambda \int_{t=a}^{\psi_j} p(t)dt = f(\psi_j),\ j = 0, \ldots, N-1, \tag{6.30}$$

we obtain the following N equations

$$\begin{aligned}
&p_0^2 = f_0,\\
&p_1^2 - \lambda\left[\frac{1}{2}p_0 + \frac{1}{2}p_1\right]h^{(N)} = f_1,\\
&p_2^2 - \lambda\left[\frac{1}{2}p_0 + p_1 + \frac{1}{2}p_2\right]h^{(N)} = f_2,\\
&\vdots\\
&p_{N-2}^2 - \lambda\left[\frac{1}{2}p_0 + p_1 + \ldots + \frac{1}{2}p_{N-2}\right]h^{(N)} = f_{N-2},\\
&p_{N-1}^2 - \lambda\left[\frac{1}{2}p_0 + p_1 + p_2 + \ldots + \frac{1}{2}p_{N-1}\right]h^{(N)} = f_{N-1}.
\end{aligned} \tag{6.31}$$

Imposing the boundary conditions given by (6.24) implies $p_0 = p_{N-1} = 0$, allowing us to eliminate the first equation in (6.31). The last equation in (6.31)

can be used to obtain an expression for $\lambda h^{(N)}$, namely,

$$\lambda h^{(N)} = -\frac{f_{N-1}}{p_1 + p_2 + \ldots + p_{N-2}}. \tag{6.32}$$

Substituting this into the remaining equations and defining

$$\alpha = \sum_{i=1}^{N-2} p_i, \quad \beta = \sum_{i=1}^{N-3} p_i. \tag{6.33}$$

we are left with $N-2$ nonlinear simultaneous equations to solve for p_i, $i = 1, 2, \ldots, N-2$

$$\begin{aligned}
&2p_1^2\alpha + f_{N-1}p_1 - 2f_1\alpha = 0,\\
&2p_2^2\alpha + f_{N-1}\left(2p_1 + p_2\right) - 2f_2\alpha = 0,\\
&2p_3^2\alpha + f_{N-1}\left(2(p_1 + p_2) + p_3\right) - 2f_3\alpha = 0,\\
&\vdots\\
&2p_{N-2}^2\alpha + f_{N-1}\left(\alpha + \beta\right) - 2f_{N-2}\alpha = 0.
\end{aligned} \tag{6.34}$$

Solving this system involves employing Newton's iterative method [84] for $N-2$ nonlinear equations. At this stage we may compute an approximate value for λ from (6.32). Alternatively, after refining the values of p_i for some value of N, we can pursue a better approximation by constructing linear interpolants connecting the points p_i. We increment the number of node points by one to $N+1$ and calculate new approximate values $\hat{p}_i$ at new node values $\hat{\psi}_i$ over the interval with $N+1$ node points and spacing

$$h^{(N+1)} = \frac{b-a}{N}. \tag{6.35}$$

The node points are calculated from

$$\hat{\psi}_i = a + ih^{(N+1)}, \; i = 0, \ldots, N, \tag{6.36}$$

and the rule for computing new interpolated points becomes

$$\hat{p}_{i+1} = \left(\frac{p_{i+1} - p_i}{\psi_{i+1} - \psi_i}\right)\left(\hat{\psi}_{i+1} - \psi_i\right) + p_i. \tag{6.37}$$

At the endpoints of the interval we make $\hat{p}_0 = 0$ and $\hat{p}_N = 0$. In addition we compute $\hat{f}_i = f(\hat{\psi}_i)$. The procedure is then repeated iteratively until a sufficiently accurate approximation is achieved.

6.6 Zero angle of inclination

We demonstrate the method on the aforementioned PDE (6.15) with the known solution and wave speed in (6.16). The numerical method was implemented using MATLAB, but could in principle be coded using any suitable package or programming language. Consider (6.15), which we recall is equivalent to (6.14) with $\sigma = 0$. For clarity we drop the $\hat{\phi}$ notation and let $\hat{\phi} \to \phi$, $X \to x$ and $T \to t$ so that (6.15) becomes

$$\frac{\partial \phi}{\partial t} = \frac{\partial^2 \phi}{\partial x^2} - 4\chi \sin \frac{\phi}{2} - 4 \sin \phi \,. \tag{6.38}$$

Then, transforming according to equations (6.18) to (6.22) and setting

$$i(\psi) = 4\chi \sin \frac{\psi}{2} + 4 \sin \psi, \tag{6.39}$$

we arrive at the equation

$$4 \left[\chi \sin \frac{\psi}{2} + \sin \psi \right] + p \left(\nu - \frac{dp}{d\psi} \right) = 0, \tag{6.40}$$

which is an Abel equation of the second kind, with solution

$$p(\psi) = \mp 4 \sin \frac{\psi}{2}, \quad \nu = \pm \chi. \tag{6.41}$$

We chose to select $\chi = -2.154$ for our example problem, a choice motivated by Stewart and Momoniat [54]. The fixed points of (6.39) for $|\chi| > 2$, lie at even multiples of π, so that $\psi = 0, \pm 2\pi, \pm 4\pi, \ldots$ are solutions of $i(\psi) = 0$ when $\chi = -2.154$. We chose the interval over which we integrated the problem to be $\psi \in (a, b)$, where $a = -2\pi$ and $b = 0$ and calculated approximate solutions for $p(\psi)$ over a range of values of N. Starting with five equally spaced points satisfying

(6.23), we have plotted the relative error between the numerically computed approximate values denoted by $p_a(\psi)$ and exact values of $p(\psi)$ computed at the same equally spaced points given by (6.41) in Fig. 6.6. The graph demonstrates that as we increase the number of points N, the approximate solution $p_a(\psi)$ converges to the true solution $p(\psi)$. In other words, as N is increased the quality of the approximation $p_a(\psi)$ improves. Of course, as the approximation

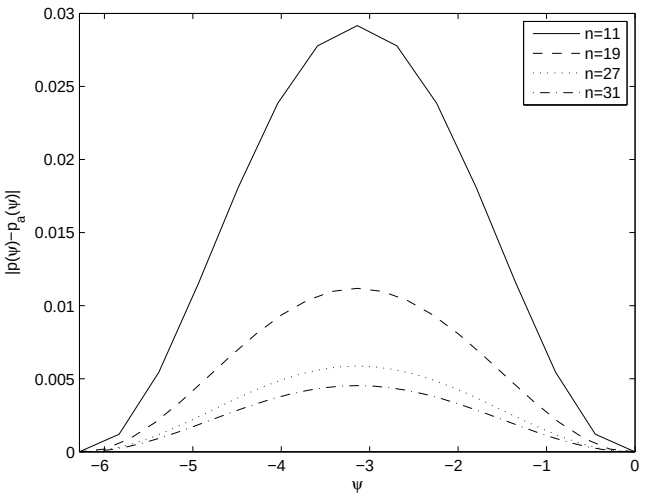

Figure 6.6: Plot of the relative error $|p(\psi) - p_a(\psi)|$ against ψ for a number of values of N with $\chi = -2.154$ and $\sigma = 0$ [8].

$p_a(\psi)$ improves, so too does the quality of the approximated wave speed. The computed wave speeds ν for the values of N shown in Fig. 6.6 are listed in Table 6.1. Compared to the magnitude of the exact wave speed for the problem which is $|\nu| = |\chi| = 2.154$, the computed wave speed for $N = 11$ is accurate to within about 1%. In addition we note that as the number of points N is increased the wave speed approximation does indeed converge to the exact value as expected. This confirms the validity of our proposed numerical scheme for $\sigma = 0$.

data points N	wave speed ν
11	2.17565
19	2.16249
27	2.15851
31	2.15750

Table 6.1: Table of computed wave speeds [8].

6.7 Nonzero angle of inclination

To demonstrate the applicability of the method, we adapted the procedure to show how varying the angle α of inclination of the electric field affects the wave speed ν for fixed $\chi = -2.154$. It is important to bear in mind that although the dimensionless quantity χ is dependent on α, we treat it as fixed by supposing that E is allowed to vary to ensure χ remains constant. Recall that $\sigma = \tan\alpha \cot\theta$ and that θ is fixed and that σ is therefore dependent on α. When $\alpha \neq 0$ we have that $\sigma \neq 0$. This introduces a third term into the nonlinearity so that now

$$i(\psi) = 4\chi \sin\frac{\psi}{2} + 4\sin\psi - 8\sigma\cos\frac{\psi}{2}. \tag{6.42}$$

Note that the fixed points of (6.42) are no longer even multiples of π if $\sigma \neq 0$ for $\chi = -2.154$, and the fixed points change as α is varied. To take account of this a simple root finding scheme was implemented to determine the fixed points of (6.42) as α was slowly incremented. Initially the problem was solved for $\alpha = 0$ on the interval $\psi \in (a, b)$ with $a = 2\pi$ and $b = 4\pi$. Then as α was varied, new fixed points were computed and new values of a and b selected as appropriate for use in the numerical scheme. The inclination of the electric field was allowed to vary over the range $0 \leq \alpha \leq 22°$. The result is shown in Fig. 6.7 below.

6.8 Discussion

The technique described in the preceding sections provides a systematic and reliable method for the numerical determination of wave speeds for PDE's of the

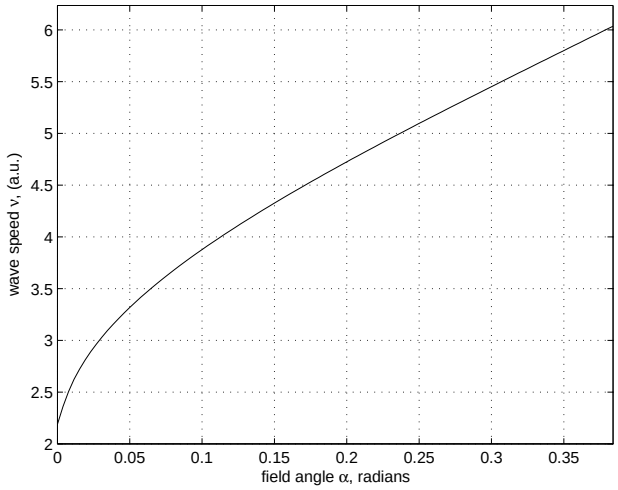

Figure 6.7: Field angle α versus wave speed ν for $\chi = -2.154$, $\theta = 0.384$ rad ($\theta = 22°$). Note the rate of change in wave speed is greatest for small inclinations of the applied field [8].

form (6.1), where a travelling wave solution may be assumed and $i(\phi)$ is taken to be a general nonlinear term. We chose to represent the problem as an integral equation and treated the equation discretely. We showed how, for a PDE with a nonlinear term which gives rise to an exact solution and analytically determined wave speed, it was possible to demonstrate convergence to the analytical wave speed using the numerical scheme. Furthermore, we demonstrated how the method may be extended to deal with problems where analytical solutions and wave speeds are not known explicitly. By developing the method of solution to the problem when $\alpha \neq 0$, we were able to extend our numerical procedure to construct a graph of wave speeds ν against the angle of inclination α for a range of values of α, and for the first time revealed for $\sigma \neq 0$ the nonlinear dependence of ν upon α. This was achieved despite there being no closed form solution to (6.1) when $i(\phi) = 4\chi \sin\frac{\phi}{2} + 4\sin\phi - 8\sigma\cos\frac{\phi}{2}$.

Future work will improve the convergence rate and accuracy of the algorithm by employing a more sophisticated quadrature scheme. Making direct comparison of wave speeds observed in the laboratory with our numerical ap-

proximations, and applying the method to other types of nonlinear problems, will form the basis of further investigations.

Chapter 7

Conclusion

So, we finally come to the end of this work and we are now in a position to review and consolidate the material presented. We began in Chapter 2 by considering a perturbation to a travelling domain wall propagating through a sample of ferroelectric liquid crystal in a planar layer geometry identical to that described in [54]. The sample was under the influence of a constant electric field and the model allowed the field to be inclined at some angle α. Making use of the fact that in the case where the field is in the plane of the sample an exact solution to the governing equation exists and where flow is assumed to be negligible, we proceeded to construct a continuum model which assumed that the exact solution was propagating in a medium where flow was not negligible.

We approached the problem of incorporating flow by locating the general wave front in a co-moving frame of reference. Then, in that co-moving frame we applied infinitesimal perturbations to the wave by imposing flow components of infinitesimal magnitude in each of three spatial directions. Working through the resulting algebra we arrived at a fully nonlinear system comprised of five separate equations one for conserved mass, three to account for conserved angular momentum in the system and a final equation, essentially a modification of the original governing equation, to account for conserved angular momentum.

Moving on from here in Chapter 3 we began the process of linearising the

perturbation equations by first making some remarks regarding the appropriateness of assuming only one elastic constant in the model. We decided that anisotropy in the model was not a significant factor and this lead us to adopt the one constant approximation. Furthermore we assumed no transverse flow which allowed us to disregard the v component of flow in our model which allowed a certain amount of simplification. Further assumptions such as the decision to model systems where $P_0 E < 0$, were guided by the need to conform to the requirements of the exact solution from the governing equation in the case where the field was at zero inclination and the linear transform to the co-moving frame within which the system was being studied.

To apply the perturbations we assumed that in a quiescent state we had simply a known solution ϕ_0 and a constant pressure p_0. The flow in the quiescent state was assumed to be zero. Perturbing the system and then linearising the result left us with four *linear* perturbation equations featuring terms which involved the solution for the quiescent state ϕ_0. By exploiting the fact that an exact solution exists in the case where the electric field in *not* inclined, that is when the field was at an angle $\alpha = 0$ we were left with four perturbation equations where the non-constant coefficients could be expressed exactly in terms of our transformed spatial variable τ.

Moving on from here to Chapter 4 we made further simplifying assumptions. We used the perturbation equation corresponding to the conserved mass to determine that the flow in the transformed x direction is infact constant. This allowed us to further reduce the system by disregarding the conserved linear momentum equation for the component of velocity in the x direction. This left us with just two equations a perturbation equation for conserved angular momentum and a perturbation equation for conserved linear momentum in the z direction.

At this point we decided to look at the problem in two different ways one involved considering the coefficients in our differential equations as if they were constant. By choosing a point in the middle of the domain wall, that is $\tau = 0$ replacing the hyperbolic terms with their numerical values at $\tau = 0$ and applying a suitable transformation we were able to construct a system of differential equations which formed a differential eigenvalue problem. The differential operator in this problem was non-self-adjoint. We chose to employ a Galerkin type method to study the eigenvalue problem and in the constant coefficient case our principal interest lay in verifying the numerical scheme and satisfying ourselves that the dominant eigenvalues were being reliably computed and were showing signs of convergence. The numerical scheme worked as expected and given a set of plausible physical values for the constants in the model we *tracked* two of the eigenvalues by using polynomial approximations of increasing greater degrees until computational limitations were reached.

For the full perturbation equations we were once again faced with a non-self-adjoint system and numerical approximation was the only feasible solution method. This time we chose a relatively low number of approximating polynomials per function. We infact chose to model our perturbation solutions with two polynomial test functions each. With a total of four Fourier coefficients this gave us a discretisation which yielded an algebraic eigenvalue problem with a fourth order characteristic equation. Using successively larger values for the magnitude of the electric field and other appropriate physical parameters typically yielded two real positive roots and two complex conjugate roots.

The time decaying components in the ansatz for the perturbation solutions were chosen so that a positive real part for the eigenvalue would yield a perturbation which decays with time. While as we mentioned, the two real roots were always found to be positive, the complex roots over the range of values

of E which we chose to use, generally started off having a negative real part as we cycled from a low magnitude field, became zero at some critical electric field strength, and then remained positive thereafter up to the maximum field strength. By recording the field strength E_c at the critical point as we varied other physical parameters, we were able to get a picture of how the material parameters influence the threshold electric field strength either side of the system was found to be in an asymptotically stable or unstable state.

So far as this analysis is concerned, the interpretation we chose to place on the critical field strength was that below the critical strength E_c travelling waves could not be initiated. Field strengths below the critical field cannot overcome the viscous and elastic forces resisting the inclination of the electric dipoles to align themselves in the field so no wave fronts appear. Above the critical field the torque exerted by the field on the dipoles is enough to overcome the viscous and elastic forces and a travelling wave is initiated. As we mentioned earlier comparison with the literature shows that the field strengths we have computed are in reasonable agreement with other researchers findings.

We could in principle improve the accuracy of the field strength calculations by adding more terms to our approximating polynomials and refining the root solving algorithm used to determine the exact point at which the real part of the complex eigenvalues changes sign. Also, using better approximating polynomial such as the Legendre polynomials would most likely increase the speed of convergence of the eigenvalues. The weighted residual method used to tackle the problems being investigated was the Galerkin method. Other weighted residual methods exist for instance the assumed modes method and the collocation method, but they generally do not deliver the accuracy of the Galerkin method. We carried out some preliminary power law analysis and this yielded some interesting results including what appears to be a *one over root B* law relating the

critical electric field to the elastic constant. Nevertheless the power law analysis is still in its early stages and more work will need to be done in order to tease out all of the available information.

The remaining two chapters focused on quantitative studies of travelling wave phenomena. In Chapter 5 we adapted an existing technique for approximating domain wall profiles and were able to find good agreement between the approximation method and a particular travelling wave problem with an exact solution. In the final chapter, Chapter 6 we looked at the problem of computing wave speeds using a novel discretisation method and presented results for a dimensionless model. The method can be straightforwardly adapted for use in other travelling wave type problems of the kind discussed in Chapter 5. Improved discretisation would no doubt improve the convergence properties of the algorithm.

Appendix A

Vector Result

Theorem A.1 *Suppose a vector* $\mathbf{v}(u)$ *has fixed modulus* $|\mathbf{v}| = C$ *where* $C \in \mathbb{R}$. *If the derivative of* $\mathbf{v}(u)$ *with respect to* u *is continuous, then*

$$\frac{d\mathbf{v}}{du} = \mathbf{w} \times \mathbf{v},$$

where $\mathbf{w}$ *may vary with with* u.

Proof We begin by noting that $\mathbf{v} \cdot \mathbf{v} = |\mathbf{v}|^2$. Then

$$\frac{d}{du}(\mathbf{v} \cdot \mathbf{v}) = 2\mathbf{v} \cdot \mathbf{v}' = 0.$$

This means that $\mathbf{v} \cdot \mathbf{v}' = 0$ and so $\mathbf{v}$ and $\mathbf{v}'$ are orthogonal. Now let

$$\mathbf{v} \times \mathbf{v}' = |\mathbf{v}|\,|\mathbf{v}'|\,\mathbf{n},$$

for some vector $\mathbf{n}(u)$ perpendicular to $\mathbf{v}$ and $\mathbf{v}'$, then

$$\begin{aligned}
\mathbf{n} \times \mathbf{v} &= \frac{1}{|\mathbf{v}|\,|\mathbf{v}'|}\left[(\mathbf{v} \times \mathbf{v}') \times \mathbf{v}\right] \\
&= \frac{1}{|\mathbf{v}|\,|\mathbf{v}'|}\left[(\mathbf{v} \cdot \mathbf{v})\,\mathbf{v}' - (\mathbf{v} \cdot \mathbf{v}')\,\mathbf{v}\right] \\
&= \frac{|\mathbf{v}|^2}{|\mathbf{v}|\,|\mathbf{v}'|}\mathbf{v}' \\
&= \frac{|\mathbf{v}|}{|\mathbf{v}'|}\mathbf{v}'.
\end{aligned}$$

Now if we define

$$\mathbf{w} = \frac{|\mathbf{v}'|}{|\mathbf{v}|}\mathbf{n},$$

then

$$\mathbf{v}' = \mathbf{w} \times \mathbf{v}. \quad \square$$

Appendix B

Elastic Constant Vector Identities

We shall now provide some justification for the identities given by (2.49) and (2.50). For the sake of brevity we shall show how, using (2.50), we may derive the K_6 term in (2.56) by considering the K_6 term in the energy density (2.46). Other terms in (2.56) and (2.55) may be derived in a similar manner. So, we start with (2.46) and consider only the vector expression for K_6

$$w = K_6(\nabla \cdot \mathbf{a})(\mathbf{b} \cdot \nabla \times \mathbf{c}), \quad \text{where} \quad \mathbf{b} = \mathbf{a} \times \mathbf{c}. \tag{B.1}$$

Expressed in Cartesian form this is equivalent to

$$\begin{aligned} w &= K_6 a_{p,p} \epsilon_{qrs} a_r c_s \epsilon_{qmn} c_{n,m} \\ &= K_6 a_{p,p} \epsilon_{qrs} \epsilon_{qmn} a_r c_s c_{n,m} \\ &= K_6 a_{p,p} (\delta_{rm}\delta_{sn} - \delta_{rn}\delta_{sm}) a_r c_s c_{n,m} \\ &= K_6 a_{p,p} a_r c_s (c_{s,r} - c_{r,s}). \end{aligned} \tag{B.2}$$

Next using (2.50) with $w = w^*$ and taking w to be equal to (B.2), we find that the first term is computed as follows

$$\begin{aligned} \frac{\partial w}{\partial c_{i,j}} &= K_6 a_{p,p} a_r c_s \left(\frac{\partial c_{s,r}}{\partial c_{i,j}} - \frac{\partial c_{r,s}}{\partial c_{i,j}} \right) \\ &= K_6 a_{p,p} a_r c_s (\delta_{ij}^{sr} - \delta_{ij}^{rs}) \\ &= K_6 a_{p,p} (a_j c_i - a_i c_j). \end{aligned} \tag{B.3}$$

Where we have used the fact that

$$\delta^{a_1 a_2 \ldots a_n}_{b_1 b_2 \ldots b_n} = \prod_{i=1}^{n} \delta_{a_i, b_i}. \tag{B.4}$$

From this we find that

$$\begin{aligned}
\left(\frac{\partial w}{\partial c_{i,j}}\right)_{,j} &= K_6[a_{p,p}(a_j c_i - a_i c_j)]_{,j} \\
&= K_6[(a_{p,p})_{,j}(a_j c_i - a_i c_j) + a_{p,p}(a_j c_i - a_i c_j)_{,j}] \\
&= K_6[(a_{p,p})_{,j}(a_j c_i - a_i c_j) \\
&\quad + a_{p,p}(a_{j,j} c_i + a_j c_{i,j} - a_{i,j} c_j - a_i c_{j,j})].
\end{aligned} \tag{B.5}$$

The second term in (2.50) yields

$$\begin{aligned}
\frac{\partial w}{\partial c_i} &= K_6 a_{p,p} a_r \delta_{si}(c_{s,r} - c_{r,s}) \\
&= K_6 a_{p,p} a_r (c_{i,r} - c_{r,i}),
\end{aligned} \tag{B.6}$$

which, on combining (B.5) with (B.6) yields the expression

$$\begin{aligned}
\left(\frac{\partial w}{\partial c_{i,j}}\right)_{,j} - \frac{\partial w}{\partial c_i} &= K_6[(a_{p,p})_{,j}(a_j c_i - a_i c_j) \\
&\quad + a_{p,p}(a_{j,j} c_i + a_j c_{i,j} - a_{i,j} c_j - a_i c_{j,j}) \\
&\quad - a_{p,p} a_r (c_{i,r} - c_{r,i})].
\end{aligned} \tag{B.7}$$

Now, the K_6 term in $\mathbf{\Pi^c}$ is

$$\mathbf{\Pi^c}_{K_6} = K_6[(\nabla \cdot \mathbf{a})(\mathbf{a} \times \nabla \times \mathbf{c}) - \nabla \times \{(\nabla \cdot \mathbf{a})\mathbf{b}\}]. \tag{B.8}$$

Taking the first term in this expression and considering the cross product we find that

$$\begin{aligned}
[\mathbf{a} \times \nabla \times \mathbf{c}]_i &= \epsilon_{ijk} a_j \epsilon_{klm} c_{m,l} \\
&= \epsilon_{kij} \epsilon_{klm} a_j c_{m,l} \\
&= (\delta_{il}\delta_{jm} - \delta_{im}\delta_{jl}) a_j c_{m,l} \\
&= a_j (c_{j,i} - c_{i,j}).
\end{aligned} \tag{B.9}$$

So that

$$(\nabla \cdot \mathbf{a})[\mathbf{a} \times \nabla \times \mathbf{c}]_i = a_{p,p} a_j (c_{j,i} - c_{i,j}). \tag{B.10}$$

The second term on the RHS of (B.8) has an i-th component given by

$$[\nabla \times \{(\nabla \cdot \mathbf{a})\mathbf{a} \times \mathbf{c}\}]_i = \epsilon_{ijk} \{(\nabla \cdot \mathbf{a})\mathbf{a} \times \mathbf{c}\}_{k,j}. \tag{B.11}$$

Now we wish to determine the k-th component of the term inside the brackets on the RHS of (B.11)

$$\{(\nabla \cdot \mathbf{a})\mathbf{a} \times \mathbf{c}\}_k = a_{p,p} \epsilon_{klm} a_l c_m, \tag{B.12}$$

and the j-th derivative of (B.12) is found to be

$$\begin{aligned} \{(\nabla \cdot \mathbf{a})\mathbf{a} \times \mathbf{c}\}_{k,j} &= (a_{p,p})_{,j} \epsilon_{klm} a_l c_m \\ &\quad + a_{p,p} \epsilon_{klm} a_{l,j} c_m \\ &\quad + a_{p,p} \epsilon_{klm} a_l c_{m,j}. \end{aligned} \tag{B.13}$$

Consequently we have that

$$\begin{aligned} [\nabla \times \{(\nabla \cdot \mathbf{a})\mathbf{a} \times \mathbf{c}\}]_i &= \epsilon_{ijk}\epsilon_{klm}[(a_{p,p})_{,j} a_l c_m + a_{p,p} a_{l,j} c_m + a_{p,p} a_l c_{m,j}] \\ &= \epsilon_{kij}\epsilon_{klm}[(a_{p,p})_{,j} a_l c_m + a_{p,p} a_{l,j} c_m + a_{p,p} a_l c_{m,j}] \\ &= (\delta_{il}\delta_{jm} - \delta_{im}\delta_{jl})[(a_{p,p})_{,j} a_l c_m + a_{p,p} a_{l,j} c_m + a_{p,p} a_l c_{m,j}] \\ &= (a_{p,p})_{,j}(a_i c_j - a_j c_i) + a_{p,p}(a_{i,j} c_j - a_{j,j} c_i) \\ &\quad + a_{p,p}(a_i c_{j,j} - a_j c_{i,j}). \end{aligned} \tag{B.14}$$

Now, combining (B.10) and (B.14) we find that the i-th component of the K_6 term is

$$\begin{aligned} K_6[(\nabla \cdot \mathbf{a})[\mathbf{a} \times \nabla \times \mathbf{c}] - \nabla \times \{(\nabla \cdot \mathbf{a})\mathbf{b}\}]_i &= K_6[a_{p,p} a_j (c_{j,i} - c_{i,j}) \\ &\quad + (a_{p,p})_{,j}(a_j c_i - a_i c_j) \\ &\quad + a_{p,p}(a_{j,j} c_i - a_{i,j} c_j) \\ &\quad + a_{p,p}(a_j c_{i,j} - a_i c_{j,j})]. \end{aligned} \tag{B.15}$$

Finally, comparing the RHS of (B.7) with the RHS of (B.15) we find that the expressions are identical which lead us to conclude that, for the energy density w defined by (B.1)

$$\left(\frac{\partial w}{\partial c_{i,j}}\right)_{,j} - \frac{\partial w}{\partial c_i} = K_6[(\nabla \cdot \mathbf{a})[\mathbf{a} \times \nabla \times \mathbf{c}] - \nabla \times \{(\nabla \cdot \mathbf{a})\mathbf{b}\}]_i. \tag{B.16}$$

Appendix C

The Rayleigh-Ritz method for an $\mathbb{R}^{2\times 2}$ linear differential operator

We present here a scheme for implementing the Rayleigh-Ritz method to a 2×2 matrix differential operator. We assume that the functions $\hat{\phi}$ and $\hat{z}$ are approximated by a sequence of trial functions up to $\mathcal{O}(2)$. In other words we choose $\hat{\phi}$ and $\hat{z}$ to be approximated by

$$\begin{aligned} \hat{\phi} &= a_1\phi_1 + a_2\phi_2, \\ \hat{z} &= b_1\phi_1 + b_2\phi_2. \end{aligned} \tag{C.1}$$

Then our operator A and the vector $\mathbf{x}$ are defined to be

$$\mathsf{A} = \begin{bmatrix} A_{11} & A_{12} \\ A_{21} & A_{22} \end{bmatrix}, \ \mathbf{x} = \begin{bmatrix} \hat{\phi} \\ \hat{z} \end{bmatrix}. \tag{C.2}$$

Our goal is to find values of λ which make the functional

$$F(\mathbf{x}) = \int \mathbf{x}^T \left(\mathsf{A} - \lambda\mathbb{I}\right)\mathbf{x}\, dx \tag{C.3}$$

a minimum with respect to the coefficients a_1, a_2, b_1 and b_2. We begin by computing the quadratic form Q given by

$$Q = \mathbf{x}^T\mathsf{A}\mathbf{x},$$

and we have that

$$\mathbf{x}^T\mathsf{A}\mathbf{x} = \begin{bmatrix} a_1\phi_1 + a_2\phi_2 & b_1\phi_1 + b_2\phi_2 \end{bmatrix} \begin{bmatrix} A_{11} & A_{12} \\ A_{21} & A_{22} \end{bmatrix} \begin{bmatrix} a_1\phi_1 + a_2\phi_2 \\ b_1\phi_1 + b_2\phi_2 \end{bmatrix}$$

$$
\begin{aligned}
&= a_1^2\phi_1 A_{11}\phi_1 + a_1a_2\phi_1 A_{11}\phi_2 + a_2a_1\phi_2 A_{11}\phi_1 + a_2^2\phi_2 A_{11}\phi_2 \\
&\quad + a_1b_1\phi_1 A_{12}\phi_1 + a_1b_2\phi_1 A_{12}\phi_2 + a_2b_1\phi_2 A_{12}\phi_1 + a_2b_2\phi_2 A_{12}\phi_2 \\
&\quad + b_1a_1\phi_1 A_{21}\phi_1 + b_1a_2\phi_1 A_{21}\phi_2 + b_2a_1\phi_2 A_{21}\phi_1 + b_2a_2\phi_2 A_{21}\phi_2 \\
&\quad + b_1^2\phi_1 A_{22}\phi_1 + b_1b_2\phi_1 A_2 2\phi_2 + b_2b_1\phi_2 A_{22}\phi_1 + b_2^2\phi_2 A_{22}\phi_2. \qquad \text{(C.4)}
\end{aligned}
$$

Also we find that the inner product of $\mathbf{x}$ with itself is given by

$$
\begin{aligned}
\mathbf{x}^T\mathbb{I}\mathbf{x} &= [a_1\phi_1 + a_2\phi_2 \;\; b_1\phi_1 + b_2\phi_2] \begin{bmatrix} 1 & 0 \\ 0 & 1 \end{bmatrix} \begin{bmatrix} a_1\phi_1 + a_2\phi_2 \\ b_1\phi_1 + b_2\phi_2 \end{bmatrix} \\
&= a_1^2\phi_1^2 + a_1a_2\phi_1\phi_2 + a_2a_1\phi_2\phi_1 + a_2^2\phi_2^2 \\
&\quad + b_1^2\phi_1^2 + b_1b_2\phi_1\phi_2 + b_2b_1\phi_2\phi_1 + b_2^2\phi_2^2. \qquad \text{(C.5)}
\end{aligned}
$$

Then integrating (C.4) and (C.5) we have that

$$
\begin{aligned}
\int \mathbf{x}^T\mathsf{A}\mathbf{x}\, d\tau &= a_1^2\langle A_{11}\phi_1, \phi_1\rangle + a_1a_2\langle A_{11}\phi_2, \phi_1\rangle + a_2a_1\langle A_{11}\phi_1, \phi_2\rangle \\
&\quad + a_2^2\langle A_{11}\phi_2, \phi_2\rangle + a_1b_1\langle A_{12}\phi_1, \phi_1\rangle + a_1b_2\langle A_{12}\phi_2, \phi_1\rangle \\
&\quad + a_2b_1\langle A_{12}\phi_1, \phi_2\rangle + a_2b_2\langle A_{12}\phi_2, \phi_2\rangle + b_1a_1\langle A_{21}\phi_1, \phi_1\rangle \\
&\quad + b_1a_2\langle A_{21}\phi_2, \phi_1\rangle + b_2a_1\langle A_{21}\phi_1, \phi_2\rangle + b_2a_2\langle A_{21}\phi_2, \phi_2\rangle \\
&\quad + b_1^2\langle A_{22}\phi_1, \phi_1\rangle + b_1b_2\langle A_2 2\phi_2, \phi_1\rangle + b_2b_1\langle A_{22}\phi_1, \phi_2\rangle \\
&\quad + b_2^2\langle A_{22}\phi_2, \phi_2\rangle, \qquad \text{(C.6)}
\end{aligned}
$$

and

$$
\begin{aligned}
\int \mathbf{x}^T\mathbb{I}\mathbf{x}\, d\tau &= a_1^2\langle \phi_1, \phi_1\rangle + a_1a_2\langle \phi_1, \phi_2\rangle + a_2a_1\langle \phi_2, \phi_1\rangle \\
&\quad + a_2^2\langle \phi_2, \phi_2\rangle + b_1^2\langle \phi_1, \phi_1\rangle + b_1b_2\langle \phi_1, \phi_2\rangle \\
&\quad + b_2b_1\langle \phi_2, \phi_1\rangle + b_2^2\langle \phi_2, \phi_2\rangle. \qquad \text{(C.7)}
\end{aligned}
$$

Now differentiating (C.3) with respect to the a_i's and b_i's we find that

$$
\begin{aligned}
\frac{\partial F}{\partial a_1} &= 2a_1\langle A_{11}\phi_1, \phi_1\rangle + a_2\langle A_{11}\phi_2, \phi_1\rangle + a_2\langle A_{11}\phi_1, \phi_2\rangle \\
&\quad + b_1\langle A_{12}\phi_1, \phi_1\rangle + b_2\langle A_{12}\phi_2, \phi_1\rangle
\end{aligned}
$$

$$
\begin{aligned}
&+ b_1\langle A_{21}\phi_1,\phi_1\rangle + b_2\langle A_{21}\phi_1,\phi_2\rangle \\
&- \lambda\left[2a_1\langle\phi_1,\phi_1\rangle + a_2\langle\phi_1,\phi_2\rangle + a_2\langle\phi_2,\phi_1\rangle\right], \qquad \text{(C.8)}\\
\frac{\partial F}{\partial a_2} &= a_1\langle A_{11}\phi_2,\phi_1\rangle + a_1\langle A_{11}\phi_1,\phi_2\rangle + 2a_2\langle A_{11}\phi_2,\phi_2\rangle \\
&+ b_1\langle A_{12}\phi_1,\phi_2\rangle + b_2\langle A_{12}\phi_2,\phi_2\rangle \\
&+ b_1\langle A_{21}\phi_2,\phi_1\rangle + b_2\langle A_{21}\phi_2,\phi_2\rangle \\
&- \lambda\left[a_1\langle\phi_1,\phi_2\rangle + a_1\langle\phi_2,\phi_1\rangle + 2a_2\langle\phi_2,\phi_2\rangle\right], \qquad \text{(C.9)}\\
\frac{\partial F}{\partial b_1} &= a_1\langle A_{12}\phi_1,\phi_1\rangle + a_2\langle A_{12}\phi_1,\phi_2\rangle \\
&+ a_1\langle A_{21}\phi_1,\phi_1\rangle + a_2\langle A_{21}\phi_2,\phi_1\rangle \\
&+ 2b_1\langle A_{22}\phi_1,\phi_1\rangle + b_2\langle A_{22}\phi_2,\phi_1\rangle + b_2\langle A_{22}\phi_1,\phi_2\rangle \\
&- \lambda\left[2b_1\langle\phi_1,\phi_1\rangle + b_2\langle\phi_1,\phi 2\rangle + b_2\langle\phi_2,\phi_1\rangle\right], \qquad \text{(C.10)}\\
\frac{\partial F}{\partial b_2} &= a_1\langle A_{12}\phi_2,\phi_1\rangle + a_2\langle A_{12}\phi_2,\phi_2\rangle \\
&+ a_1\langle A_{21}\phi_1,\phi_2\rangle + a_2\langle A_{21}\phi_2,\phi_2\rangle \\
&+ b_1\langle A_{22}\phi_2,\phi_1\rangle + b_1\langle A_{22}\phi_1,\phi_2\rangle + 2b_2\langle A_{22}\phi_2,\phi_2\rangle \\
&- \lambda\left[b_1\langle\phi_1,\phi_2\rangle + b_1\langle\phi_2,\phi_1\rangle + 2b_2\langle\phi_2,\phi_2\rangle\right]. \qquad \text{(C.11)}
\end{aligned}
$$

So we wish to solve the following system of homogeneous simultaneous linear equations

$$
\begin{aligned}
&2\left[\langle A_{11}\phi_1,\phi_1\rangle - \lambda\langle\phi_1,\phi_1\rangle\right]a_1 + \left[\langle A_{11}\phi_2,\phi_1\rangle + \langle A_{11}\phi_1,\phi_2\rangle - 2\lambda\langle\phi_1,\phi_2\rangle\right]a_2 \\
&+ \left[\langle A_{12}\phi_1,\phi_1\rangle + \langle A_{21}\phi_1,\phi_1\rangle\right]b_1 + \left[\langle A_{12}\phi_2,\phi_1\rangle + \langle A_{21}\phi_1,\phi_2\rangle\right]b_2 = 0, \qquad \text{(C.12)}\\
&\left[\langle A_{11}\phi_2,\phi_1\rangle + \langle A_{11}\phi_1,\phi_2\rangle - 2\lambda\langle\phi_1,\phi_2\rangle\right]a_1 + 2\left[\langle A_{11}\phi_2,\phi_2\rangle - \lambda\langle\phi_2,\phi_2\rangle\right]a_2 \\
&+ \left[\langle A_{12}\phi_1,\phi_2\rangle + \langle A_{21}\phi_2,\phi_1\rangle\right]b_1 + \left[\langle A_{12}\phi_2,\phi_2\rangle + \langle A_{21}\phi_2,\phi_2\rangle\right]b_1 = 0, \qquad \text{(C.13)}\\
&2\left[\langle A_{22}\phi_1,\phi_1\rangle - \lambda\langle\phi_1,\phi_1\rangle\right]b_1 + \left[\langle A_{22}\phi_2,\phi_1\rangle + \langle A_{22}\phi_1,\phi_2\rangle + \lambda\langle\phi_1,\phi_2\rangle\right]b_2 \\
&+ \left[\langle A_{12}\phi_1,\phi_1\rangle + \langle A_{21}\phi_1,\phi_1\rangle\right]a_1 + \left[\langle A_{12}\phi_1,\phi_2\rangle + \langle A_{21}\phi_2,\phi_1\rangle\right]a_2 = 0, \qquad \text{(C.14)}\\
&\left[\langle A_{22}\phi_2,\phi_1\rangle + \langle A_{22}\phi_1,\phi_2\rangle - \lambda\langle\phi_1,\phi_2\rangle\right]b_1 + 2\left[\langle A_{22}\phi_2,\phi_2\rangle - \lambda\langle\phi_2,\phi_2\rangle\right]b_2 \\
&+ \left[\langle A_{12}\phi_2,\phi_1\rangle + \langle A_{21}\phi_1,\phi_2\rangle\right]a_1 + \left[\langle A_{12}\phi_2,\phi_2\rangle + \langle A_{21}\phi_2,\phi_2\rangle\right]a_2 = 0. \qquad \text{(C.15)}
\end{aligned}
$$

Appendix D

Determination of $a(t)$, $b(t)$, $c(t)$, $\xi_0(t)$ and $\xi_1(t)$

Equations (5.68)-(5.71) may be solved using Gaussian elimination. We outline the steps required here and derive a relationship between $\xi_0(t)$ and $\xi_1(t)$. This in turn will allow us to derive expressions for $a(t)$ and $c(t)$. We start by adding (5.70) and (5.71) and then solve the following system of three equations in three unknowns $a(t)$, $b(t)$ and $c(t)$

$$a(t)\xi_0 + \tfrac{1}{2}b(t)\xi_0^2 + \tfrac{1}{6}c(t)\xi_0^3 = \tfrac{1}{2}\left(\phi_0 - \phi_1\right), \tag{D.1}$$

$$a(t)\xi_1 - \tfrac{1}{2}b(t)\xi_1^2 + \tfrac{1}{6}c(t)\xi_1^3 = \tfrac{1}{2}\left(\phi_0 - \phi_1\right), \tag{D.2}$$

$$2a(t) + b(t)\left(\xi_0 - \xi_1\right) + \tfrac{1}{2}c(t)\left(\xi_0^2 + \xi_1^2\right) = 0. \tag{D.3}$$

Writing (D.1)-(D.3) system in augmented matrix form we reduce the problem to row echelon form by performing elementary row operations (ERO) as follows

$$\left[\begin{array}{ccc|c} \xi_0 & \frac{1}{2}\xi_0^2 & \frac{1}{6}\xi_0^3 & \frac{1}{2}\left(\phi_0 - \phi_1\right) \\ \xi_1 & -\frac{1}{2}\xi_1^2 & \frac{1}{6}\xi_1^3 & \frac{1}{2}\left(\phi_0 - \phi_1\right) \\ 2 & \xi_0 - \xi_1 & \frac{1}{2}\left(\xi_0^2 + \xi_1^2\right) & 0 \end{array}\right] \tag{D.4}$$

First ERO $R_3 := R_3 - \frac{2}{\xi_0}R_1$

$$\left[\begin{array}{ccc|c} \xi_0 & \frac{1}{2}\xi_0^2 & \frac{1}{6}\xi_0^3 & \frac{1}{2}\left(\phi_0 - \phi_1\right) \\ \xi_1 & -\frac{1}{2}\xi_1^2 & \frac{1}{6}\xi_1^3 & \frac{1}{2}\left(\phi_0 - \phi_1\right) \\ 0 & -\xi_1 & \frac{1}{6}\xi_0^2 + \frac{1}{2}\xi_1^2 & -\frac{1}{\xi_0}\left(\phi_0 - \phi_1\right) \end{array}\right] \tag{D.5}$$

Second ERO $R_2 := R_2 - \frac{\xi_1}{\xi_0} R_1$

$$\left[\begin{array}{ccc|c} \xi_0 & \frac{1}{2}\xi_0^2 & \frac{1}{6}\xi_0^3 & \frac{1}{2}(\phi_0 - \phi_1) \\ 0 & -\frac{1}{2}\xi_1(\xi_1 - \xi_0) & \frac{1}{6}\xi_1(\xi_1^2 - \xi_0^2) & \frac{1}{2}(\phi_0 - \phi_1)(1 - \xi_1/\xi_0) \\ 0 & -\xi_1 & \frac{1}{6}\xi_0^2 + \frac{1}{2}\xi_1^2 & -\frac{1}{\xi_0}(\phi_0 - \phi_1) \end{array}\right] \tag{D.6}$$

Third ERO $R_3 := R_3 - \frac{2}{\xi_1 - \xi_0} R_2$

$$\left[\begin{array}{ccc|c} \xi_0 & \frac{1}{2}\xi_0^2 & \frac{1}{6}\xi_0^3 & \frac{1}{2}(\phi_0 - \phi_1) \\ 0 & -\frac{1}{2}\xi_1(\xi_1 - \xi_0) & \frac{1}{6}\xi_1(\xi_1^2 - \xi_0^2) & \frac{1}{2}(\phi_0 - \phi_1)(1 - \xi_1/\xi_0) \\ 0 & 0 & \frac{1}{6}(\xi_1 - \xi_0)^2 & 0 \end{array}\right] \tag{D.7}$$

Now for consistency we see that the the last row of (D.7) yields $\xi_0(t) = \xi_1(t)$ so that (D.1), (D.2) and (D.3) may be reduced to the following pair of simultaneous equations

$$2a(t)\xi_0 + \tfrac{1}{3}c(t)\xi_0^3 = \phi_0 - \phi_1, \tag{D.8}$$

$$2a(t) + c(t)\xi_0^2 = 0. \tag{D.9}$$

This immediately implies that $b(t) = 0$. Then from (D.9) we have that

$$c(t) = -\frac{2a(t)}{\xi_0^2}, \tag{D.10}$$

which on substitution into (D.8) yields

$$a(t) = \frac{3}{4}\frac{(\phi_0 - \phi_1)}{\xi_0}, \tag{D.11}$$

so that

$$\xi_0(t) = \frac{3}{4}\frac{(\phi_0 - \phi_1)}{a(t)}, \tag{D.12}$$

which on substituting back into (D.10) gives

$$c(t) = -\frac{32}{9}\frac{1}{(\phi_0 - \phi_1)^2}a^3(t). \tag{D.13}$$

Appendix E

Weighted Residual Methods

The principle behind the method of weighted residuals is relatively straightforward. What we aim to do is solve a generally non-self-adjoint differential eigenvalue problem by discretising the differential eigenvalue problem and in so doing form an algebraic eigenvalue problem which we may solve using standard methods taken from linear algebra [61, p.27]. Here we follow the general treatment given by Meirovitch [64] on the subject of weighted residuals. In addition we shall regard the operator eigenvalue problem more generally and so we shall also take into account the general eigenvalue problem in Finlayson [67] and adapt our discussion to suit. Suppose we have the following differential eigenvalue problem

$$\mathcal{A}y = \Lambda \mathcal{B}y, \tag{E.1}$$

with homogeneous boundary conditions

$$B_i y = 0, \quad i = 1, 2, \ldots, n \ \text{ at } \ x = -\delta \ \text{ and } \ x = \delta, \tag{E.2}$$

where operators $\mathcal{A}$ and $\mathcal{B}$ are general differential operators. Consider a trial function $w(x)$. In general $w(x)$ does not satisfy (E.1) which means that if we substitute the trial function for y in (E.1) the measure of the error when we do this is given by the *residual* which we define to be

$$R(w, x) = \mathcal{A}w - \Lambda \mathcal{B}w. \tag{E.3}$$

If we chose as the trial function the eigenfunction w_i and associated eigenvalue Λ_i the residual would be zero. Next we choose a *weighting* function $v(x)$ and define the *weighted residual*

$$vR = v(\mathcal{A}w - \Lambda\mathcal{B}w). \tag{E.4}$$

If $v(x)$ is chosen so that $v(x)$ is *orthogonal* to $R(w,x)$ then the integral of the weighted residual is zero

$$(v,R) = \int_{-\delta}^{\delta} v(\mathcal{A}w - \Lambda\mathcal{B}w)dx = 0. \tag{E.5}$$

Now specify an approximate solution of (E.1) by defining the function

$$y^n = \sum_{j=1}^{n} a_j\phi_j, \tag{E.6}$$

where $\phi_1, \phi_2, \cdots, \phi_n$ are n functions which are chosen from a complete set of test functions. The completeness property is crucial as is the condition that the functions ϕ_j be *linearly independent* [67]. Then we choose another set of functions $\psi_1, \psi_2, \cdots, \psi_n$ from another complete set. The coefficients $a_1, a_2, \cdots, a_n$ are determined by demanding that the functions ψ_i be orthogonal to the weighted residual $R = R(y^n, x)$ so that

$$(\psi_i, R) = \int_{-\delta}^{\delta} \psi_i(\mathcal{A}y^n - \Lambda^n\mathcal{B}y^n)dx = 0, \quad i = 1, 2, \ldots, n, \tag{E.7}$$

where Λ^n is the approximate eigenvalue associated with y^n. The eigenvalue Λ^n is generally determined by numerical means. Then introducing (E.6) into (E.7) we find that

$$\begin{aligned}(\psi_i, R) &= \int_{-\delta}^{\delta} \psi_i \left(\sum_{j=1}^{n} a_j\mathcal{A}\phi_j - \Lambda^n \sum_{j=1}^{n} a_j\mathcal{B}\phi_j \right) dx \\ &= \sum_{j=1}^{n} (k_{ij} - \Lambda^n m_{ij})a_j = 0, \quad i = 1, 2, \ldots, n, \end{aligned} \tag{E.8}$$

where

$$\begin{aligned} k_{ij} &= (\psi_i, \mathcal{A}\phi_j) = \int_{-\delta}^{\delta} \psi_i \mathcal{A}\phi_j dx, \quad i,j = 1,2,\ldots,n, \\ m_{ij} &= (\psi_i, \mathcal{B}\phi_j) = \int_{-\delta}^{\delta} \psi_i \mathcal{B}\phi_j dx, \quad i,j = 1,2,\ldots,n. \end{aligned} \tag{E.9}$$

where we find that the elements k_{ij} and m_{ij} are constant coefficients. Then defining the vector $\mathbf{a} = (a_1, a_2, \ldots, a_n)^T$ and the matrices $\mathsf{K} = [k_{ij}]$ and $\mathsf{M} = [m_{ij}]$ we may write this down as follows

$$\mathsf{K}\mathbf{a} = \Lambda^n \mathsf{M}\mathbf{a}, \tag{E.10}$$

which we recognise as an eigenvalue problem. Now (E.10) has a non-trivial solution, that is the a_j's are non-zero, provided its determinant vanishes

$$\det(k_{ij} - \Lambda^n m_{ij}) = 0. \tag{E.11}$$

This gives a characteristic equation in Λ^n of degree n. The coefficients a_i may then be determined by a process of Gaussian elimination.

The method of weighted residuals can be extended to problems where the differential operators are such that $\mathcal{A}, \mathcal{B} \in \mathbb{R}^{n\times n}$ with $n \geq 1$. Then the problem becomes one of solving the generalised operator problem

$$\mathcal{A}\mathbf{y} = \Lambda \mathcal{B}\mathbf{y}, \tag{E.12}$$

where $\mathbf{y} \in \mathbb{R}^n$. Now choosing the trial function so that $\mathbf{w} \in \mathbb{R}^n$ we define the residual to be

$$\mathbf{R}(\mathbf{w}, x) = \mathcal{A}\mathbf{w} - \Lambda \mathcal{B}\mathbf{w}. \tag{E.13}$$

Once again if we are given a Λ^i representing an eigenvalue of (E.12) along with an associated eigenvector w_i the residual $\mathbf{R}(w_i, x)$ is zero. At this point we want to form a weighted residual which we may use to determine an orthogonality condition.

Previously we chose a trial function w and a weighting function v and ensured orthogonality via (E.5). Now however the problem is complicated due to the presence of $\mathbb{R}^{n\times n}$ operators. Somehow we need to weight our residual $\mathbf{R}(\mathbf{w}, x)$ with respect to a weighting function.

To do so we follow the procedures outlined in [85, p.193-204] and [64, p.312-319]. In both of these treatments a weighted residual method is applied to a pair of coupled ODE's arising from a problem in aeroelasticity theory. Applied to the current problem the procedure for tackling the system involves the following. In order to weight the residual the trial function is chosen to be an approximate solution to the governing operator problem (E.12), viz

$$\mathbf{y}^n = \begin{bmatrix} y_1^n \\ y_2^n \end{bmatrix}, \quad \text{where} \quad y_1^n = \sum_{j=1}^{n} a_j \phi_j \quad \text{and} \quad y_2^n = \sum_{j=n+1}^{2n} a_j \phi_j. \tag{E.14}$$

Then taking the residual $\mathbf{R}(\mathbf{w}, x)$ to be $\mathbf{R} \in \mathbb{R}^{2\times 1}$ and writing $\mathbf{R}$ in component form $\mathbf{R} = (R_1, R_2)^T$, we choose $2n$ weighting functions ψ_i and form $2n$ weighted residuals as follows

$$\psi_i R_1 = \psi_i \left[\mathcal{A}_{11} y_1^n + \mathcal{A}_{12} y_2^n - \Lambda^{2n} \left(\mathcal{B}_{11} y_1^n + \mathcal{B}_{12} y_2^n\right)\right], \; i = 1, 2, \cdots, n, \tag{E.15}$$

$$\psi_i R_2 = \psi_i \left[\mathcal{A}_{21} y_1^n + \mathcal{A}_{22} y_2^n - \Lambda^{2n} \left(\mathcal{B}_{21} y_1^n + \mathcal{B}_{22} y_2^n\right)\right], \; i = n+1, n+2, \cdots, 2n, \tag{E.16}$$

Note that the eigenvalues for this system Λ^{2n} are of multiplicity $2n$. We shall use the notation given in Stewart [4] for the *tensor product* or *dyadic product*, so that the symbol $\otimes$ is used to represent the tensor product in the sense

$$[\mathbf{a} \otimes \mathbf{b}]_{ij} = a_i b_j. \tag{E.17}$$

This means that in Cartesians $\mathbf{a} \otimes \mathbf{b}$ corresponds roughly to a matrix with components given by (E.17). Consider the weighted residual given at (E.15). If we substitute for y_1^n and y_2^n from (E.14) in (E.15) we can write the problem

down as

$$\begin{aligned}
\psi_i R_1 &= \psi_i \left[\mathcal{A}_{11} \sum_{j=1}^{n} a_j \phi_j + \mathcal{A}_{12} \sum_{j=n+1}^{2n} a_j \phi_j - \Lambda^{2n} \left(\mathcal{B}_{11} \sum_{j=1}^{n} a_j \phi_j + \mathcal{B}_{12} \sum_{j=n+1}^{2n} a_j \phi_j \right) \right] \\
&= \sum_{j=1}^{n} a_j \left[\psi_i \mathcal{A}_{11} \phi_j - \Lambda^{2n} \psi_i \mathcal{B}_{11} \phi_j \right] + \sum_{j=n+1}^{2n} a_j \left[\psi_i \mathcal{A}_{12} \phi_j - \Lambda^{2n} \psi_i \mathcal{B}_{12} \phi_j \right] \\
&= \sum_{j=1}^{n} a_j \left[\left(\boldsymbol{\psi} \otimes \boldsymbol{\upsilon}^{\mathcal{A}_{11}} \right)_{ij} - \Lambda^{2n} \left(\boldsymbol{\psi} \otimes \boldsymbol{\upsilon}^{\mathcal{B}_{11}} \right)_{ij} \right] \\
&\quad + \sum_{j=n+1}^{2n} a_j \left[\left(\boldsymbol{\psi} \otimes \boldsymbol{\upsilon}^{\mathcal{A}_{12}} \right)_{ij} - \Lambda^{2n} \left(\boldsymbol{\psi} \otimes \boldsymbol{\upsilon}^{\mathcal{B}_{12}} \right)_{ij} \right] \qquad \text{(E.18)}
\end{aligned}$$

where we define the vectors

$$\boldsymbol{\psi} = \begin{bmatrix} \psi_1 \\ \psi_2 \\ \vdots \\ \psi_n \end{bmatrix}, \qquad \text{(E.19)}$$

along with

$$\boldsymbol{\upsilon}^{\mathcal{A}_{11}} = \begin{bmatrix} \mathcal{A}_{11}\phi_1 \\ \mathcal{A}_{11}\phi_2 \\ \vdots \\ \mathcal{A}_{11}\phi_n \end{bmatrix}, \boldsymbol{\upsilon}^{\mathcal{B}_{11}} = \begin{bmatrix} \mathcal{B}_{11}\phi_1 \\ \mathcal{B}_{11}\phi_2 \\ \vdots \\ \mathcal{B}_{11}\phi_n \end{bmatrix}, \boldsymbol{\upsilon}^{\mathcal{A}_{12}} = \begin{bmatrix} \mathcal{A}_{12}\phi_1 \\ \mathcal{A}_{12}\phi_2 \\ \vdots \\ \mathcal{A}_{12}\phi_n \end{bmatrix}, \boldsymbol{\upsilon}^{\mathcal{B}_{12}} = \begin{bmatrix} \mathcal{B}_{12}\phi_1 \\ \mathcal{B}_{12}\phi_2 \\ \vdots \\ \mathcal{B}_{12}\phi_n \end{bmatrix} \qquad \text{(E.20)}$$

In a similar fashion we define the weighted residual associated with R_2 with respect to ψ_i as

$$\begin{aligned}
\psi_i R_2 &= \sum_{j=1}^{n} a_j \left[\left(\boldsymbol{\psi} \otimes \boldsymbol{\upsilon}^{\mathcal{A}_{21}} \right)_{ij} - \Lambda^{2n} \left(\boldsymbol{\psi} \otimes \boldsymbol{\upsilon}^{\mathcal{B}_{21}} \right)_{ij} \right] \\
&\quad + \sum_{j=n+1}^{2n} a_j \left[\left(\boldsymbol{\psi} \otimes \boldsymbol{\upsilon}^{\mathcal{A}_{22}} \right)_{ij} - \Lambda^{2n} \left(\boldsymbol{\psi} \otimes \boldsymbol{\upsilon}^{\mathcal{B}_{22}} \right)_{ij} \right] \qquad \text{(E.21)}
\end{aligned}$$

where we define

$$\boldsymbol{\upsilon}^{\mathcal{A}_{21}} = \begin{bmatrix} \mathcal{A}_{21}\phi_1 \\ \mathcal{A}_{21}\phi_2 \\ \vdots \\ \mathcal{A}_{21}\phi_n \end{bmatrix}, \boldsymbol{\upsilon}^{\mathcal{B}_{21}} = \begin{bmatrix} \mathcal{B}_{21}\phi_1 \\ \mathcal{B}_{21}\phi_2 \\ \vdots \\ \mathcal{B}_{21}\phi_n \end{bmatrix}, \boldsymbol{\upsilon}^{\mathcal{A}_{22}} = \begin{bmatrix} \mathcal{A}_{22}\phi_1 \\ \mathcal{A}_{22}\phi_2 \\ \vdots \\ \mathcal{A}_{22}\phi_n \end{bmatrix}, \boldsymbol{\upsilon}^{\mathcal{B}_{22}} = \begin{bmatrix} \mathcal{B}_{22}\phi_1 \\ \mathcal{B}_{22}\phi_2 \\ \vdots \\ \mathcal{B}_{22}\phi_n \end{bmatrix}. \qquad \text{(E.22)}$$

Then the orthogonality conditions follow by integrating (E.15) and (E.16) with respect to x over the interval $-\delta \leq x \leq \delta$ as follows

$$\begin{aligned}
\int_{-\delta}^{\delta} \psi_i R_1 \, dx &= \int_{-\delta}^{\delta} \sum_{j=1}^{n} a_j \left[\left(\boldsymbol{\psi} \otimes \boldsymbol{\upsilon}^{\mathcal{A}_{11}} \right)_{ij} - \Lambda^{2n} \left(\boldsymbol{\psi} \otimes \boldsymbol{\upsilon}^{\mathcal{B}_{11}} \right)_{ij} \right] \\
&\quad + \sum_{j=n+1}^{2n} a_j \left[\left(\boldsymbol{\psi} \otimes \boldsymbol{\upsilon}^{\mathcal{A}_{12}} \right)_{ij} - \Lambda^{2n} \left(\boldsymbol{\psi} \otimes \boldsymbol{\upsilon}^{\mathcal{B}_{12}} \right)_{ij} \right] dx \\
&= 0, \quad i = 1, 2, \cdots, n, \qquad \text{(E.23)} \\
\int_{-\delta}^{\delta} \psi_i R_2 \, dx &= \int_{-\delta}^{\delta} \sum_{j=1}^{n} a_j \left[\left(\boldsymbol{\psi} \otimes \boldsymbol{\upsilon}^{\mathcal{A}_{21}} \right)_{ij} - \Lambda^{2n} \left(\boldsymbol{\psi} \otimes \boldsymbol{\upsilon}^{\mathcal{B}_{21}} \right)_{ij} \right] \\
&\quad + \sum_{j=n+1}^{2n} a_j \left[\left(\boldsymbol{\psi} \otimes \boldsymbol{\upsilon}^{\mathcal{A}_{22}} \right)_{ij} - \Lambda^{2n} \left(\boldsymbol{\psi} \otimes \boldsymbol{\upsilon}^{\mathcal{B}_{22}} \right)_{ij} \right] dx \\
&= 0, \quad i = n+1, 2, \cdots, 2n, \qquad \text{(E.24)}
\end{aligned}$$

Suppose now that we select $n = 2$ so that the orthogonality conditions at (E.23) yield

$$\begin{aligned}
\int_{-\delta}^{\delta} \psi_1 R_1 \, dx &= \int_{-\delta}^{\delta} a_1 \left[\left(\boldsymbol{\psi} \otimes \boldsymbol{\upsilon}^{\mathcal{A}_{11}} \right)_{11} - \Lambda^{2n} \left(\boldsymbol{\psi} \otimes \boldsymbol{\upsilon}^{\mathcal{B}_{11}} \right)_{11} \right] \\
&\quad + a_2 \left[\left(\boldsymbol{\psi} \otimes \boldsymbol{\upsilon}^{\mathcal{A}_{11}} \right)_{12} - \Lambda^{2n} \left(\boldsymbol{\psi} \otimes \boldsymbol{\upsilon}^{\mathcal{B}_{11}} \right)_{12} \right] \\
&\quad + a_3 \left[\left(\boldsymbol{\psi} \otimes \boldsymbol{\upsilon}^{\mathcal{A}_{12}} \right)_{13} - \Lambda^{2n} \left(\boldsymbol{\psi} \otimes \boldsymbol{\upsilon}^{\mathcal{B}_{12}} \right)_{13} \right] \\
&\quad + a_4 \left[\left(\boldsymbol{\psi} \otimes \boldsymbol{\upsilon}^{\mathcal{A}_{12}} \right)_{14} - \Lambda^{2n} \left(\boldsymbol{\psi} \otimes \boldsymbol{\upsilon}^{\mathcal{B}_{12}} \right)_{14} \right] \, dx \\
&= 0, \qquad \text{(E.25)}
\end{aligned}$$

and

$$\begin{aligned}
\int_{-\delta}^{\delta} \psi_2 R_1 \, dx &= \int_{-\delta}^{\delta} a_1 \left[\left(\boldsymbol{\psi} \otimes \boldsymbol{\upsilon}^{\mathcal{A}_{11}} \right)_{21} - \Lambda^{2n} \left(\boldsymbol{\psi} \otimes \boldsymbol{\upsilon}^{\mathcal{B}_{11}} \right)_{21} \right] \\
&\quad + a_2 \left[\left(\boldsymbol{\psi} \otimes \boldsymbol{\upsilon}^{\mathcal{A}_{11}} \right)_{22} - \Lambda^{2n} \left(\boldsymbol{\psi} \otimes \boldsymbol{\upsilon}^{\mathcal{B}_{11}} \right)_{22} \right] \\
&\quad + a_3 \left[\left(\boldsymbol{\psi} \otimes \boldsymbol{\upsilon}^{\mathcal{A}_{12}} \right)_{23} - \Lambda^{2n} \left(\boldsymbol{\psi} \otimes \boldsymbol{\upsilon}^{\mathcal{B}_{12}} \right)_{23} \right] \\
&\quad + a_4 \left[\left(\boldsymbol{\psi} \otimes \boldsymbol{\upsilon}^{\mathcal{A}_{12}} \right)_{24} - \Lambda^{2n} \left(\boldsymbol{\psi} \otimes \boldsymbol{\upsilon}^{\mathcal{B}_{12}} \right)_{24} \right] \, dx \\
&= 0, \qquad \text{(E.26)}
\end{aligned}$$

whereas the orthogonality conditions at (E.24) yield the following expressions

$$\begin{aligned}\int_{-\delta}^{\delta}\psi_3 R_2\,dx &= \int_{-\delta}^{\delta} a_1\left[\left(\boldsymbol{\psi}\otimes\boldsymbol{\upsilon}^{\mathcal{A}_{21}}\right)_{31}-\Lambda^{2n}\left(\boldsymbol{\psi}\otimes\boldsymbol{\upsilon}^{\mathcal{B}_{21}}\right)_{31}\right]\\ &\quad +a_2\left[\left(\boldsymbol{\psi}\otimes\boldsymbol{\upsilon}^{\mathcal{A}_{21}}\right)_{32}-\Lambda^{2n}\left(\boldsymbol{\psi}\otimes\boldsymbol{\upsilon}^{\mathcal{B}_{21}}\right)_{32}\right]\\ &\quad +a_3\left[\left(\boldsymbol{\psi}\otimes\boldsymbol{\upsilon}^{\mathcal{A}_{22}}\right)_{33}-\Lambda^{2n}\left(\boldsymbol{\psi}\otimes\boldsymbol{\upsilon}^{\mathcal{B}_{22}}\right)_{33}\right]\\ &\quad +a_4\left[\left(\boldsymbol{\psi}\otimes\boldsymbol{\upsilon}^{\mathcal{A}_{22}}\right)_{34}-\Lambda^{2n}\left(\boldsymbol{\psi}\otimes\boldsymbol{\upsilon}^{\mathcal{B}_{22}}\right)_{34}\right]\,dx\\ &= 0, \end{aligned} \tag{E.27}$$

$$\begin{aligned}\int_{-\delta}^{\delta}\psi_4 R_2\,dx &= \int_{-\delta}^{\delta} a_1\left[\left(\boldsymbol{\psi}\otimes\boldsymbol{\upsilon}^{\mathcal{A}_{21}}\right)_{41}-\Lambda^{2n}\left(\boldsymbol{\psi}\otimes\boldsymbol{\upsilon}^{\mathcal{B}_{21}}\right)_{41}\right]\\ &\quad +a_2\left[\left(\boldsymbol{\psi}\otimes\boldsymbol{\upsilon}^{\mathcal{A}_{21}}\right)_{42}-\Lambda^{2n}\left(\boldsymbol{\psi}\otimes\boldsymbol{\upsilon}^{\mathcal{B}_{21}}\right)_{42}\right]\\ &\quad +a_3\left[\left(\boldsymbol{\psi}\otimes\boldsymbol{\upsilon}^{\mathcal{A}_{22}}\right)_{43}-\Lambda^{2n}\left(\boldsymbol{\psi}\otimes\boldsymbol{\upsilon}^{\mathcal{B}_{22}}\right)_{43}\right]\\ &\quad +a_4\left[\left(\boldsymbol{\psi}\otimes\boldsymbol{\upsilon}^{\mathcal{A}_{22}}\right)_{44}-\Lambda^{2n}\left(\boldsymbol{\psi}\otimes\boldsymbol{\upsilon}^{\mathcal{B}_{22}}\right)_{44}\right]\,dx\\ &= 0. \end{aligned} \tag{E.28}$$

Finally we may write the orthogonality condition down as a generalised eigenvalue problem so that

$$\mathsf{Aa} = \Lambda^{2n}\mathsf{Ba}, \tag{E.29}$$

where the matrix elements A_{ij} and B_{ij} are given by

$$\begin{aligned} A_{ij} &= \int_{-\delta}^{\delta}\left(\boldsymbol{\psi}\otimes\boldsymbol{\upsilon}^{\mathcal{A}_{11}}\right)_{ij}\,dx, \quad i,j=1,2,\\ A_{ij} &= \int_{-\delta}^{\delta}\left(\boldsymbol{\psi}\otimes\boldsymbol{\upsilon}^{\mathcal{A}_{12}}\right)_{ij}\,dx, \quad i=1,2; j=3,4,\\ A_{ij} &= \int_{-\delta}^{\delta}\left(\boldsymbol{\psi}\otimes\boldsymbol{\upsilon}^{\mathcal{A}_{21}}\right)_{ij}\,dx, \quad i=3,4; j=1,2,\\ A_{ij} &= \int_{-\delta}^{\delta}\left(\boldsymbol{\psi}\otimes\boldsymbol{\upsilon}^{\mathcal{A}_{22}}\right)_{ij}\,dx, \quad i,j=3,4, \end{aligned}$$

and

$$B_{ij} = \int_{-\delta}^{\delta}\left(\boldsymbol{\psi}\otimes\boldsymbol{\upsilon}^{\mathcal{B}_{11}}\right)_{ij}\,dx, \quad i,j=1,2,$$

$$
\begin{aligned}
B_{ij} &= \int_{-\delta}^{\delta} \left(\boldsymbol{\psi} \otimes \boldsymbol{\upsilon}^{\mathcal{B}_{12}}\right)_{ij} \, dx, \quad i = 1, 2; j = 3, 4, \\
B_{ij} &= \int_{-\delta}^{\delta} \left(\boldsymbol{\psi} \otimes \boldsymbol{\upsilon}^{\mathcal{B}_{21}}\right)_{ij} \, dx, \quad i = 3, 4; j = 1, 2, \\
B_{ij} &= \int_{-\delta}^{\delta} \left(\boldsymbol{\psi} \otimes \boldsymbol{\upsilon}^{\mathcal{B}_{22}}\right)_{ij} \, dx, \quad i, j = 3, 4,
\end{aligned}
$$

E.1 The Galerkin method

The Galerkin method [67] is the name given to a scheme whereby the weighting functions are made equal to the trial functions used to form the approximate solution. So, for example, suppose we have a linear operator problem of the form

$$\mathcal{L}y = \lambda y, \tag{E.30}$$

and we wish to approximate its solution using the function

$$y^n(x) = \sum_{j=1}^{n} a_j \phi_j(x) \tag{E.31}$$

where the ϕ_j are a complete set of trial functions chosen to match the boundary conditions of the problem in question. We form the residual as described in Appendix E thus

$$R(y^n, x) = \mathcal{L}y^n - \lambda y^n, \tag{E.32}$$

Then choosing the weighting functions to be equal to the trial functions, so that $\psi_i = \phi_i$ we multiply the residual by the weighting functions so that on integrating to form the orthogonality condition we see that

$$(\phi_i, R) = \int_{-\delta}^{\delta} \phi_i \mathcal{L}\phi_j \, dx = 0, \quad \text{for} \quad i, j = 1, 2, \cdots, n. \tag{E.33}$$

By contrast in the multidimensional case as given in (E.12), choosing the weighting functions to be equal to the trial functions is achieved by making $\boldsymbol{\psi} = \boldsymbol{\phi}$.

Appendix F

The adjoint of an $\mathbb{R}^{2\times 2}$ general second order linear differential operator

First, suppose that we have a general linear differential operator $\mathcal{L} \in \mathbb{R}^{2\times 2}$ and two vectors $\mathbf{u}, \mathbf{v} \in \mathbb{R}^{1\times 2}$ such that

$$\mathcal{L} = \begin{bmatrix} l_{11} & l_{12} \\ l_{21} & l_{22} \end{bmatrix}, \mathbf{u} = \begin{bmatrix} u_1 \\ u_2 \end{bmatrix} \text{ and } \mathbf{v} = \begin{bmatrix} v_1 \\ v_2 \end{bmatrix}. \tag{F.1}$$

We define the inner product as follows

$$\begin{aligned} (\mathbf{v}, \mathcal{L}\mathbf{u}) &= \int_a^b \mathbf{v} \cdot \mathcal{L}\mathbf{u}\, dx \\ &= \int_a^b v_1 l_{11} u_1 + v_1 l_{12} u_2 + v_2 l_{21} u_1 + v_2 l_{22} u_2\, dx \end{aligned} \tag{F.2}$$

$$\tag{F.3}$$

Then typically following an integration by parts we find that

$$\begin{aligned} (\mathbf{v}, \mathcal{L}\mathbf{u}) &= \int_a^b u_1 l_{11}^* v_1 + u_2 l_{12}^* v_1 + u_1 l_{21}^* v_2 + u_2 l_{22}^* v_2\, dx + B(\eta_1, \eta_2, \zeta_1, \zeta_2) \\ &= \int_a^b u_1 l_{11}^* v_1 + u_1 l_{21}^* v_2 + u_2 l_{12}^* v_1 + u_2 l_{22}^* v_2\, dx + B(\eta_1, \eta_2, \zeta_1, \zeta_2) \\ &= \int_a^b \mathbf{u} \cdot \mathcal{L}^* \mathbf{v}\, dx + B(\eta_1, \eta_2, \zeta_1, \zeta_2) \\ &= (\mathbf{u}, \mathcal{L}^* \mathbf{v}) + B(\eta_1, \eta_2, \zeta_1, \zeta_2), \end{aligned} \tag{F.4}$$

where $B(\eta_1, \eta_2, \zeta_1, \zeta_2)$ is a certain bi-linear form in the variables [86]

$$\eta_1 = (u_1(a), u_1'(a), \cdots, u_1^{(n-1)}(a), u_1(b), u_1'(b), \cdots, u_1^{(n-1)}(b)), \tag{F.5}$$

$$\eta_2 = (u_2(a), u_2'(a), \cdots, u_2^{(n-1)}(a), u_2(b), u_2'(b), \cdots, u_2^{(n-1)}(b)), \quad \text{(F.6)}$$

$$\zeta_1 = (v_1(a), v_1'(a), \cdots, v_1^{(n-1)}(a), v_1(b), v_1'(b), \cdots, v_1^{(n-1)}(b)), \quad \text{(F.7)}$$

$$\zeta_2 = (v_2(a), v_2'(a), \cdots, v_2^{(n-1)}(a), v_2(b), v_2'(b), \cdots, v_2^{(n-1)}(b)), \quad \text{(F.8)}$$

Then we may write the adjoint as

$$\mathcal{L}^* = \begin{bmatrix} l_{11}^* & l_{21}^* \\ l_{12}^* & l_{22}^* \end{bmatrix}, \quad \text{(F.9)}$$

Suppose now we have a general linear differential operator of second order given by

$$l = a_2(x)\frac{d^2}{dx^2} + a_1(x)\frac{d}{dx} + a_0(x). \quad \text{(F.10)}$$

It can be shown (see Lanczos [87, p.184]) using a suitable integration by parts that the adjoint operator of l is given by

$$l^* = a_2\frac{d^2}{dx^2} + (2a_2' - a_1)\frac{d}{dx} + (a_2'' - a_1' + a_0). \quad \text{(F.11)}$$

Suppose further that our operator $\mathcal{L}$ is such that the elements of $\mathcal{L}$ are given by

$$\mathcal{L}_{ij} = l_{ij}, \quad \text{(F.12)}$$

and in addition the elements of $\mathcal{L}$ are general second order differential operators $l_{ij} \in C^2[a, b]$ so that

$$l_{ij} = [a_{ij}]_2\frac{d^2}{dx^2} + [a_{ij}]_1\frac{d}{dx} + [a_{ij}]_0, \quad \text{(F.13)}$$

then the adjoint of (F.13) is

$$l_{ij}^* = [a_{ij}]_2\frac{d^2}{dx^2} + (2[a_{ij}]_2' - [a_{ij}]_1)\frac{d}{dx} + ([a_{ij}]_2'' - [a_{ij}]_1' + [a_{ij}]_0). \quad \text{(F.14)}$$

We know, again see Lanczos [87, p.184], that the most general self-adjoint linear differential operator of second order is

$$\mathcal{D} = A(x)\frac{d^2}{dx^2} + A'(x)\frac{d}{dx} + C(x). \quad \text{(F.15)}$$

Then in order for $l_{ij} = l_{ij}^*$ we require that

$$[a_{ij}]_1 = [a_{ij}]_2' \;\Rightarrow\; [a_{ij}]_1' = [a_{ij}]_2''. \tag{F.16}$$

Then

$$\begin{aligned} l_{ij}^* &= [a_{ij}]_2 \frac{d^2}{dx^2} + (2[a_{ij}]_2' - [a_{ij}]_1)\frac{d}{dx} + ([a_{ij}]_2'' - [a_{ij}]_1' + [a_{ij}]_0) \\ &= [a_{ij}]_2 \frac{d^2}{dx^2} + [a_{ij}]_2' \frac{d}{dx} + [a_{ij}]_0. \end{aligned}$$

So using the notation developed above the most general linear differential operator of second order is

$$l_{ij} = [a_{ij}]_2 \frac{d^2}{dx^2} + [a_{ij}]_2' \frac{d}{dx} + [a_{ij}]_0. \tag{F.17}$$

This means that all of the elements of l_{ij} must at least satisfy (F.17) in order for the operator $\mathcal{L}$ to be self-adjoint. Moreover the off diagonal elements of $\mathcal{L}$ and $\mathcal{L}^*$, that is the elements l_{12}, l_{21}, l_{12}^* and l_{21}^* must satisfy the following requirements

$$\begin{aligned} l_{12} &= [a_{12}]_2 \frac{d^2}{dx^2} + [a_{12}]_2' \frac{d}{dx} + [a_{12}]_0, \\ l_{12}^* &= [a_{12}]_2 \frac{d^2}{dx^2} + [a_{12}]_2' \frac{d}{dx} + [a_{12}]_0, \\ l_{21} &= [a_{21}]_2 \frac{d^2}{dx^2} + [a_{21}]_2' \frac{d}{dx} + [a_{21}]_0, \\ l_{12}^* &= [a_{21}]_2 \frac{d^2}{dx^2} + [a_{21}]_2' \frac{d}{dx} + [a_{21}]_0, \end{aligned}$$

and since

$$\mathcal{L} = \begin{bmatrix} l_{11} & l_{12} \\ l_{21} & l_{22} \end{bmatrix}, \text{ and } \mathcal{L}^* = \begin{bmatrix} l_{11}^* & l_{21}^* \\ l_{12}^* & l_{22}^* \end{bmatrix}, \tag{F.18}$$

a further requirement for $\mathcal{L}$ to be self-adjoint is that

$$l_{12} = l_{21}^*, \text{ and } l_{21} = l_{12}^*. \tag{F.19}$$

This means that the final requirement for the self-adjointness of $\mathcal{L}$ is that we must have $[a_{12}]_2 = [a_{21}]_2$, $[a_{12}]_2' = [a_{21}]_2'$ and $[a_{12}]_0 = [a_{21}]_0$. If any of the elements do not satisfy at a minimum the requirement (F.17) then $\mathcal{L}$ *cannot* be shown to be self-adjoint.

Appendix G

Rayleigh-Ritz methods

Given the ansatz postulated at (4.1) to (4.4), we expect the perturbations to decay when $\omega > 0$. Consequently our goal now is to determine the sign of the constant ω, and in the problem being considered ω plays the role of an eigenvalue of A. We note from [88, p.121-2] that a compact self-adjoint operator $\mathsf{A} \in L(\mathcal{H})$ is positive definite if and only if its eigenvalues are positive. By positive definite we mean a compact self-adjoint operator A for which

$$(\mathsf{A}\mathbf{x}, \mathbf{x}) > 0 \; \forall \mathbf{x} \in \mathcal{H} \tag{G.1}$$

holds. Moreover, the first eigenvalue ω_1 maybe calculated by considering

$$\omega_1 = \max_{\|\mathbf{x}\|=1} (\mathsf{A}\mathbf{x}, \mathbf{x}), \tag{G.2}$$

with the spectrum of eigenvalues for the operator A such that $\omega_1 \geq \omega_2 \geq \cdots \geq \omega_n \geq \cdots \geq 0$. Premultiplying both sides of (4.24) by $\mathbf{x}^T$, and integrating over the interval $\tau \in [-\frac{L}{2}, \frac{L}{2}]$ we get

$$(\mathsf{A}\mathbf{x}, \mathbf{x}) = \omega(\mathbf{x}, \mathbf{x}), \tag{G.3}$$

where we define

$$(\mathsf{A}\mathbf{x}, \mathbf{x}) = \int_{-\frac{L}{2}}^{\frac{L}{2}} \mathbf{x}^T \mathsf{A}\mathbf{x} \; d\tau, \tag{G.4}$$

and

$$(\mathbf{x}, \mathbf{x}) = \int_{-\frac{L}{2}}^{\frac{L}{2}} \mathbf{x}^T \mathbf{x} \; d\tau. \tag{G.5}$$

From (G.4) and using integration by parts, we identify the following form for the integral

$$(\mathsf{A}\mathbf{x},\mathbf{x}) = \int_{-\frac{L}{2}}^{\frac{L}{2}} \tilde{a}\hat{\phi}_{,\tau}^2 - \tilde{c}\hat{\phi}^2 + \tilde{d}\hat{z}_{,\tau}^2 - \tilde{e}\hat{z}_{,\tau}\hat{\phi}_{,\tau} - \tilde{f}\hat{z}_{,\tau}\hat{\phi}\ d\tau. \tag{G.6}$$

If we let $F(\hat{\phi}_{,\tau},\hat{\phi},\hat{z}_{,\tau})$ be equal to the integrand of (G.6), so that

$$F(\hat{\phi}_{,\tau},\hat{\phi},\hat{z}_{,\tau}) = \tilde{a}\hat{\phi}_{,\tau\tau}^2 - \tilde{c}\hat{\phi}^2 + \tilde{d}\hat{z}_{,\tau}^2 - \tilde{e}\hat{z}_{,\tau}\hat{\phi}_{,\tau} - \tilde{f}\hat{z}_{,\tau}\hat{\phi}, \tag{G.7}$$

and furthermore assume that $\tilde{e}$ and $\tilde{f}$ have arbitrary sign and that $\tilde{a} > 0$, $\tilde{d} > 0$ and $\tilde{e} > 0$, we may write

$$F(\hat{\phi}_{,\tau},\hat{\phi},\hat{z}_{,\tau}) = \mathbf{y}^T\mathsf{B}\mathbf{y}, \tag{G.8}$$

where

$$\mathsf{B} = \begin{bmatrix} \tilde{a} & 0 & -\frac{\tilde{e}}{2} \\ 0 & -\tilde{c} & -\frac{\tilde{f}}{2} \\ -\frac{\tilde{e}}{2} & -\frac{\tilde{f}}{2} & \tilde{d} \end{bmatrix},\ \mathbf{y} = \begin{bmatrix} \hat{\phi}_{,\tau} \\ \hat{\phi} \\ \hat{z}_{,\tau} \end{bmatrix}. \tag{G.9}$$

Note that (G.8) is a quadratic form. Note also that

$$\mathbf{x}^T\mathsf{A}\mathbf{x} = \mathbf{y}^T\mathsf{B}\mathbf{y}. \tag{G.10}$$

Recall we are attempting to establish that the eigenvalues of (4.24) are all positive. This is equivalent to showing that $\mathbf{x}^T\mathsf{A}\mathbf{x} > 0$. This in turn is equivalent to demanding that the quadratic form given at (G.8) is positive definite. If we can show $\mathbf{y}^T\mathsf{B}\mathbf{y} > 0$ then the matrix B is said to be a positive definite matrix, and this in turn means that the matrix B has positive eigenvalues.

It is well known that a symmetric matrix is positive definite if and only if the determinant of every principal submatrix is positive [89]. Here we denote the principal submatrices of B by $\mathsf{B}_r,\ r = 1, 2, \cdots, n$. Considering the principal submatrices of B then we find that the first and second submatrices are given by

$$\mathsf{B}_1 = \tilde{c} > 0,\ \ \mathsf{B}_2 = -\tilde{a}\tilde{c} < 0. \tag{G.11}$$

This test is inconclusive, and the result means that we must resort to integral inequalities to demonstrate that make A positive definite.

G.1 Integral Inequalities

Consider again the integral given by (G.6). This maybe re-written as follows

$$(\mathsf{A}\mathbf{x},\mathbf{x}) = \int_{-\frac{L}{2}}^{\frac{L}{2}} \tilde{d}\, Q^2 + \left[\tilde{a} - \frac{\tilde{e}^2}{4\tilde{d}}\right]\hat{\phi}_{,\tau}^2 - \left[\tilde{c} + \frac{\tilde{f}^2}{4\tilde{d}}\right]\hat{\phi}^2\, d\tau, \tag{G.12}$$

where

$$Q = \hat{z}_{,\tau} - \frac{\tilde{f}}{2\tilde{d}}\hat{\phi} - \frac{\tilde{e}}{2\tilde{d}}\hat{\phi}_{,\tau}. \tag{G.13}$$

We shall assume that

$$\tilde{a} - \frac{\tilde{e}^2}{4\tilde{d}} > 0. \tag{G.14}$$

Then appealing to Hardy's inequality [90, p.105]

$$\int_{a_0}^{b_0}\left(\frac{dy}{dx}\right)^2 \geq \int_{a_0}^{b_0}\frac{y^2}{4[f(x)]^2}\, dx, \quad \text{where } f(x) = min\{x - a_0, b_0 - x\}, \tag{G.15}$$

and noticing that on $x \in (a_0, b_0)$

$$|f(x)| \leq \left(\frac{b_0 - a_0}{2}\right), \tag{G.16}$$

so that we may write

$$\left(\frac{1}{f(x)}\right)^2 \geq \left(\frac{2}{b_0 - a_0}\right)^2. \tag{G.17}$$

we find that

$$\begin{aligned}
(\mathsf{A}\mathbf{x},\mathbf{x}) &= \int_{-\frac{L}{2}}^{\frac{L}{2}} \tilde{d}\, Q^2 + \left[\tilde{a} - \frac{\tilde{e}^2}{4\tilde{d}}\right]\hat{\phi}_{,\tau}^2 - \left[\tilde{c} + \frac{\tilde{f}^2}{4\tilde{d}}\right]\hat{\phi}^2\, d\tau \\
&\geq \int_{-\frac{L}{2}}^{\frac{L}{2}} \tilde{d}\, Q^2 + \left[\tilde{a} - \frac{\tilde{e}^2}{4\tilde{d}}\right]\frac{\hat{\phi}^2}{4[f(x)]^2} - \left[\tilde{c} + \frac{\tilde{f}^2}{4\tilde{d}}\right]\hat{\phi}^2\, d\tau \\
&\geq \int_{-\frac{L}{2}}^{\frac{L}{2}} \left[\tilde{a} - \frac{\tilde{e}^2}{4\tilde{d}}\right]\frac{\hat{\phi}^2}{4[f(x)]^2} - \left[\tilde{c} + \frac{\tilde{f}^2}{4\tilde{d}}\right]\hat{\phi}^2\, d\tau \\
&\geq \int_{-\frac{L}{2}}^{\frac{L}{2}} \left[\frac{1}{L^2}\left[\tilde{a} - \frac{\tilde{e}^2}{4\tilde{d}}\right] - \left[\tilde{c} + \frac{\tilde{f}^2}{4\tilde{d}}\right]\right]\hat{\phi}^2\, d\tau \\
&\geq 0.
\end{aligned} \tag{G.18}$$

Then provided (G.14) is true and

$$\frac{1}{L^2}\left[\tilde{a}-\frac{\tilde{e}^2}{4\tilde{d}}\right]-\left[\tilde{c}+\frac{\tilde{f}^2}{4\tilde{d}}\right]>0, \tag{G.19}$$

we have that

$$\mathbf{x}^T\mathsf{A}\mathbf{x}>0, \tag{G.20}$$

and so we are guaranteed that the quadratic form $\mathbf{x}^T\mathsf{A}\mathbf{x}$ is positive definite.

Appendix H

Root solver

The root solver `Root()` used to determine critical field strengths is shown here. Written in MAPLE it requires a function `f()` declared externally to the procedure and takes as arguments upper and lower values `X2` and `X1` respectively along with a tolerance `EPS`. The code has been adapted from a root solver found in [91, p.116].

```
    # proc[Root] Adapted from the book Advanced Mathematical Methods
with Maple pg.  116.
Root:=proc(X1,X2,EPS)
local FL,FH,XL,XH,swap,dx,k,rtf,F,del,eps;
FL:=f(X1);FH:=f(X2);eps:=EPS;
if FL*FH>0 then RETURN(0) fi;
if FL < 0 then
XL:=X1; XH:=X2;
else
XL:=X2; XH:=X1; swap:=FL; FL:=FH; FH:=swap;
fi:
dx:=XH-XL;
for k from 1 to 50 do;
rtf:=XL+dx*FL/(FL-FH); F:=f(rtf);
```

```
if F < 0 then
del:=XL-rtf:  XL:=rtf; FL:=F;
else
del:=XH-rtf:  XH:=rtf; FH:=F;
fi;
dx:=XH-XL;
if abs(del) < eps or abs(F) < eps then break fi;
od;
rtf
end:
```

Bibliography

[1] P. Palffy-Muhoray, "The diverse world of liquid crystals," *Physics Today*, vol. 60, no. 9, pp. 54–60, 2007.

[2] R. A. Soref, "Field effects in nematic liquid crystals obtained with interdigital electrodes," *J. Appl. Phys.*, vol. 45, no. 12, pp. 5466–5468, 1974.

[3] I. W. Stewart and R. J. Atkin, "Static domain wall solutions for smectic C liquid crystals and nematic liquid crystals in cylindrical geometry," *J. Non-Newtonian Fluid Mech.*, vol. 119, pp. 105–113, 2004.

[4] I. W. Stewart, *The Static and Dynamic Continuum Theory of Liquid Crystals*. London and New York: Taylor and Francis, 2004.

[5] N. A. Clark and S. T. Lagerwall, "Submicrosecond bistable electro-optic switching in liquid crystals," *Appl. Phys. Lett.*, vol. 36, pp. 899–901, 1980.

[6] S. Elston, "The optics of ferroelectric liquid crystals," *Journal of Modern Optics*, vol. 42, no. 1, pp. 19–56, 1995.

[7] I. W. Stewart and E. J. Wigham, "Dynamics of cylindrical domain walls in smectic C liquid crystals," *J. Phys. A: Math. Theor.*, vol. 42, April 2009.

[8] L. J. Seddon and I. W. Stewart, "Computing the wave speed of soliton-like solutions in SmC* liquid crystals," *Mol. Cryst. Liq. Cryst.*, vol. 525, pp. 167–175, 2010.

[9] F. Reinitzer, "Beiträge zur Kenntniss des Cholesterins," *Monatsh. Chem.*, vol. 9, pp. 421–441, 1888.

[10] H. Kelker, "History of liquid crystals," *Mol. Cryst. Liq. Cryst.*, vol. 21, pp. 1–48, 1969.

[11] G. Friedel, "Les états mésomorphes de la matière," *Ann. Phys. (Paris)*, vol. 18, pp. 273–474, 1922.

[12] T. Carlsson and F. M. Leslie, "The development of theory for flow and dynamic effects for nematic liquid crystals," *Liq. Cryst.*, vol. 26, pp. 1267–1280, 1999.

[13] C. W. Oseen, "Beiträge zur Theorie der anisotropen Flüssigkeiten," *Arkiv För Matematik, Astronomi Och Fysik*, vol. 19A, no. part 9, pp. 1–19, 1925.

[14] C. W. Oseen, "The theory of liquid crystals," *Trans. Faraday Soc.*, vol. 29, pp. 883–899, 1933.

[15] H. Zocher, "Über die Einwirkung magnetischer, elektrischer und mechanischer Kräfte auf Mesophasen," *Physik. Zeitschr.*, vol. 28, pp. 790–796, 1927.

[16] F. C. Frank, "On the theory of liquid crystals," *Discuss. Faraday Soc.*, vol. 25, pp. 19–28, 1958.

[17] J. L. Ericksen, "Conservation laws for liquid crystals," *Trans. Soc. Rheol.*, vol. 5, pp. 23–34, 1961.

[18] F. M. Leslie, "Some constitutive equations for anisotropic fluids," *Q. Jl. Mech. Appl. Math.*, vol. 19, pp. 357–370, 1966.

[19] F. M. Leslie, "Some constitutive equations for liquid crystals," *Arch. Rat. Mech. Anal.*, vol. 28, pp. 265–283, 1968.

[20] J. Fisher and A. G. Fredrickson, "Interfacial effects on the viscosity of a nematic mesophase," *Mol. Cryst. Liq. Cryst.*, vol. 8, pp. 267–284, 1969.

[21] R. J. Atkin, "Poiseuille flow of liquid crystals of the nematic type," *Arch. Rat. Mech. Anal.*, vol. 38, pp. 224–240, 1970.

[22] F. M. Leslie, I. W. Stewart, and M. Nakagawa, "A continuum theory for smectic C liquid crystals," *Mol. Cryst. Liq. Cryst.*, vol. 198, pp. 443–454, 1991.

[23] P. G. de Gennes and J. Prost, *The Physics of Liquid Crystals*. Oxford: Oxford University Press, second ed., 1993.

[24] L. Gattermann and A. Ritschke, "Über azoxyphenoläther," *Ber. Deutsch. Chem. Ges.*, vol. 23, pp. 1738–1750, 1890.

[25] H. Kelker and B. Scheurle, "A liquid-crystalline (nematic) phase with a particularly low solidification point," *Angew. Chem. Internat. Edit.*, vol. 8, pp. 884–885, 1969.

[26] I. Dierking, *Textures of liquid crystals*. Weinheim: Vch Verlagsgesellschaft Mbh, 2003.

[27] H. Sackmann, "Smectic liquid crystals: A historical review," *Liq. Cryst.*, vol. 5, pp. 43–55, 1989.

[28] I. W. Stewart, "Dynamic theory for smectic A liquid crystals," *Continuum Mech. Thermodyn.*, vol. 18, pp. 343–360, November 2007.

[29] R. B. Meyer, L. Liébert, L. Strzelecki, and P. Keller, "Ferroelectric liquid crystals," *J. de Physique Lett.*, vol. 36, pp. L69–L71, 1975.

[30] S. T. Lagerwall, *Ferroelectric and Antiferroelectric Liquid Crystals*. Weinheim, Germany: Wiley-VCH, 1999.

[31] I. W. Stewart, "The pumping phenomenon in smectic C* liquid crystals," *Liq. Cryst.*, vol. 37, pp. 799–809, 2010.

[32] P. Das and W. H. Schwarz, "Solitons in cell membranes," *Phys. Rev. E.*, vol. 51, no. 4, pp. 3588–3612, 1995.

[33] F. Gouda, G. Anderson, M. Matuszczyk, T. Matuszczyk, K. Skarp, and S. Lagerwall, "Dielectric anisotropy and dielectric torque in ferroelectric liquid crystals and their importance for electro-optic device performance," *J. Appl. Phys.*, vol. 67, no. 1, pp. 180–186, 1990.

[34] J. L. Ericksen, "Hydrostatic theory of liquid crystals," *Arch. Rat. Mech. Anal.*, vol. 9, pp. 371–378, 1962.

[35] W. H. de Jeu, *Physical Properties of Liquid Crystalline Materials*. New York: Gordon and Breach, 1990.

[36] F. M. Leslie, I. W. Stewart, T. Carlsson, and M. Nakagawa, "Equivalent smectic C liquid crystal energies," *Continuum Mech. Thermodyn.*, vol. 3, pp. 237–250, 1991.

[37] Orsay Group, "Simplified elastic theory for smectics C," *Solid State Commun.*, vol. 9, pp. 653–655, 1971.

[38] A. Rapini, "Instabilités magnétique d'un smectique C," *J. de Physique*, vol. 33, pp. 237–247, 1972.

[39] M. Nakagawa, "On the elastic theory of ferroelectric SmC* liquid crystals," *J. Phys. Soc. Japan*, vol. 58, pp. 2346–2354, 1989.

[40] T. Carlsson, I. W. Stewart, and F. M. Leslie, "An elastic energy for the ferroelectric chiral smectic C* phase," *J. Phys. A: Math. Gen.*, vol. 25, pp. 2371–2374, 1992.

[41] A. Saupe, "On molecular structure and physical properties of thermotropic liquid crystals," *Mol. Cryst. Liq. Cryst.*, vol. 7, pp. 59–74, 1969.

[42] T. Carlsson, I. W. Stewart, and F. M. Leslie, "Theoretical studies of smectic C liquid crystals confined in a wedge: Stability considerations and Frederiks transitions," *Liq. Cryst.*, vol. 9, pp. 661–678, 1991.

[43] I. Dahl and S. T. Lagerwall, "Elastic and flexoelectric properties of chiral smectic-C phase and symmetry considerations on ferroelectric liquid-crystal cells," *Ferroelectrics*, vol. 58, pp. 215–243, 1984.

[44] D. A. Alexander, *The Mathematics of Instabilities in Smetic C Liquid Crystals*. PhD thesis, Department of Mathematics, University of Strathclyde, UK, 2000.

[45] S. P. A. Gill and F. M. Leslie, "Shear flow and magnetic field effects on smectic C, C^*, C_M and C_M^* liquid crystals," *Liq. Cryst.*, vol. 14, pp. 1905–1923, 1993.

[46] P. Maltese, R. Piccolo, and V. Ferrara, "An addressing effective computer model for surface stabilized ferroelectric liquid crystal cells," *Liq. Cryst.*, vol. 15, pp. 819–834, 1993.

[47] C. V. Brown, P. E. Dunn, and J. C. Jones, "The effect of the elastic constants on the alignment and electro-optic behaviour of smectic C liquid crystals," *Euro. Jnl. of Applied Mathematics*, vol. 8, pp. 281–291, 1997.

[48] P. G. de Gennes, "Conjectures sur l'état smectique," *J. de Physique Colloq.*, vol. 30, no. C4, pp. 65–71, 1969.

[49] T. Carlsson, F. M. Leslie, and N. A. Clark, "Macroscopic theory for the flow behavior of smectic-C and smectic-C* liquid crystals," *Phys. Rev. E*, vol. 51, pp. 4509–4525, 1995.

[50] M. A. Osipov, T. J. Sluckin, and E. M. Terentjev, "Viscosity coefficients of smectics C*," *Liq. Cryst.*, vol. 19, pp. 197–205, 1995.

[51] W. van Saarloos, M. van Hecke, and R. Holyst, "Front propagation into unstable and metastable states in smectic-C* liquid crystals: Linear and nonlinear marginal-stability analysis," *Phys. Rev. E*, vol. 52, pp. 1773–1777, 1995.

[52] J. E. Maclennan, M. A. Handschy, and N. A. Clark, "Director reorientation dynamics in chevron ferroelectric liquid crystal cells," *Liq. Cryst.*, vol. 7, pp. 787–796, 1990.

[53] R. Stannarius and C. Langer, "Kink propagation in freely suspended Smc* films," *Mol. Cryst. Liq. Cryst.*, vol. 358, pp. 209–224, 2001.

[54] I. W. Stewart and E. Momoniat, "Travelling waves in ferroelectric smectic C liquid crystals," *Phys. Rev. E*, vol. 69, 2004.

[55] M. Nakagawa, "A hydrodynamic theory of compressible SmC* liquid crystals," *J. Phys. Soc. Japan*, vol. 65, pp. 100–106, 1996.

[56] M. Nakagawa, "A hydrodynamic theory of compressible SmC* liquid crystals," *J. Non-Newtonian Fluid Mech.*, vol. 119, pp. 123–129, 2004.

[57] A. J. Chorin and J. E. Marsden, *A Mathematical Introduction to Fluid Mechanics, Third Edition*. New York, Berlin, Heidelberg, London, Paris, Tokyo, Hong Kong, Barcelona, Budapest: Springer-Verlag, 1990.

[58] J. S. R. Chisolm, *Vectors in three-dimensional space*. London, New York and Melbourne: Cambridge University Press, 1978.

[59] J. D. Logan, *An Introduction to Nonlinear Partial Differential Equations, Second Edition*. Hoboken, New Jersey and Canada: John Wiley & Sons, Inc., 2008.

[60] K. J. Kidney, I. W. Stewart, and G. McKay, "Anisotropy of the elastic constants in SmC* liquid crystal films," *Mol. Cryst. Liq. Cryst.*, vol. 449, pp. 117–125, 2006.

[61] J. Thomsen, *Vibrations and stability: advanced theory, analysis, and tools*. Berlin Heidelberg: Springer Verlag, second ed., 2003.

[62] E. B. Davies, "Non-self-adjoint differential operators," *Bulletin of the London Mathematical Society*, vol. 34, no. 5, p. 513, 2002.

[63] I. W. Stewart, "Stability of equilibrium states in finite samples of smectic C* liquid crystals," *J. Phys. A: Math. Gen.*, vol. 38, pp. 1853–1873, 2005.

[64] L. Meirovitch, *Computational Methods in Structural Dynamics*. Alphen aan den Rijn, The Netherlands: Sijthoff & Noordhoff International Publishers B. V., 1980.

[65] L. Meirovitch, *Analytical Methods in Vibrations, 1967*. London: Macmillan Company, 1967.

[66] S. Rao, *Vibration of continuous systems*. Hoboken, New Jersey: John Wiley & Sons Inc, 2007.

[67] B. A. Finlayson, *The method of Weighted Residuals and Variational Principles*. New York and London: Academic Press, 1972.

[68] A. Quarteroni, R. Sacco, and F. Saleri, *Numerical mathematics*. Berlin Heidelberg: Springer Verlag, second ed., 2007.

[69] H. J. Müller and S. Jayaraman, "Dielectric properties of nematic and ferroelectric liquid crystals," *Mol. Cryst. and Liq. Cryst.*, vol. 309, no. 1, pp. 93–110, 1998.

[70] A. R. MacGregor, "A method for computing the optical properties of a smectic C* liquid crystal cell with a chevron layer structure," *J. Mod. Optics*, vol. 37, pp. 919–935, 1990.

[71] Merck, *Liquid Crystal Mixtures*. Darmstadt, Federal Republic of Germany: Industrial Chemicals Division, Business Unit Liquid Crystals, 1992.

[72] I. Stewart and F. Stewart, "Shear flow in smectic a liquid crystals," *J. Phys.: Condens. Matter*, vol. 21, 2009.

[73] A. Hill and B. Straughan, "A legendre spectral element method for eigenvalues in hydrodynamic stability," *Journal of Computational and Applied Mathematics*, vol. 193, no. 1, pp. 363–381, 2006.

[74] J. Stelzer and H. Arodź, "Dynamics of cylindrical domain walls in nematic liquid crystals," *Phys. Rev. E*, vol. 56, pp. 1784–1790, 1997.

[75] H. Arodź and A. L. Larsen, "Dynamics of cylindrical and spherical relativistic domain walls of finite thickness," *Phys. Rev. D*, vol. 49, pp. 4154–4166, 1994.

[76] A. Vilenkin, "Cosmic strings and domain walls," *Physics Reports*, vol. 121, pp. 263–315, 1985.

[77] M. L. Boas, *Mathematical Methods in the Physical Sciences*. Chichester: Wiley, second ed., 1983.

[78] J. Nagumo, S. Yoshizawa, and S. Arimoto, "Bistable transmission lines," *Circuit Theory, IEEE Transactions on*, vol. 12, no. 3, pp. 400–412, 1965.

[79] P. Schiller, G. Pelzl, and D. Demus, "Bistability and domain wall motion in smectic C phases induced by strong electric fields," *Liq. Cryst.*, vol. 2, pp. 21–30, 1987.

[80] I. W. Stewart, "Painlevé analysis for a semi-linear parabolic equation arising in smectic liquid crystals," *IMA J. Appl. Math.*, vol. 61, pp. 47–60, 1998.

[81] I. Abdulhalim, G. Moddel, and N. A. Clark, "Soliton switching in ferroelectric liquid crystals and their transient electro-optic response," *J. Appl. Phys.*, vol. 76, pp. 820–831, 1994.

[82] Y. B. Chernyak, "Steady state plane wave propagation speed in excitable media," *Phys. Rev. E*, vol. 56, pp. 2061–2073, 1997.

[83] J. Kondo, *Integral Equations*. Oxford: Clarendon, 1991.

[84] R. L. Burden and J. D. Faires, *Numerical Analysis*. Pacific Grove: Brooks Cole, seventh ed., 2001.

[85] Y. Fung, *An introduction to the theory of aeroelasticity*. Dover Publications, 2002.

[86] M. Naimark, *Linear differential operators, Part I: Elementary theory of linear differential operators with additional material by the author. Translated by ER Dawson. English translation edited by WN Everitt*. New York: Frederick Ungar Publishing Co, Inc., 1967.

[87] C. Lanczos, *Linear Differential Operators*. Mineola, N. Y.: Dover, 1997.

[88] I. Gohberg and S. Goldberg, *Basic Operator Theory*. Boston, Basel, Stuttgart: Birkhäuser, 1980.

[89] C. Anton, H. & Rorres, *Elementary Linear Algebra, Applications Version*. New York: Wiley, eighth ed., 2000.

[90] E. B. Davies, *Spectral Theory and Differential Operators*. Cambridge: Cambridge University Press, 1995.

[91] D. Richards, *Advanced mathematical methods with Maple*. Cambridge: Cambridge University Press, 2002.